Exploring the intraperitoneal route of administration for siRNA delivery in the treatment of peritoneal carcinomatosis

George Dakwar

M.Med.Sc – Pharmacology

Thesis submitted to obtain the degree of
Doctor in Pharmaceutical Sciences

Proefschrift voorgedragen tot het bekomen van de graad van
Doctor in de Farmaceutische Wetenschappen

2016

Faculty of Pharmaceutical Sciences

Dean

Prof. dr. Jan Van Bocxlaer

Promoters

Prof. dr. Katrien Remaut

Prof. dr. Stefaan De Smedt

Co-promoter

Prof. dr. Wim Ceelen

Members of the Exam Committee:

Prof. dr. **Chris Vervaet** (chairman)	Ghent University
Dr. **Pieter Colin** (secretary)	Ghent University
Prof. dr. **Véronique Preat**	Catholic University of Louvain
Prof. dr. **Enrico Mastrobattista**	Utrecht University
Dr. **Wouter Willaert**	Ghent University Hospital

Ghent, November 23rd, 2016

The promoters:

Prof. dr. Katrien Remaut

Prof. dr. Stefaan De Smedt

The author:

M.Med.Sc. George Dakwar

The co-promoter:

Prof. Dr. Wim Ceelen

Table of contents

List of abbreviations

ABZ	Albendazole
AUC	Area Under Curve
BSA	Bovine Serum Albumin
CRS	Cytoreductive Surgery
CER	Ceramide
CTLs	Cytotoxic T Lymphocytes
DCs	Dendritic Cells
DDSs	Drug Delivery Systems
DLS	Dynamic Light Scattering
DOX	Doxorubicin
DT-A	Diphtheria Toxin A
FACS	Fluorescence-Activated Cell Sorting
FAK	Focal Adhesion Kinase
FBS	Fetal Bovine Serum
FCS	Fluorescence Correlation Spectroscopy
FD	FITC-Dextran
FDA	Food and Drug Administration
FITC	Fluorescein Isothiocyanate
FRAP	Fluorescence Recovery After Photobleaching
fSPT	Fluorescence Single Particle Tracking
GM-CSF	Granulocyte Macrophage Colony Stimulating Factor

HA	Hyaluronic Acid
(H)IPEC	(Hyperthermic) IntraPeritoneal Chemotherapy
IFP	Interstitial Fluid Pressure
IV	Intravenous
IP	IntraPeritoneal
LC-MS	Liquid Chromatography Mass Spectrometry
LF	Lipofectamine
LPs	Liposomes
LPXs	Lipoplexes
MHCs	Major Histocompatibility Complexes
MPS	Mononuclear Phagocyte System
miRNA	microRNA
mRNA	messenger RNA
MTD	Maximally Tolerated Dose
MTT	(3-(4,5 Dimethylthiazol-2-yl)-2,5-Diphyneltetrazolium Bromide)
PC	Peritoneal Carcinomatosis
pDNA	plasmid DNA
PEG	Poly-Ethylene-Glycol
PEI	PolyEthylenImine
PIPAC	Pressurized Intraperitoneal Aerosol Chemotherapy
PK	Pharmacokinetics
PLGA	Poly(Lactic-co-Glycolic Acid)

PS	Polystyrene
Pt	Platinum
PTX	Paclitaxel
RES	Reticulo-Endothelial System
RISC	RNA Induced Silencing Complex
RNAi	RNA inteference
SDS-PAGE	Sodium Dodecyl Sulfate Polyacrylamide Gel Electrophoresis
siRNA	short/small interfering RNA
Th	helper T cells
VEGF	Vascular Endothelial Growth Factor

List of symbols

h	Hours
min	Minutes
µ	Micro
f	Frequency
η	Dynamic viscosity
d	Diameter
cP	Centipoise
ζ	Zeta
ρ	Density
v	Kinematic viscosity

AIM AND OUTLINE OF THIS THESIS

Cancer is one of the most lethal diseases worldwide, affecting millions of people annually. The past three decades have witnessed a significant progress in the diagnosis and treatment of several cancer types. In spite of this progress, cancer is still a hard to treat disease. For instance, cancer that arises from organs confined within the peritoneal cavity (e.g. ovarian, pancreatic, colorectal and liver), leading to peritoneal carcinomatosis (PC), represents an enormous challenge for both the medical and scientific community due to its late stage of discovery and low survival rates of the treated patients. In this context, different post-surgical therapies are currently being employed in the clinic in order to prolong the survival of patients diagnosed with PC. Nevertheless, most of the patients relapse and succumb to their disease.

Due to their potential to increase the specificity and consequently decrease the adverse effects of different drugs, nanoparticles (NPs) loaded with anti-cancer agents have been a topic of interest for many researchers and pharmaceutical companies during the last 30 years, leading to several products that are used nowadays in clinical oncology. The suitability of nanomedicines for the treatment of PC via the intraperitoneal (IP) route of administration, however, has not been thoroughly investigated yet. Also, the discovery of the RNA interference (RNAi) pathway about two decades ago has opened new avenues in cancer therapy. The RNAi mechanism involves the use of small interfering RNAs (siRNAs) or microRNAs (miRNAs) to knockdown a specific gene. To date, specific gene knockdown is mainly achieved using siRNAs. Therefore, in this project we will limit our focus on siRNAs.

Therefore, the aim of this thesis was to shed the light on the ability of NPs loaded with small interfering RNA (siRNA) for IP therapy of PC. Specifically, we investigate the colloidal stability and biological performance of different lipid-based nano-sized formulations loaded with siRNA in a relevant model of ascites fluid obtained from a PC patient, as well as, we explore the behavior of NPs following IP administration in mice.

In **Chapter 1**, we provide a brief introduction on PC, the anatomy and role of the peritoneal membrane, as well as on the current techniques used in the clinical management of PC following surgical debulking. Importantly, we focus on the hurdles of using nanomedicines for IP therapy of PC in suspension and suggest possible strategies to resolve these challenges.

While **Chapter 1** reports mainly on the use of nanomedicines for chemotherapeutic drugs, in **Chapter 2,** we review the recent progress in the use of nanomedicines for the delivery of nucleic acids, mainly plasmid DNA (pDNA) and siRNA, administered via the IP route for the treatment of PC. In **Chapter 3**, we evaluate the colloidal stability of model polystyrene (PS) NPs possessing cationic, neutral and anionic surface charge, as well as of nano-sized liposomes with different degrees of poly-ethylene glycol (PEG) surface coating in peritoneal fluids from murine and human

origin. The aggregation in peritoneal fluids obtained from mice and the ascites fluid obtained from a PC patient was assessed using an in-house advanced microscopy technique known as fluorescence single particle tracking (fSPT). Similarly, pre-mature release of the siRNA from the different liposomal formulations in undiluted mice peritoneal fluid and ascites fluid was determined using fluorescence correlation spectroscopy (FCS).

In **Chapter 4** and **Chapter 5** we attempt to investigate the influence of the extracellular stability of different siRNA-liposomes complexes (i.e. lipoplexes) on the ability to knockdown a specific gene in the SKOV-3 human ovarian cancer cell line. In **Chapter 4** we tested the colloidal stability, as well as the cellular uptake and knockdown efficiency of different lipoplexes (LPXs) following incubation in ascites fluid. We also provided an evidence that aggregation is not the sole determinant of the downregulation efficiency *in vitro.* The LPXs described in **Chapter 4** were prepared using the classic method for the preparation of LPXs – electrostatic interactions between the positively charged liposomes and the negatively charged siRNA. A similar evaluation of the colloidal stability and knockdown efficiency was performed in **Chapter 5** on LPXs prepared with the hydration method. In both cases the loss of cellular uptake following incubation in the ascites fluid but not in reduced serum medium was the bottleneck for achieving high gene knockdown.

In **Chapter 6,** we elucidate the reason behind the loss of cellular uptake observed in **Chapter 4** and **Chapter 5**, and question whether this phenomenon is restricted only for liposomes possessing the specific lipid composition and biological fluid (i.e. ascites fluid) we used. We carry-out uptake and transfection experiments with LPXs with a different lipid composition in fetal bovine serum, ascites fluid and human serum. Furthermore, we analyze the composition of the proteins bound on the surface of LPXs (known as "protein corona") qualitatively and quantitatively by SDS-PAGE and liquid-chromatography mass spectroscopy (LC-MS), respectively.

In **Chapter 7**, we examine the effect of the carrier solution on the abdominal residence time and biodistribution of NPs following IP administration in mice. Size distributions of 200 nm PS NPs coated with PEG and a mixture containing different molecular weight of FITC-dextrans were obtained at different time points following injection using fSPT and fluorescence recovery after photobleaching (FRAP), respectively. The biodistribution of the PS NPs was determined by fluorescence imaging of the collected organs 24 h following administration.

In **Chapter 8**, we discuss the significance and global impact of translating post-operative strategies for the treatment of PC into the clinic. Furthermore, we elaborate on the contribution of the data presented in this thesis on developing nanomedicine-based IP therapy for the treatment of PC, with emphasis on the hurdles and challenges to be overcome in future studies, in order to ensure successful translation into the clinic.

1

NANOMEDICINE-BASED INTRAPERITONEAL THERAPY FOR THE TREATMENT OF PERITONEAL CARCINOMATOSIS – MISSION POSSIBLE?

Parts of this chapter are published as:

George R. Dakwar[1], Molood Shariati[1], Wouter Willaert[2,3], Wim Ceelen[2,3], Stefaan C. De Smedt[1], Katrien Remaut[1,3], Nanomedicine-based intraperitoneal therapy for the treatment of peritoneal carcinomatosis – Mission possible?. *Advanced Drug Delivery Reviews* (2016).

[1] Ghent Research Group on Nanomedicines, Faculty of Pharmaceutical Sciences, Laboratory for General Biochemistry and Physical Pharmacy, Ghent University, Ghent, Belgium

[2] Department of Surgery, Laboratory of Experimental Surgery, Ghent University Hospital, Ghent, Belgium

[3] Cancer Research Institute Ghent (CRIG), Ghent, Belgium

Abstract

Intraperitoneal (IP) drug delivery represents an attractive strategy for the local treatment of peritoneal carcinomatosis (PC). Over the past decade, a lot of effort has been put both in the academia and clinic in developing IP therapeutic approaches that maximize local efficacy while limiting systemic side effects. Also nanomedicines are under investigation for the treatment of tumors confined to the peritoneal cavity, due to their potential to increase the peritoneal retention and to target drugs to the tumor sites as compared to free drugs. Despite the progress reported by multiple clinical studies, there are no FDA approved drugs or formulations for specific use in the peritoneal cavity yet. This review discusses the current clinical management of PC, as well as recent advances in nanomedicine-based IP delivery. We address important challenges to be overcome towards designing optimal nanocarriers for IP therapy *in vivo*.

Keywords: Peritoneal Carcinomatosis, Intraperitoneal delivery, Sustained release, Biodistribution, Nanomedicines

1. Introduction

Primary cancer occurring in organs confined to the peritoneal cavity (e.g. ovary, liver, colon, and pancreas) might lead to the migration of cancer cells to the peritoneal cavity. Attachment of free-flowing cancer cells to the mesothelial layer of the peritoneal membrane results in the formation of peritoneal carcinomatosis (PC). In the USA alone, there are about 250,000 cases of cancer originating from organs in the peritoneal cavity (e.g., ovarian, pancreatic, colorectal, gastric and liver)[1]. Unfortunately, most primary tumor sites do not cause clear clinical symptoms that enable the early detection of the peritoneal spread of cancer cells. The detection of PC thus mostly occurs at a later disease stage when a large amount of tumor nodules is already distributed over the peritoneal surfaces. The presence of these multiple peritoneal metastases confers a poor prognosis [2].

Selected patients with PC benefit from surgical cytoreduction, aiming to remove all visible peritoneal metastases. Depending on the histology and grade of the disease, either perioperative or postoperative intravenous (IV) chemotherapy can be administered. Despite macroscopically complete cytoreductive surgery (CRS), many patients develop recurrent PC [3]. Hence, active adjuvant treatments are needed to remove persisting minimal residual disease and improve the survival of patients diagnosed with PC. The past decade has witnessed a significant progress in developing IP adjuvant techniques. Most newly developed techniques focus on the local administration of chemotherapeutics. The rationale for IP therapy is the ability to achieve a high locoregional (peritoneal) drug concentration, while avoiding systemic toxicity [4]. Conventional chemotherapeutics might, however, rapidly leak from the peritoneal cavity and display little specificity towards cancer cells. Therefore, the use of nanomedicines to prolong the residence time in the peritoneal cavity and to specifically target tumor cells is being explored. In this review we aim to discuss the progress, barriers and challenges in employing nanomedicines for IP therapy of PC, with a special focus on strategies that are employed to increase the residence time of nanomedicines in the peritoneal cavity. To do so, we first focus on the main techniques that are currently used in the clinical management of PC using local administration of conventional chemotherapeutics. We also address the challenges and hurdles in tailoring nanomedicines for IP delivery *in vivo*, including biodistribution and tumor penetration. Finally, we discuss ongoing clinical trials with nanomedicines for PC therapy and reflect on the possible strategies to overcome current limitations upon administration of nanomedicines.

2. Anatomy and role of the peritoneal membrane

The peritoneal membrane covers the visceral, abdominal and pelvic organs and has a total surface of 1.5 m² on average [5]. It is composed of several layers of connective tissue as demonstrated by Baron [6]. The first layer is comprised of mesothelial cells interconnected by tight junctions, which secrete surface hyaluronan as depicted in Figure 1A. The mesothelial layer functions as a barrier that protects from physical damage and surface adhesion [7]. A submesothelial basement membrane separates the mesothelial layer from the interstitial space, which contains fibroblasts, collagen and other molecules as a first "defense line" against macromolecules (Figure 1A). The last layer consists of vessels with negatively charged endothelial cells – a second "defense line" that prevents the passage of large macromolecules into the peritoneal cavity (Figure 1A).

Under normal conditions (Figure 1A), the oncotic pressure that is exerted by plasma proteins (mainly albumin) across the peritoneal membrane (between the endothelial layer and the mesothelial layer) restricts the diffusion of water into the abdominal cavity due to the reabsorption of water that occurs into the capillaries from the interstitial space [8]. In the majority of the PC cases, however, this homeostasis is disrupted by an increased microvascular permeability which is believed to be mainly induced by the vascular endothelial growth factor (VEGF) [9, 10]. Together with the secretion of cytokines and chemokines in the surrounding of the peritoneum, the structure of the membrane is altered leading eventually to a net change in the flow direction of the fluid (i.e. oncotic pressure) into the peritoneal cavity and consequently, to the formation of an albumin-rich ascites fluid in the peritoneal cavity (Figure 1B). The exact mechanism by which the ascites fluid accumulates in the abdomen is very complex, and not fully elucidated yet. It is hypothesized that different factors play an important role in the formation of the ascites fluid, such as lymphatic obstruction and osmotic water transport following the leakage of proteins from microcapillaries into the peritoneal cavity [11].

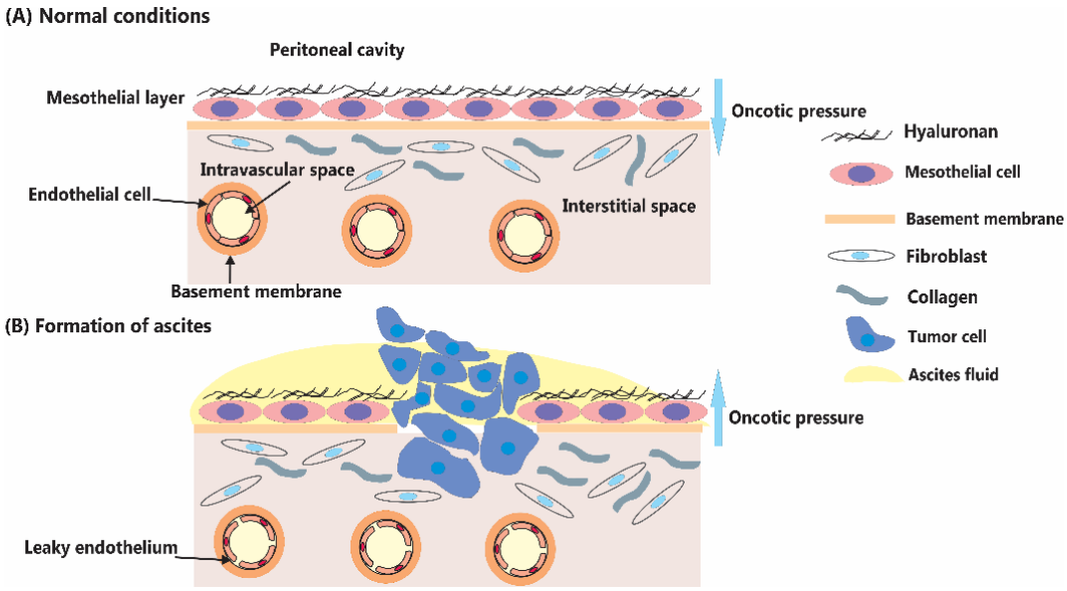

Figure 1. The peritoneal membrane and formation of ascites fluid. (A) Structure of the peritoneal membrane under normal conditions and **(B)** disruption of the peritoneal membrane in peritoneal carcinomatosis, leading to the formation of ascites.

Interestingly, it has been shown that the peritoneal membrane does not correspond to the classic semi-permeable model, but rather is highly permeable to both water, small solutes and proteins [7]. In fact, the peritoneal membrane does not represent a substantial physical barrier for IP administered low-molecular weight drugs, indicating that small chemotherapeutics can easily redistribute to the systemic circulation [7, 12, 13]. There is no consensus, however, as to which extent the peritoneal membrane poses a barrier to nano-or micrometer sized particles. Also, it is not known if the permeability of the peritoneal membrane changes in function of peritoneal disease progression due to the infiltration of tumor cells in the mesothelial cell layer and disruption of the basement membrane.

3. Local chemotherapy for the treatment of PC

3.1 Rationale behind using IP therapy

IP therapy aimed at targeting tumors within the peritoneal cavity offers pharmacokinetic advantages when compared to systemic (IV) administration of chemotherapeutics. As postulated by Dedrick et al., higher concentrations of drug are expected to reach peritoneal tumors following IP delivery compared with the systemic delivery [14, 15]. Also, IP delivery increases the concentration of drug in the vicinity of hypoxic, small peritoneal metastases (less than 1 mm in diameter), which lack an established vasculature and are therefore difficult to treat using IV administration [16]. Finally, similar to any other regional cancer therapy, administration of drugs directly into the site of action lowers systemic toxic effects [17]. It should be noted that none of the available chemotherapeutics has been specifically approved for IP administration. Therefore, IP chemotherapy is currently used off label with agents developed for IV administration such as

Doxorubicin [18], Fluorouracil analogs [19], Paclitaxel (PTX) [20], and Platinum-based compounds [21].

3.2 Current clinical management of PC

Nowadays, the most common IP delivery technique in many clinical centers is repeated IP instillation of chemotherapeutics using a port catheter after cytoreductive surgery (CRS) [22, 23]. During CRS, all macroscopic disease is removed by a combination of organ resections and peritonectomy procedures. The IP cycles are usually initiated 1-3 weeks after surgical debulking, and the catheter is removed after the last cycle of IP chemotherapy is completed. Another option for IP delivery of chemotherapeutics involves intraoperative continuous chemoperfusion (IPEC), immediately after CRS. Intraperitoneal chemoperfusion is usually performed under hyperthermic conditions (41.5°C), known as HIPEC [24] (Figure 2). It is assumed that HIPEC leads to a homogeneous distribution of the administered drug throughout the abdominal cavity and enhances penetration of the drug into the remaining solid tumor nodules [25, 26]. During the combined procedure, the peritoneal cavity is perfused during 30-120 min with chemotherapy using a closed or semi-open perfusion circuit consisting of inflow and outflow drains, a roller pump, reservoir, and heating element. In the largest single-center study, between the years 1991 until 2013, 1,000 patients with PC underwent CRS followed by HIPEC [27]. The authors showed a significant improvement in the survival rate and a substantial decrease in complications, stoma creation and transfusion requirement over time. It should be noted that surgery combined with HIPEC is invasive and time consuming. Also, standardized treatment protocols regarding drug schedule and dose, perfusion temperature, and perfusion duration are currently unavailable [28].

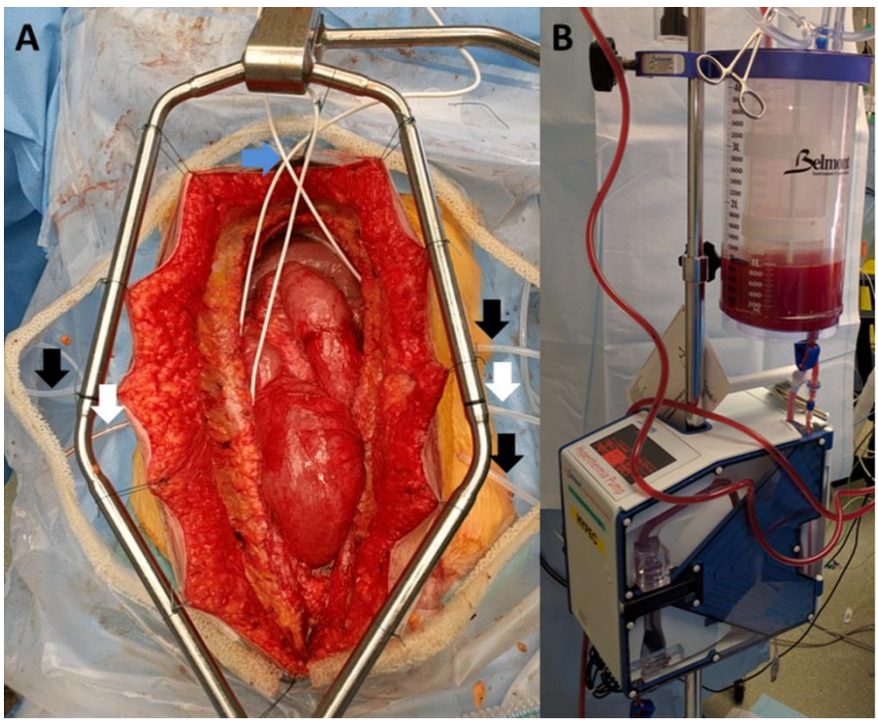

Figure 2. Surgical procedure of HIPEC. (A) View of the open abdomen after cytoreductive surgery for peritoneal carcinomatosis. Then, hyperthermic intraperitoneal chemotherapy (HIPEC) is performed through inflow (white arrows) and outflow (black arrows) tubes that are inserted in the abdominal cavity and connected with a pump, which installs an ongoing circulation. Temperature is continuously measured using three probes (blue arrow) placed in the abdominal cavity. **(B)** A roller pump establishes a continuous circulation of chemotherapy in and out the abdominal cavity.

A very recent new method of intraperitoneal cytotoxic drug delivery for the treatment of PC is Pressurized IntraPeritoneal Aerosol Chemotherapy (PIPAC) [29], which is performed during laparoscopy. After creation of a standard CO_2 pneumoperitoneum (working pressure of 12 mmHg), several balloon trocars are introduced into the abdominal cavity. A disposable nebulizer or micropump (MIP®, Reger Medizintechnik, and Rottweil, Germany) is positioned into the abdomen through one of the trocars connected with a high pressure injector through a dedicated high-pressure line. The cytotoxic solution (Figure 3B) is injected under a pressure of 20 bar, and the resulting aerosol dispersed in the abdomen (Figure 3C). After complete administration, a generator (Ultravision, Alesi Surgical Ltd., UK) is activated, inducing electrostatic precipitation of the airborne particles on the peritoneal surface (i.e., electrostatic PIPAC or E-PIPAC). This pressurized state at 12 mmHg is maintained for 30 min. Thereafter, the capnoperitoneum is deflated through a closed suction system.

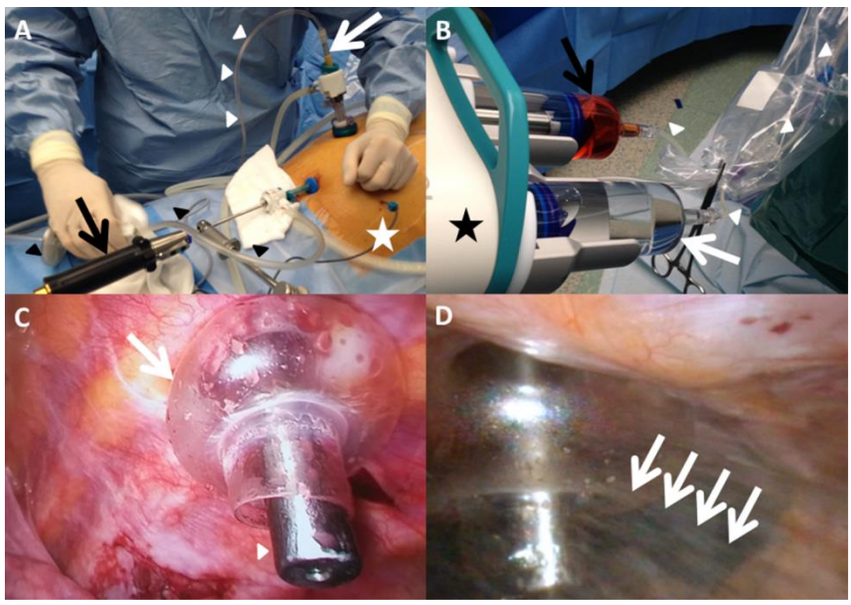

Figure 3. Surgical procedure of E-PIPAC. **(A)** A capnoperitoneum is established during laparoscopy. A nebulizer (white arrow) placed in a 10 mm balloon trocar is connected with a high-pressure line (white arrowheads). A 5 mm camera (black arrow) is inserted in a 5 mm balloon trocar to inspect the nebulization in the abdomen. Once all the cytotoxic agents are injected, electrostatic precipitation of aerosol on the peritoneum is induced through a dedicated catheter (star) connected with a generator. After E-PIPAC, the abdomen is deflated through a closed aerosol waste system with filter (black arrowheads). **(B)** Double head injector (star) with 2 syringes for doxorubicin (black arrow) and cisplatin (white arrow) administration. Both syringes are connected with a high-pressure line (white arrowheads). **(C)** Intra-abdominal view of the tip of the nebulizer (white arrowhead) inserted in the 10 mm balloon trocar (white arrow) before initiation of E-PIPAC. **(D)** Intra-abdominal movement of airborne cytotoxic particles (multiple arrows) during injection.

The working mechanism of PIPAC is based on local administration of cytotoxic agents on the tumoral surface in the abdominal cavity. The aerosol form accomplishes homogeneous drug distribution [30], while it is believed that the high intra-abdominal pressure enhances tissue penetration and antitumor effects [31, 32]. As a consequence, a low dose of chemotherapy can be used, causing low systemic drug uptake and toxicity [29, 33]. Interestingly, Solass and coworkers indeed showed that clinical PIPAC therapy with Doxorubicin achieves high tissue drug concentrations, even though a relatively low dose is nebulized [29].

Other possible advantages include minimal patient discomfort, the repeatability of the procedure, the global quality of life improvement, and the possibility to combine PIPAC with systemic chemotherapy [34, 35]. Experimental and clinical studies show that PIPAC has promising antitumor activity in ovarian, gastric, and colorectal carcinomatosis [36, 37]. Prospective studies (NCT02604784, NCT02320448, NCT01854255), investigating the efficacy of PIPAC in recurrent gastric cancer are currently recruiting patients. A phase 1 dose-escalation trial has been initiated recently in recurrent ovarian cancer (NCT02475772). It is clear, however, that PIPAC is still in its infancy and further clinical research is needed.

4. Future directions in PC therapy

A major drawback of currently used local therapies for PC is the significant risk of recurrent peritoneal disease [38, 39]. Due to the short exposure time to conventional small chemotherapeutics, which rapidly leak from the peritoneal cavity, there is a need for therapeutic approaches that enable a prolonged residence time of chemotherapeutics in the peritoneal cavity following CRS. One such approach that is investigated, is the use of nanoparticles that carry and deliver chemotherapeutics specifically into tumors.

4.1 Rationale for using nanomedicines for IP therapy

Nanoparticles (NPs) are particles with a size that ranges from 1 to 1000 nanometer (nm) in diameter. Due to their size, versatility and the ability to easily modify their surface, NPs are excellent candidates to cross biological barriers and deliver different therapeutics into cells. Also, NPs can potentially slow down systemic absorption, decrease systemic toxicity [40] and extend the exposure time of the drugs to peritoneal tumors. Furthermore, NPs can be functionalized to selectively accumulate at tumor sites [41, 42]. NPs that are used as vehicles for the delivery of drugs and biopharmaceuticals are known as "nanomedicines".

Generally speaking, NPs are roughly divided into two main types: (1) lipid-based NPs and (2) polymer-based NPs. The most used lipid-based nanomedicines for biomedical applications are liposomes [43], while Poly (lactic-co-glycolic acid) (PLGA) is one of the most successfully developed polymers used in drug delivery [44]. The choice of NPs for a specific application mostly depends on the physico-chemical properties of the desired cargo (e.g. hydrophilicity/hydrophobicity, charge, and solubility, etc.) and the route of administration, as well as on the extracellular and intracellular barriers it is expected to cross in order to successfully reach the site of action. To date, there are some nanomedicines approved for clinical use and several more in clinical trials [45]. Nanomedicines have also played a vital role in cancer therapy [41, 42], with a total of 12 clinically approved nanomedicines for anti-cancer therapies [46]. None of these nanomedicines, however, are intended for IP cancer therapy.

Numerous attempts have been made to deliver chemotherapeutics into tumors confined to the peritoneal cavity using NPs (Figure 4A), via both IV and IP routes [47-49]. We have also recently reviewed different non-viral nucleic acid delivery systems that were IP administered for the treatment of peritoneal cancer [50]. In the current review, we do not aim to overview the different types of nanoparticle systems and their building blocks as such, but to focus on general *in vitro* and *in vivo* aspects related to IP delivery of nanomedicines that are currently still often overlooked.

4.2 *In vitro* stability and biological activity of NPs in the presence of ascites fluid

Generally speaking, *in vitro* optimization of nanomedicines is required as a first development step, and this includes basic characterization of the size and surface charge, followed by toxicity, uptake, and biological activity assays in the relevant cell type. Nevertheless, *in vitro* optimization is often carried out in biofluids that do not resemble the *in vivo* situation, and the impact of the relevant biofluids that nanomedicines will encounter upon *in vivo* administration is often not investigated. It is becoming increasingly clear that NPs present in biofluids (e.g. blood, plasma, serum, saliva, and peritoneal fluid, etc.) interact with different components including proteins and degrading enzymes that may lead to their aggregation, premature release of cargo, loss of targeting capabilities, decrease of cellular uptake, and eventually dramatic limitation of biological activity [51-56]. In this context, we have recently established an *in vitro* model to evaluate the performance of NPs in the presence of ascites fluid obtained from a patient diagnosed with PC. By using advanced microscopy techniques, we were able to determine the aggregation and disintegration of NPs in the undiluted ascites fluid, as parameters to follow their colloidal stability in function of time [57]. Our data demonstrate that the ascites fluid does not only influence the colloidal stability of the NPs, but also drastically lowers cellular uptake of liposome-siRNA complexes. Thus, even NPs such as PEGylated liposomes that were colloidally stable in ascites fluid (in terms of aggregation and release), lost their ability to silence genes in SKOV-3 human ovarian cancer cells due to their incapability to carry the siRNA into the cells [51]. It should be noted that generally, only limited amount of ascites fluid has developed in the patients which are eligible for CRS and adjuvant IP therapy. Before the development of ascites, only a small amount of IP fluid is present, which cannot be extracted from patients to optimize *in vitro* performance of NPs. Whether or not the small amount of IP fluid limits the therapeutic potential of *in vivo* administered nanoparticles to the same extent as ascites fluid remains to be elucidated. Nevertheless, we do recommend to optimize the *in vitro* behavior of NPs in ascites fluid, before moving on to the *in vivo* evaluation of NPs.

4.3 *In vivo* barriers and challenges upon IP administration of NPs

4.3.1 Biodistribution of NPs following IP injection

Apart from colloidal stability, an important feature in anti-tumor activity of nanomedicines is their fate following administration. Ideally, nanomedicines should circulate, extravasate (in the case of IV injection), accumulate and finally penetrate into the tumor. Unlike for IV administration, where tens of studies investigated the biodistribution and ability of different nanomedicines to accumulate at tumor sites [58, 59], only (very) limited data are available on the biodistribution of NPs following IP injection (Table 1). The biodistribution of non-PEGylated (450 nm in size) and PEGylated (30-100 nm in size) graphene oxide NPs was assessed in healthy animals following IP

administration [60]. Aggregated and immobile NPs were found in the abdomen for the non-PEGylated formulation, whereas the mobile PEGylated formulations accumulated mainly in the liver and spleen. Langer and coworkers evaluated 265 nm PLGA NPs of 90 kDa as strategy to prolong drug delivery in the murine peritoneum and compared the biodistribution with 5-250 μm sized PLGA microparticles (MPs) [61]. All NPs were cleared from the peritoneum within 2 days after administration, and accumulated in the mononuclear phagocyte system (MPS) organs, namely the liver and spleen. MPs were retained in the peritoneal cavity for a longer time period, but a high incidence of adhesions 2 weeks after injection of the MPs made them unsuitable for long term delivery to the peritoneum [61]. Similarly, Tsai et al. examined the effect of carrier size on the disposition and anti-tumor activity of paclitaxel (PTX) [62]. In particular, PTX loaded gelatin MPs and NPs, as well as Cremophor micelles were systematically studied in mice bearing Hs766T pancreatic human cancer cells. Again, NPs were more rapidly cleared from the peritoneal cavity, with less than 0.1% remaining in peritoneal lavage samples 24 h following IP administration. MPs exhibited the slowest clearance and the longest residence time in the abdominal cavity, which was correlated with a ~2 fold increase in the survival time when compared to the NPs and Cremophor micelles. The authors attributed this clearance profile to the dimensions they found for the lymphatic duct openings (known as stomata) on the diaphragm of mice, which ranged on average from 0.7 to 15.5 μm in length and 0.5 to 8.2 μm in width. Therefore, NPs smaller than these openings were rapidly cleared into the systemic circulation, while a more slow absorption occurred for MPs which were similar in size to the openings [62]. Also, Hirano and Hunt investigated the size effect on the peritoneal retention of liposomes of 48, 170, 460 and 720 nm in rats [63]. They observed no size effect in this range, as all liposomes remained below the estimated size limits that would restrict their entrance into the lymphatic capillaries. When Sadzuka et al. investigated the size effect for negatively charged liposomes of 155, 605 and 4225 nm, they came to comparable conclusions [64]. Again, no significant difference in clearance was observed for the small and medium sized vesicles, while the larger liposomes indeed were retained for a longer time in the peritoneal cavity 8 and 24 h after injection. When neutral liposomes were used, Mirahmadi concluded that 1000 nm sized particles were the most optimal to achieve high peritoneal retention [65]. Dadashzadeh et al., however, looked into the effect of size, charge, lipid composition and PEG coating on peritoneal retention in healthy female NMRI mice using 100 nm and 1000 nm radiolabeled liposomes [66]. The charge of the liposomes seemed to be the most important factor that determined the retention in the abdominal cavity, with cationic liposomes being longer retained than negatively charged liposomes. The effect of size on peritoneal clearance was dependent on the charge of the liposomes. 100 and 1000 nm negatively charged liposomes were equally rapidly cleared, most likely through macrophage uptake. Size did matter for the cationic liposomes, where the 1000 nm cationic liposomes had the highest retention in the peritoneal cavity, with up to 25% of the initial dose still remaining 48 h following administration. For 100 nm cationic liposomes, 20% of the injected dose could still be retrieved after 24 h. In the first hours following injection, PEGylation of the cationic liposomes even further increased the peritoneal

retention, presumably because of interference with the uptake of PEGylated liposomes in the macrophages. The authors concluded, overall, that the 100 nm cationic liposomes are the most suitable for IP drug delivery due to uniform distribution in the peritoneal cavity and resistance to uptake by peritoneal macrophages. It should be noted that the authors did not determine the actual size of liposomes after injection into the abdomen. As we previously demonstrated that especially cationic liposomes are sensitive to aggregation, we speculate that the high retention of the 100 nm cationic liposomes observed by Dadashzadeh et al. could potentially be attributed to aggregation of the cationic liposomes in the peritoneal cavity to micrometer sized aggregates [57], which no longer efficiently cross the lymphatic openings. Also, it is of importance to mention that the vast majority of the above mentioned biodistribution studies were performed in healthy animals (see Table 1). Therefore, at the moment it is not clear whether or not the residence time of particles in the peritoneal cavity would be changed in the presence of PC, for example by changing the barrier function of the peritoneum, by altering the amount and activity of macrophages present in the peritoneal cavity or by changes in the content and composition of proteins in the peritoneal fluids, which might bind and alter the biological activity of NPs as mentioned under section 4.2.

In general, two major mechanisms for drug clearance from the peritoneal cavity to the systemic circulation are suggested: (1) direct absorption through the peritoneum and (2) drainage via the lymphatic ducts. For small molecules with a molecular weight of less than 20 kDa, absorption through the peritoneum is the major pathway, as shown by Flessner and co-workers [12]. For larger compounds such as NPs and MPs, the studies above demonstrate that lymphatic drainage represents the major clearance pathway [63, 67]. The lymphatic drainage and rapid clearance of colloidally stable NPs (that are diffusing and do not form aggregates) from the peritoneal cavity seem inevitable, in such a way that NPs are cleared within several hours (depending on the size) following administration, resulting in a low residence time in the abdomen. Nevertheless, it should be noted that NPs that are larger than 500 nm in size tend to stay in the lymph nodes, while smaller NPs pass through the lymph nodes and end up in the systemic circulation [63]. This lymphatic targeting of NPs has long time ago already been proposed by Maincent et al. [68] as a promising strategy to treat tumors that make use of the lymphatic pathways to spread and metastasize in the peritoneal cavity.

Table 1. Biodistribution of NPs following IP administration

Formulation	Hydrodynamic diameter & surface charge (if available)	animal model	Outcome	Reference
PEGylated and non-PEGylated Graphene oxide NPs	25, 27, 50 nm PEGylated 450 nm negatively charged	Healthy mice	450 nm non-PEGylated formed aggregates in the abdomen, the PEGylated particles were cleared mainly in the liver and spleen	[60]
PLGA	265 nm negatively charged	Healthy mice	NPs were cleared from the abdomen within 2 days and accumulated in the spleen and liver	[61]
Gelatin NPs loaded with Paclitaxel	60, 90 nm	Nude mice bearing human xenograft tumor model - pancreatic Hs766T tumor cells	Rapid clearance (within 24 hours) of the NPs from the abdomen and poor efficacy *in vivo* compared with MPs	[62]
Egg lecithin liposomes encapsulating [^{14}C] sucrose	48, 170, 460, and 720 nm	Healthy rats	Rate and extent of absorption from the peritoneal cavity was independent on size. The Smallest liposomes accumulated in the lymph with little lymph node retention, larger liposomes were collected in the lymph nodes	[63]
Liposomes encapsulating doxorubicin (different lipid compositions)	150, 605 and 4225 nm negatively charged liposomes	CDF_1 mice bearing Ehrlich ascites carcinoma tumors	Lipid composition did not affect the clearance of the liposomes. Large liposomes were superior over the small liposomes and free drug solution in inducing cytotoxicity	[64]
^{99m}Tc DSPC/CHOL liposomes	100, 400, 1000 and 3000 nm neutral liposomes	Healthy mice	Highest peritoneal concentration was measured for the 1000 nm liposomes. The 3000 nm sedimented upon abdominal organs	[65]
PEGylated and non-PEGylated liposomal formulations	100 and 1000 nm PEGylated, cationic and	Healthy mice	Positively charged liposomes of 1000 nm exhibited the highest retention time in the	[66]

	negatively charged liposomes		peritoneal cavity	
[^{14}C] Polyacrylic polymeric particles composed of carbon-14 polyhexylcyanoacrylate nanoparticles (PHCA) and polymethylmethacrylate (PMMA)	543 nm for PHCA and 1.4 µm for PMMA	Healthy rats	Targeting the lymphatics via the IP route was 70-2000 fold higher when compared to the IV route	[68]

4.3.2 The size dilemma for optimal tumor penetration of NPs

To ensure maximal efficacy of cytotoxic drugs, penetration of the drug deep into the tumor tissue is crucial. From a clearance point of view, ideally, large particles (above 1 µm) such as MPs and microspheres are used as depot systems to prolong the retention time of drugs in the peritoneal cavity. In this respect, different MPs loaded with chemotherapeutics were used for the treatment of abdominal cancer [49, 69, 70]. Nevertheless, it has been shown that micro-sized formulations bear the risk of inducing peritoneal adhesions and inflammations [4, 61, 71]. The optimal balance between retention time, adhesions and efficacy of MPs is currently a topic of interest for several research groups [72].

With regard to nanomedicines, the size dilemma consists of having a delivery system that efficiently penetrates on the level of the tumor, but on the other hand, also sufficiently remains present in the peritoneal cavity for this penetration to take place. The poor retention time of chemotherapeutics and nanomedicines in the abdomen, however, is expected to limit peritoneal tumor penetration and anti-tumor activity of these nanomedicines. Also, the microenvironment of many solid tumors makes the penetration of drugs very difficult or even impossible in some cases [73]. Tumors are characterized by a dense extracellular matrix, limiting the penetration not only of cytotoxic drugs but also of nanomedicines [74]. Also, the abundant and leaky vasculature in tumors results in a high interstitial fluid pressure (IFP) which counteracts the penetration of drugs and nanomedicines into the tumors by convective flow [75]. It has been demonstrated that smaller sized nanomedicines penetrate into tumors more efficiently than larger ones [76, 77]. Apart from the size of the nanomedicines, it has been recently shown that the surface charge plays a very important role in tumor penetration. Wang et al. [78] provided a strong experimental evidence in different tumor models that 100 nm positively charged PEGylated nanomedicines are superior in terms of tumor penetration over their neutral and anionic counterparts, and consequently exhibit enhanced tumor killing efficiency. In the context of NPs penetration into peritoneal tumors, Ding et al. [79] studied the antitumor efficacy and tumor penetration of 100 nm negatively charged (at pH 7.4) cisplatin-loaded gelatin-poly(acrylic acid) NPs in mice bearing hepatic H22 tumors. The nanoparticulate system significantly decreased the tumor volume when

compared to the cisplatin solution. However, tumor sections obtained 2 days following IP administration, showed that NPs are not able to effectively permeate the tumor deeply, but rather affect the cells near the vasculature. This suggests that IP injected NPs first entered the systemic circulation before reaching the tumor site. On the other hand, a recent study demonstrated that nanoscale PTX-polymersomes [80, 81] were detected deep inside the tumor's parenchyma, indicating efficient tumor penetration [82] . Interestingly, the fluorescence signal showed higher accumulation of PTX-polymersomes in tumors compared with other organs (lung, kidney, heart, liver and spleen). Following IV administration, however, PTX-polymersomes accumulated less in peritoneal tumors and more in other organs. Overall, the data suggest that NPs penetrated into the tumor nodules both (1) directly, from the peritoneal cavity and (2) systemically after clearance from the peritoneal cavity, so that both small poorly vascularized and large vascularized tumors are affected by the drug.

A possible strategy to lower the IFP is to decrease the vasculature in tumor nodules. It has been recently shown by Gremonprez et al. [83] that the inhibition of VEGF by Bevacizumab enhances the penetration of chemotherapeutics into peritoneal tumors and inhibits tumor growth in mice bearing colorectal carcinomatosis. Whether the tumor penetration of nanomedicines would also improve upon inhibition of VEGF remains to be investigated. However, given the important role of VEGF in the angiogenesis and formation of ascites [8, 9] (see section 2.), VEGF inhibitors seem excellent candidates for the treatment of peritoneal metastatic cancer. Albendazole (ABZ) is a widely investigated anti-parasite drug for its ability to inhibit VEGF [84], as well as tumor growth via the inhibition of tubulin polymerization and G2 M phase of the cell cycle. Noorani et al. [85] formulated ABZ bovine serum albumin (BSA) NPs of respectively 7-10 nm and 200-250 nm for the sustained release of ABZ in the peritoneum. The anti-tumor efficacy of both formulations following IP injection was tested *in vivo* in OVCAR3 xenograft tumor model. The 10 nm ABZ BSA particles significantly suppressed the tumors at a much lower dose than the free drug, whereas non-significant tumor inhibition compared with free drug was observed for the 200 nm ABZ BSA. Yet, both formulations significantly reduced the ascites volume and number of malignant ascites cells in the abdomen of the treated nude mice. The authors attributed the significant decrease in tumor burden between both formulations to the penetration of NPs into the tumor tissue, which is highly likely more pronounced for the 10 nm ABZ BSA. Therefore, it seems that smaller NPs are beneficial for optimal tumor penetration, in spite of the short residence time expected in the peritoneal cavity.

5. Strategies for IP delivery and sustained release of nanomedicines in the peritoneal cavity

Possible strategies to enhance the biodistribution and residence time of nanomedicines in the peritoneal cavity are depicted in Table 2 and Figure 4. As mentioned above, for most NPs rapid clearance from the peritoneum to the systemic circulation takes place. Therefore, to overcome the obstacles associated with intraperitoneally injected nanomedicines as such (i.e. dispersed in solution), release of NPs in a sustained manner in the peritoneum seems an optimal solution (Figure 4B, 4E). Conceptually, controlled release of small doses of NPs loaded with anti-cancer therapeutics, nucleic acids or a combination of both from depot systems could attenuate lymphatic drainage of the NPs, prolong the retention time in the abdomen, increase the exposure time of the tumors with the drug, and as a result augment its efficacy (see Table 2). Aiming to increase the residence time of platinum (Pt) in the peritoneal cavity for the local treatment of ovarian cancer, Cho et al. encapsulated Pt within Hyaluronic acid (HA) NPs forming PtNPs [86]. These NPs were then loaded on a biocompatible and biodegradable *in-situ* crosslinkable HA gel (PtNP/gel). Both systems (PtNPs and PtNP/gel) showed *in vitro* sustained release kinetics of Pt, and *in vivo* drug release for the PtNP/gel depot system of less than 2 weeks in the peritoneal cavity. Unexpectedly, when these systems were IP instilled in the abdomen of mice bearing SKOV-3 tumors, no enhancement in anti-tumor efficacy was measured compared with a solution of the free drug (i.e. cisplatin solution) [86]. Therefore, these findings do not support the expected synergy between the residence time of the drug and its therapeutic effect. The same research group evaluated the efficacy of PTX nanocrystals and microparticulate PTX precipitates loaded on a similar crosslinkable HA hydrogel for the treatment of mice bearing SKOV-3 ovarian cancer tumors [87]. Contrary to outcomes obtained with the PtNP/gel, the PTX nanocrystals exhibited significant tumor suppression upon single IP administration compared with the commercially available Taxol®. The microparticulate PTX precipitates, did not, however, result in a significant tumor inhibition compared with Taxol®. Since both studies were performed with the same depot system (i.e. HA hydrogel) and cancer model, the differences in efficacy between the studies most probably arise from the PK properties of the drug encapsulated within the hydrogel. In particular, PTX, with a molecular weight of approximately 854 Da and a bulky structure, is probably cleared slowly from the peritoneal cavity [88], resulting in increased exposure to peritoneal tumors. Indeed, when compared with a lower molecular weight platinum-based compound, PTX exhibited the highest peritoneal-to-plasma area under curve (AUC) ratio [89]. Importantly, a high peritoneal-to-plasma AUC ratio is not always translated in enhanced antitumor activity, since drug penetration also plays an important role [90]. Fan et al. [91] did find that sustained release of NPs from a hydrogel may hold a promise for future clinical applications. A thermosensitive hydrogel (i.e. liquid at room temperature, gel at the body temperature) composed of polylactic acid and Pluronic L64, co-encapsulating NPs loaded with the anti-cancer agent docetaxel and the anti-microbial tumor suppressing peptide LL37 (Figure 4B), significantly inhibited tumor growth in a mice model derived

from colorectal cancer HCT116 cells following IP administration. This significant inhibition was accompanied by an increase in the survival of the treated mice when compared with a solution containing both drugs and the hydrogel containing only docetaxel NPs. Similarly, Xu et al. [92] developed a thermosensitive hydrogel assembled by PTX NPs of amphiphilic copolymer, termed as PTX/PECT^{gel} [93]. Upon IP administration of PTX/PECT^{gel} in mice bearing CT26 colorectal PC model, the hydrogel degraded over 8 days in the peritoneal cavity and significantly decreased the tumor weight compared with the free PTX solution – Taxol®. Furthermore, the authors showed higher abdominal PTX concentration for the PTX/PECT^{gel} compared with Taxol® for an extended period of time.

Another possible interesting strategy to improve the biodistribution of nanomedicines in the peritoneal cavity is, similarly to the PIPAC method described in section 3.2., the aerosolization of nanomedicines in the peritoneum (Figure 4C). In theory, nanomedicines can be nebulized in the peritoneal cavity. Whether or not the nanomedicines' structure or function is affected by the high pressure nebulization, however, remains to be elucidated.

In contrast to PIPAC, NPs have already been used in the setting of (H)IPEC (Figure 4D). In a recent study by Nowacki et al.[94], HIPEC was performed in mice using a nano-sized drug delivery system based on carbon nanotubes (CNTs) [95]. Briefly, CNTs loaded with cisplatin were functionalized with the anti-CD133 antibody to reduce the resistance to chemotherapy, emerging from the CD133 antigen. When the CNTs functionalized with anti-CD133 were applied IP via the HIPEC procedure in the abdomen of mice bearing peritoneal B16 melanoma tumors, the best general survival (12.6 days) observed was for the functionalized CNTs, and the shortest general survival (8 days) was for the mice in which the HIPEC procedure was not carried-out [94]. Likewise, De Smet et al. [96] investigated the suitability of PTX nanosuspension stabilized by Pluronic F127® for HIPEC treatment in rats bearing SKOV-3 ovarian cancer. Compared with the commercially available PTX formulation - Taxol®, no significant tumor volume reduction was documented 7 days and 14 days after HIPEC treatment. A significant reduction in tumor volume was, however, observed when the PTX nanosuspension was compared with the non-treated group. Also, the rats treated with the PTX nanosuspension recovered faster following the HIPEC procedure.

Overcoming the resistance of cancer cells remains one of the main hurdles in cancer therapy [97]. In many cancer patients, even after complete remission, a relapse can occur due to multi-drug resistant (MDR) tumors. One approach to limit drug resistance is to minimize the periods between drug doses. In addition to the localized delivery strategies aiming to enhance the exposure of tumors to chemotherapeutics, metronomic dosing represents a novel approach defined as the frequent and continuous administration of conventional chemotherapy drugs at low doses without drug-free breaks (Figure 4E) [98]. Goldberg and coworkers developed slow-release drug delivery systems based on dual layer surface coating of PLGA PEGylated NPs loaded with PTX for IP

treatment of mice bearing BR5FVB1-Akt drug resistant ovarian cancer tumors. Compared with free PTX, metronomic dosing obtained by sustained release of PTX in the peritoneum significantly prolonged the survival of the treated animals [99]. A synergy in anti-tumor activity was documented when metronomic dosing was achieved with PLGA-PRINT NPs encapsulating docetaxel in combination with the antiangiogenic complex of chitosan NPs loaded with the enhancer of zeste homolog 2 (mEZH2) siRNA in HeyA8 and SKOV3ip1 ovarian tumor models. The chemotherapeutic agent (i.e. PLGA-PRINT docetaxel) was IP administered, whereas the siRNA-NP complex was intravenously injected [100].

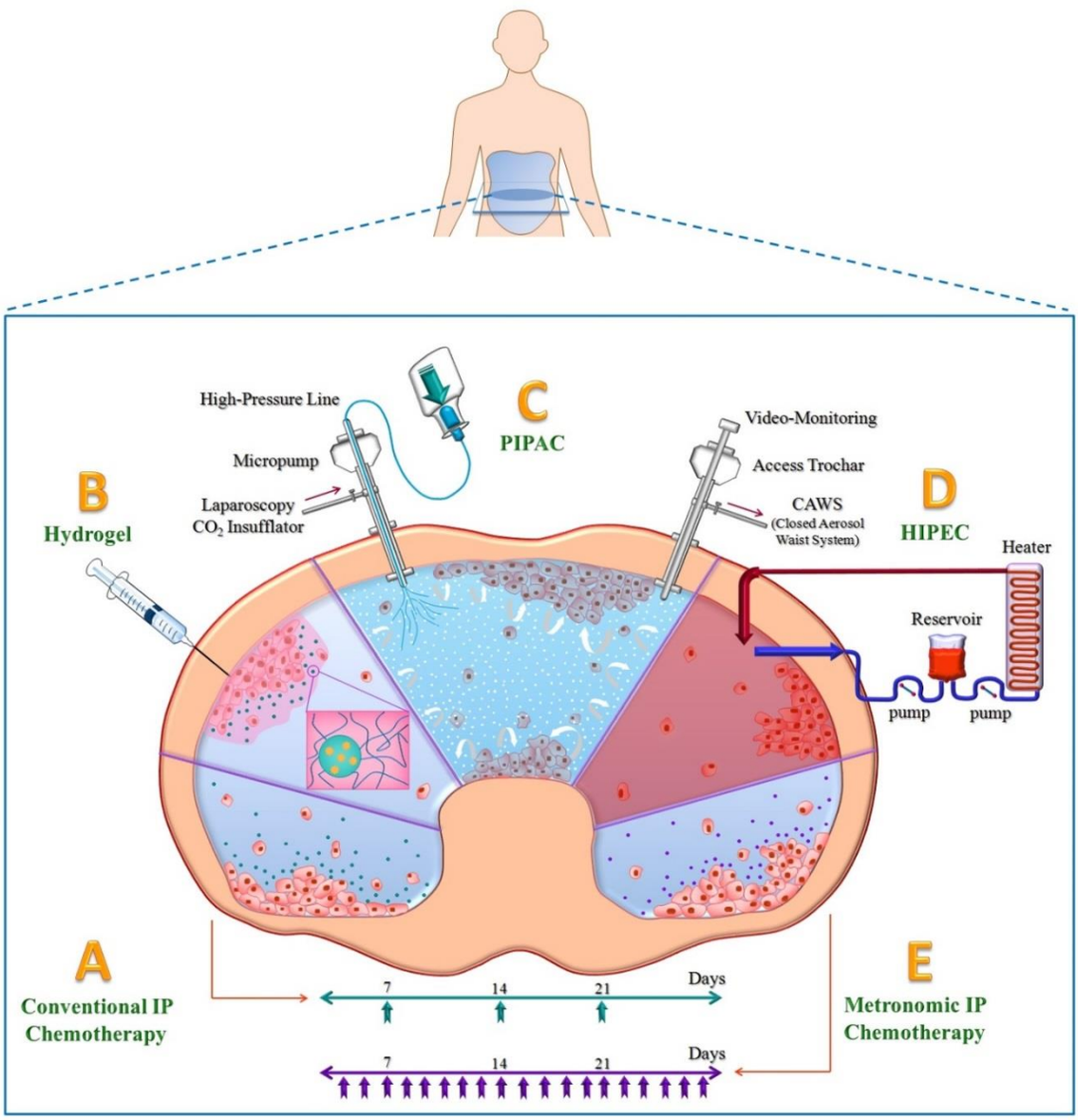

Figure 4. Schematic illustration of the different therapies involving nanomedicines from left to right. (A) NPs loaded with chemotherapeutics or other macromolecules. **(B)** Sustained release of NPs loaded with anti-cancer drugs from a depot system (e.g. hydrogel). **(C)** Nebulization of NPs using PIPAC. **(D)** HIPEC of NPs. **(E)** Continuous administration of NPs loaded with chemotherapeutics at low doses without drug-free breaks known as metronomic therapy.

In addition to drug resistance, the lack of tumor specificity is a major obstacle in IP chemotherapy. Ideally, the nanomedicines should specifically accumulate at the target site, and leave healthy tissues unaffected. In general, this targeting can be accomplished by incorporating antibodies or targeting ligands at the NPs' surface to enhance the interaction between the NPs and the tumor site. The folate receptor alpha (FR-alpha) has already been identified as a suitable target for cancer therapy and imaging [101]. Also, VEGF and Human Epidermal Growth Factor Receptor 2 (HER2) targeted antibodies show potential for specific tumor targeting [102]. In these studies, the targeting moieties were coupled to fluorophores, to improve debulking in cytoreductive surgery after tumor-specific intraoperative fluorescence imaging. When a HER2 targeting antibody was coupled to PTX containing NPs, however, no difference in overall tumor accumulation between targeted and non-targeted NPs was seen [103]. It should be noted that due to the heterogeneous origin of primary tumors that can lead to PC, suitable targeting agents will greatly differ from patient to patient [104]. Therefore, a personalized medicine approach seems recommended, in which individual suitable tumor-specific targets can be identified and validated.

Table 2. Investigated IP administered formulations to overcome the rapid clearance of nanomedicines in solution following IP injection

Formulation	**Hydrodynamic diameter & surface charge (if available)**	**Cancer model**	**Outcome**	**Reference**
Bovine serum albumin NPs encapsulating ABZ	~ 10 nm ~ 200 nm	Nude mice bearing OVCAR3 tumors	Significant reduction in the ascites fluid volume, as well as in the VEGF expression	[85]
Pt solution, PtNPs and PtNPs loaded on HA hydrogel	PtNP – 270 nm, negatively charged	Balb/c mice bearing SKOV-3 ovarian cancer tumors	Pt solution was superior over the PtNPs and PtNP/gel in terms of tumor inhibition	[86]
PTX nanocrystals and microparticulate PTX loaded on HA hydrogel compared with the commercially available PTX formulation – Taxol®	PTX nanocrystals – rods shaped ~ 260nm and a surface charge of -6 mV, microparticulate PTX – needle shaped ~ 11.5 µm in length and 2 µm in width, negatively charged (-3mV)	Balb/c mice bearing SKOV-3 ovarian cancer tumors	PTX nanocrystals loaded on the HA hydrogel, but not the microparticulate PTX, significantly prolonged the survival of mice compared with the commercially available PTX formulation - Taxol®	[87]
PLA-L35-PLA NPs loaded with docetaxel and LL37 formulated into PLA-L64-PLA	PLA-L35-PLA NPs ~ 130 nm, neutral NPs	HCT116 PC model	Sustained release of docetaxel and the suppressing peptide LL37 efficiently	[91]

thermosensitive hydrogel			suppressed the growth of PC in mice	
Thermosensitive hydrogel assembled with PTX nanoparticles (PTX/PECT^{gel})	PTX/PECT NPs ~120 nm	Mice bearing CT 26 colorectal PC model and ascites fluid	IP administration of PTX/PECT hydrogel efficiently inhibited tumor growth and metastasis compared with Taxol®	[92]
Carbon nanotubes (CNTs) loaded with cisplatin and functionalized with the CD-133 antibody	NA	IP B16 melanoma tumors	Longer survival (12.6 days) was obtained for CNTs delivery systems after HIPEC compared to the situation where HIPEC was not carried-out	[94]
Nanocrystalline PTX stabilized by Pluronic F127®	~ 400 nm	Rats bearing SKOV-3 ovarian cancer tumors	HIPEC treatment using the PTX nanosuspension resulted in a significant tumor suppression compared to the non-treated group. No significant reduction in tumor growth was observed when the PTX formulation was compared to the commercially available Taxol®	[96]
Dual-layer surface PLGA PEGylated NPs loaded with PTX for metronomic dosing	~150 nm, negatively charged	mice bearing BR5FVB1-Akt drug resistant ovarian cancer tumors	Significant increase in the survival of mice compared to the free drug	[99]
PLGA-PRINT docetaxel NPs (IP administered metronomic dosing) and chitosan NPs complexed with mEZH2 siRNA (administered IV)	PLGA-PRINT docetaxel 80 x 320 nm 230 nm Negatively charged	HeyA8 and SKOV3ip1 ovarian tumors	Significant anti-tumor activity in both cancer models	[100]

6. Nanomedicine-based IP therapy – ongoing clinical trials

Here, we focus on two NP formulations that were evaluated for IP therapy in humans (Table 3). A recent phase I study evaluated the toxicity, tolerability, and pharmacokinetics (PK) of intraperitoneally administered nanoparticulate Cremophor-free PTX (NanoTaX®) in 21 patients with peritoneal solid tumors malignancies, following CRS [105]. The selected patients received six escalating doses of NanoTaX® (50-275 mg/m^2) every 28 days. Compared with the IV administered PTX, no additional increase in the toxicity was documented. Moreover, the treatment resulted in a favorable peritoneal PK profile, exhibited by peak concentrations of PTX in the peritoneal fluid that are 450-2900 folds higher than the peak concentrations of PTX in plasma 2 days following injection. Response was determined in 16 patients. Among those, four patients remained stable, while in twelve patients the tumors continued to grow (i.e. disease progression). Remarkably, five patients with advanced cancers survived more than 400 days after the beginning of the treatment. In summary, this study provided a clinical evidence in humans showing that NanoTax® administered via IP catheter exhibits lower systemic toxicity and higher levels of drugs in the peritoneal cavity compared with the IV administered PTX. This low toxicity and high peritoneal PTX retention is explained by the fact that NanoTax® is actually a 600-700 nm rod shaped reservoir which allows continuous release of PTX in the peritoneum. The study was completed in 2013 and it is unclear yet whether a subsequent phase II trial is planned.

The second NP-based formulation under clinical investigation for IP therapy in humans is Abraxane®. Abraxane® is a Cremophor®-free, albumin-based NP with PTX (~130 nm), used in clinical oncology for the treatment of metastatic breast and pancreatic cancer, as well as neoplasms. The Food and Drug Administration (FDA) and the European Medicines Association (EMA) approved Abraxane® for IV administration [106]. Abraxane® has however not been approved yet for use in IP therapy. A recent phase I trial [107] aimed to examine the maximally tolerated dose (MTD), adverse effects and PK of dose-escalating intraperitoneally administered (via IP catheter) Abraxane®. 27 patients with advanced peritoneal malignancies showed high peritoneal exposure of Abraxane® compared to the plasma exposure (i.e. pharmacologic advantage) with a low inter – and intra-patient variability.

Table 3. Ongoing clinical trials using nanomedicines for the IP treatment of peritoneal tumors

Formulation	Diameter	Clinical trial (phase/No. of patients)	Outcome	Reference
NanoTax® - nanoparticulate reservoir of PTX	Rod-shaped 600-700 nm	Phase 1 included 21 patients with peritoneal solid tumor malignancies after CRS	IP administration of NanoTax® results in high PTX levels, minimal systemic exposure and reduced toxicity compared with the IV administration	[105]
Abraxane® - albumin based NPs bound to PTX	~ 130 nm	Phase 1 included 27 patients with advanced peritoneal malignancy	Significant peritoneal exposure of Abraxane® compared to the plasma, low inter- and intra-patient variability	[107]

7. Conclusions and future perspectives

IP therapy for the treatment of PC is a rapidly growing niche that is being explored through an intensive effort of clinicians, pharmacologists and material scientists. To date, IP therapy of PC has not become a standard of care. An important aspect to take into account when developing IP therapies is to retain anti-cancer agents as much as possible in the peritoneal cavity, to achieve maximal tumor exposure to the drug. NPs are being utilized to deliver drugs to the peritoneum, however, when administered as such in dispersion, rapid clearance to the systemic circulation hampers their biological activity. Therefore, to unravel the potential of nanomedicines for IP therapies, future research should focus on improving the biodistribution of nanomedicines in the peritoneum, and correlate it with tumor accumulation, penetration, and killing efficacy. The balance between these is not easy to achieve in the peritoneal cavity. On the one hand, the use of small nanomedicines (below 100 nm) would be very efficient for tumor penetration and maximizing drug efficacy. On the other hand, those small nanomedicines will highly likely be associated with a short residence time in the abdomen. In light of these limitations, it seems that injecting nanomedicines dispersed in a solvent will not be the optimal strategy for the treatment of PC. Nevertheless, to give a clear-cut answer whether the mission is possible with nanomedicines, in-depth investigation of the sustained release platforms described in this article, such as release of NPs from biodegradable hydrogels in the peritoneum and metronomic dosing is a prerequisite. Also, the identification and validation of tumor-specific targets will further help to develop targeting agents that increase tumor specificity of the nanomedicines. In addition, IP aerosol

delivery (PIPAC) of nanomedicines or (H)IPEC of NPs as an adjunct to surgery may hold promise in selected patients.

Acknowledgements

George Dakwar is a doctoral fellow at the Ghent Research Group on Nanomedicines. W.C. is a senior clinical investigator of the Fund for Scientific Research Flanders, (FWO). This work was supported by the FWO (grant No. G006714N) for G.D., K.R., S.D., and W.C.

References

[1] A.C. Society, Cancer Facts & Figures 2015, Atlanta: American Cancer Society, (2015).
[2] B. Sadeghi, C. Arvieux, O. Glehen, A.C. Beaujard, M. Rivoire, J. Baulieux, E. Fontaumard, A. Brachet, J.L. Caillot, J.L. Faure, J. Porcheron, J.L. Peix, Y. Francois, J. Vignal, F.N. Gilly, Peritoneal carcinomatosis from non-gynecologic malignancies - Results of the EVOCAPE 1 multicentric prospective study, Cancer, 88 (2000) 358-363.
[3] L. Bijelic, T.D. Yan, P.H. Sugarbaker, Failure analysis of recurrent disease following complete cytoreduction and Perioperative intraperitoneal chemotherapy in patients with peritoneal carcinomatosis from colorectal cancer, Annals of Surgical Oncology, 14 (2007) 2281-2288.
[4] G. Bajaj, Y. Yeo, Drug Delivery Systems for Intraperitoneal Therapy, Pharm Res, 27 (2010) 735-738.
[5] J. Esquivel, Current status of colorectal cancer with peritoneal carcinomatosis, Ann Surg Oncol, 17 (2010) 1968-1969.
[6] M.A. Baron, Structure of the intestinal peritoneum in man, American Journal of Anatomy, 69 (1941) 439-497.
[7] M.F. Flessner, The transport barrier in intraperitoneal therapy, Am J Physiol Renal Physiol, 288 (2005) F433-442.
[8] E. Kipps, D.S. Tan, S.B. Kaye, Meeting the challenge of ascites in ovarian cancer: new avenues for therapy and research, Nat Rev Cancer, 13 (2013) 273-282.
[9] D.R. Senger, Vascular Endothelial Growth Factor: Much More than an Angiogenesis Factor, Mol Biol Cell, 21 (2010) 377-379.
[10] D.R. Senger, S.J. Galli, A.M. Dvorak, C.A. Perruzzi, V.S. Harvey, H.F. Dvorak, Tumor-Cells Secrete a Vascular-Permeability Factor That Promotes Accumulation of Ascites-Fluid, Science, 219 (1983) 983-985.
[11] G.B. Feldman, R.C. Knapp, S.E. Order, S. Hellman, The role of lymphatic obstruction in the formation of ascites in a murine ovarian carcinoma, Cancer Res, 32 (1972) 1663-1666.
[12] M.F. Flessner, J.D. Fenstermacher, R.G. Blasberg, R.L. Dedrick, Peritoneal Absorption of Macromolecules Studied by Quantitative Autoradiography, Am J Physiol, 248 (1985) H26-H32.
[13] R.L. Dedrick, M.F. Flessner, Pharmacokinetic problems in peritoneal drug administration: Tissue penetration and surface exposure, J Natl Cancer I, 89 (1997) 480-487.
[14] R.L. Dedrick, C.E. Myers, P.M. Bungay, V.T. DeVita, Jr., Pharmacokinetic rationale for peritoneal drug administration in the treatment of ovarian cancer, Cancer Treat Rep, 62 (1978) 1-11.
[15] M. Markman, Strategies to examine new compounds for intraperitoneal use in ovarian cancer, Int J Gynecol Cancer, 18 (2008) 33-35.
[16] X.F. Li, S. Carlin, M. Urano, J. Russell, C.C. Ling, J.A. O'Donoghue, Visualization of hypoxia in microscopic tumors by immunofluorescent microscopy, Cancer Research, 67 (2007) 7646-7653.
[17] J.B. Wolinsky, Y.L. Colson, M.W. Grinstaff, Local drug delivery strategies for cancer treatment: Gels, nanoparticles, polymeric films, rods, and wafers, J Control Release, 159 (2012) 14-26.
[18] P. Jacquet, A. Averbach, O.A. Stuart, D. Chang, P.H. Sugarbaker, Hyperthermic intraperitoneal doxorubicin: pharmacokinetics, metabolism, and tissue distribution in a rat model, Cancer Chemoth Pharm, 41 (1998) 147-154.
[19] S. Harada, L. Ping, T. Obara, H. Oikawa, M. Miyata, M. Matsuo, T. Takahashi, T. Yanagisawa, The Antitumor Effect of Hyperthermia Combined with Fluorouracil and Its Analogs, Radiat Res, 142 (1995) 232-241.
[20] H.J. Kuh, S.H. Jang, M.G. Wientjes, J.R. Weaver, J.L.S. Au, Determinants of paclitaxel penetration and accumulation in human solid tumor, J Pharmacol Exp Ther, 290 (1999) 871-880.
[21] P.J.M. van de Vaart, N. van der Vange, F.A.N. Zoetmulder, A.R. van Goethem, O. van Tellingen, W.W.T. Huinink, J.H. Beijnen, H. Bartelink, A.C. Begg, Intraperitoneal cisplatin with regional hyperthermia in advanced ovarian cancer: Pharmacokinetics and cisplatin-DNA adduct formation in patients and ovarian cancer cell lines, Eur J Cancer, 34 (1998) 148-154.
[22] M. Markman, Intraperitoneal antineoplastic drug delivery: rationale and results, Lancet Oncol, 4 (2003) 277-283.
[23] M. Markman, J.L. Walker, Intraperitoneal chemotherapy of ovarian cancer: A review, with a focus on practical aspects of treatment, J Clin Oncol, 24 (2006) 988-994.
[24] J.S. Spratt, R.A. Adcock, M. Muskovin, W. Sherrill, J. McKeown, Clinical delivery system for intraperitoneal hyperthermic chemotherapy, Cancer Res, 40 (1980) 256-260.
[25] W.P. Ceelen, M.F. Flessner, Intraperitoneal therapy for peritoneal tumors: biophysics and clinical evidence, Nat Rev Clin Oncol, 7 (2010) 108-115.
[26] G. Los, P. Sminia, J. Wondergem, P.H. Mutsaers, J. Havemen, D. ten Bokkel Huinink, O. Smals, D. Gonzalez-Gonzalez, J.G. McVie, Optimisation of intraperitoneal cisplatin therapy with regional hyperthermia in rats, Eur J Cancer, 27 (1991) 472-477.
[27] E.A. Levine, J.H.t. Stewart, P. Shen, G.B. Russell, B.L. Loggie, K.I. Votanopoulos, Intraperitoneal chemotherapy for peritoneal surface malignancy: experience with 1,000 patients, J Am Coll Surg, 218 (2014) 573-585.

[28] K. Turaga, E. Levine, R. Barone, R. Sticca, N. Petrelli, L. Lambert, G. Nash, M. Morse, R. Adbel-Misih, H.R. Alexander, F. Attiyeh, D. Bartlett, A. Bastidas, T. Blazer, Q. Chu, K. Chung, L. Dominguez-Parra, N.J. Espat, J. Foster, K. Fournier, R. Garcia, M. Goodman, N. Hanna, L. Harrison, R. Hoefer, M. Holtzman, J. Kane, D. Labow, B. Li, A. Lowy, P. Mansfield, E. Ong, C. Pameijer, J. Pingpank, M. Quinones, R. Royal, G. Salti, A. Sardi, P. Shen, J. Skitzki, J. Spellman, J. Stewart, J. Esquivel, Consensus guidelines from The American Society of Peritoneal Surface Malignancies on standardizing the delivery of hyperthermic intraperitoneal chemotherapy (HIPEC) in colorectal cancer patients in the United States, Ann Surg Oncol, 21 (2014) 1501-1505.
[29] W. Solass, R. Kerb, T. Murdter, U. Giger-Pabst, D. Strumberg, C. Tempfer, J. Zieren, M. Schwab, M.A. Reymond, Intraperitoneal Chemotherapy of Peritoneal Carcinomatosis Using Pressurized Aerosol as an Alternative to Liquid Solution: First Evidence for Efficacy, Annals of Surgical Oncology, 21 (2014) 553-559.
[30] W. Solass, A. Hetzel, G. Nadiradze, E. Sagynaliev, M.A. Reymond, Description of a novel approach for intraperitoneal drug delivery and the related device, Surg Endosc, 26 (2012) 1849-1855.
[31] P. Esquis, D. Consolo, G. Magnin, P. Pointaire, P. Moretto, M.D. Ynsa, J.L. Beltramo, C. Drogoul, M. Simonet, L. Benoit, P. Rat, B. Chauffert, High intra-abdominal pressure enhances the penetration and antitumor effect of intraperitoneal cisplatin on experimental peritoneal carcinomatosis, Ann Surg, 244 (2006) 106-112.
[32] W. Solass, A. Herbette, T. Schwarz, A. Hetzel, J.S. Sun, M. Dutreix, M.A. Reymond, Therapeutic approach of human peritoneal carcinomatosis with Dbait in combination with capnoperitoneum: proof of concept, Surg Endosc, 26 (2012) 847-852.
[33] A. Blanco, U. Giger-Pabst, W. Solass, J. Zieren, M.A. Reymond, Renal and hepatic toxicities after pressurized intraperitoneal aerosol chemotherapy (PIPAC), Ann Surg Oncol, 20 (2013) 2311-2316.
[34] A.R. Marc, W. Solass, C. Tempfer, Pressurized intraperitoneal aerosol chemotherapy (PIPAC), Intraperitoneal Cancer Therapy, CRC Press2015, pp. 389-402.
[35] C.B. Tempfer, G.A. Rezniczek, P. Ende, W. Solass, M.A. Reymond, Pressurized Intraperitoneal Aerosol Chemotherapy with Cisplatin and Doxorubicin in Women with Peritoneal Carcinomatosis: A Cohort Study, Anticancer Res, 35 (2015) 6723-6729.
[36] C. Demtroder, W. Solass, J. Zieren, D. Strumberg, U. Giger-Pabst, M.A. Reymond, Pressurized intraperitoneal aerosol chemotherapy with oxaliplatin in colorectal peritoneal metastasis, Colorectal Dis, 18 (2016) 364-371.
[37] G. Nadiradze, U. Giger-Pabst, J. Zieren, D. Strumberg, W. Solass, M.A. Reymond, Pressurized Intraperitoneal Aerosol Chemotherapy (PIPAC) with Low-Dose Cisplatin and Doxorubicin in Gastric Peritoneal Metastasis, J Gastrointest Surg, 20 (2016) 367-373.
[38] H.J. Braam, T.R. Van Oudheusden, I.H.J.T. De Hingh, S.W. Nienhuijs, D. Boerma, M.J. Wiezer, B. Van Ramshorst, Patterns of recurrence following complete cytoreductive surgery and hyperthermic intraperitoneal chemotherapy in patients with peritoneal carcinomatosis of colorectal cancer, J Surg Oncol, 109 (2014) 841-847.
[39] P.H. Sugarbaker, Update on the prevention of local recurrence and peritoneal metastases in patients with colorectal cancer, World J Gastroenterol, 20 (2014) 9286-9291.
[40] P.E. Colombo, M. Boustta, S. Poujol, M. Jarlier, F. Bressolle, I. Teulon, M.Z. Ladjemi, F. Pinguet, P. Rouanet, M. Vert, Intraperitoneal administration of novel doxorubicin loaded polymeric delivery systems against peritoneal carcinomatosis: Experimental study in a murine model of ovarian cancer, Gynecologic Oncology, 122 (2011) 632-640.
[41] K.J. Cho, X. Wang, S.M. Nie, Z. Chen, D.M. Shin, Therapeutic nanoparticles for drug delivery in cancer, Clin Cancer Res, 14 (2008) 1310-1316.
[42] A.Z. Wang, R. Langer, O.C. Farokhzad, Nanoparticle Delivery of Cancer Drugs, Annu Rev Med, 63 (2012) 185-198.
[43] T.M. Allen, P.R. Cullis, Liposomal drug delivery systems: From concept to clinical applications, Adv Drug Deliver Rev, 65 (2013) 36-48.
[44] F. Danhier, E. Ansorena, J.M. Silva, R. Coco, A. Le Breton, V. Preat, PLGA-based nanoparticles: An overview of biomedical applications, J Control Release, 161 (2012) 505-522.
[45] M.L. Etheridge, S.A. Campbell, A.G. Erdman, C.L. Haynes, S.M. Wolf, J. McCullough, The big picture on nanomedicine: the state of investigational and approved nanomedicine products, Nanomed-Nanotechnol, 9 (2013) 1-14.
[46] L. Bregoli, D. Movia, J.D. Gavigan-Imedio, J. Lysaght, J. Reynolds, A. Prina-Mello, Nanomedicine applied to translational oncology: A future perspective on cancer treatment, Nanomed-Nanotechnol, 12 (2016) 81-103.
[47] Z. Lu, J. Wang, M.G. Wientjes, J.L.S. Au, Intraperitoneal therapy for peritoneal cancer, Future Oncol, 6 (2010) 1625-1641.
[48] J. Tomasina, S. Lheureux, P. Gauduchon, S. Rault, A. Malzert-Freon, Nanocarriers for the targeted treatment of ovarian cancers, Biomaterials, 34 (2013) 1073-1101.
[49] T.R. van Oudheusden, H. Grull, P.Y.W. Dankers, I.H.J.T. de Hingh, Targeting the Peritoneum with Novel Drug Delivery Systems in Peritoneal Carcinomatosis: A Review of the Literature, Anticancer Research, 35 (2015) 627-634.

[50] R.D. George, S.C.D.S. Stefaan, R. Katrien, Intraperitoneal nonviral nucleic acid delivery in the treatment of peritoneal cancer, Intraperitoneal Cancer Therapy, CRC Press2015, pp. 359-371.
[51] G.R. Dakwar, K. Braeckmans, J. Demeester, W. Ceelen, S.C. De Smedt, K. Remaut, Disregarded Effect of Biological Fluids in siRNA Delivery: Human Ascites Fluid Severely Restricts Cellular Uptake of Nanoparticles, Acs Appl Mater Inter, 7 (2015) 24322-24329.
[52] M. Hadjidemetriou, Z. Al-Ahmady, M. Mazza, R.F. Collins, K. Dawson, K. Kostarelos, In Vivo Biomolecule Corona around Blood-Circulating, Clinically Used and Antibody-Targeted Lipid Bilayer Nanoscale Vesicles, Acs Nano, 9 (2015) 8142-8156.
[53] Z.H. Liu, Y.P. Jiao, T. Wang, Y.M. Zhang, W. Xue, Interactions between solubilized polymer molecules and blood components, J Control Release, 160 (2012) 14-24.
[54] A. Salvati, A.S. Pitek, M.P. Monopoli, K. Prapainop, F.B. Bombelli, D.R. Hristov, P.M. Kelly, C. Aberg, E. Mahon, K.A. Dawson, Transferrin-functionalized nanoparticles lose their targeting capabilities when a biomolecule corona adsorbs on the surface, Nat Nanotechnol, 8 (2013) 137-143.
[55] C.D. Walkey, W.C.W. Chan, Understanding and controlling the interaction of nanomaterials with proteins in a physiological environment, Chem Soc Rev, 41 (2012) 2780-2799.
[56] D. Zhong, Y.P. Jiao, Y. Zhang, W. Zhang, N. Li, Q.H. Zuo, Q. Wang, W. Xue, Z.H. Liu, Effects of the gene carrier polyethyleneimines on structure and function of blood components, Biomaterials, 34 (2013) 294-305.
[57] G.R. Dakwar, E. Zagato, J. Delanghe, S. Hobel, A. Aigner, H. Denys, K. Braeckmans, W. Ceelen, F.C. De Smedt, K. Remaut, Colloidal stability of nano-sized particles in the peritoneal fluid: Towards optimizing drug delivery systems for intraperitoneal therapy, Acta Biomater, 10 (2014) 2965-2975.
[58] J.I. Hare, T. Lammers, M.B. Ashford, S. Puri, G. Storm, S.T. Barry, Challenges and strategies in anti-cancer nanomedicine development: An industry perspective, Adv Drug Deliv Rev, (2016).
[59] T. Lammers, F. Kiessling, W.E. Hennink, G. Storm, Drug targeting to tumors: Principles, pitfalls and (pre-) clinical progress, J Control Release, 161 (2012) 175-187.
[60] K. Yang, H. Gong, X.Z. Shi, J.M. Wan, Y.J. Zhang, Z. Liu, In vivo biodistribution and toxicology of functionalized nano-graphene oxide in mice after oral and intraperitoneal administration, Biomaterials, 34 (2013) 2787-2795.
[61] D.S. Kohane, J.Y. Tse, Y. Yeo, R. Padera, M. Shubina, R. Langer, Biodegradable polymeric microspheres and nanospheres for drug delivery in the peritoneum, J Biomed Mater Res A, 77a (2006) 351-361.
[62] M. Tsai, Z. Lu, J. Wang, T.K. Yeh, M.G. Wientjes, J.L.S. Au, Effects of carrier on disposition and antitumor activity of intraperitoneal paclitaxel, Pharm Res, 24 (2007) 1691-1701.
[63] K. Hirano, C.A. Hunt, Lymphatic transport of liposome-encapsulated agents: effects of liposome size following intraperitoneal administration, J Pharm Sci, 74 (1985) 915-921.
[64] Y. Sadzuka, S. Hirota, T. Sonobe, Intraperitoneal administration of doxorubicin encapsulating liposomes against peritoneal dissemination, Toxicol Lett, 116 (2000) 51-59.
[65] N. Mirahmadi, M.H. Babaei, A.M. Vali, S. Dadashzadeh, Effect of liposome size on peritoneal retention and organ distribution after intraperitoneal injection in mice, Int J Pharmaceut, 383 (2010) 7-13.
[66] S. Dadashzadeh, N. Mirahmadi, M.H. Babaei, A.M. Vali, Peritoneal retention of liposomes: Effects of lipid composition, PEG coating and liposome charge, J Control Release, 148 (2010) 177-186.
[67] W.J. Shih, J.J. Coupal, H.L. Chia, Communication between peritoneal cavity and mediastinal lymph nodes demonstrated by Tc-99m albumin nanocolloid intraperitoneal injection, Proc Natl Sci Counc Repub China B, 17 (1993) 103-105.
[68] P. Maincent, P. Thouvenot, C. Amicabile, M. Hoffman, J. Kreuter, P. Couvreur, J.P. Devissaguet, Lymphatic Targeting of Polymeric Nanoparticles after Intraperitoneal Administration in Rats, Pharm Res, 9 (1992) 1534-1539.
[69] Z. Lu, M. Tsai, D. Lu, J. Wang, M.G. Wientjes, J.L.S. Au, Tumor-Penetrating Microparticles for Intraperitoneal Therapy of Ovarian Cancer, J Pharmacol Exp Ther, 327 (2008) 673-682.
[70] F. Ramazani, C.F. van Nostrum, G. Storm, F. Kiessling, T. Lammers, W.E. Hennink, R.J. Kok, Locoregional cancer therapy using polymer-based drug depots, Drug Discov Today, 21 (2016) 640-647.
[71] D.S. Kohane, R. Langer, Biocompatibility and drug delivery systems, Chem Sci, 1 (2010) 441-446.
[72] J.L.S. Au, Z. Lu, M.G. Wientjes, Versatility of Particulate Carriers: Development of Pharmacodynamically Optimized Drug-Loaded Microparticles for Treatment of Peritoneal Cancer, Aaps J, 17 (2015) 1065-1079.
[73] A.I. Minchinton, I.F. Tannock, Drug penetration in solid tumours, Nat Rev Cancer, 6 (2006) 583-592.
[74] A.A. Manzoor, L.H. Lindner, C.D. Landon, J.Y. Park, A.J. Simnick, M.R. Dreher, S. Das, G. Hanna, W. Park, A. Chilkoti, G.A. Koning, T.L.M. ten Hagen, D. Needham, M.W. Dewhirst, Overcoming Limitations in Nanoparticle Drug Delivery: Triggered, Intravascular Release to Improve Drug Penetration into Tumors, Cancer Research, 72 (2012) 5566-5575.
[75] C.H. Heldin, K. Rubin, K. Pietras, A. Ostman, High interstitial fluid pressure - An obstacle in cancer therapy, Nature Reviews Cancer, 4 (2004) 806-813.
[76] M.J. Ernsting, M. Murakami, A. Roy, S.-D. Li, Factors controlling the pharmacokinetics, biodistribution and intratumoral penetration of nanoparticles, J Control Release, 172 (2013) 782-794.
[77] S. Huo, H. Ma, K. Huang, J. Liu, T. Wei, S. Jin, J. Zhang, S. He, X.J. Liang, Superior penetration and retention behavior of 50 nm gold nanoparticles in tumors, Cancer Res, 73 (2013) 319-330.

[78] H.-X. Wang, Z.-Q. Zuo, J.-Z. Du, Y.-C. Wang, R. Sun, Z.-T. Cao, X.-D. Ye, J.-L. Wang, K.W. Leong, J. Wang, Surface charge critically affects tumor penetration and therapeutic efficacy of cancer nanomedicines, Nano Today.
[79] D. Ding, Z.S. Zhu, Q. Liu, J. Wang, Y. Hu, X.Q. Jiang, B.R. Liu, Cisplatin-loaded gelatin-poly(acrylic acid) nanoparticles: Synthesis, antitumor efficiency in vivo and penetration in tumors, European Journal of Pharmaceutics and Biopharmaceutics, 79 (2011) 142-149.
[80] C. Pegoraro, D. Cecchin, L.S. Gracia, N. Warren, J. Madsen, S.P. Armes, A. Lewis, S. MacNeil, G. Battaglia, Enhanced drug delivery to melanoma cells using PMPC-PDPA polymersomes, Cancer Lett, 334 (2013) 328-337.
[81] L. Messager, J. Gaitzsch, L. Chierico, G. Battaglia, Novel aspects of encapsulation and delivery using polymersomes, Curr Opin Pharmacol, 18 (2014) 104-111.
[82] L. Simon-Gracia, H. Hunt, P.D. Scodeller, J. Gaitzsch, G.B. Braun, A.M.A. Willmore, E. Ruoslahti, G. Battaglia, T. Teesalu, Paclitaxel-Loaded Polymersomes for Enhanced Intraperitoneal Chemotherapy, Mol Cancer Ther, 15 (2016) 670-679.
[83] F. Gremonprez, B. Descamps, A. Izmer, C. Vanhove, F. Vanhaecke, O. De Wever, W. Ceelen, Pretreatment with VEGF(R)-inhibitors reduces interstitial fluid pressure, increases intraperitoneal chemotherapy drug penetration, and impedes tumor growth in a mouse colorectal carcinomatosis model, Oncotarget, 6 (2015) 29889-29900.
[84] M.H. Pourgholami, Z. Yan Cai, Y. Lu, L. Wang, D.L. Morris, Albendazole: a potent inhibitor of vascular endothelial growth factor and malignant ascites formation in OVCAR-3 tumor-bearing nude mice, Clin Cancer Res, 12 (2006) 1928-1935.
[85] L. Noorani, M. Stenzel, R. Liang, M.H. Pourgholami, D.L. Morris, Albumin nanoparticles increase the anticancer efficacy of albendazole in ovarian cancer xenograft model, J Nanobiotechnol, 13 (2015).
[86] E.J. Cho, B. Sun, K.O. Doh, E.M. Wilson, S. Torregrosa-Allen, B.D. Elzey, Y. Yeo, Intraperitoneal delivery of platinum with in-situ crosslinkable hyaluronic acid gel for local therapy of ovarian cancer, Biomaterials, 37 (2015) 312-319.
[87] B. Sun, M.S. Taha, B. Ramsey, S. Torregrosa-Allen, B.D. Elzey, Y. Yeo, Intraperitoneal chemotherapy of ovarian cancer by hydrogel depot of paclitaxel nanocrystals, J Control Release, 235 (2016) 91-98.
[88] C. Hasovits, S. Clarke, Pharmacokinetics and Pharmacodynamics of Intraperitoneal Cancer Chemotherapeutics, Clin Pharmacokinet, 51 (2012) 203-224.
[89] M. Markman, Intraperitoneal Chemotherapy, Semin Oncol, 18 (1991) 248-254.
[90] G. Los, E.M.E. Verdegaal, P.H.A. Mutsaers, J.G. Mcvie, Penetration of Carboplatin and Cisplatin into Rat Peritoneal Tumor Nodules after Intraperitoneal Chemotherapy, Cancer Chemoth Pharm, 28 (1991) 159-165.
[91] R. Fan, A. Tong, X. Li, X. Gao, L. Mei, L. Zhou, X. Zhang, C. You, G. Guo, Enhanced antitumor effects by docetaxel/LL37-loaded thermosensitive hydrogel nanoparticles in peritoneal carcinomatosis of colorectal cancer, Int J Nanomedicine, 10 (2015) 7291-7305.
[92] S. Xu, H. Fan, L. Yin, J. Zhang, A. Dong, L. Deng, H. Tang, Thermosensitive hydrogel system assembled by PTX-loaded copolymer nanoparticles for sustained intraperitoneal chemotherapy of peritoneal carcinomatosis, European Journal of Pharmaceutics and Biopharmaceutics.
[93] W.W. Wang, L.D. Deng, S.X. Xu, X.M. Zhao, N. Lv, G.X. Zhang, N. Gu, R.J. Hu, J.H. Zhang, J.J. Liu, A.J. Dong, A reconstituted "two into one" thermosensitive hydrogel system assembled by drug-loaded amphiphilic copolymer nanoparticles for the local delivery of paclitaxel, J Mater Chem B, 1 (2013) 552-563.
[94] M. Nowacki, M. Wisniewski, K. Werengowska-Ciecwierz, K. Roszek, J. Czarnecka, I. Lakomska, T. Kloskowski, D. Tyloch, R. Debski, K. Pietkun, M. Pokrywczynska, D. Grzanka, R. Czajkowski, G. Drewa, A. Jundzill, J.K. Agyin, S.L. Habib, A.P. Terzyk, T. Drewa, Nanovehicles as a novel target strategy for hyperthermic intraperitoneal chemotherapy: a multidisciplinary study of peritoneal carcinomatosis, Oncotarget, 6 (2015) 22776-22798.
[95] S. Marchesan, K. Kostarelos, A. Bianco, M. Prato, The winding road for carbon nanotubes in nanomedicine, Mater Today, 18 (2015).
[96] L. De Smet, P. Colin, W. Ceelen, M. Bracke, J. Van Bocxlaer, J.P. Remon, C. Vervaet, Development of a Nanocrystalline Paclitaxel Formulation for Hipec Treatment, Pharm Res, 29 (2012) 2398-2406.
[97] C. Holohan, S. Van Schaeybroeck, D.B. Longley, P.G. Johnston, Cancer drug resistance: an evolving paradigm, Nature Reviews Cancer, 13 (2013) 714-726.
[98] N. Andre, M. Carre, E. Pasquier, Metronomics: towards personalized chemotherapy?, Nat Rev Clin Oncol, 11 (2014) 413-431.
[99] Z. Amoozgar, L. Wang, T. Brandstoetter, S.S. Wallis, E.M. Wilson, M.S. Goldberg, Dual-layer surface coating of PLGA-based nanoparticles provides slow-release drug delivery to achieve metronomic therapy in a paclitaxel-resistant murine ovarian cancer model, Biomacromolecules, 15 (2014) 4187-4194.
[100] K.M. Gharpure, K.S. Chu, C.J. Bowerman, T. Miyake, S. Pradeep, S.L. Mangala, H.D. Han, R. Rupaimoole, G.N. Armaiz-Pena, T.B. Rahhal, S.Y. Wu, J.C. Luft, M.E. Napier, G. Lopez-Berestein, J.M. DeSimone, A.K. Sood, Metronomic Docetaxel in PRINT Nanoparticles and EZH2 Silencing Have Synergistic Antitumor Effect in Ovarian Cancer, Mol Cancer Ther, 13 (2014) 1750-1757.
[101] G.M. van Dam, G. Themelis, L.M.A. Crane, N.J. Harlaar, R.G. Pleijhuis, W. Kelder, A. Sarantopoulos, J.S. de Jong, H.J.G. Arts, A.G.J. van der Zee, J. Bart, P.S. Low, V. Ntziachristos, Intraoperative tumor-specific

fluorescence imaging in ovarian cancer by folate receptor-alpha targeting: first in-human results, Nat Med, 17 (2011) 1315-U1202.
[102] A.G.T.T. van Scheltinga, G.M. van Dam, W.B. Nagengast, V. Ntziachristos, H. Hollema, J.L. Herek, C.P. Schroder, J.G.W. Kosterink, M.N. Lub-de Hoog, E.G.E. de Vries, Intraoperative Near-Infrared Fluorescence Tumor Imaging with Vascular Endothelial Growth Factor and Human Epidermal Growth Factor Receptor 2 Targeting Antibodies, J Nucl Med, 52 (2011) 1778-1785.
[103] A. Cirstoiu-Hapca, F. Buchegger, N. Lange, L. Bossy, R. Gurny, F. Delie, Benefit of anti-HER2-coated paclitaxel-loaded immuno-nanoparticles in the treatment of disseminated ovarian cancer: Therapeutic efficacy and biodistribution in mice, J Control Release, 144 (2010) 324-331.
[104] J. McLachlan, J.P.D.N. Lima, L. Dumas, S. Banerjee, Targeted agents and combinations in ovarian cancer: where are we now?, Expert Rev Anticanc, 16 (2016) 441-454.
[105] S.K. Williamson, G.A. Johnson, H.A. Maulhardt, K.M. Moore, D.S. McMeekin, T.K. Schulz, G.A. Reed, K.F. Roby, C.B. Mackay, H.J. Smith, S.J. Weir, J.A. Wick, M. Markman, G.S. diZerega, M.J. Baltezor, J. Espinosa, C.J. Decedue, A phase I study of intraperitoneal nanoparticulate paclitaxel (Nanotax(R)) in patients with peritoneal malignancies, Cancer Chemother Pharmacol, 75 (2015) 1075-1087.
[106] A. Moreno-Aspitia, E.A. Perez, Nanoparticle albumin-bound paclitaxel (ABI-007): a newer taxane alternative in breast cancer, Future Oncol, 1 (2005) 755-762.
[107] M.C. Cristea, T.W. Synold, P.H. Frankel, S.E. Rivkin, D. Lim, V.M. Chung, J. Chao, M.T. Wakabayashi, I.B. Paz, E.S. Han, P. Lin, L.A. Leong, A. Hakim, M.I. Carroll, H. Openshaw, N. Prakash, T.H. Dellinger, M.S. Park, R. Morgan, Pharmacologic advantage (PA) of intraperitoneal (IP) nab-paclitaxel in patients with advanced malignancies primarily confined to the peritoneal cavity., J Clin Oncol, 33 (2015).

2

INTRAPERITONEAL NONVIRAL NUCLEIC ACID DELIVERY IN THE TREATMENT OF PERITONEAL CANCER

Parts of this chapter are published as:

George R. Dakwar[1], Stefaan C. De Smedt[1], Katrien Remaut[1], Intraperitoneal nonviral nucleic acid delivery in the treatment of peritoneal cancer. Intraperitoneal Cancer Therapy: Principles and Practice, CRC Press Taylor & Francis, 359-371 (2015).

[1] Ghent Research Group on Nanomedicines, Faculty of Pharmaceutical Sciences, Laboratory for General Biochemistry and Physical Pharmacy, Ghent University, Ghent, Belgium

1. Introduction

Peritoneal carcinomatosis (PC) is a secondary cancer in the peritoneal cavity that originates from gynaecological or non-gynaecological organs. Due to the late stage of discovery, these peritoneal metastasis are often widely spread in the peritoneal cavity and difficult to treat. Current treatment is based on cytoreductive surgery followed by intravenous (IV) administration of conventional chemotherapeutic agents. However, complete surgical removal is often not possible. Also, remaining tumor cells can spread and lead to the formation of new metastasis. Therefore, the majority of the patients unfortunately develop disease recurrence and relapse. Intraperitoneal (IP) administration has shown several advantages over the IV one, due to the ability to inject higher concentrations of anti-cancer agents into the site of action (i.e. the peritoneal cavity), with limited systemic side effects [1]. Also here, however, the IP administration of cytostatics suffers from the fact that the action of the currently used cytostatics is not tumor-specific and not long-lasting.

The rapid progress that has been made during the last 20 years in medical sciences led to the development of new strategies in the treatment of cancer [2,3]. Gene therapy, for example, enables to specifically express or silence genes, thereby minimizing side effects which are often observed with the conventional chemotherapy. Given this, IP gene therapy is an attractive strategy to target tumors within the peritoneal cavity, taking advantage of the direct administration to the tumor site, and also the selectivity that could be achieved in gene targeting. Therefore, IP nucleic acid delivery could prove to be useful to specifically target the metastases in the peritoneum. In this chapter we will provide a brief introduction on the delivery of nucleic acids into tumor cells confined within the peritoneal cavity, with a focus on the mechanism of action of lipidic and polymeric carriers that have been administered intraperitoneally. It should be noted that none of these delivery systems has received FDA approval yet.

2. Delivery of nucleic acids for the treatment of PC

2.1 Plasmid DNA

Plasmid DNA is a powerful tool to induce the expression of proteins, and offers great opportunities for cancer treatment. Plasmids are circular, double stranded DNA molecules that can be engineered to carry any gene of interest and can range between 1 to 1000 kilo base pair (kbp) in size. The rational beyond using DNA as a therapeutic agent is to take advantage of the body's cell machinery to produce the encoded proteins at the site of action, thereby overcoming the need to produce and repeatedly administer highly purified proteins [4]. Generally speaking, the encoded proteins that result from the expression of a therapeutic gene can act either on intracellular targets, or extracellular when the formed proteins are released outside the cells and act on neighboring or distant cells [5]. In most applications using non-viral gene delivery, the resulting

gene expression is transient (e.g. limited in function of time). Alternatively, stable long-lasting gene expression can be obtained when a mutated gene is replaced with the wild type one.

To ensure biological activity of DNA-based therapeutics, the genetic material should enter the nucleus of the target cell, and later on be transcribed into messenger RNA (mRNA) and translated into active protein. There are however several barriers for the delivery of DNA into cells, which will be discussed later in this chapter.

2.1.1 DNA for cancer therapy

The use of DNA for cancer therapy can be accomplished by targeting tumor cells directly or indirectly. Direct targeting includes the expression of tumor suppressors and the delivery of suicide genes. Tumor suppressor genes control the cell division rate of normal cells, preventing them to divide excessively and form tumor tissue. Cancer cells carrying mutated tumor suppression genes can be treated by the DNA induced expression of correct tumor suppressor genes, resulting in cell cycle arrest or death. The most common tumor suppressors are P53, PTEN, ARF and APC [6-9]. Also the delivery of suicide genes is being used to specifically kill cancer cells. Once delivered into the nucleus of cancer cells, suicide genes encode for enzymes that allow to metabolize a prodrug into a cytotoxin which is capable of diffusing into neighboring cells. Suicide genes can also directly encode for toxins, such as for example the diphtheria toxin A (DT-A), which inhibits protein synthesis thereby causing cell death. Indirect strategies include immunotherapy and chemoprotection. Chemoprotection is a process by which bone marrow cells are infected with viruses that protect them from the toxic effects of chemotherapy [10]. Immunotherapy aims to activate a local and systemic immune response against cancer cells, and is thought to be the least toxic approach in cancer therapy [11,12]. As an example for immunotherapy, genes encoding for anti-inflammatory cytokines can be incorporated into plasmid DNA (pDNA) and delivered into tumor microenvironment to enhance the immune response against cancer cells [13]. Alternatively, dendritic cells can be challenged with tumor specific antigens, after which they activate the immune system to specifically target the tumor cells where the antigens were derived from. Finally, plasmid DNA can also be used as a precursor to form short hairpin RNA (shRNAs) that can be processed by the cell to small interfering RNA (siRNA). Unlike pDNA, siRNA is used to downregulate the expression of the target proteins, in a process called RNA interference (RNAi) as will be discussed below.

2.2 RNAi

In 1998, Fire and Mello reported the discovery of double-stranded RNA (dsRNA) which is capable to knockdown gene activity [14]. Small interfering RNA (siRNA) is a 21-23 nucleotide double stranded RNA that binds to a complementary mRNA sequence in the cytoplasm of cells, causing degradation of the desired mRNA, and consequently a decrease in the expression of the corresponding protein [15]. In principle, siRNA can be designed to be complementary for any mRNA sequence. For cancer applications, genes involved in apoptotic and proliferative pathways are subject to silencing in order to treat tumors that are resistant to chemotherapy or nonresectable tumors [16]. Currently, several RNAi-based drugs are in clinical trials, including treatments against solid tumors and advanced cancer [17]. As mentioned above, another type of RNAi uses shRNAs which are synthesized in living cells after the delivery of plasmids or viral or bacterial vectors into cells encoding for these shRNAs [18]. shRNAs consist of two complementary 19-22 (bp) RNA sequences linked by a short loop, which is similar in structure to the natural microRNA (miRNA), and are processed intracellular into functional siRNA.

2.2.1 RNAi for cancer therapy

The last two decades have witnessed a revolution in genomics and proteomics during which tens of molecular pathways involved in proliferation of cancer cells were identified. These include immune evasion, angiogenesis, and metastasis. Theoretically, knockdown of every gene should be possible, however, for successful and specific gene knockdown it is important to screen targets that are over-expressed by cancer cells. As we will discuss later in section 4, RNAi opens the opportunity for designing personalized medicine [19], since it can influence the expression or knockdown of a specific gene in a particular cancer patient. To date, the most common RNAi targets related to cancer are the multidrug resistance (MDR) proteins [20]. MDR is a situation in which cancer cells develop resistance against anticancer drugs by several mechanisms such as decreased drug uptake, increased drug efflux, and induction of DNA repair mechanisms. For instance, P-glycoprotein (P-gp) is a transporter protein encoded by the MDR-1 gene that pump drugs into the extracellular space before reaching the target. It has been shown that P-gp is over-expressed in several cancer types following chemotherapeutic treatment, making it an attractive target for RNAi [21]. Another common example of MDR encoded protein is survivin, a member of the inhibitor of apoptosis (IAP) protein family, since it is up-regulated in solid tumors and has been involved with drug resistance [22,23]. Recently, co-delivery of conventional anti-cancer chemotherapeutics and siRNA has received tremendous attention to overcome cancer resistance [24].

2.3 Mechanisms of DNA and RNAi

The aim of DNA therapy is to bring wild type genes into the nucleus of cells or to correct mutated genes. The second requires a process called homologous recombination by which new exogenously administered DNA sequences can be introduced into the genome of a living cell [25]. Homologous recombination is considered a rare event, therefore most of the DNA therapies are based on transient delivery of the DNA sequence into the nucleus. Once in the nucleus, the DNA can be transcribed into mRNA, which relocates to the cytoplasm where it is translated into the corresponding proteins (Figure 1C, step 8). The extent by which the delivered gene is expressed depends on the number of DNA copies being transcribed. It has been suggested that the minimum number of copies required to measure gene expression ranges from 75 to 4000 [26,27]. For RNAi medicines, however, the site of action is the cytoplasm of the cell. Briefly, in the cytoplasm of the cell, a protein complex known as RNA-induced silencing complex (RISC) mediates the cleavage of one RNA strand, while the other guide-strand is involved in degrading the targeted mRNA (Figure 1B, step 5, 6 and 7). Double stranded siRNAs can be produced endogenously (by cells) or chemically synthesized and applied. Exogenously administered RNA can either interact with the RISC complex immediately as double strand or after cleavage by an enzyme known as RNAse III Dicer [28]. The mechanism by which shRNA is processed within the cells is very similar to that of siRNA. Shortly, after its transcription in the nucleus, it is exported to the cytosol where it interacts with Dicer, which in turn converts shRNA into siRNA and binds to the RICS complex as described above [29].

Naked nucleic acids suffer from instability and are prone to enzymatic degradation in the biological environment. Moreover, naked nucleic acids are rapidly excreted by kidney filtration, and are not able to interact with biological membranes due to their anionic charge. Hence, naked nucleic acids suffer from low transfection efficiency [30,31] and are complexed with viral or non-viral carriers to optimize their cellular delivery, as discussed below.

2.4 Viral and non-viral vectors for nucleic acids delivery

Viruses are infectious agents that can internalize into the host cell and take advantage of its cellular machinery to replicate its own genetic material and to infect other cells [32]. Different viruses have been exploited to deliver therapeutic DNA and siRNA into cells [33,34]. Importantly, viruses are genetically modified before their use *in vivo*, by removing the pathogenic part and replacing it with the desired therapeutic nucleic acid [35], without changing its structural properties and ability to infect other cells [32]. The non-pathogenic virus is then called a viral vector and can be used for *in vivo* transfection. Despite their high transfection efficiency [33], several limitations have been reported when viral vectors were used. First of all, acute immune response and toxicity continue to be a major concern for viral vectors [35]. Also, viral vectors are generally produced in small quantities and scaling up the process would come with a large cost

[36,37]. Finally, due to size limitations of the viral vectors, not all genes can be carried by the virus [35].

The drawbacks of viral vectors made scientists think of other safer and possibly cheaper alternatives. Over the past decade, non-viral vectors have been widely investigated for DNA and siRNA delivery into cells both *in vitro* and *in vivo*. In this respect, non-viral vectors possess several advantages over their viral counterparts. They are relatively safe, and do not induce a strong immune response. Also, they can be more easily prepared in large quantities [38,39]. Nevertheless, the application of non-viral nucleic acid delivery systems is still limited due to low cellular uptake and poor transfection efficiency [36].

Most non-viral nucleic acid delivery systems are based on polymeric or lipid nano-sized carriers. Nanotechnology in general and nano-based drug delivery in particular, have played a vital role in cancer therapy [40-42]. The ultimate goal for non-viral nucleic acid delivery systems is to obtain site-specific delivery of therapeutic nucleic acids, and release these nucleic acids in a controlled fashion, in order to maximize the treatment efficacy while minimizing side effects [43,44]. It has been shown that complexation or encapsulation of nucleic acids with lipid-based or polymer-based nanoparticles significantly enhances their uptake into tumor cells. In the majority of the cases, negatively charged nucleic acids are added to positively charged lipid or polymer particles, taking advantage of the electrostatic interactions to form liposome/nucleic acid complexes (LPXs) or polymer/nucleic acid complexes (polyplexes). These complexes generally have a positive charge and a size range between 80 – 600 nm.

2.5 Barriers for IP DNA and siRNA delivery

Clinical applications of non-viral DNA and siRNA carriers are still hampered by inefficient *in vivo* delivery. To obtain the desired therapeutic effect of nucleic acids, several extra- and intracellular barriers should be overcome, which will largely depend on the administration route of the complexes.

For efficacious IP nucleic acid delivery, non-viral vectors should meet several requirements on both the extracellular (Figure 1A) and intracellular (Figure 1B and C) level. Following IP administration, non-viral vectors are present in the peritoneal fluid. Hence, they should remain stable in this IP fluid until the target cells are reached (Figure 1A, step 1). Non-viral vectors can however interact with components of the peritoneal fluid, especially proteins. This potentially leads to: (1) aggregation of the vectors (Figure 1A, step 3) and (2) pre-mature release of the cargo (i.e. nucleic acid) (Figure 1A, step 2), which results in the loss of transfection efficiency [45]. In this regard, the stability of different nano-sized particles should be studied in the extracellular fluids they will reside in, namely the peritoneal fluid in the case of IP delivery [45]. Also the ascites fluid is being investigated to understand and develop different clinical strategies for the treatment of peritoneal

cancer [46]. Ideally, non-viral vectors should protect nucleic acids from interaction with different molecules in the biological fluids without inducing immune responses [47]. Extracellular stability is a prerequisite to ensure interaction of the non-viral vectors with biological membranes of cells, which is essential towards reaching the site of action and to ensure good intracellular uptake. To enhance extracellular stability, carriers are often grafted with polyethylene glycol (PEG) chains to minimize binding of proteins, thereby preventing aggregation and recognition by the mononuclear phagocyte system (MPS). However, PEGylation has several disadvantages, especially on the intracellular level. It is known that the PEG chains can limit the interaction of carriers with intracellular organelles, such as the endosomal membrane. This on its turn prevents or seriously lowers endosomal escape of the carriers and thus the amount of nucleic acids that can be successfully delivered [48]. Also, we have shown that PEGylation may interfere with the electrostatic interactions formed between the negatively charged nucleic acid and the positively charged carrier, resulting in a more rapid pre-mature release of the cargo in the biological fluid [45]. It is therefore clear that a good balance should be reached between extracellular stability of the carriers and the ability to still efficiently deliver the nucleic acids in the intracellular environment. Also, carriers intended for IP delivery, should remain in the peritoneum for a sufficient long time, without relocation to the blood stream (Figure 1A, step 4). Which physicochemical properties are best to prevent leakage from the nanocarriers through the peritoneal/plasma barrier remains to be elucidated.

Once a carrier has reached its target cell, it should enter the cells, which mostly occurs through endocytosis (Figure 1B and C step 1). Following uptake by cells via endocytosis, delivery vectors are present in the early endosome (Figure 1B and C, step 2), which mature to late endosome and eventually deliver their content to lysosomes. To avoid degradation in the lysosomal compartment (Figure 1B and C, step 3), the delivery vector needs to destabilize the endosomal membrane, leading to the release of the cargo into the cytoplasm of the cell, in a process which is known as endosomal escape (Figure 1B and C, step 4) [49]. It is often argued that endosomal escape is the most critical step in nucleic acid delivery. In the case of siRNA delivery, the cytoplasm is the intracellular site where the RISC machinery can be engaged (Figure 1B, step 5) and eventually, recognize the target mRNA leading to its degradation (Figure 1B, step 6 and 7). DNA vectors, however, have to efficiently migrate through the cytoplasm of the cell towards the nucleus in addition to the endosomal escape (Figure 1C, step 5). Then, crossing the nuclear membrane is required for DNA to be transcribed (Figure 1C, step 7) and translated (Figure 1C, step 8) into the encoded proteins [50,51]. It is generally accepted that the nuclear membrane is one of the most difficult intracellular barriers to overcome for DNA delivery. Also, degradation of DNA in the cytoplasm of the cells should be avoided (Figure 1C, step 6).

Despite the progress that has been made over the last decade in overcoming the above-mentioned extracellular and intracellular challenges in non-viral nucleic acid delivery, their translation into clinical oncology is still premature. In the following section, we will review the non-viral DNA and

siRNA delivery systems that were investigated *in vivo* for their ability to target tumors confined within the peritoneal cavity following IP administration up to date.

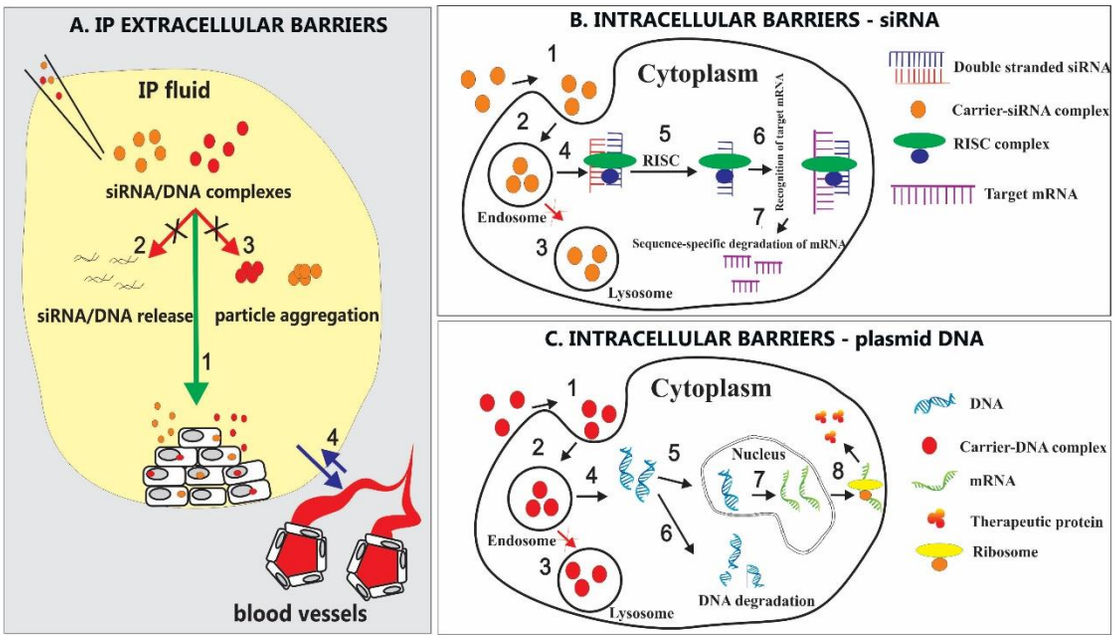

Figure 1. Schematic overview over the different barriers in non-viral nucleic acid delivery. (A) extracellular barriers. **(B)** and **(C)** intracellular barriers.

3. Current *in vivo* use of plasmid DNA for PC

Table 1 summarizes the current *in* vivo studies that have been performed with pDNA for the treatment of PC up to date. As mentioned above, pDNA aims to induce the expression of deficient proteins, suicide genes or proteins that stimulate the host immune system, with the goal to target tumor cells. Some studies also made use of reporter proteins such as luciferase, to explore the suitability of DNA carriers to reach tumor cells. For example Zhang et al. performed a proof of concept study of a delivery system for its ability to express luciferase in peritoneal tumors *in vivo*, without investigating its effect on tumor growth [53]. They studied 'stabilized plasmid-lipid particles' (SPLP) composed of DOPE, the cationic lipid dioleoydimethylammonium chloride (DODAC) and C8 Ceramide-PEG (C8 Cer-PEG) in an IP human melanoma B16 tumor model. C8 Cer-PEG was chosen to PEGylate the lipid nanoparticles, because of its ability to diffuse out of the nanoparticles with a certain kinetic, ensuring good PEGylation in the extracellular biofluids, while the de-PEGylation over time restores the intracellular trafficking of the complexes. This in contrast to the commonly used DSPE-PEG which results in stable PEGylation that ensures good extracellular stability, but interferes on the level of cellular uptake and endosomal escape [52]. The authors reported high expression of luciferase in B16 tumors 24 h following IP injection [53]. In a study by Louis et al., the widely used linear polymer polyethylenimine (L-PEI) was used to deliver DNA

expressing luciferase in mice bearing SKOV-3 human ovarian cancer cells. Multiple IP injections of PEI/DNA complexes resulted in high transgene expression, without any toxicity signs [54].

Immunotherapy is receiving increasing attention in the treatment of cancer. In this respect, several cytokines have been suggested to induce immune response, particularly IL-12 [55]. Fewell et al. synthesized PEG-PEI-cholesterol lipopolymers complexed with IL-12 plasmid and tested its ability to induce an anticancer immune response in mice bearing ovarian adenocarcinomas tumors. The authors reported a significant increase in murine IL-12 and interferon (IFN-*γ)* in ascites fluid and an increased survival of the animals. Additionally, a significant decrease was noted in vascular endothelial growth factor (VEGF), which plays an important role in ascites formation. As expected, when combined with chemotherapy, an additional increase in the survival of the treated mice was observed [56]. These successful *in vivo* experiments paved the way to clinical trials in humans. A phase I clinical trial was carried out on women diagnosed with chemotherapy-resistant ovarian cancer. In this study, 13 patients received four increasing doses of the formulated plasmid, namely 0.6, 3, 12, or 24 $mg*m^{-2}$, once every four weeks, via IP infusion. No major side effects were reported, except for fever and abdominal pain. High levels of IL-12 plasmid and (IFN-*γ)* were measured in the peritoneal fluid but not in serum during the treatment, suggesting that this IL-12 delivery system is suitable for local delivery and the treatment of recurrent ovarian cancer [57]. Recently, the results of a phase II clinical trial addressing the toxicity and antitumor activity of the formulation in 20 platinum resistant patients were published [58]. Briefly, patients received a weekly IP infusion of the IL-12 plasmid containing lipopolymer at a dose of 24 $mg*m^{-2}$. Common adverse effects were reported including fatigue, fever, chills, abdominal pain, nausea, vomiting, anemia, thrombocytopenia and leukopenia. No patients with partial or complete response were reported. In summary, seven patients had stable disease, nine had progressive disease, and six had survival progression-free survival (PFS) for six months. Therefore, the authors deduced that the treatment had insufficient and limited biological activity in platinum resistant ovarian cancer patients [58]. To this end, a phase I clinical trial is ongoing to evaluate the efficacy and toxicity of combined therapy of the IL-12 formulation (gene therapy) with a liposomal doxorubicin formulation (conventional chemotherapy) in ovarian cancer patients.

Colon cancer is among the most common diseases in the world, with about 50,000 deaths yearly in the United States [59]. The difficulty in treating colon cancer is due to rapid spread and metastases. Vesicular stomatitis virus matrix protein (VSVMP) has been shown to inhibit host gene expression by interacting with the nucleoporin Nup 98, an important component of the nuclear core complex which is responsible for the transport of different molecules across the nuclear envelope, thereby blocking nuclear export and inducing apoptosis [60]. Guo et al. synthesized and investigated heparin-polyethyleneimine (HPEI) nanogels complexed with plasmids encoding for VSVMP (pVSVMP) for their ability to induce apoptosis in C-26 colon carcinoma cells. HPEI/pVSVMP nanogels efficiently inhibited peritoneal metastasis of C-26 colon carcinoma in mice following IP injection, and prolonged their survival [61]. Worth mentioning the fact that intravenous

administration of HPEI/pVSVMP nanogels resulted in rapid degradation of the complexes and their excretion through urine. Therefore, the data demonstrate a clear advantage of the IP route for the treatment of colon carcinoma when compared with the systemic one. In another study, the same research group used the same HPEI nanogels to deliver Filamin A interacting protein 1-like (FILIP1L). FILIP1L plays a role in regulating angiogenesis, apoptosis and proliferation of tumor cells. Interestingly, it has been proposed that FILIP1L is absent in ovarian cancer cell lines [62]. When tested in SKOV-3 IP ovarian carcinomatosis model, HPEI incorporating plasmids expressing FILIP1L suppressed tumor growth, and decreased tumor weight about 72% compared to the control group [63].

As mentioned in section 2.5. , the use of PEG posts a challenge for the drug delivery community, especially within the field of nucleic acid delivery. It is becoming more common to coat different nanoparticles with PEG chains that can be detached upon trigger, or diffuse spontaneously out of the complexes in function of time [64]. Addressing this point, Kumagai et al. compared the toxicity and gene expression efficiency of two block copolymers that are able to form nano-sized micelles. The first is poly (ethylene glycol)-block-poly (PEG-P [Asp (DET)]) and the second is PEG-SS-P [Asp (DET)] containing a disulfide bond (S-S) between the cationic polymer and the PEG chains. The idea behind the disulfide bond is to trigger detachment of the PEG chains upon exposure to the intracellular reducing environment of the cells, and consequently facilitate interactions with intracellular organelles. When both polymers loaded with plasmid DNA encoding for human tumor necrosis factor α (hTNF-α) were IP injected in mice bearing a peritoneally disseminated cancer model, higher antitumor activity was observed for the polymer containing S-S bonds, without any differences in toxicity [65]. Similarly, in a study carried out by the same research group, a mixture of block/homo-mixed polymers were used to prepare micelles. More specifically, poly{N'-[N-(2-aminoethyl)-2-aminoethyl]aspartamide} P[Asp(DET)] and (PEG)-b-P[Asp(DET)] was compared to (PEG)-b-P[Asp(DET)] alone for their ability to express luciferase in mice with peritoneal dissemination following IP administration. The mixture showed 12 folds higher luciferase expression 24 h after the injection. Additionally, antitumor activity of the mixed polymer loaded with granulocyte macrophage colony stimulating factor (GM-CSF) in mice as well as in cynomolgus monkeys was observed following IP injection via the activation of natural killer cells [66].

Within the frame of gene therapy, delivery of suicide DNA to epithelial ovarian cancer cells has also been investigated. To date, several attempts have been reported. Langer and co-workers have developed a DNA construct that contains the diphtheria toxin A (DT-A) and a recombinase, to regulate gene expression on both the transcriptional and recombination level. This construct was delivered into ovarian cancer cells and inhibited tumor growth in mice [67]. Huang et al. showed that IP administration of cationic biodegradable poly(β-amino ester) to deliver DNA encoding for DT-A in mice bearing metastatic ovarian cancer tumors, not only inhibited tumor growth and prolonged the survival of mice, but also was more efficient in terms of tumor suppression than the conventional anticancer agents paclitaxel and cisplatin [68]. Taking advantage of the DT-A toxin,

Hine et al. proved that the fusion of the recombinase Rad51 promoter, which is overexpressed in many tumors, to the DT-A gene results in a specific killing of tumors, and thus is an attractive strategy for cancer treatment [69]. Later on, Hine et al. brought evidence for the efficiency of the system *in vivo*. In this study a Rad-51-luciferase construct was IP delivered using a cationic linear PEI, known as jetPEI, in mice bearing HeLa cells xenografts. Due to the luciferase expression it was possible to specifically detect tumors, with an *in vivo* bioluminescent camera, while no bioluminescence was detected in healthy mice. Furthermore, the treatment decreased tumor mass by fourfold, which was accompanied with a reduction in malignant ascites and a 90% increase in the life span of the treated mice compared to the control mice [70]. Finally, the study recommends to use pRad51-Luc-DT-A/jetPEI to image and treat different types of cancer.

As explained above, plasmids can also be used to express short hairpin RNA (shRNA) that is further processed by the cell into siRNA. Therefore, plasmid delivery can also be used to downregulate specific proteins. Claudin-3 (CLDN3) is a tight junction, integral membrane protein that is overexpressed in ovarian tumors, but not in healthy ovarian tissue. CLDN3 overexpression eventually leads to invasion and survival of ovarian tumors [71,72]. Hence, downregulation of CLDN3 offers an attractive strategy for cancer treatment. Sun et al. developed a plasmid expressing shRNA against CLDN3 and encapsulated the plasmids within biodegradable poly (lactic-co-glycolic acid) (PLGA) nanoparticles. Following 12 IP administrations to nude mice bearing SKOV-3 ovarian cancer, a significant reduction in the tumor weight of 67.4% compared to the control was measured [73].

Table 1. Summary of *in vivo* studies evaluating IP delivery of nanoparticles for cancer DNA therapy

Gene type	Carrier	Cancer model	Results	Ref.
Luciferase DNA (Reporter gene)	Stabilized plasmid-lipid particles coated with diffusible Ceramide-poly(ethylene-glycol)	B16BL-6 human melanoma cells were seeded in the peritoneal cavity of C57BL/6 mice	High luciferase expression in tumor tissue compared to healthy tissue	[53]
Luciferase DNA (Reporter gene)	(L-PEI) Linear polyethylenimine	SKOV-3 IP ovarian carcinomatosis	Dose dependent significant level of transgene expression, preferentially in tumors compared to other organs, without toxicity	[54]
pmIL-12 (Immunotherapy)	Polyethylenimine covalently attached to methoxy polyethylene glycol and cholesteryl chloroformate	*In vivo:* ID8 IP Ovarian cancer which lead to PC Phase I: 13 women with chemotherapy-resistant recurrent ovarian cancer Phase II: 20 patients with platinum resistant recurrent ovarian cancer	*In vivo:* Suppression of ascites accumulation, dramatic decrease in VEGF levels, no signs of toxicity Phase I: high levels of (IFN-*γ)* in PF but not in serum Phase II: seven patients had a stable disease, nine patients had progressive disease and six had a progression free survival for 6 months	[56-58]
pVSVMP	Heparin conjugated to polyethylenimine	C-26 colon carcinoma	The treatment prevented growth of abdominal metastasis and increased the life span of the treated mice	[61]
FILIP1LΔC103	Heparin conjugated to polyethylenimine	SKOV-3 IP ovarian carcinomatosis	Significant inhibition of ovarian cancer, reduction in angiogenesis, decrease in cell	[63]

			proliferation and increase in tumor apoptosis	
hTNF-α	PEG-SS-P[Asp(DET)]	SUIT-2 IP human pancreatic carcinoma	High antitumor activity without renal and hepatic toxicity	[65]
(GM-CSF) (Immune therapy)	(PEG)-b-P[Asp(DET)] /P[Asp(DET)]	SUIT-2 IP human pancreatic carcinoma	Efficient uptake in tumor nodules, and prolongation of the survival rate in treated mice	[66]
Diphtheria toxin (DT-A) (Suicide therapy)	cationic biodegradable poly(β-amino ester)	Epithelial ovarian cancer	Reduction in tumor mass, and increase in survival rate. Tumor suppression was superior over cisplatin and paclitaxel treatment	[68]
pRad51-DT-A (Suicide therapy)	Linear polyethylenimine (jetPEI)	IP HeLa tumor cells	Efficient inhibition of malignant ascites, fourfold decrease in tumor mass, 90% increase in the mean survival time of treated mice	[70]
Plasmid expressing shRNA-against Claudin-3 (CLDN3) (Short hairpin RNA)	poly(lactic-co-glycolic acid) PLGA	SKOV-3 IP ovarian carcinomatosis	Efficient downregulation of CLDN3, tumor suppression, reduction in tumor weight, and increase in tumor apoptosis	[73]

4. Current *in vivo* use of RNAi for PC

As mentioned earlier, since its discovery, siRNA has attracted remarkable attention for cancer applications. In general, RNAi aims to downregulate cancer-related proteins which are often overexpressed in cancer cells and contribute to their invasiveness and increased proliferation. Table 2 summarizes the siRNA based therapies that have been explored *in* vivo so far. In an attempt to downregulate the expression of focal adhesion kinase (FAK) which plays an important role in survival, migration and invasion of cancer cells [74], FAK siRNA complexed with 1,2-dioleoyl-sn-glycero-3-phosphatidylcholine (DOPC) liposomes was IP injected in mice bearing an ovarian cancer model. This treatment reduced the mean tumor weight by 44% to 72% in three cell lines [75]. Similarly, the same research group employed the same ovarian cancer model in mice, evaluating the ability of Interleukin-8 (IL-8) siRNA-DOPC complexes to suppress IL-8 activity. IL-8 is a proangiogenic cytokine that is overexpressed in many human cancers. The authors reported a significant reduction in the tumor weight that varies between 32%-52% in the tested cell lines, proposing that IL-8 gene silencing decreases tumor growth via an antiangiogenic mechanism [76].

As mentioned above, the downregulation of Claudin-3 (CLDN3) offers possibilities for anti-cancer treatments. Huang et al. investigated whether the siRNA induced knockdown of CLDN3 prevented the growth of metastasis in a mice model derived from ovarian surface epithelial ID8 cells. Interestingly, IP injection of LPXs containing siRNA against CLDN3 to mice significantly decreased not only tumor growth, but also the development of ascites, indicating that suppression of metastasis occurred [77]. Likewise, Fujita et al. proposed an atelocollagen delivery system loaded with siRNA against NEDD1, a centrosomal protein that associates with the gamma-tubulin ring complex protein and plays an important role in regulating the metaphase of the cell cycle [78]. NEDD1 downregulation prolonged the survival of mice bearing a gastric and peritoneal metastasis model from ascites producing tumors [79]. In addition to CLDN3, IL-8 and FAK, inhibition of oncogenes is also an attractive strategy to suppress tumors. Briefly, oncogenes are genes that tend to cause cancer, and are mutated or overexpressed in tumor cells [80]. In a study by Ren et al., an inhibitor of DNA binding 4 (ID4) was characterized, and shown to be overexpressed on the surface of human ovarian cancer cells. In the same study, the authors demonstrate *in vitro* and *in vivo* silencing when nanocomplexes of cell-penetrating peptides containing siRNA against ID4 were injected IP to mice with disseminated intra-abdominal tumors, every 3 days for 30 days. The treatment remarkably increased the survival rate of 80% of the animals, with the ability to live 60 days or even more, without inducing a strong immune response [81]. Recently, survivin, a member of the inhibitor of apoptosis (IAP) protein family, is receiving increased attention in cancer therapy, since it is up-regulated in solid tumors [80]. In an attempt to knockdown survivin expression in mice bearing a metastatic human pancreatic tumor model, Wang et al. investigated the ability of liposomes composed of 1,2-dioleoyl-3-trimethylammoniumpropane (DOTAP), 1,2-dioleoyl-sn-glycero-3-phosphoethanolamine (DOPE) and 1,2-distearoyl-sn-glycero-3-

phosphoethanolamine-N-[methoxy(polyethylene glycol)-2000 (DSPE-PEG) complexed with siRNA against survivin. The study revealed that these complexes successfully decreased the expression of survivin, but only when they were co-administered with the conventional chemotherapeutic paclitaxel (PTX) [82]. The data presented in the study thus encourages the co-delivery of siRNA and other chemotherapeutic agents to tumors.

Other RNAi strategies are especially useful for personalized medicine purposes. BRCA1 is a tumor suppressor which is mutated in about 5% of the ovarian cancer population, leading to defects in the DNA repair process, such as mutations in chromosomal rearrangements [83,84]. On the contrary, Poly(ADP-ribose) polymerase-1 (PARP1) is involved in preventing DNA damage and genomic stability [85]. It has been postulated that orally administered PARP-1 inhibitors in patients with BRCA mutations resulted in antitumor activity [86]. When PARP-1 siRNA was IP delivered using lipid-like nanostructures called 'lipidoids' in mice bearing disseminated BRCA1-deficient murine ovarian carcinoma allografts, a significant cell growth inhibition and extended survival of the treated mice was noticeable [87].

Table 2. Summary of *in vivo* studies evaluating IP delivery of nanoparticles for cancer RNAi therapy

siRNA against	Carrier	Cancer model	Results	Ref.
Focal adhesion kinase (FAK)	DOPC liposomes	Human ovarian cancer using 3 cell lines SKOV-3ip1, HeyA8 (taxane sensitive), and HeyA8MDR (taxane resistant) in nude mice	Reduction in tumor weight by 44% to 72% depending on the cell line, Synergistic effect when siRNA was combined with docetaxel	[75]
IL-8	DOPC liposomes	Human ovarian cancer cell lines SKOV-3ip1, HeyA8 (taxane sensitive), and SKOV-3ip2.TR (taxane resistant) in nude mice	Reduction in tumor weight 32% to 52% depending on the cell line, Synergistic effect when siRNA was combined with docetaxel	[76]
CLDN3	lipidoid	ID8 IP Ovarian cancer	Suppression of tumor growth, reduction in ascites, without any toxicity following multiple administrations	[77]
NEDD1	Atelocollagen	HSC-60 IP gastric cancer in scid mice	Significant increase in the life span of the treated mice	[79]
ID4	Cell penetrating peptides (CPPs)	OVCAR-8 IP tumors	Remarkable prolongation in survival , 80% of the animals survived at least 60 days without inducing immune response following one injection every 3 days for 30 days	[81]
Survivin	Liposomes composed of DOTAP DOPE PEG and cholesterol	H766T IP pancreatic human metastatic xenograft	Efficient knockdown of survivin was possible only when combined with paclitaxel	[82]
PARP-1	lipidoid	Genetically defined murine ovarian cancer	High specificity of the treatment, prolongation of the survival of mice	[87]

5. Concluding remarks and future prospective

In this chapter, we restricted our discussion on IP injection of non-viral vectors to deliver nucleic acids into tumors residing in the peritoneal space. IP delivery of nucleic acids is indeed an attractive approach to target PC. Although several non-viral gene delivery systems carrying plasmid DNA or siRNA have proven anti-tumor effect to some extent, none of the tested formulations have been approved for use in clinical oncology so far. Translation into the clinic still awaits a new class of formulations that can overcome both the intracellular and extracellular barriers as discussed above. The main problem in optimizing non-viral gene delivery systems remains the lack of knowledge on the relation between the physicochemical properties of delivery systems (e.g. charge and size) and their obtained therapeutic effect. Also, carrier properties which assure stability on the extracellular level (for example surface PEGylation) still often interfere with the intracellular performance of the same carrier. It should be noted that the efficiency of a delivery system can greatly depend on the extracellular barriers which are encountered, and thus on the administration route. It is crucial to evaluate and optimize gene delivery vehicles with the intended administration route in mind. For IP delivery, this implies that carrier properties should be studied in the peritoneal fluid. In an attempt to perform reliable measurements in more complex biological fluids, we have proven that advanced microscopy techniques such as fluorescence correlation spectroscopy (FCS) and single particle tracking (SPT) enable to monitor the disassembly and aggregation of non-viral vectors in undiluted biological fluids [45]. By employing these powerful techniques, we can simulate the *in vivo* situation, and screen for formulations that show minimal aggregation properties while keeping the maximal amount of their siRNA or pDNA load in the IP fluid. For local IP delivery, it should be noted that having colloidal stable particles in the peritoneal cavity is not the only requirement for optimal tumor targeting. It has been reported that nano-sized vectors are rapidly cleared from the peritoneal cavity following IP administration compared to microparticles [88] (Figure 1A, step 4). This rapid absorption from the peritoneal cavity to the systemic circulation, most likely seriously limits the amount of complexes that actually reach and enter the tumor target cells. The rapid clearance of nanoparticles from the peritoneal cavity has however also been exploited in some studies, where the IP route is being used for systemic gene delivery, to target systemic tumors. In a study by Aigner and co-workers, siRNA against c-erbB2/neu (HER-2) receptor complexed with PEI was injected IP into mice bearing subcutaneous SKOV-3 tumors and exhibited a remarkable reduction in tumor growth, whereas no reduction in tumor growth was observed following injection of naked siRNA [89]. In this case, the IP delivery is thus used as a depot system, from which systemic delivery of nanoparticles is aimed.

In the vast majority of the studies we reviewed, it is important to stress out the fact that long-term biological activity by silencing or overexpressing genes was obtained only after multiple administrations of the formulations to the peritoneal cavity. Therefore, future strategies will most likely also depend on delivery systems that can increase the residence time of non-viral nucleic acid delivery systems in the peritoneal cavity, with limited distribution to the systemic circulation. In this respect, sustained release of non-viral vectors from an injectable depot system might be an advantage, due to the ability to maintain stable gene silencing or expression for a prolonged period of time. It is expected that the constantly increasing knowledge on possible gene targets in tumor cells will continue to fine-tune the use of plasmid DNA and siRNA delivery for the treatment of PC. Also, nucleic acid delivery will play a major role in personalized cancer treatments as screening methods allow more and more cancer associated genes to be identified on a person-to-person basis. Finally, the combination of nucleic acids with conventional chemotherapeutics can also contribute to the translation of IP gene therapy to the clinic.

References

[1] W.P. Ceelen, M.F. Flessner, Intraperitoneal therapy for peritoneal tumors: biophysics and clinical evidence, Nature reviews. Clinical oncology, 7 (2010) 108-115.
[2] D. Hanahan, R.A. Weinberg, Hallmarks of cancer: the next generation, Cell, 144 (2011) 646-674.
[3] A.M. Scott, J.D. Wolchok, L.J. Old, Antibody therapy of cancer, Nature reviews. Cancer, 12 (2012) 278-287.
[4] H.M. Blau, M.L. Springer, Gene therapy--a novel form of drug delivery, The New England journal of medicine, 333 (1995) 1204-1207.
[5] J.S. Sandhu, A. Keating, N. Hozumi, Human gene therapy, Crit Rev Biotechnol, 17 (1997) 307-326.
[6] T. Minaguchi, T. Mori, Y. Kanamori, M. Matsushima, H. Yoshikawa, Y. Taketani, Y. Nakamura, Growth suppression of human ovarian cancer cells by adenovirus-mediated transfer of the PTEN gene, Cancer research, 59 (1999) 6063-6067.
[7] P.J. Morin, B. Vogelstein, K.W. Kinzler, Apoptosis and APC in colorectal tumorigenesis, Proceedings of the National Academy of Sciences of the United States of America, 93 (1996) 7950-7954.
[8] J.A. Roth, D. Nguyen, D.D. Lawrence, B.L. Kemp, C.H. Carrasco, D.Z. Ferson, W.K. Hong, R. Komaki, J.J. Lee, J.C. Nesbitt, K.M. Pisters, J.B. Putnam, R. Schea, D.M. Shin, G.L. Walsh, M.M. Dolormente, C.I. Han, F.D. Martin, N. Yen, K. Xu, L.C. Stephens, T.J. McDonnell, T. Mukhopadhyay, D. Cai, Retrovirus-mediated wild-type p53 gene transfer to tumors of patients with lung cancer, Nature medicine, 2 (1996) 985-991.
[9] C.T. Yang, L. You, C.C. Yeh, J.W. Chang, F. Zhang, F. McCormick, D.M. Jablons, Adenovirus-mediated p14(ARF) gene transfer in human mesothelioma cells, Journal of the National Cancer Institute, 92 (2000) 636-641.
[10] F. McCormick, Cancer gene therapy: fringe or cutting edge?, Nature reviews. Cancer, 1 (2001) 130-141.
[11] I. Mellman, G. Coukos, G. Dranoff, Cancer immunotherapy comes of age, Nature, 480 (2011) 480-489.
[12] M. Vanneman, G. Dranoff, Combining immunotherapy and targeted therapies in cancer treatment, Nature reviews. Cancer, 12 (2012) 237-251.
[13] G. Dranoff, Cytokines in cancer pathogenesis and cancer therapy, Nature reviews. Cancer, 4 (2004) 11-22.
[14] A. Fire, S. Xu, M.K. Montgomery, S.A. Kostas, S.E. Driver, C.C. Mello, Potent and specific genetic interference by double-stranded RNA in Caenorhabditis elegans, Nature, 391 (1998) 806-811.
[15] S.M. Elbashir, J. Harborth, W. Lendeckel, A. Yalcin, K. Weber, T. Tuschl, Duplexes of 21-nucleotide RNAs mediate RNA interference in cultured mammalian cells, Nature, 411 (2001) 494-498.
[16] S.I. Pai, Y.Y. Lin, B. Macaes, A. Meneshian, C.F. Hung, T.C. Wu, Prospects of RNA interference therapy for cancer, Gene therapy, 13 (2006) 464-477.
[17] R. Kanasty, J.R. Dorkin, A. Vegas, D. Anderson, Delivery materials for siRNA therapeutics, Nature materials, 12 (2013) 967-977.
[18] P.J. Paddison, A.A. Caudy, E. Bernstein, G.J. Hannon, D.S. Conklin, Short hairpin RNAs (shRNAs) induce sequence-specific silencing in mammalian cells, Gene Dev, 16 (2002) 948-958.
[19] M.A. Hamburg, F.S. Collins, The path to personalized medicine, The New England journal of medicine, 363 (2010) 301-304.
[20] B.C. Baguley, Multidrug resistance in cancer, Methods in molecular biology, 596 (2010) 1-14.
[21] T.B. Lee, J.H. Park, Y.D. Min, K.J. Kim, C.H. Choi, Epigenetic mechanisms involved in differential MDRI mRNA expression between gastric and colon cancer cell lines and rationales for clinical chemotherapy, Bmc Gastroenterol, 8 (2008).
[22] D.C. Altieri, Survivin, cancer networks and pathway-directed drug discovery, Nature reviews. Cancer, 8 (2008) 61-70.
[23] A.W. Tolcher, D.I. Quinn, A. Ferrari, F. Ahmann, G. Giaccone, T. Drake, A. Keating, J.S. de Bono, A phase II study of YM155, a novel small-molecule suppressor of survivin, in castration-resistant taxane-pretreated prostate cancer, Annals of oncology : official journal of the European Society for Medical Oncology / ESMO, 23 (2012) 968-973.
[24] M. Creixell, N.A. Peppas, Co-delivery of siRNA and therapeutic agents using nanocarriers to overcome cancer resistance, Nano Today, 7 (2012) 367-379.
[25] M.R. Capecchi, Altering the genome by homologous recombination, Science, 244 (1989) 1288-1292.
[26] R.N. Cohen, M.A. van der Aa, N. Macaraeg, A.P. Lee, F.C. Szoka, Jr., Quantification of plasmid DNA copies in the nucleus after lipoplex and polyplex transfection, Journal of controlled release : official journal of the Controlled Release Society, 135 (2009) 166-174.
[27] S. Hama, H. Akita, S. Iida, H. Mizuguchi, H. Harashima, Quantitative and mechanism-based investigation of post-nuclear delivery events between adenovirus and lipoplex, Nucleic Acids Res, 35 (2007) 1533-1543.
[28] D. De Paula, M.V. Bentley, R.I. Mahato, Hydrophobization and bioconjugation for enhanced siRNA delivery and targeting, Rna, 13 (2007) 431-456.
[29] C.B. Moore, E.H. Guthrie, M.T. Huang, D.J. Taxman, Short hairpin RNA (shRNA): design, delivery, and assessment of gene knockdown, Methods in molecular biology, 629 (2010) 141-158.

[30] A. Malek, O. Merkel, L. Fink, F. Czubayko, T. Kissel, A. Aigner, In vivo pharmacokinetics, tissue distribution and underlying mechanisms of various PEI(-PEG)/siRNA complexes, Toxicol Appl Pharmacol, 236 (2009) 97-108.
[31] J. Soutschek, A. Akinc, B. Bramlage, K. Charisse, R. Constien, M. Donoghue, S. Elbashir, A. Geick, P. Hadwiger, J. Harborth, M. John, V. Kesavan, G. Lavine, R.K. Pandey, T. Racie, K.G. Rajeev, I. Rohl, I. Toudjarska, G. Wang, S. Wuschko, D. Bumcrot, V. Koteliansky, S. Limmer, M. Manoharan, H.P. Vornlocher, Therapeutic silencing of an endogenous gene by systemic administration of modified siRNAs, Nature, 432 (2004) 173-178.
[32] M.A. Kay, State-of-the-art gene-based therapies: the road ahead, Nat Rev Genet, 12 (2011) 316-328.
[33] C.E. Thomas, A. Ehrhardt, M.A. Kay, Progress and problems with the use of viral vectors for gene therapy, Nat Rev Genet, 4 (2003) 346-358.
[34] R.S. Tomar, H. Matta, P.M. Chaudhary, Use of adeno-associated viral vector for delivery of small interfering RNA, Oncogene, 22 (2003) 5712-5715.
[35] D. Bouard, D. Alazard-Dany, F.L. Cosset, Viral vectors: from virology to transgene expression, Br J Pharmacol, 157 (2009) 153-165.
[36] J. Nguyen, F.C. Szoka, Nucleic acid delivery: the missing pieces of the puzzle?, Accounts of chemical research, 45 (2012) 1153-1162.
[37] T. Nagasaki, S. Shinkai, The concept of molecular machinery is useful for design of stimuli-responsive gene delivery systems in the mammalian cell, J Incl Phenom Macro, 58 (2007) 205-219.
[38] M.S. Al-Dosari, X. Gao, Nonviral Gene Delivery: Principle, Limitations, and Recent Progress, Aaps J, 11 (2009) 671-681.
[39] X. Gao, K.S. Kim, D.X. Liu, Nonviral gene delivery: What we know and what is next, Aaps J, 9 (2007) E92-E104.
[40] O.C. Farokhzad, R. Langer, Impact of Nanotechnology on Drug Delivery, ACS nano, 3 (2009) 16-20.
[41] J.S. Ross, D.P. Schenkein, R. Pietrusko, M. Rolfe, G.P. Linette, J. Stec, N.E. Stagliano, G.S. Ginsburg, W.F. Symmans, L. Pusztai, G.N. Hortobagyi, Targeted therapies for cancer 2004, Am J Clin Pathol, 122 (2004) 598-609.
[42] A. Schroeder, D.A. Heller, M.M. Winslow, J.E. Dahlman, G.W. Pratt, R. Langer, T. Jacks, D.G. Anderson, Treating metastatic cancer with nanotechnology, Nature Reviews Cancer, 12 (2012) 39-50.
[43] R. Langer, Drug delivery and targeting, Nature, 392 (1998) 5-10.
[44] S.M. Moghimi, A.C. Hunter, J.C. Murray, Long-circulating and target-specific nanoparticles: Theory to practice, Pharmacol Rev, 53 (2001) 283-318.
[45] G.R. Dakwar, E. Zagato, J. Delanghe, S. Hobel, A. Aigner, H. Denys, K. Braeckmans, W. Ceelen, F.C. De Smedt, K. Remaut, Colloidal stability of nano-sized particles in the peritoneal fluid: Towards optimizing drug delivery systems for intraperitoneal therapy, Acta Biomater, 10 (2014) 2965-2975.
[46] E. Kipps, D.S.P. Tan, S.B. Kaye, Meeting the challenge of ascites in ovarian cancer: new avenues for therapy and research, Nature Reviews Cancer, 13 (2013) 273-282.
[47] R. Barbalat, S.E. Ewald, M.L. Mouchess, G.M. Barton, Nucleic Acid Recognition by the Innate Immune System, Annual Review of Immunology, Vol 29, 29 (2011) 185-214.
[48] K. Knop, R. Hoogenboom, D. Fischer, U.S. Schubert, Poly(ethylene glycol) in Drug Delivery: Pros and Cons as Well as Potential Alternatives, Angew Chem Int Edit, 49 (2010) 6288-6308.
[49] A.K. Varkouhi, M. Scholte, G. Storm, H.J. Haisma, Endosomal escape pathways for delivery of biologicals, Journal of controlled release : official journal of the Controlled Release Society, 151 (2011) 220-228.
[50] A.T. Dinh, C. Pangarkar, T. Theofanous, S. Mitragotri, Understanding intracellular transport processes pertinent to synthetic gene delivery via stochastic simulations and sensitivity analyses, Biophys J, 92 (2007) 831-846.
[51] G.L. Lukacs, P. Haggie, O. Seksek, D. Lechardeur, N. Freedman, A.S. Verkman, Size-dependent DNA mobility in cytoplasm and nucleus, J Biol Chem, 275 (2000) 1625-1629.
[52] L.C. Gomes-da-Silva, N.A. Fonseca, V. Moura, M.C. Pedroso de Lima, S. Simoes, J.N. Moreira, Lipid-based nanoparticles for siRNA delivery in cancer therapy: paradigms and challenges, Accounts of chemical research, 45 (2012) 1163-1171.
[53] Y.P. Zhang, L. Sekirov, E.G. Saravolac, J.J. Wheeler, P. Tardi, K. Clow, E. Leng, R. Sun, P.R. Cullis, P. Scherrer, Stabilized plasmid-lipid particles for regional gene therapy: formulation and transfection properties, Gene therapy, 6 (1999) 1438-1447.
[54] M.H. Louis, S. Dutoit, Y. Denoux, P. Erbacher, E. Deslandes, J.P. Behr, P. Gauduchon, L. Poulain, Intraperitoneal linear polyethylenimine (L-PEI)-mediated gene delivery to ovarian carcinoma nodes in mice, Cancer Gene Ther, 13 (2006) 367-374.
[55] M.J. Robertson, J. Ritz, Interleukin 12: Basic Biology and Potential Applications in Cancer Treatment, The oncologist, 1 (1996) 88-97.
[56] J.G. Fewell, M.M. Matar, J.S. Rice, E. Brunhoeber, G. Slobodkin, C. Pence, M. Worker, D.H. Lewis, K. Anwer, Treatment of disseminated ovarian cancer using nonviral interleukin-12 gene therapy delivered intraperitoneally, J Gene Med, 11 (2009) 718-728.

[57] K. Anwer, M.N. Barnes, J. Fewell, D.H. Lewis, R.D. Alvarez, Phase-I clinical trial of IL-12 plasmid/lipopolymer complexes for the treatment of recurrent ovarian cancer, Gene therapy, 17 (2010) 360-369.
[58] R.D. Alvarez, M.W. Sill, S.A. Davidson, C.Y. Muller, D.P. Bender, R.L. DeBernardo, K. Behbakht, W.K. Huh, A phase II trial of intraperitoneal EGEN-001, an IL-12 plasmid formulated with PEG-PEI-cholesterol lipopolymer in the treatment of persistent or recurrent epithelial ovarian, fallopian tube or primary peritoneal cancer: a gynecologic oncology group study, Gynecologic oncology, 133 (2014) 433-438.
[59] A. Jemal, R. Siegel, E. Ward, Y. Hao, J. Xu, T. Murray, M.J. Thun, Cancer statistics, 2008, CA: a cancer journal for clinicians, 58 (2008) 71-96.
[60] C. von Kobbe, J.M. van Deursen, J.P. Rodrigues, D. Sitterlin, A. Bachi, X. Wu, M. Wilm, M. Carmo-Fonseca, E. Izaurralde, Vesicular stomatitis virus matrix protein inhibits host cell gene expression by targeting the nucleoporin Nup98, Mol Cell, 6 (2000) 1243-1252.
[61] M. Gou, K. Men, J. Zhang, Y. Li, J. Song, S. Luo, H. Shi, Y. Wen, G. Guo, M. Huang, X. Zhao, Z. Qian, Y. Wei, Efficient inhibition of C-26 colon carcinoma by VSVMP gene delivered by biodegradable cationic nanogel derived from polyethyleneimine, ACS nano, 4 (2010) 5573-5584.
[62] S.C. Mok, K.K. Wong, R.K.W. Chan, C.C. Lau, S.W. Tsao, R.C. Knapp, R.S. Berkowitz, Molecular-Cloning of Differentially Expressed Genes in Human Epithelial Ovarian-Cancer, Gynecologic oncology, 52 (1994) 247-252.
[63] C. Xie, M.L. Gou, T. Yi, H.X. Deng, Z.Y. Li, P. Liu, X.R. Qi, X. He, Y.Q. Wei, X. Zhao, Efficient Inhibition of Ovarian Cancer by Truncation Mutant of FILIP1L Gene Delivered by Novel Biodegradable Cationic Heparin-Polyethyleneimine Nanogels, Human gene therapy, 22 (2011) 1413-1422.
[64] B. Romberg, W.E. Hennink, G. Storm, Sheddable coatings for long-circulating nanoparticles, Pharmaceutical research, 25 (2008) 55-71.
[65] M. Kumagai, S. Shimoda, R. Wakabayashi, Y. Kunisawa, T. Ishii, K. Osada, K. Itaka, N. Nishiyama, K. Kataoka, K. Nakano, Effective transgene expression without toxicity by intraperitoneal administration of PEG-detachable polyplex micelles in mice with peritoneal dissemination, Journal of Controlled Release, 160 (2012) 542-551.
[66] M. Ohgidani, K. Furugaki, K. Shinkai, Y. Kunisawa, K. Itaka, K. Kataoka, K. Nakano, Block/homo polyplex micelle-based GM-CSF gene therapy via intraperitoneal administration elicits antitumor immunity against peritoneal dissemination and exhibits safety potentials in mice and cynomolgus monkeys, Journal of Controlled Release, 167 (2013) 238-247.
[67] J.A. Sawicki, D.G. Anderson, R. Langer, Nanoparticle delivery of suicide DNA for epithelial ovarian cancer therapy, Ovarian Cancer: State of the Art and Future Directions in Translational Research, 622 (2008) 209-219.
[68] Y.H. Huang, G.T. Zugates, W.D. Peng, D. Holtz, C. Dunton, J.J. Green, N. Hossain, M.R. Chernick, R.F. Padera, R. Langer, D.G. Anderson, J.A. Sawicki, Nanoparticle-Delivered Suicide Gene Therapy Effectively Reduces Ovarian Tumor Burden in Mice, Cancer research, 69 (2009) 6184-6191.
[69] C.M. Hine, A. Seluanov, V. Gorbunova, Use of the Rad51 promoter for targeted anti-cancer therapy, Proceedings of the National Academy of Sciences of the United States of America, 105 (2008) 20810-20815.
[70] C.M. Hine, A. Seluanov, V. Gorbunova, Rad51 Promoter-Targeted Gene Therapy Is Effective for In Vivo Visualization and Treatment of Cancer, Mol Ther, 20 (2012) 347-355.
[71] P.J. Morin, Claudin proteins in ovarian cancer, Dis Markers, 23 (2007) 453-457.
[72] L.B.A. Rangel, R. Agarwal, T. D'Souza, E.S. Pizer, P.L. Alo, W.D. Lancaster, L. Gregoire, D.R. Schwartz, K.R. Cho, P.J. Morin, Tight junction proteins claudin-3 and claudin-4 are frequently overexpressed in ovarian cancer but not in ovarian cystadenomas, Clinical Cancer Research, 9 (2003) 2567-2575.
[73] C.T. Sun, T. Yi, X.R. Song, S.Z. Li, X.R. Qi, X.C. Chen, H.G. Lin, X. He, Z.Y. Li, Y.Q. Wei, X. Zhao, Efficient inhibition of ovarian cancer by short hairpin RNA targeting claudin-3, Oncol Rep, 26 (2011) 193-200.
[74] M.D. Schaller, J.T. Parsons, Focal adhesion kinase: an integrin-linked protein tyrosine kinase, Trends in cell biology, 3 (1993) 258-262.
[75] J. Halder, A.A. Kamat, C.N. Landen, L.Y. Han, S.K. Lutgendorf, Y.G. Lin, W.M. Merritt, N.B. Jennings, A. Chavez-Reyes, R.L. Coleman, D.M. Gershenson, R. Schmandt, S.W. Cole, G. Lopez-Berestein, A.K. Sood, Focal adhesion kinase targeting using in vivo short interfering RNA delivery in neutral liposomes for ovarian carcinoma therapy, Clinical Cancer Research, 12 (2006) 4916-4924.
[76] W.M. Merritt, Y.G. Lin, W.A. Spannuth, M.S. Fletcher, A.A. Kamat, L.Y. Han, C.N. Landen, N. Jennings, K. De Geest, R.R. Langley, G. Villares, A. Sanguino, S.K. Lutgendorf, G. Lopez-Berestein, M.M. Bar-Eli, A.K. Sood, Effect of interleukin-8 gene silencing with liposome-encapsulated small interfering RNA on ovarian cancer cell growth, Journal of the National Cancer Institute, 100 (2008) 359-372.
[77] Y.H. Huang, Y.H. Bao, W.D. Peng, M. Goldberg, K. Love, D.A. Bumcrot, G. Cole, R. Langer, D.G. Anderson, J.A. Sawicki, Claudin-3 gene silencing with siRNA suppresses ovarian tumor growth and metastasis, Proceedings of the National Academy of Sciences of the United States of America, 106 (2009) 3426-3430.
[78] L. Haren, M.H. Remy, I. Bazin, I. Callebaut, M. Wright, A. Merdes, NEDD1-dependent recruitment of the gamma-tubulin ring complex to the centrosome is necessary for centriole duplication and spindle assembly, J Cell Biol, 172 (2006) 505-515.

[79] T. Fujita, K. Yanagihara, F. Takeshita, K. Aoyagi, T. Nishimura, M. Takigahira, F. Chiwaki, T. Fukagawa, H. Katai, T. Ochiya, H. Sakamoto, H. Konno, T. Yoshida, H. Sasaki, Intraperitoneal delivery of a small interfering RNA targeting NEDD1 prolongs the survival of scirrhous gastric cancer model mice, Cancer science, 104 (2013) 214-222.
[80] J. Luo, N.L. Solimini, S.J. Elledge, Principles of Cancer Therapy: Oncogene and Non-oncogene Addiction, Cell, 136 (2009) 823-837.
[81] Y. Ren, H.W. Cheung, G. von Maltzhan, A. Agrawal, G.S. Cowley, B.A. Weir, J.S. Boehm, P. Tamayo, A.M. Karst, J.F. Liu, M.S. Hirsch, J.P. Mesirov, R. Drapkin, D.E. Root, J. Lo, V. Fogal, E. Ruoslahti, W.C. Hahn, S.N. Bhatia, Targeted Tumor-Penetrating siRNA Nanocomplexes for Credentialing the Ovarian Cancer Oncogene ID4, Sci Transl Med, 4 (2012).
[82] J. Wang, Z. Lu, B.Z. Yeung, M.G. Wientjes, D.J. Cole, J.L.S. Au, Tumor priming enhances siRNA delivery and transfection in intraperitoneal tumors, Journal of Controlled Release, 178 (2014) 79-85.
[83] M.E. Moynahan, J.W. Chiu, B.H. Koller, M. Jasin, Brca1 controls homology-directed DNA repair, Mol Cell, 4 (1999) 511-518.
[84] J.F. Stratton, S.A. Gayther, P. Russell, J. Dearden, M. Gore, P. Blake, D. Easton, B.A.J. Ponder, Contribution of BRCA1 mutations to ovarian cancer, New Engl J Med, 336 (1997) 1125-1130.
[85] R. Krishnakumar, W.L. Kraus, The PARP Side of the Nucleus: Molecular Actions, Physiological Outcomes, and Clinical Targets, Mol Cell, 39 (2010) 8-24.
[86] P.C. Fong, D.S. Boss, T.A. Yap, A. Tutt, P.J. Wu, M. Mergui-Roelvink, P. Mortimer, H. Swaisland, A. Lau, M.J. O'Connor, A. Ashworth, J. Carmichael, S.B. Kaye, J.H.M. Schellens, J.S. de Bono, Inhibition of Poly(ADP-Ribose) Polymerase in Tumors from BRCA Mutation Carriers., New Engl J Med, 361 (2009) 123-134.
[87] M.S. Goldberg, D.Y. Xing, Y. Ren, S. Orsulic, S.N. Bhatia, P.A. Sharp, Nanoparticle-mediated delivery of siRNA targeting Parp1 extends survival of mice bearing tumors derived from Brca1-deficient ovarian cancer cells, Proceedings of the National Academy of Sciences of the United States of America, 108 (2011) 745-750.
[88] M. Tsai, Z. Lu, J. Wang, T.K. Yeh, M.G. Wientjes, J.L.S. Au, Effects of carrier on disposition and antitumor activity of intraperitoneal paclitaxel, Pharmaceutical research, 24 (2007) 1691-1701.
[89] B. Urban-Klein, S. Werth, S. Abuharbeid, F. Czubayko, A. Aigner, RNAi-mediated gene-targeting through systemic application of polyethylenimine (PEI)-complexed siRNA in vivo, Gene therapy, 12 (2005) 461-466.

3

COLLOIDAL STABILITY OF NANO-SIZED PARTICLES IN THE PERITONEAL FLUID: TOWARDS OPTIMIZING DRUG DELIVERY SYSTEMS FOR INTRAPERITONEAL THERAPY

Parts of this chapter are published as:

George R. Dakwar[1], Elisa Zagato[1,2], Joris Delanghe[3], Sabrina Hobel[4], Achim Aigner[4], Kevin Braeckmans[1,2], Wim Ceelen[5], Stefaan C. De Smedt[1], Katrien Remaut[1], Colloidal stability of nano-sized particles in the peritoneal fluid: Towards optimizing drug delivery systems for intraperitoneal therapy. *Acta Biomaterialia*, 10, 2965-2975 (2014).

[1] Ghent Research Group on Nanomedicines, Faculty of Pharmaceutical Sciences, Laboratory for General Biochemistry and Physical Pharmacy, Ghent University, Ghent, Belgium

[2] Center for Nano- and Biophotonics, Ghent University, Ghent, Belgium

[3] Laboratory for Clinical Biology, Department of Clinical Chemistry, Microbiology and Immunology, Ghent University Hospital, Ghent, Belgium

[4] Rudolf Boehm Institute of Pharmacology and Toxicology, Clinical Pharmacology, Leipzig University, Leipzig, Germany

[5] Department of Surgery, Laboratory of Experimental Surgery, Ghent University Hospital, Ghent, Belgium

Abstract

Intraperitoneal (IP) administration of nano-sized delivery vehicles containing small interfering RNA (siRNA) is recently gaining attention as an alternative route for the efficient treatment of peritoneal carcinomatosis (PC). The colloidal stability of nanomatter following IP administration has, however, not been thoroughly investigated yet. Here, enabled by advanced microscopy methods such as Single Particle Tracking (SPT) and Fluorescence Correlation Spectroscopy (FCS), we follow the aggregation and cargo release of nano-scaled systems directly in peritoneal fluids from healthy mice and ascites fluid from a patient diagnosed with PC. The colloidal stability in the peritoneal fluids was systematically studied in function of the charge (positive or negative) and Poly-Ethylene Glycol (PEG) degree of liposomes and polystyrene nanoparticles (NPs), and compared to human serum. Our data demonstrate strong aggregation of cationic and anionic NPs in the peritoneal fluids, while only slight aggregation was observed for the PEGylated ones. PEGylated liposomes, however, lead to a fast and premature release of siRNA cargo in the peritoneal fluids. Based on our observations, we reflect on how to tailor improved delivery systems for IP therapy.

Keywords: Drug delivery, Aggregation, Peritoneal Carcinomatosis, Intraperitoneal administration, Release, siRNA

1. Introduction

Peritoneal metastases are one of the major causes of death in patients diagnosed with ovarian cancer [2]. Also in colorectal cancer, cancer cells often migrate to the abdomen where they spread and form PC [1]. The often late stage of discovery of peritoneal metastases, which can spread over the entire surface of the peritoneum (~2 m²), make the treatment very difficult. This fact is well-demonstrated from clinical trials indicating the low median survival of patients diagnosed with PC [3].

Current treatment of PC involves removing the majority of peritoneal metastases (cytoreductive surgery) followed by intravenous (IV) administration of chemotherapeutic agents such as oxaliplatin in combination with 5-fluorouracil or leucovorin [4,5] to kill remaining tumor cells. Also platinum-based (i.e. oxaliplatin, cisplatin) chemotherapeutics in combination with paclitaxel [6,7] are used. Unfortunately, the majority of the patients develop disease recurrence [8,9]. Therefore, more efficient post-surgical strategies to kill remaining tumor cells are needed [10]. In this context, intraperitoneal (IP) administration of chemotherapeutics has shown to be superior over the IV route [11,12], particularly due to the ability to maintain high concentrations of cytotoxic agents in the peritoneal cavity [13]. Also, promising data have resulted from clinical trials evaluating hyperthermic intraperitoneal chemoperfusion (HIPEC) immediately after cytoreductive surgery [14,15]. HIPEC involves flushing the peritoneal cavity with chemotherapeutic agents at an elevated temperature of 41-42°C. It is hypothesized that HIPEC is more efficacious compared to conventional IP therapy since it not only takes advantage of the hyperthermic effect, but also enables distribution of the drug in all parts of the peritoneal cavity [16]. Nevertheless, the efficacy of HIPEC is still controversial as several studies claim that no synergistic effect exists between the anti-cancer agent and the hyperthermia [15,17].

One strategy to improve the anticancer effect upon cytoreductive surgery is to use specialized drug delivery systems (DDSs) with the ability to reside in the peritoneal cavity for a prolonged period of time. Interestingly, recent *in vivo* data suggest that the IP administration of DDSs that release chemotherapeutics results in an enhanced body distribution in general, and on the intratumoral level in particular [18]. Also the delivery of small interfering RNA (siRNA) for the treatment of ovarian cancer and PC has recently attracted considerable attention [19]. siRNAs are small (20-21 nucleotides) double stranded RNA molecules that can downregulate specific protein production. siRNA has the benefit that it can target genes which are specific for tumor cells, leaving healthy, non-tumor tissue unaffected. Interestingly, carriers for combinatorial therapy of (specific) siRNA and conventional (non-specific) anti-cancer drugs (e.g. paclitaxel (PTX) or doxorubicin (DOX)) have been reported to result in some benefits compared to each one alone [20].

In the past few years, different DDSs were evaluated for IP administration [21,22], Among them are targeted nanocarriers [23], NPs for IP gene delivery [24], micelles [25], microparticle (MP) [26,27] and hydrogels for sustained release in the peritoneal cavity [28-30]. For nanosized drug carriers, the state of aggregation and the release profile following IP administration may play a crucial role in their delivery performance. Indeed, the colloidal stability of nanocarriers influences e.g. the internalization of the cargo into cancer cells, and thus may alter the expected anti-tumor efficacy. Following administration, nano-carriers tend to bind/interact with various components that are present in biofluids [31], including proteins and enzymes forming the so called 'protein corona' [32,33]. For instance, recent reports suggest that the targeting capability of ligands conjugated to nanomaterials is lost by adsorption of a protein corona to their surface [34,35]. Increasing our knowledge on the relation between the physicochemical properties of delivery systems and their obtained therapeutic effect is crucial. Since the route of administration plays a major role in whether or not certain carriers will work, each carrier should be optimized for the *in vivo* situation where it is intended to be used, e.g. the peritoneal fluid in the case of IP delivery. Although several studies have addressed the colloidal stability of NPs in biofluids like blood, plasma and serum [36,37], the physicochemical behavior of delivery vehicles in terms of aggregation and release of cargo in peritoneal fluids has not been investigated yet.

The main objective of this study is to provide insight in the requirements for IP delivery systems in terms of charge and PEGylation degree, to be colloidally stable and to have an optimal release profile in the peritoneal fluid. Herein, for the first time, we study the aggregation of polystyrene (PS) NPs and liposomal formulations in peritoneal fluid from healthy mice (transsudate) and ascites fluid (exudate) from a patient diagnosed with PC. Additionally, we study the release profile of liposomal formulations carrying siRNA in the peritoneal fluids. For this purpose, we utilize state of the art fluorescence techniques that were previously developed in our laboratory, namely Single Particle Tracking (SPT) and Fluorescence Correlation Spectroscopy (FCS) to respectively gain information on the aggregation of NPs and the release of siRNA in undiluted biofluids [36,38]. The results are compared to measurements of the same NPs dispersed in human serum.

2. Materials and Methods

2.1 Materials

(2,3-Dioleoyloxy-propyl)-Trimethylammonium-chloride (DOTAP) and 1,2-Dioleoyl-sn-glycero-3-phosphoethanolamine (DOPE) were purchased from Corden Pharma LLC (Liestal, Switzerland).

1,2-distearoyl-*sn*-glycero-3-phosphoethanolamine-N-[methoxy(polyethyleneglycol)-2000] (DSPE-PEG) was purchased from Avanti Polar Lipids (Alabaster, AL, USA). Chloroform, 4-(2-hydroxyethyl)-1-piperazineethanesulfonic acid (HEPES), N-hydroxysulfosuccinimide (Sulfo-NHS), 1-ethyl-3-(3-dimethylaminopropyl) carbodiimide hydrochloride (EDC), Dimethylethylenediamine (DMEDA) and sodium chloride (NaCl) were purchased from Sigma Aldrich (Bornem, Belgium). Yellow-green fluorescent (λ_{ex}= 505 nm, λ_{em}= 515 nm) carboxylated PS FluoSpheres (0.1 µm in size) and 1, 1'-dioctadecyl-3, 3, 3', 3'-tetramethylindodicarbocyanine perchlorate (DID) (λ_{ex}= 644 nm, λ_{em}= 665 nm) were purchased from Invitrogen (Merelbeke, Belgium). Methoxy-polyethylene glycol-amine (mPEGa) 2 kDa was purchased from Creative PEGWorks (Winston Salem, USA). Alexa Fluor-488 Negative Control siRNA ((Eurogentec, Seraing, Belgium).

2.2 Animals

Mice, heterozygous for Foxn1 (nu/+) were purchased from Charles River (Sulzfeld, Germany) and maintained by the animal core facility. Animals were kept at 22°C in a humidified atmosphere with food and water ad libitum.

2.3 Collection of biofluids

To collect samples containing mouse peritoneal fluid, a lavage of the peritoneal cavity was performed. To this end, mice were euthanized by an overdose of the inhalation anesthetic isoflurane followed by cervical dislocation. The abdominal wall was opened immediately and the peritoneal cavity was washed with 1 mL of water. The lavage was taken and stored frozen until use. The procedure was approved and carried out in compliance with the guidelines for animal experiments of Leipzig University.

Human serum was obtained from a healthy donor. Briefly, blood was collected at the Ghent University Hospital into Venosafe™ 6 mL tubes containing gel and clotting activator (Terumo Europe™, Leuven, Belgium). Then the tubes were centrifuged for 10 minutes at 4,000 × g and 20°C. The supernatant (serum) was transferred into microvette® 500 Z-Gel (SARSTEDT, Numbrecht, Germany) and centrifuged for 5 min at 1,0000 × g and 20°C. The serum was portioned into 50 µl aliquots (to avoid freezing-thawing cycles) in sterile polypropylene tubes and stored in -20°C until use. Human ascites fluid was obtained from a patient diagnosed with PC at

the medical oncology department, Ghent University hospital. The experiments with the ascites fluid were approved by the ethics committee of the Ghent University hospital (# 2013/589).

2.4 Protein analysis and capillary electrophoresis

Total protein in human serum, human ascites fluid, and mice peritoneal fluid was assayed using a pyrogallol red-molybdate method on a Cobas 8000 analyzer (Roche, Mannheim, Germany) [39].

Human serum and human ascites fluid protein electrophoresis was performed using a Capillarys 2™ CE system (Sebia, Paris, France) that is routinely employed in clinical laboratories [40,41]. Prior to the hydrodynamic injection (4”), 40 µl of serum is automatically diluted 5x in the running buffer (pH 10). Then, 7 kV is applied in the 8 silica-fused capillaries (effective length 15.5 cm; internal diameter 25 µm; optical cell 100 µm) for 4’ at 35.5°C (Peltier device). Proteins are detected at the cathode (deuterium lamp; 200 nm) as 5 fractions (γ-globulins, β-globulins, α2-globulins, α1-globulins and albumin) that are automatically quantified as percentages of the total signal.

For mice peritoneal fluid (characterized by low protein concentrations), agarose gel electrophoresis was carried out, followed by a sensitive staining using the Protur HiSi 100 system (Analis, Suarlée, Belgium).

2.5 Viscosity measurements

Viscosity measurements of human ascites fluid and human serum were performed using a micro-Ubbelohde viscometer (53610/I) (Schott-Geräte (Mainz, Germany) at 22°C. 4 mL of each bio fluid were loaded on a capillary (ID number 100-002 with capillary constant K= 0.009671 mm^2/s^2) and the flow time (in seconds) was measured 3 times for each biofluid. The averaged flow time was used to calculate the kinematic viscosity according to the following equation:

$$v = K\times (t-y)$$

Where t is the averaged flow time, and y (in seconds) is the kinetic energy correction for the flow time provided by the manufacturer. For human serum, the calculated kinematic viscosity is 1.6 mm^2/s and for the human ascites fluid is 1.39 mm^2/s. The dynamic viscosity η is defined using the following relation:

$$\eta = \rho \times v$$

Where ρ is the density of fluid (g/mL) and 1 cSt = 1 mm^2/s. Since the density of human serum and human ascites fluid is very close to 1 g/mL [42], we assume all the densities of fluids used in this study are equal to 1, and thus in all Single Particle Tracking measurements the following values of dynamic viscosity were used: 1.39 cP for human ascites fluid, 1.6 cP for human serum, and 0.94 cP for mice IP fluid and HEPES buffer.

2.6 Functionalization of anionic polystyrene NPs

Functionalization of 100 nm anionic NPs to PEGylated and positively charged ones was performed according to previously published procedures [43]. The charge and size of the NPs was measured using the Zetasizer Nano-ZS (Malvern, Worcestershire, UK). The average size of all the NPs in HEPES buffer (pH 7.4) was around 110 nm, and zeta-potential around 30 mV for the positively charged NPs, -13 mV for the PEGylated NPs, and around -33 mV for the anionic NPs.

2.7 Preparation of liposomes

DOTAP and DOPE lipids were dissolved in chloroform and mixed in a round bottomed flask. A lipid film was formed by rotary evaporation of the chloroform at 40°C. The dried lipid film was rehydrated with 20 mM HEPES buffer pH 7.4, resulting in a final concentration of 5 mM DOTAP and 5 mM DOPE. Thereafter, liposomes were sonicated using a probe sonicator (Branson Ultrasonics Digital Sonifier®, Danbury, USA). For the preparation of PEGylated liposomes, the desired amounts of DSPE-PEG dissolved in chloroform (corresponding to 5 mol% or 10 mol% of the total lipids) were added to the lipids in the round bottomed flask before evaporation. For SPT experiments, liposomes were fluorescently labeled by incorporation of 1 mol% (of the total lipids) with DID. The average size and zeta potential of the liposomes was measured using Zetasizer Nano-ZS (Malvern, Worcestershire, UK). The average diameter of the liposomes was around 90 nm for the cationic liposomes and 100 nm for the PEGylated ones. The zeta potential around + 45 mV for the cationic liposomes, 15 mV for the 5 mol% PEGylated liposomes and 7 mV for the 10 mol% liposomes.

2.8 Size and zeta-potential measurements

The average size and the zeta potential of the liposomes and the PS NPs were measured using the Nano-ZS Zetasizer (Malvern, Worcestershire, UK) in 4 different biofluids: HEPES buffer, mice IP fluid, human ascites fluid, and human serum. Equal volumes of respectively cationic, 5% PEGylated and 10% PEGylated liposomes and biofluids were mixed and incubated for 1 h at 37°C. At the end of the incubation period, these mixtures were diluted with 20 mM HEPES buffer to a final concentration of 125 μM DOTAP (~2.5 vol% of biofluids). The size and ζ-potential measurements were performed at 25°C. The size and the zeta potential of the PS NPs were determined following the same procedure.

2.9 Fluorescence single particle tracking (fSPT)

Single particle tracking (SPT) is a fluorescence microscopy technique that uses wide-field laser illumination and a fast and sensitive CCD camera to record high speed movies of individual diffusing particles in biofluids. Thereafter, the movies are analyzed by a specific image processing algorithm to obtain the motion trajectories for all individual particles. The trajectories are then used to calculate the diffusion coefficient of each particle. After analyzing many particles, a

distribution of diffusion coefficients is obtained which is transformed into size distribution using the Stokes-Einstein equation and refined by the maximal entropy method (MEM), as previously described [36]. The conversion of diffusion coefficients to sizes requires knowledge of the viscosity of the biofluid and the temperature at which the experiment is performed.

SPT measurements on different PS NPs (Anionic, PEGylated, Cationic) and DID labeled liposomes dispersed in biofluids were performed as follows. First, formulations were diluted 400 times in HEPES buffer. Then 5 µl was added to 45 µl of biofluid (e.g. 90 vol% of mice IP fluid, human ascites fluid and human serum), and incubated for 1 h at 37°C in a 96-well plate (Greiner bio-one, Frickenhausen, Germany). At the end of the incubation time, the sample was placed on the custom-built SPT set-up [36] and movies were recorded focused at about 5 µm above the bottom of the glassbottom 96-well plate. Videos were recorded at room temperature (22.5°C) with the NIS Elements software (Nikon) driving the EMCCD camera (Cascade II:512, Roper Scientific, AZ, USA) and a TE2000 inverted microscope equipped with a 100× NA1.4 oil immersion lens (Nikon). Analysis of the videos was performed using in-house developed software. During the incubation and measurements, the well plate was covered with Adhesive Plates Seals (Thermo Scientific, UK) to avoid evaporation of the sample and allow diffusion only.

2.10 FCS on siRNA containing liposomes (lipoplexes)

FCS is a microscopy-based technique that monitors the fluorescence intensity fluctuations of molecules diffusing in and out of the focal volume of a confocal microscope. Shortly, when free siRNA molecules are present in the focal volume, a fluorescence signal (baseline) is obtained which is proportional to the local siRNA concentration. When the siRNA is complexed with NPs, the concentration of free siRNA (e.g. the baseline) drops and peaks of high fluorescence intensity appear each time a nanocomplex containing many fluorescent siRNA molecules passes the detection volume. Vice versa, when siRNA dissociates from the complexes, the concentration of free siRNA increases again, resulting in an increase of the baseline. The drop/increase in the intensity of the baseline can be used to calculate the percentage of the complexed/released siRNA as was previously described by Buyens et al. [38]. Single color FCS measurements were performed on LPXs containing Alexa-488 siRNA Negative Control siRNA (Eurogentec, Seraing, Belgium). To follow the release of the complexed siRNA in function of time, LPXs with charge ratio of ±8 were prepared by adding appropriate amounts DOTAP DOPE liposomes to siRNA. The mixture was then incubated at room temperature for 30 minutes to allow formation of the LPXs. The size of the LPXs was measured using dynamic light scattering and was about 100 nm for cationic ones and 110 nm for the PEGylated. For FCS measurements, 5 µl of the LPXs were diluted in 45 µl of each biofluid (resulting in 90 vol% of mice IP fluid, human ascites fluid and human serum in the final samples) and the fluorescent signal was measured respectively immediately after mixing the LPXs with the biofluids and after one hour of incubation at 37°C. During the

incubation and the FCS measurements, the well plate was covered with Adhesive Plates Seals (Thermo Scientific, UK) to avoid evaporation of the sample and to minimize flow.

FCS measurements were performed on C1si laser scanning confocal microscope (Nikon, Japan), equipped with a Time-Correlated Single Photon Counting (TCSPC) Data Acquisition module (Picoquant, Berlin, Germany). The laser beam was held stationary and was focused through a water immersion objective lens (Plan Apo 60×, NA 1.2, collar rim correction, Nikon, Japan), at about 50 μm above the bottom of the glassbottom 96-well plate (Grainer Bio-one, Frickenhausen, Germany), which contained the fluorescent samples (free Alexa488-siRNA and Alexa488-siRNA complexed to non-PEGylated, 5% PEGylated or 10% PEGylated liposomes (5 nM Alexa488-siRNA in all samples). The 488 nm laser beam of a krypton–argon laser (Bio-Rad, Cheshire, UK) was used and the green fluorescence intensity fluctuations were recorded using Symphotime (Picoquant, Berlin, Germany) during at least 60 seconds.

3. Results

3.1 Protein content of the biofluids

The data in Table 1 depicts the total protein content in each biofluid. The highest protein content was determined in the human serum samples obtained from a healthy donor. Ascites fluid from the peritoneal cavity of a patient diagnosed with PC contained almost half the amount of proteins when compared to human serum. Peritoneal fluid extracted from mice was found to contain a rather low protein concentration. This most likely can be attributed to the collection procedure in which the peritoneal fluid of mouse was diluted between 10-50 times at least, unlike the human serum and ascites fluid, where the collection procedure did not involve any dilution. With regard to the type of proteins found in each sample, capillary electrophoresis of the human serum and ascites fluid reveals a very similar composition, with a major fraction of albumin (Figure 1A and 1B). Also mouse peritoneal fluid contains a major albumin fraction (68 KDa) and a prominent transferrin (Tfr) fraction (80 KDa) (Figure 1C).

Table 1. Total protein of the studied biofluids

Sample analyzed	Total protein (mg/dl)
Mice IP fluid	183.84
Human ascites fluid	3296.4
Human serum	6244

It should be noted that in the case of PC, the high protein content observed in the ascites fluid is attributed to the increased permeability of the peritoneal membrane induced mainly by vascular endothelial growth factor (VEGF) [44]. In patients with an earlier stage of PC, the total amount of proteins present in the peritoneal fluid is expected to be less. Nevertheless, a relative protein composition, similar as in Figure 1B is expected.

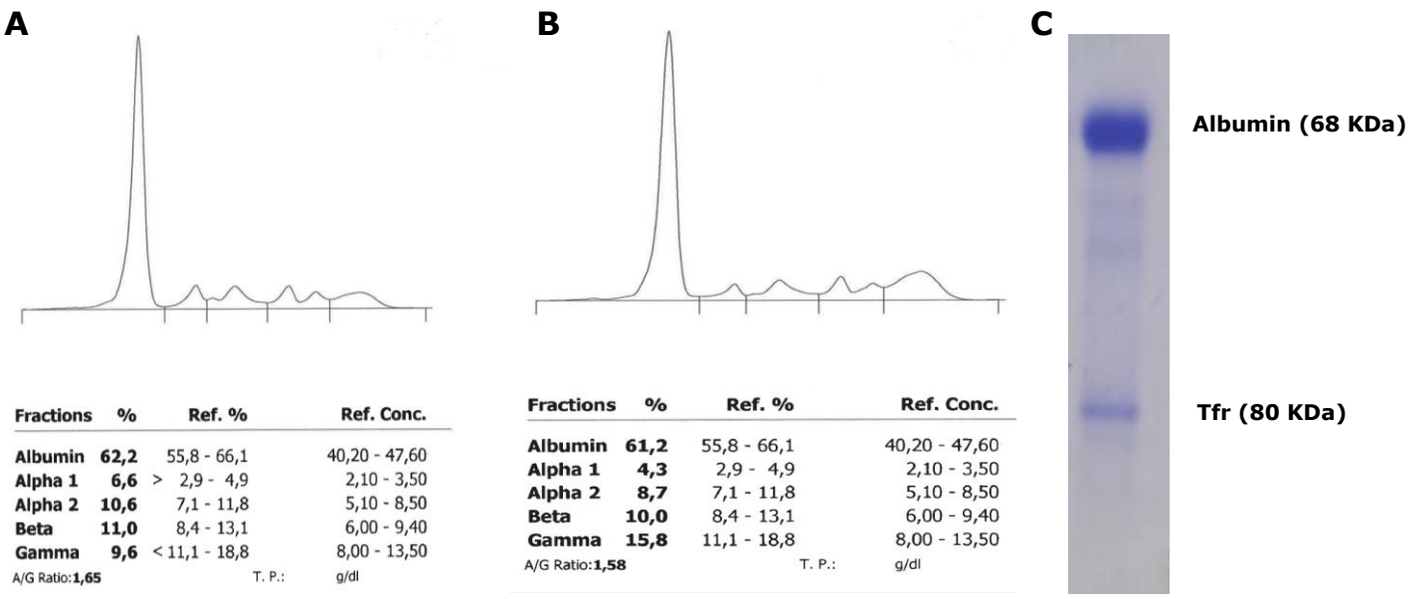

Fractions	%	Ref. %	Ref. Conc.
Albumin	62,2	55,8 - 66,1	40,20 - 47,60
Alpha 1	6,6	> 2,9 - 4,9	2,10 - 3,50
Alpha 2	10,6	7,1 - 11,8	5,10 - 8,50
Beta	11,0	8,4 - 13,1	6,00 - 9,40
Gamma	9,6	< 11,1 - 18,8	8,00 - 13,50

A/G Ratio:**1,65** T. P.: g/dl

Fractions	%	Ref. %	Ref. Conc.
Albumin	61,2	55,8 - 66,1	40,20 - 47,60
Alpha 1	4,3	2,9 - 4,9	2,10 - 3,50
Alpha 2	8,7	7,1 - 11,8	5,10 - 8,50
Beta	10,0	8,4 - 13,1	6,00 - 9,40
Gamma	15,8	11,1 - 18,8	8,00 - 13,50

A/G Ratio:**1,58** T. P.: g/dl

Figure 1. Capillary electrophoresis of (A) ascites fluid, **(B)** human serum and **(C)** agarose gel electrophoresis of peritoneal fluid collected from mice.

3.2 Colloidal stability of PS NPs and liposomes in diluted peritoneal fluids and serum

The data in Figure 2 demonstrate the size and the zeta-potential of PS NPs measured by DLS following 1 h of incubation at 37°C in each of the studied biofluids. Samples were incubated in 50 vol% of biofluids and further diluted to 2.5% biofluids for the actual measurements. As illustrated in Figure 2A (note the broken axis), cationic NPs (white bars) show pronounced aggregation in biofluids with a low protein concentration and less aggregation in biofluids with a high protein content. This aggregation is accompanied by a significant decrease in the zeta potential: the positively charged NPs (+ 28 mV) in HEPES buffer turn negative upon dispersing them in the biofluids (Figure 2B). Interestingly, an "opposite" aggregation pattern was observed with the anionic NPs (dark grey bars), whose state of aggregation seemed to be correlated with the protein content of the biofluids. Yet, when compared to cationic polystyrene NPs, this aggregation was less pronounced. Notably, the zeta potential of the anionic NPs increases from -33 mV in HEPES buffer to less negative NPs in the rest of the biofluids. The size of the PEGylated NPs (Figure 2A, grey bars) did not change upon incubation in the biofluids, indicating that the PEG-chains effectively inhibit aggregation.

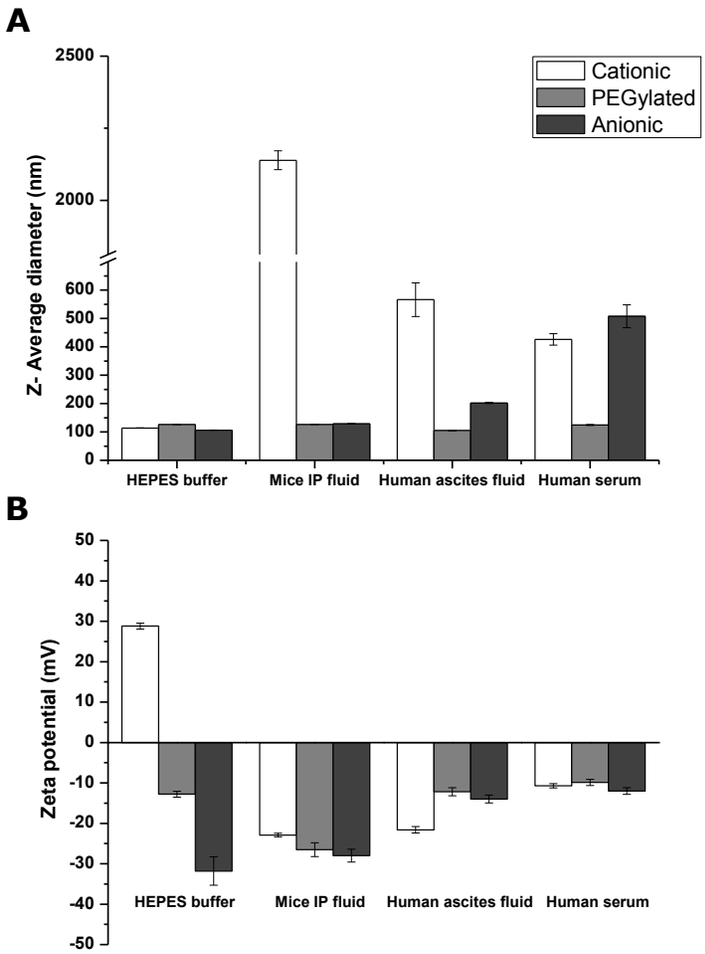

Figure 2. (A) average size and **(B)** zeta-potential of cationic (white bars), PEGytlated (grey bars)and anionic (dark grey bars) PS NPs following 1 h incubation at 37°C with the different biofluids: HEPES buffer, mice IP fluid, ascites fluid and human serum (n=3).

As liposomes are widely used in drug delivery and hold potential for siRNA delivery in the peritoneal cavity, it is of interest to have an insight on the aggregation profile of different liposomal formulations in IP fluid. Therefore, we investigated the colloidal stability upon incubating non-PEGylated, 5% PEGylated and 10% PEGylated liposomes in the biofluids. The data in Figure 3 show the hydrodynamic diameter and the zeta potential of cationic and PEGylated liposomal formulations following 1 h of incubation in the biofluids. It can be seen that the extent of aggregation (Figure 3A, broken axis) is more severe in human serum > ascites fluid > mice IP fluid which correlates with the protein content of the biofluids (Table 1). In particular, the aggregation is the most pronounced for the cationic liposomes (white bars), while PEGylation significantly diminishes aggregation of cationic liposomes, indicating that the PEG chains improve the colloidal stability of the cationic liposomes. As can be seen from Figure 3B, a drop in the zeta potential was observed for all the liposomal formulations upon dispersing them in the biofluids (especially in human serum and ascites fluid).

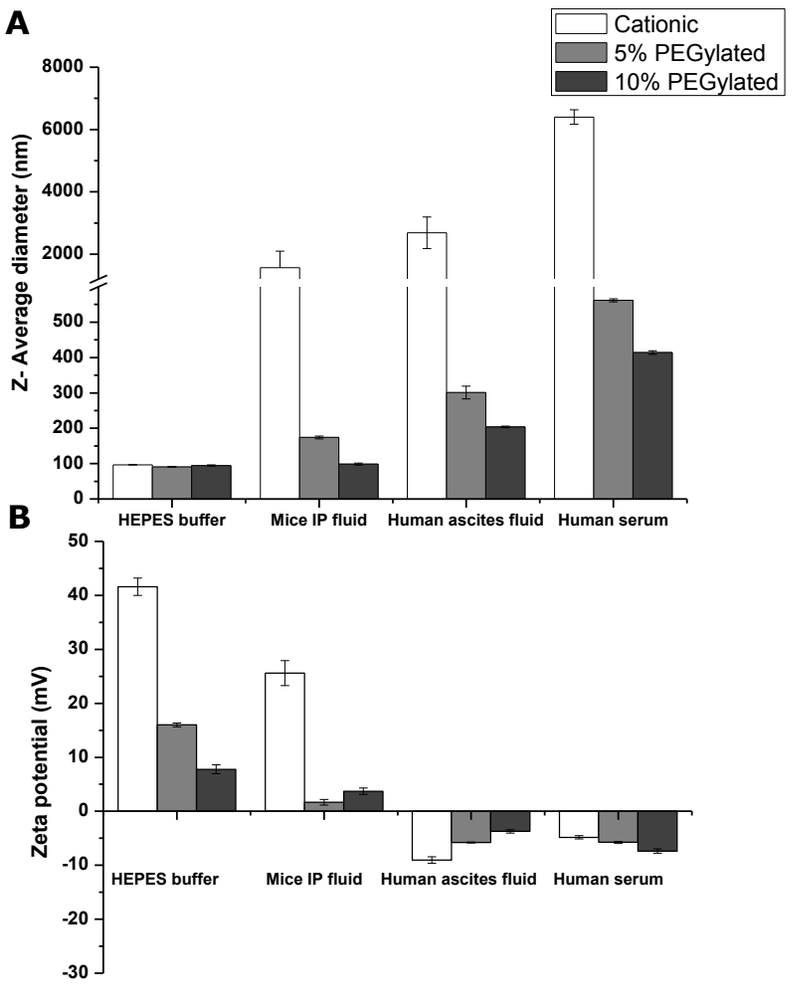

Figure 3. (A) average size and **(B)** zeta-potential of cationic (white bars), 5% PEGytlated (grey bars) and 10% PEGylated (dark grey bars) DOTAP DOPE liposomes following 1 h incubation at 37°C with the different biofluids: HEPES buffer, mice IP fluid, ascites fluid and human serum (n=3).

3.3 Aggregation of PS NPs and liposomes in undiluted biofluids

Dynamic light scattering (DLS) is the most common technique to measure the average size of NPs in aqueous media. However, measuring the size of NPs in biofluids by DLS is challenging as proteins in the biofluids can scatter the light and interfere with the measurements. As an example size distributions of the biological fluids only diluted in HEPES buffer are shown in Supplemental Figure 1A and Figure 1B. Therefore, the DLS measurements in the previous sections were performed on highly diluted samples (only 2.5 vol% of biofluids in Figure 2 and Figure 3).

We have previously shown that SPT is a powerful technique to measure the size of NPs in undiluted biofluids such as serum and blood [36,45,46]. Here, we present for the first time the aggregation behavior of NPs in undiluted peritoneal fluids, and compared the aggregation profile with the one obtained in buffer and human serum. A particular benefit of SPT is that size measurements are performed on a per particle basis so that, contrary to DLS, there is no bias towards larger sizes.

The size distributions of the PS NPs, as obtained by SPT in undiluted biofluids, are depicted in Figure 4 in line with the DLS data (Figure 2A), on average 100 nm size particles are observed in HEPES buffer. In the biological fluids, particles sizes increase to about 200 nm in human serum, 300 nm in ascites fluid and even μm sized aggregates in mice IP fluid, again confirming the DLS results. For the anionic NPs (Figure 4B), a different aggregation pattern was observed: only a slight increase in size was noticed for the ascetic and mice IP fluid, while a broadened distribution was observed in human serum. In the case of PEGylated NPs (Figure 4C), the particles remained stable in mice and ascites IP fluid. Also, human serum resulted only in a very minor increase in size compared to the buffer sample. These findings are all consistent with the trends observed by DLS (Figure 2A).

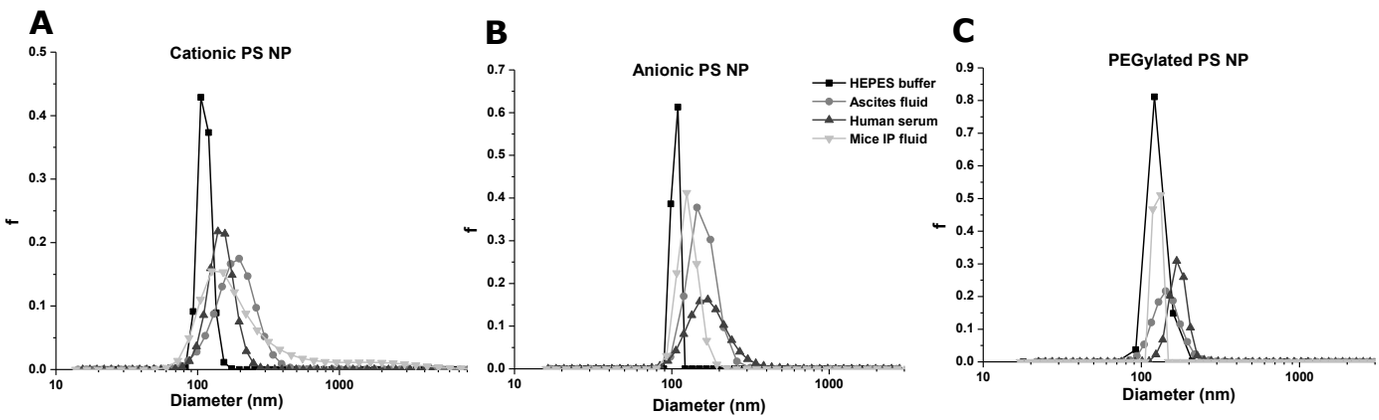

Figure 4. SPT sizing of (A) cationic, **(B)** anionic and **(C)** PEGylated PS NPs following 1 h incubation at 37°C with 90 vol% of biofluids: HEPES buffer, mice IP fluid, ascites fluid and human serum.

The aggregation behavior of the liposomes dispersed in the undiluted biofluids is shown in Figure 5 and Figure 6. For the cationic liposomes, large non-diffusing aggregates (up to 2-3 μm) in size were observed at the bottom of the well following 1 h of incubation in mice IP fluid, ascites fluid and human serum (Figure 5). As these aggregates did not show Brownian motion, SPT data could not be obtained.

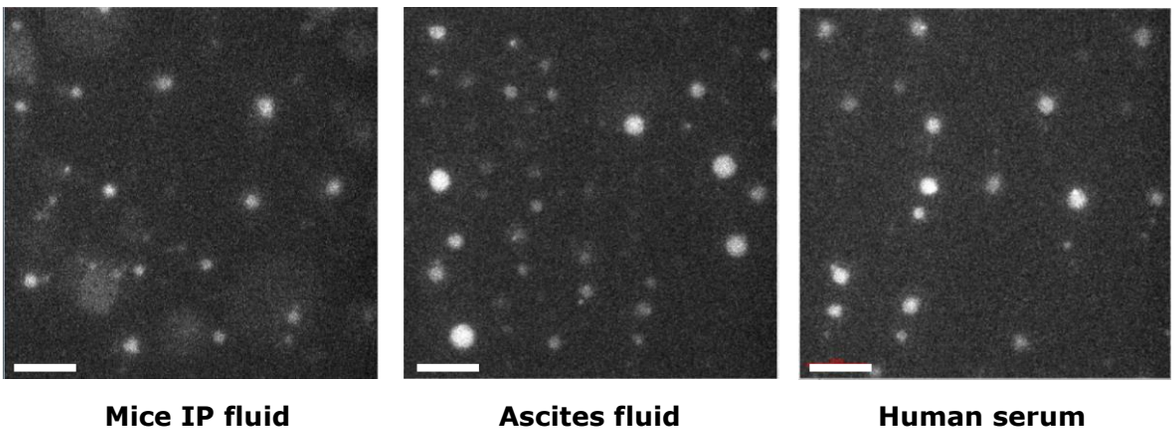

Figure 5. Snapshots of non-diffusing aggregates following 1 h incubation at 37°C of cationic DOTAP DOPE liposomes with 90 vol% of biofluids: HEPES buffer, mice IP fluid, ascites fluid and human serum. The scale bar corresponds to 10 µm.

The size distributions of the 5% PEGylated liposomes (Figure 6A) confirm the outcome of the DLS data in Figure 3A, and show the profound aggregation of these liposomes in human serum. In the mice IP fluid and ascetic fluid, this aggregation is less prominent. Finally, the 10% PEGylated liposomes hardly aggregate in the peritoneal fluids. In human serum, at least a part of the liposomes did not aggregate as can be seen from the bimodal behavior. Note that the size distribution for the 10% PEGylated liposomes in HEPES buffer seems broader than the one for the 5% PEGylated liposomes. Possibly, this is due to the structure the liposomes adopt with higher degrees of PEGylation, including small disks and large aggregates which contribute to the polydispersity of the sample [47].

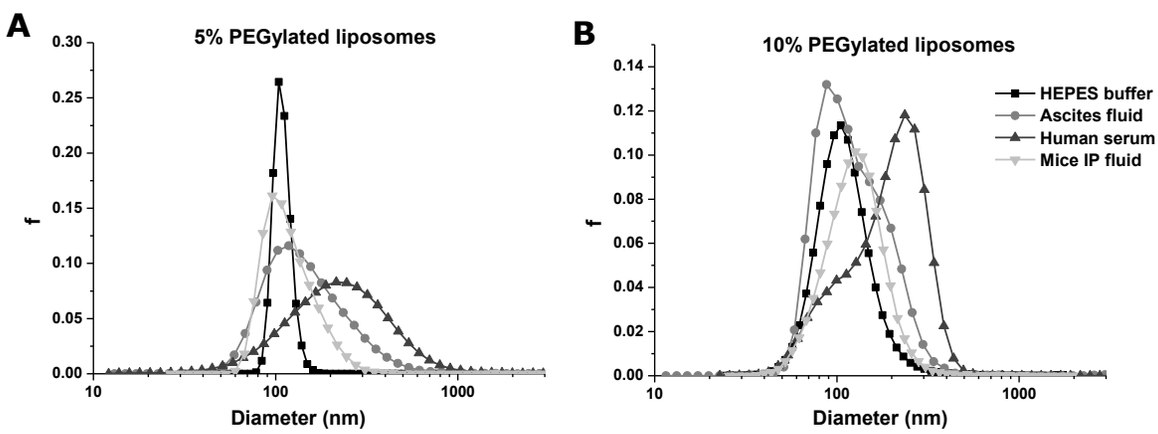

Figure 6. SPT sizing of (A) 5% PEGylated liposomes and **(B)** 10% PEGylated DOTAP DOPE liposomes following 1 h incubation at 37°C with 90 vol% of biofluids: HEPES buffer, mice IP fluid, ascites fluid and human serum.

3.4 Release of siRNA from liposomes in undiluted biofluids

siRNA has the potential to treat peritoneal metastasis by preventing the growth and spread of circulating tumor cells. For siRNA to be biologically active, it needs to reach the cytoplasm of the tumor cells. Therefore, it is generally 'complexed' with cationic carriers such as polymers or liposomes, as 'naked' siRNA is not taken up by cells. In the next set of experiments, we aimed to determine the stability of siRNA-liposome complexes in peritoneal fluids, with respect to siRNA release from the formulations. When siRNA is prematurely released from the complexes in the biofluids, the biological activity will be lost. The percentage of free siRNA in HEPES buffer at the zero hour time point (Figure 7A, grey bars), shows the amount of siRNA that remained free (e.g. uncomplexed) when the siRNA/liposome complexes were formed. About 2%, 6% and 15% of siRNA is not encapsulated in respectively the cationic, 5% PEGylated and 10% PEGylated liposomes. This indicates that a higher PEGylation degree lowers the siRNA encapsulation efficiency. Following 1 h of incubation, the effect of PEGylation becomes even more pronounced: only the non-PEGylated liposomes retain the complexed siRNA. For the 5% and 10% PEGylated liposomes, respectively 30% and even 85% of siRNA is released into HEPES buffer. Next, the siRNA containing complexes were incubated with the undiluted biofluids. When compared to HEPES buffer (Figure 7A, grey bars), we observe an immediate release of siRNA at the zero time point upon dispersing the complexes in the biofluids (Figure 7, B-D, grey bars). This immediate release most likely corresponds to the release of surface-bound siRNA and increases with PEGylation degree. Further incubating the complexes in the biofluids for 1 h did not result in a substantial additional release of siRNA (Figure 7B-D**,** white bars), except for the 5% PEGylated complexes in human serum (Figure 7D, white bars). Overall, the siRNA release was limited to maximally 30% for the cationic liposomes, while for the 5% and 10% PEGylated liposomes, between 65-80% of siRNA was released into the peritoneal fluids and even close to 100% siRNA was released in human serum after 1 h.

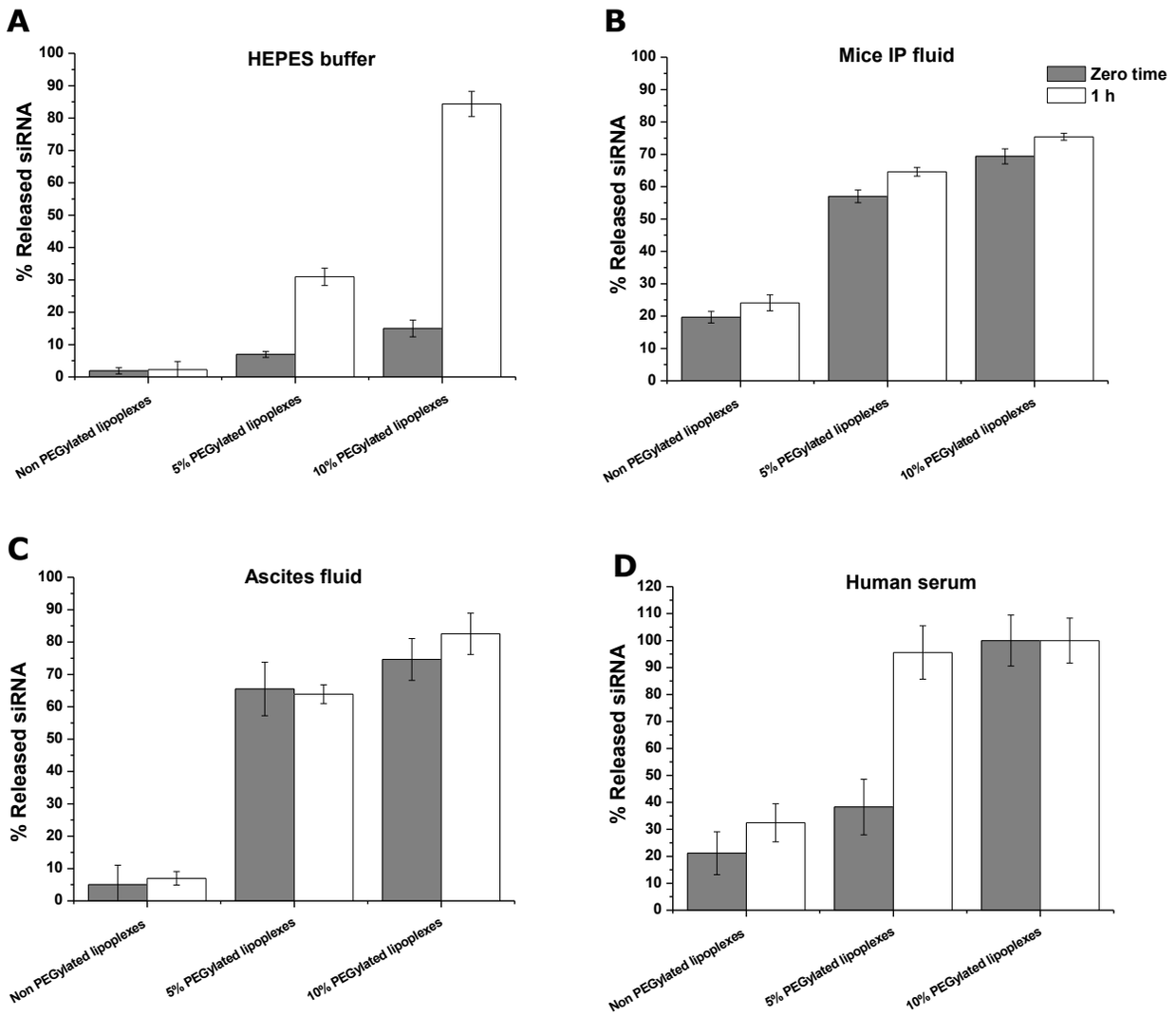

Figure 7. Percentage of siRNA release of non-PEGylated and PEGylated AF-488 siRNA-liposome complexes (±8) determined by FCS analysis, in 90 vol% biofluids: of **(A)** HEPES buffer, **(B)** mice IP fluid, **(C)** ascites fluid and **(D)** human serum immediately after preparation (grey bars) and following 1 h incubation at 37°C (white bars).

4. Discussion

Designing new delivery systems for targeting peritoneal cancer cells is a major challenge. Apart from the IV route of administration, IP delivery of NPs that target cancer cells over a prolonged period of time is being explored. Upon IP delivery, NPs are directly administered at the target site. Hence, interactions of the NPs with blood components that potentially induce immune responses or stability issues could be avoided [48]. The stability of NPs in the IP fluid is a major determinant for their efficacy. Indeed, either particle aggregation or premature release of cargo in the IP fluid could diminish the biological effect. The colloidal stability of NPs in IP fluids has, however, not been

studied in detail before. In this study, we employed advanced microscopy techniques to directly assess stability of NPs in terms of aggregation and cargo release, in undiluted biofluids such as mice IP fluid and ascites fluid from a patient diagnosed with PC and compared it to human serum.

4.1 Aggregation of model PS NPs and liposomes in peritoneal fluids

Aggregation of different PS NPs and liposomal formulations in the peritoneal fluids was tested using DLS and SPT. Two main questions were addressed, namely: (1) does the physicochemical properties of the material (e.g. charge and PEGylation degree) influence aggregation and (2) does the concentration of the proteins in each of the biofluids correlate with the aggregation profiles?

PS NPs were used in this study as an inert hydrophobic model system. Liposomes, on the other hand, are frequently used to deliver therapeutic agents to target cells. A summary of their aggregation profiles can be found in Table 2. It was already demonstrated before that serum induces quick aggregation of positively charged NPs [36]. This was confirmed in our study, especially for the positively charged liposomes. Also in mice and human IP fluid, severe aggregation of positively charged particles was observed. As seen in Figure 1, albumin is the major protein fraction in both mice and human IP fluid, as well as in human serum (~60%). Under physiological conditions (pH 7-7.4) albumin and other negatively charged proteins are capable of binding to cationic NPs, inducing the formation of micrometer sized protein-NP complexes [31]. It is thus most likely that albumin is the most abundant component in the protein corona around the positively charged NPs, as was observed before [49]. The formation of protein-nanoparticle complexes also explains the drop observed in the zeta potential in Figure 2A and 2B. It should be noted that negatively charged NPs tend to bind proteins with an isoelectric point greater than 5.5, such as IgG [50]. This explains why the zeta potential of the negatively charged polystyrene beads becomes less negative upon incubation with the biofluids.

Table 2. Aggregation of the studied formulations in the different biofluids. / indicates no aggregation, +, ++ and +++ indicate aggregates up to respectively 200 nm, 500 nm and >1 µm.

Formulation	HEPES buffer	Mice IP fluid	Ascites fluid	Human serum
+ PS	---	+++	+	+
- PS	---	+	+	+
PEG PS	---	---	+	+
+ liposomes	---	+++	+++	+++
5% PEG liposomes	---	+	+	++
10% PEG liposomes	---	---	+	+

The adsorption of proteins to the NPs described above is drastically diminished when the surface of the PS NPs and liposomes is decorated with PEG (Table 2). Despite the role of PEG in avoiding aggregation, the data presented in Figure 6B indicate that there is a limit to which extent the protein adsorption could be prevented. This finding is significant, suggesting that 10% PEGylated liposomes are very stable in the peritoneal fluids, but not in human serum where aggregation still takes place due to the high density of proteins bound on the surface of the PEG residues (Table 1). In general, it seems that PEGylation is necessary to avoid the formation of aggregation in peritoneal fluids. Both positively and negatively charged non-PEGylated NPs tend to form large aggregates upon incubation with peritoneal fluids or human serum.

Among all the studied formulations the aggregation tendency seemed proportional to the protein concentration of the incubation fluid, except for positively charged PS NPs, which show the greatest aggregation in mice IP fluid with lowest protein content. The exact reason for this is unclear. It should be noted, however, that the positively charged PS NPs become negatively charged upon incubation with the biofluids. The negatively charged PS NPs, on the other hand, become slightly less negative. Therefore, the actual proteins that bind to the NPs are expected to be different for cationic or anionic NPs, respectively, which might influence their aggregation behavior. Another observation is that the liposomes tend to aggregate more than PS NP in all biofluids. This most probably stems from the intrinsic properties of the building blocks. In particular, when collisions between two liposomes occur (especially non-PEGylated ones), hydrophobic interactions between lipids from both liposomes can take place, supporting the formation of aggregates. On the contrary, PS NP are 'inert' plastic particles that could 'bounce' upon collision and shown no additional attracting forces that would support the formation of aggregates.

4.2 Release of siRNA from liposomes in the peritoneal fluids

Apart from colloidal stability in terms of aggregation, the NPs should be able to bring their cargo to the target site. The release of siRNA from liposomal formulations in the peritoneal fluids was evaluated using Fluorescence Correlation Spectroscopy (FCS). As we previously demonstrated, FCS is an elegant technique to follow the complexation behavior of small nucleic acids to NPs, both in buffer and in living cells [38,51]. The data in Figure 7 clearly suggest better complexation and slower release of siRNA for the non-PEGylated LPXs over the PEGylated ones. The higher the PEGylation degree, the more rapid the siRNA molecules dissociate from the complexes, even in buffer conditions. This most likely stems from the proposed mechanism for LPX formation [52-54]. When cationic liposomes are added to negatively charged siRNA, strong electrostatic interactions occur, and the majority of the siRNA molecules attach to the surface of the liposomes. These siRNA-coated liposomes can subsequently fuse with other liposomes, so that siRNA is entrapped within the bilayer of the liposomes. In the case of PEGylated LPXs, the PEG chains prevent the fusion of different liposomes, resulting in LPXs in which siRNA is only bound to the outer surface

and not "sandwiched" in between the multilayers of the liposomes. Also, the lower surface charge leads to less complexation, resulting in an increasing amount of free siRNA at zero time with higher degree of PEGylation as seen in Figure 7.

The release is also dependent on the composition of the biofluid in which the LPXs were incubated afterwards. For the PEGylated LPXs, the excess of albumin and other negatively charged proteins triggers the release of the surface bound siRNA from the complexes by competing for binding to the cationic lipids. In human serum, the release percentage of the siRNA is the highest when compared to other biofluids, as these samples contain the highest protein concentration. Interestingly, only small differences occur in the percentages of release of siRNA from non-PEGylated LPXs in between zero time and 1 h of incubation in the different biofluids. This shows that negatively charged proteins in serum and IP fluids only compete with siRNA bound to the surface of the LPXs, leaving siRNA sandwiched in between the lipid bilayers unaffected.

4.3 Tailoring delivery systems for IP therapy

Nano-sized delivery vehicles for IP administration for the treatment PC should meet several efficacy and safety requirements: (1) long retention time in the peritoneal cavity to ensure maximal therapeutic efficiency, (2) limited leakage into the systemic circulation to avoid toxic side effects, (3) a specific targeting of tumor cells and (4) limited immune and inflammation responses. All these are still major challenges in IP delivery systems [22].

Figure 8 schematically represents the different steps and hurdles for NPs administered to the peritoneal cavity. In the case of siRNA, internalization of the carrier into the cells is needed, before knock down of proteins responsible for the proliferation of cancer cells can occur. The data presented in this study undoubtedly propose rapid aggregation of positively and negatively charged NPs in the peritoneal fluids. Large size aggregates, however, are not efficiently taken up by cells anymore. Therefore, the siRNA activity of these aggregates will be lost (Figure 8A, step 1). Also, premature release of siRNA from the carrier in the peritoneal fluid is not desired (Figure 8A, step 2) as free siRNA is not able to penetrate into the cytosol of the cancer cells. While reduced aggregation is achieved by PEGylation of NPs, the PEGylated liposomes suffered from a fast release of the complexed siRNA upon exposure to the IP fluids. Also, PEGylation has been associated with low transfection efficiency due to poor uptake and/or interaction with the endosomal membrane. Nevertheless, different PEGylation strategies can be exploited to prevent aggregation, while keeping the transfection efficiency [55]. An interesting strategy is the use of sheddable PEG-chains that protect the NPs from aggregation in the extracellular environment, but dissociate once the NPs enter certain intracellular compartments. Also, altering the formation procedure of liposomes is an option. By hydrating the lipid film with a solution of siRNA at least part of the loaded siRNA is entrapped inside the liposomal core, even when PEGylated liposomes are used [56]. Also post PEGylation of preformed siRNA/liposome formulations (in which all siRNA

is entrapped between lipid bilayers) is feasible. Apart from aggregation and premature cargo release, the clearance of NPs from the peritoneal cavity is an important parameter. Ideally, NPs should reside in the peritoneal cavity as long as possible, without leakage into the systemic circulation (Figure 8B, step 4). It has been suggested, however, that NPs are cleared from the peritoneal cavity within 2 days [57]. Therefore, for developing RNAi-based therapy for the treatment of peritoneal cancer (which preferentially makes use of nano-sized particles for optimized cell internalization), a future strategy could be to load NPs into a sustained release system. Taking into account the clearance rate of NPs from the peritoneal cavity, such a controlled release system can be tuned so that a constant amount of NPs is present in the peritoneal cavity. It should be noted that a good retention time in the peritoneal cavity was reported for 100 nm positively charged liposomes by Dadashzadeh et al. [58]. The size of the liposomes upon IP administration was however not continuously monitored. In our opinion, this slower clearance rate can be attributed to the aggregation of these NPs to micrometer sized particles in the IP fluid. As has been suggested, these MPs do indeed show a slower clearance rate from the peritoneal cavity when compared to NPs [59].

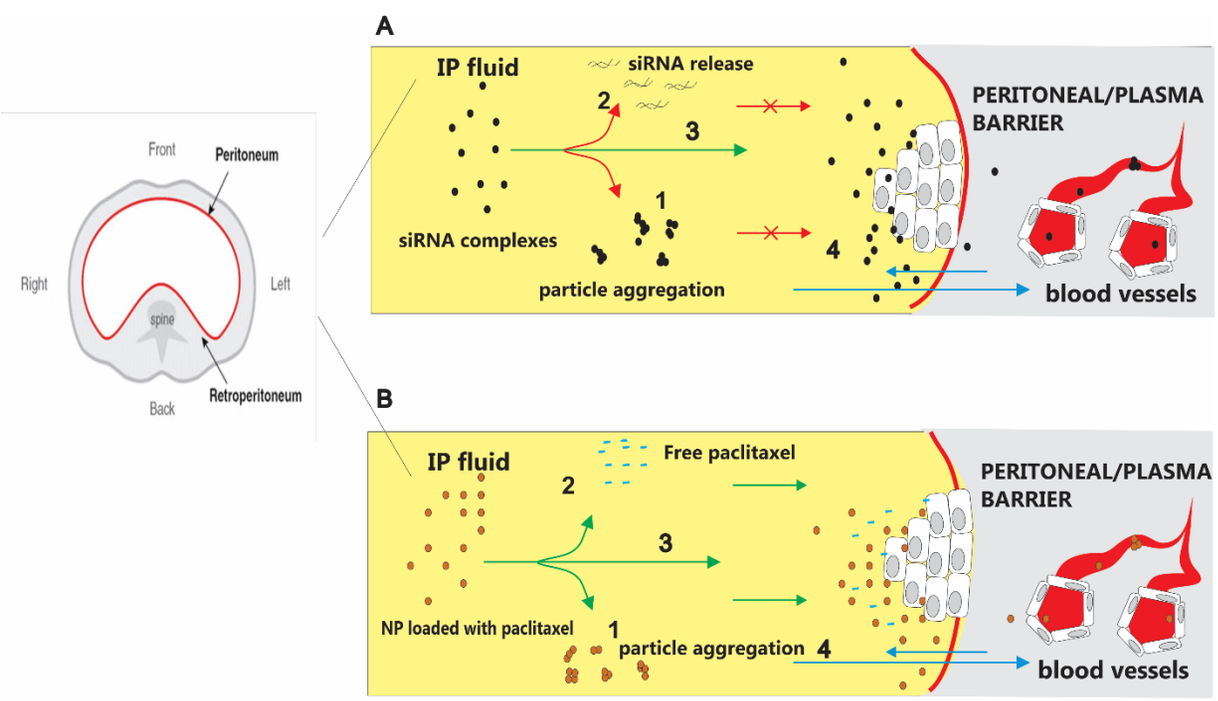

Figure 8. Schematic overview of the different pathways of siRNA complexes or NPs loaded with paclitaxel following IP injection.

Unlike for siRNA, conventional anti-cancer agents such as paclitaxel and doxorubicin (DOX) do not need a carrier system to be taken up in cells. Therefore, the aggregation of NPs or premature cargo release might not be a major problem for these type of formulations (Figure 8B). Aggregation of NPs would however lead to large size aggregates which could lead to increasing difficulty of drug dissolution in the IP fluid (Figure 8B, step 1). Also, Kohane et al. concluded that

MPs do not appear to be good candidates for IP drug delivery due to the risk of adhesions [57]. Also, a disadvantage of the conventional cytostatics, is the non-specificity of the drugs which also affect healthy non-tumor cells and the fact that tumor cells can develop resistance after long-term treatment and exposure.

It should be noted that the environment of the peritoneal cavity seems to be less aggressive than the one of the systemic circulation: while 5% PEGylated liposomes remained stable in IP fluid, aggregation was still observed in the human serum. Therefore, one could argue that less colloidal stable NPs could still be used for IP administration. We have the opinion, however, that IP administered NPs should also be stable enough in the systemic circulation, since clearance of these particles from the peritoneal cavity to the systemic circulation is most likely inevitable (Figure 8, step 4). When a colloidal stable nanoparticle, once it leaves the peritoneal cavity, starts aggregating in the blood circulation, there is a risk of clogging blood capillaries, which should obviously be avoided.

Finally, it is important to stress out that the outcomes from the stability testing *in vitro* in biofluids with the techniques used in this study (FCS and SPT) represent a good prediction of the stability for the *in vivo* situation. Therefore, formulations that are not stable enough *in vitro* should not be considered for *in vivo* applications. Rather, further *in vitro* optimization should take place to enhance the stability of NPs and to ensure that only stable formulations are used for further animal studies. It should be noted, however, that the *in vivo* situation is expected to be more complex than the *in vitro* one in biological fluids. Therefore, particles that showed good stability in the biofluids should always be further tested *in vivo* to determine their biological activity.

5. Conclusions

There is increasing interest from clinicians in treating carcinomatosis patients with some form of IP therapy. Unfortunately, none of the currently used drugs in this setting have been specifically designed or tested for IP application. In this study, for the first time, we investigate the aggregation and release of cargo from NPs in peritoneal fluids. Our data indicate fast aggregation of positively and negatively charged NPs in the peritoneal fluids, which can be prevented by decorating the surface with PEG. Conventional complexation of nucleic acids with our PEGylated liposomes results however in a rapid release of the nucleic acids in the peritoneal fluids, which is not preferred.

Acknowledgments

KR is a post-doctoral fellow of the Research Foundation-Flanders (FWO). GD is a doctoral fellow of the Flemish Government (Vlaamse overheid). EZ is a doctoral fellow of the Institute for the Promotion of Innovation through Science and Technology in Flanders (IWT). WC is a senior clinical investigator of the Fund for Scientific Research – Flanders (FWO). We thank Dr. Bart Lucas for his assistance with the viscosity measurements. The research was supported by the Research Foundation-Flanders (research project G006714N).

Supplementary information

Supplementary Figure 1.

A

			Size (d.nm):	% Intensity:	St Dev (d.nm):
Z-Average (d.nm):	96,90	Peak 1:	205,7	83,5	100,5
PdI:	0,546	Peak 2:	28,64	13,3	8,951
Intercept:	0,907	Peak 3:	6,999	3,2	1,404
Result quality :	Refer to quality report				

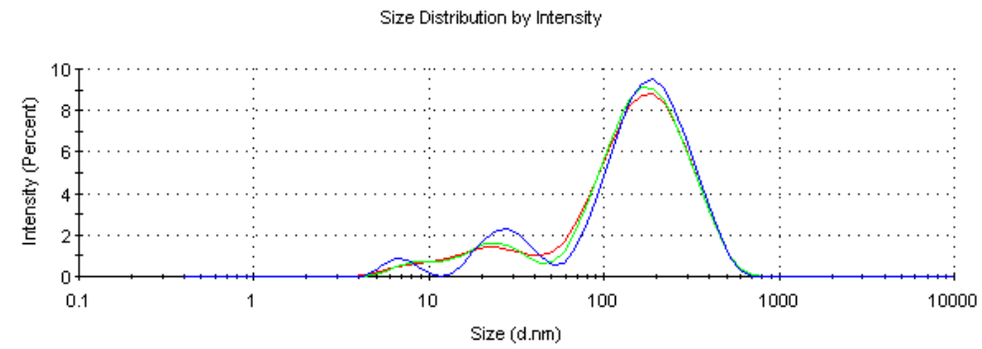

B

			Size (d.nm):	% Intensity:	St Dev (d.nm):
Z-Average (d.nm):	58,98	Peak 1:	255,2	62,6	139,6
PdI:	0,651	Peak 2:	35,53	28,0	14,75
Intercept:	0,930	Peak 3:	8,284	9,4	2,488
Result quality :	Refer to quality report				

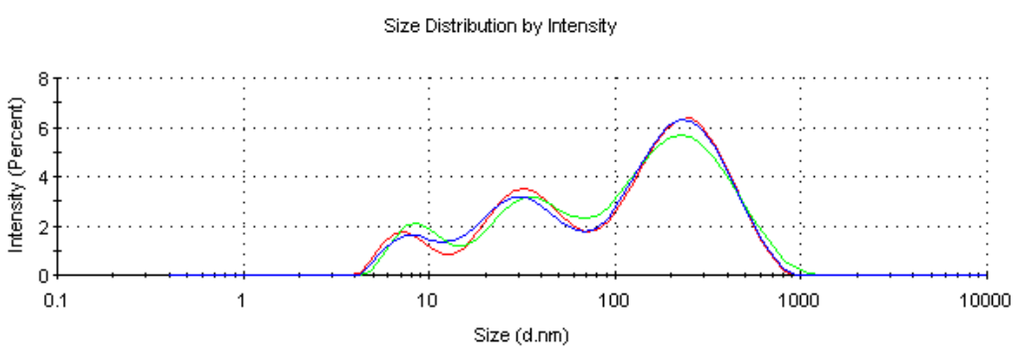

DLS size distributions of (A) human serum and (B) ascites fluid diluted in HEPES buffer.

References

[1] J. Hunn, G.C. Rodriguez, Ovarian Cancer: Etiology, Risk Factors, and Epidemiology, Clin Obstet Gynecol, 55 (2012) 3-23.
[2] Y.L.B. Klaver, V.E.P.P. Lemmens, S.W. Nienhuijs, M.D.P. Luyer, I.H.J.T. de Hingh, Peritoneal carcinomatosis of colorectal origin: Incidence, prognosis and treatment options, World Journal of Gastroenterology, 18 (2012) 5489-5494.
[3] A. Poveda, R. Salazar, J.M. del Campo, C. Mendiola, J. Cassinello, B. Ojeda, J.A. Arranz, A. Oaknin, J. Garcia-Foncillas, M.J. Rubio, A.G. Martin, Update in the management of ovarian and cervical carcinoma, Clinical & Translational Oncology, 9 (2007) 443-451.
[4] J. Cassidy, S. Clarke, E. Diaz-Rubio, W. Scheithauer, A. Figer, R. Wong, S. Koski, M. Lichinitser, T.S. Yang, F. Rivera, F. Couture, F. Sirzeen, L. Saltz, Randomized phase III study of capecitabine plus oxaliplatin compared with fluorouracil/folinic acid plus oxaliplatin as first-line therapy for metastatic colorectal cancer, Journal of Clinical Oncology, 26 (2008) 2006-2012.
[5] R. Porschen, H.T. Arkenau, S. Kubicka, R. Greil, T. Seufferlein, W. Freier, A. Kretzschmar, U. Graeven, A. Grothey, A. Hinke, W. Schmiegel, H.J. Schmoll, Phase III study of capecitabine plus oxaliplatin compared with fluorouracil and leucovorin plus oxaliplatin in metastatic colorectal cancer: A final report of the AIO colorectal study group, Journal of Clinical Oncology, 25 (2007) 4217-4223.
[6] D.S. Alberts, P.Y. Liu, E.V. Hannigan, R. OToole, S.D. Williams, J.A. Young, E.W. Franklin, D.L. ClarkePearson, V.K. Malviya, B. DuBeshter, M.D. Adelson, W.J. Hoskins, Intraperitoneal cisplatin plus intravenous cyclophosphamide versus intravenous cisplatin plus intravenous cyclophosphamide for stage III ovarian cancer, New England Journal of Medicine, 335 (1996) 1950-1955.
[7] R.F. Ozols, B.N. Bundy, B.E. Greer, J.M. Fowler, D. Clarke-Pearson, R.A. Burger, R.S. Mannel, K. DeGeest, E.M. Hartenbach, R. Baergen, Phase III trial of carboplatin and paclitaxel compared with cisplatin and paclitaxel in patients with optimally resected stage III ovarian cancer: A Gynecologic Oncology Group study, Journal of Clinical Oncology, 21 (2003) 3194-3200.
[8] D. Jelovac, D.K. Armstrong, Recent Progress in the Diagnosis and Treatment of Ovarian Cancer, Ca-a Cancer Journal for Clinicians, 61 (2011) 183-203.
[9] M.J. Koppe, O.C. Boerman, W.J.G. Oyen, R.P. Bleichrodt, Peritoneal carcinomatosis of colorectal origin - Incidence and current treatment strategies, Annals of Surgery, 243 (2006) 212-222.
[10] B.T. Hennessy, R.L. Coleman, M. Markman, Ovarian cancer, Lancet, 374 (2009) 1371-1382.
[11] D.K. Armstrong, B. Bundy, L. Wenzel, H.Q. Huang, R. Baergen, S. Lele, L.J. Copeland, J.L. Walker, R.A. Burger, G.O. Grp, Intraperitoneal cisplatin and paclitaxel in ovarian cancer, New England Journal of Medicine, 354 (2006) 34-43.
[12] O. Glehen, F. Kwiatkowski, P.H. Sugarbaker, D. Elias, E.A. Levine, M. De Simone, R. Barone, Y. Yonemura, F. Cavaliere, F. Quenet, M. Gutman, A.A.K. Tentes, G. Lorimier, J.L. Bernard, J.M. Bereder, J. Porcheron, A. Gomez-Portilla, P. Shen, M. Deraco, P. Rat, F.N. Gilly, Cytoreductive surgery combined with perioperative intraperitoneal chemotherapy for the management of peritoneal carcinomatosis from colorectal cancer: A multi-institutional study, Journal of Clinical Oncology, 22 (2004) 3284-3292.
[13] R.L. Dedrick, C.E. Myers, P.M. Bungay, V.T. Devita, Pharmacokinetic Rationale for Peritoneal Drug Administration in Treatment of Ovarian Cancer, Cancer Treatment Reports, 62 (1978) 1-11.
[14] D. Hompes, A. D'Hoore, E. Van Cutsem, S. Fieuws, W. Ceelen, M. Peeters, K. Van der Speeten, C. Bertrand, H. Legendre, J. Kerger, The Treatment of Peritoneal Carcinomatosis of Colorectal Cancer with Complete Cytoreductive Surgery and Hyperthermic Intraperitoneal Peroperative Chemotherapy (HIPEC) with Oxaliplatin: A Belgian Multicentre Prospective Phase II Clinical Study, Annals of Surgical Oncology, 19 (2012) 2186-2194.
[15] P.H. Sugarbaker, Cytoreductive Surgery Plus Hyperthermic Perioperative Chemotherapy for Selected Patients with Peritoneal Metastases from Colorectal Cancer: A New Standard of Care or an Experimental Approach?, Gastroenterology Research and Practice, (2012).
[16] W.P. Ceelen, M.F. Flessner, Intraperitoneal therapy for peritoneal tumors: biophysics and clinical evidence, Nature Reviews Clinical Oncology, 7 (2010) 108-115.
[17] Y.L.B. Klaver, T. Hendriks, R.M.L.M. Lomme, H.J.T. Rutten, R.P. Bleichrodt, I.H.J.T. de Hingh, Intraoperative versus Early Postoperative Intraperitoneal Chemotherapy after Cytoreduction for Colorectal Peritoneal Carcinomatosis: an Experimental Study, Annals of Surgical Oncology, 19 (2012) S475-S482.
[18] P. Zahedi, J. Stewart, R. De Souza, M. Piquette-Miller, C. Allen, An injectable depot system for sustained intraperitoneal chemotherapy of ovarian cancer results in favorable drug distribution at the whole body, peritoneal and intratumoral levels, Journal of Controlled Release, 158 (2012) 379-385.
[19] M.S. Goldberg, siRNA Delivery for the treatment of ovarian cancer, Methods, (2013) In press.
[20] M. Creixell, N.A. Peppas, Co-delivery of siRNA and therapeutic agents using nanocarriers to overcome cancer resistance, Nano Today, 7 (2012) 367-379.
[21] G. Bajaj, Y. Yeo, Drug Delivery Systems for Intraperitoneal Therapy, Pharmaceutical Research, 27 (2010) 735-738.
[22] Z. Lu, J. Wang, M.G. Wientjes, J.L.S. Au, Intraperitoneal therapy for peritoneal cancer, Future Oncology, 6 (2010) 1625-1641.

[23] J. Tomasina, S. Lheureux, P. Gauduchon, S. Rault, A. Malzert-Freon, Nanocarriers for the targeted treatment of ovarian cancers, Biomaterials, 34 (2013) 1073-1101.
[24] S. Hallaj-Nezhadi, C.R. Dass, F. Lotfipour, Intraperitoneal delivery of nanoparticles for cancer gene therapy, Future Oncology, 9 (2013) 59-68.
[25] H. Cho, T.C. Lai, G.S. Kwon, Poly(ethylene glycol)-block-poly(epsilon-caprolactone) micelles for combination drug delivery: Evaluation of paclitaxel, cyclopamine and gossypol in intraperitoneal xenograft models of ovarian cancer, Journal of Controlled Release, 166 (2013) 1-9.
[26] J. Fujiyama, Y. Nakase, K. Osaki, C. Sakakura, H. Yamagishi, A. Hagiwara, Cisplatin incorporated in microspheres: development and fundamental studies for its clinical application, Journal of Controlled Release, 89 (2003) 397-408.
[27] Z. Lu, M. Tsai, D. Lu, J. Wang, M.G. Wientjes, J.L.S. Au, Tumor-Penetrating Microparticles for Intraperitoneal Therapy of Ovarian Cancer, Journal of Pharmacology and Experimental Therapeutics, 327 (2008) 673-682.
[28] W.K. Bae, M.S. Park, J.H. Lee, J.E. Hwang, H.J. Shim, S.H. Cho, D.E. Kim, H.M. Ko, C.S. Cho, I.K. Park, I.J. Chung, Docetaxel-loaded thermoresponsive conjugated linoleic acid-incorporated poloxamer hydrogel for the suppression of peritoneal metastasis of gastric cancer, Biomaterials, 34 (2013) 1433-1441.
[29] G. Bajaj, M.R. Kim, S.I. Mohammed, Y. Yeo, Hyaluronic acid-based hydrogel for regional delivery of paclitaxel to intraperitoneal tumors, Journal of Controlled Release, 158 (2012) 386-392.
[30] J. Yu, H.J. Lee, K. Hur, M.K. Kwak, T.S. Han, W.H. Kim, S.C. Song, K. Yanagihara, H.K. Yang, The antitumor effect of a thermosensitive polymeric hydrogel containing paclitaxel in a peritoneal carcinomatosis model, Investigational New Drugs, 30 (2012) 1-7.
[31] C.D. Walkey, W.C.W. Chan, Understanding and controlling the interaction of nanomaterials with proteins in a physiological environment, Chemical Society Reviews, 41 (2012) 2780-2799.
[32] Z.H. Liu, Y.P. Jiao, T. Wang, Y.M. Zhang, W. Xue, Interactions between solubilized polymer molecules and blood components, Journal of Controlled Release, 160 (2012) 14-24.
[33] D. Zhong, Y.P. Jiao, Y. Zhang, W. Zhang, N. Li, Q.H. Zuo, Q. Wang, W. Xue, Z.H. Liu, Effects of the gene carrier polyethyleneimines on structure and function of blood components, Biomaterials, 34 (2013) 294-305.
[34] V. Mirshafiee, M. Mahmoudi, K.Y. Lou, J.J. Cheng, M.L. Kraft, Protein corona significantly reduces active targeting yield, Chemical Communications, 49 (2013) 2557-2559.
[35] A. Salvati, A.S. Pitek, M.P. Monopoli, K. Prapainop, F.B. Bombelli, D.R. Hristov, P.M. Kelly, C. Aberg, E. Mahon, K.A. Dawson, Transferrin-functionalized nanoparticles lose their targeting capabilities when a biomolecule corona adsorbs on the surface, Nature Nanotechnology, 8 (2013) 137-143.
[36] K. Braeckmans, K. Buyens, W. Bouquet, C. Vervaet, P. Joye, F. De Vos, L. Plawinski, L. Doeuvre, E. Angles-Cano, N.N. Sanders, J. Demeester, S.C. De Smedt, Sizing Nanomatter in Biological Fluids by Fluorescence Single Particle Tracking, Nano Letters, 10 (2010) 4435-4442.
[37] M.A. Dobrovolskaia, A.K. Patri, J.W. Zheng, J.D. Clogston, N. Ayub, P. Aggarwal, B.W. Neun, J.B. Hall, S.E. McNeil, Interaction of colloidal gold nanoparticles with human blood: effects on particle size and analysis of plasma protein binding profiles, Nanomedicine-Nanotechnology Biology and Medicine, 5 (2009) 106-117.
[38] K. Buyens, B. Lucas, K. Raemdonck, K. Braeckmans, J. Vercammen, J. Hendrix, Y. Engelborghs, S.C. De Smedt, N.N. Sanders, A fast and sensitive method for measuring the integrity of siRNA-carrier complexes in full human serum, Journal of Controlled Release, 126 (2008) 67-76.
[39] J.L. Orsonneau, P. Douet, C. Massoubre, P. Lustenberger, S. Bernard, An Improved Pyrogallol Red Molybdate Method for Determining Total Urinary Protein, Clinical Chemistry, 35 (1989) 2233-2236.
[40] X. Bossuyt, B. Lissoir, G. Marien, D. Maisin, J. Vunckx, N. Blanckaert, P. Wallemacq, Automated serum protein electrophoresis by Capillarys (R), Clinical Chemistry and Laboratory Medicine, 41 (2003) 704-710.
[41] C. Gay-Bellile, D. Bengoufa, P. Houze, D. Le Carrer, M. Benlakehal, B. Bousquet, B. Gourmel, T. Le Bricon, Automated multicapillary electrophoresis for analysis of human serum proteins, Clinical Chemistry, 49 (2003) 1909-1915.
[42] L.T. Sniegoski, J.R. Moody, Determination of Serum and Blood Densities, Analytical Chemistry, 51 (1979) 1577-1578.
[43] N. Symens, R. Walczak, J. Demeester, I. Mattaj, S.C. De Smedt, K. Remaut, Nuclear Inclusion of Nontargeted and Chromatin-Targeted Polystyrene Beads and Plasmid DNA Containing Nanoparticles, Molecular Pharmaceutics, 8 (2011) 1757-1766.
[44] B.K. Zebrowski, W.B. Liu, K. Ramirez, Y. Akagi, G.B. Mills, L.M. Ellis, Markedly elevated levels of vascular endothelial growth factor in malignant ascites, Annals of Surgical Oncology, 6 (1999) 373-378.
[45] B. Naeye, H. Deschout, V. Caveliers, B. Descamps, K. Braeckmans, C. Vanhove, J. Demeester, T. Lahoutte, S.C. De Smedt, K. Raemdonck, In vivo disassembly of IV administered siRNA matrix nanoparticles at the renal filtration barrier, Biomaterials, 34 (2013) 2350-2358.
[46] B. Naeye, H. Deschout, M. Roding, M. Rudemo, J. Delanghe, K. Devreese, J. Demeester, K. Braeckmans, S.C. De Smedt, K. Raemdonck, Hemocompatibility of siRNA loaded dextran nanogels, Biomaterials, 32 (2011) 9120-9127.
[47] M. Johnsson, K. Edwards, Liposomes, disks, and spherical micelles: Aggregate structure in mixtures of gel phase phosphatidylcholines and poly(ethylene glycol)-phospholipids, Biophysical Journal, 85 (2003) 3839-3847.

[48] B.S. Zolnik, A. Gonzalez-Fernandez, N. Sadrieh, M.A. Dobrovolskaia, Minireview: Nanoparticles and the Immune System, Endocrinology, 151 (2010) 458-465.
[49] G.W. Doorley, C.K. Payne, Cellular binding of nanoparticles in the presence of serum proteins, Chemical Communications, 47 (2011) 466-468.
[50] A. Gessner, A. Lieske, B.R. Paulke, R.H. Muller, Functional groups on polystyrene model nanoparticles: Influence on protein adsorption, Journal of Biomedical Materials Research Part A, 65A (2003) 319-326.
[51] B. Lucas, K. Remaut, N.N. Sanders, K. Braeckmans, S.C. De Smedt, J. Demeester, Towards a better understanding of the dissociation behavior of liposome-oligonucleotide complexes in the cytosol of cells, Journal of Controlled Release, 103 (2005) 435-450.
[52] K. Remaut, B. Lucas, K. Braeckmans, N.N. Sanders, J. Demeester, S.C. De Smedt, Protection of oligonucleotides against nucleases by pegylated and non-pegylated liposomes as studied by fluorescence correlation spectroscopy, Journal of Controlled Release, 110 (2005) 212-226.
[53] K. Remaut, B. Lucas, K. Braeckmans, N.N. Sanders, J. Demeester, S.C. De Smedt, Delivery of phosphodiester oligonucleotides: Can DOTAP/DOPE liposomes do the trick?, Biochemistry, 45 (2006) 1755-1764.
[54] K. Remaut, B. Lucas, K. Raemdonck, K. Braeckmans, J. Demeester, S.C. De Smedt, Can we better understand the intracellular behavior of DNA nanoparticles by fluorescence correlation spectroscopy?, Journal of Controlled Release, 121 (2007) 49-63.
[55] L.C. Gomes-da-Silva, N.A. Fonseca, V. Moura, M.C.P. de Lima, S. Simoes, J.N. Moreira, Lipid-Based Nanoparticles for siRNA Delivery in Cancer Therapy: Paradigms and Challenges, Accounts of Chemical Research, 45 (2012) 1163-1171.
[56] K. Buyens, J. Demeester, S.C. De Smedt, N.N. Sanders, Elucidating the Encapsulation of Short Interfering RNA in PEGylated Cationic Liposomes, Langmuir, 25 (2009) 4886-4891.
[57] D.S. Kohane, J.Y. Tse, Y. Yeo, R. Padera, M. Shubina, R. Langer, Biodegradable polymeric microspheres and nanospheres for drug delivery in the peritoneum, Journal of Biomedical Materials Research Part A, 77A (2006) 351-361.
[58] S. Dadashzadeh, N. Mirahmadi, M.H. Babaei, A.M. Vali, Peritoneal retention of liposomes: Effects of lipid composition, PEG coating and liposome charge, Journal of Controlled Release, 148 (2010) 177-186.
[59] M. Tsai, Z. Lu, J. Wang, T.K. Yeh, M.G. Wientjes, J.L.S. Au, Effects of carrier on disposition and antitumor activity of intraperitoneal paclitaxel, Pharmaceutical Research, 24 (2007) 1691-1701.

4

DISREGARDED EFFECT OF BIOLOGICAL FLUIDS IN SIRNA DELIVERY: HUMAN ASCITES FLUID SEVERELY RESTRICTS CELLULAR UPTAKE OF NANOPARTICLES

Parts of this chapter are published as:

George R. Dakwar[1], Kevin Braeckmans[1,2], Joseph Demeester[1], Wim Ceelen[3], Stefaan C. De Smedt[1], Katrien Remaut[1], Disregarded effect of biological fluids in siRNA delivery: Human ascites fluid severely restricts cellular uptake of nanoparticles. *ACS Applied Materials and Interfaces,* 7, 24322-24329 (2015).

[1] Ghent Research Group on Nanomedicines, Faculty of Pharmaceutical Sciences, Laboratory for General Biochemistry and Physical Pharmacy, Ghent University, Ghent, Belgium

[2] Center for Nano- and Biophotonics, Ghent University, Ghent, Belgium

[3] Department of Surgery, Laboratory of Experimental Surgery, Ghent University Hospital, Ghent, Belgium

Abstract

Small interfering RNA (siRNA) offers a great potential for the treatment of various diseases and disorders. Nevertheless, inefficient *in vivo* siRNA delivery hampers its translation into the clinic. While numerous successful *in vitro* siRNA delivery stories exist in reduced-protein conditions, most studies so far overlook the influence of the biological fluids present in the *in vivo* environment. In this study, we compared the transfection efficiency of liposomal formulations in Opti-MEM® (low protein content, routinely used for *in vitro* screening) and human undiluted ascites fluid obtained from a PC patient (high protein content, representing the *in vivo* situation). In Opti-MEM®, all formulations are biologically active. In ascites fluid, however, the biological activity of all lipoplexes (LPXs) is lost except for lipofectamine RNAiMAX. The drop in transfection efficiency was not correlated to the physicochemical properties of the nanoparticles (NPs), such as premature siRNA release and aggregation of the NPs in the human ascites fluid. Remarkably, however, all of the formulations except for lipofectamine RNAiMAX lost their ability to be taken up by cells following incubation in ascites fluid. To take into account the possible effects of a protein corona formed around the NPs, we recommend always using undiluted biological fluids for the *in vitro* optimization of nano-sized siRNA formulations next to conventional screening in low-protein content media. This should tighten the gap between *in vitro* and *in vivo* performance of NPs and ensure the optimal selection of NPs for further *in vivo* studies.

Keywords: liposomes, siRNA delivery, ascites, protein corona, lipofectamine, peritoneal metastasis

1. Introduction

Since the discovery of small interfering RNA (siRNA) [1,2] a lot of effort has been put into translating it into the clinic for the treatment of different diseases [3]. *In vitro* there are numerous options for successfully delivering siRNA to cells under "reduced serum conditions". In more complex "protein-rich" biological fluids, however, the effect of the protein corona (being formed at the surface of the nanoparticles (NPs)) on the aggregation, release, uptake, intracellular trafficking, and transfection of NPs should not be underestimated [4-6]. Unfortunately, upon screening tens of papers that aim to optimize siRNA carriers for future *in vivo* use, the NPs are only evaluated in unrealistic protein-free conditions in spite of the fact that human biological fluids, e.g., blood, serum, plasma, ascites fluids, sputa, and synovial fluids, are easily accessible. As these undiluted biological fluids contain high concentration of proteins, they more closely resemble the *in vivo* situation. *In vivo* siRNA delivery is a complex process that includes both extracellular and intracellular barriers. Generally speaking, NPs are expected to keep the cargo (i.e., siRNA) in an intact form while circulating in the biological fluids of the body. Also, premature release of the siRNA from the NPs and aggregation of siRNA NPs in biological fluids are referred to as extracellular barriers for siRNA delivery [7]. While it is possible to determine the overall biological activity (i.e., gene knockdown) of siRNA formulations in vivo, it is impossible to monitor siRNA release, aggregation, and interaction of the formulations with biological membranes directly *in vivo*. Therefore, *in vitro* optimization of nanoparticle-based siRNA delivery is still needed, although it should be done under conditions that are as similar as possible to the *in vivo* situation in which the NPs are intended to be used.

A better understanding of our failure to efficiently deliver siRNA *in vivo* [8] should arise from a stronger knowledge of the physicochemical and biophysical properties of siRNA delivery systems in the biofluids that are expected to be encountered. For patients diagnosed with PC, for example, the delivery of NPs in the peritoneal cavity is being considered as a promising future therapy. Locoregional anticancer therapy allows the targeting of the PC while at the same time limiting systemic toxicity. After locoregional administration, NPs come into contact with the peritoneal fluid present in the peritoneal cavity of these patients. Hence, understanding the influence of peritoneal fluid on the performance of the NPs is crucial. In the current study, we investigated the ability of different PEGylated and non-PEGylated cationic liposomes to induce siRNA-mediated knockdown in a human ovarian cancer cell line. We resembled the expected *in vivo* situation by incubating the NPs in undiluted ascites fluid isolated from a PC patient. Important parameters of the liposomal formulations that we studied were (i) the release of siRNA in the ascites fluid, (ii) the aggregation of the LPXs, and (iii) the effect of the biofluid on the cellular uptake of NPs. All parameters were correlated with the biological performance of the liposomal formulations. Our results indicate that there is a large discrepancy between the high transfection potential of the NPs seen under protein-

free conditions and their performance that remains after exposing them to a protein-rich biofluid, such as human ascites fluid.

2. Materials and methods

2.1 Materials

(2, 3-Dioleoyloxy-propyl)-Trimethylammonium-chloride (DOTAP), 1, 2-dioleoyl-sn-glycero-3-phosphoethanolamine (DOPE), and N-palmitoyl-sphingosine-1-{succinyl [methoxy (polyethylene glycol) 2000]} (C16 mPEG 2000 ceramide) were purchased from Avanti Polar Lipids (Alabaster, AL). Chloroform, 4-(2-hydroxyethyl)-1-piperazineethanesulfonic acid (HEPES), 3-(4,5-dimethyl-2-thiazolyl)-2,5-diphenyl-2H-tetrazolium bromide (MTT), and sodium chloride (NaCl) were purchased from Sigma-Aldrich (Bornem, Belgium). Penicillin–streptomycin (5000 U/ml), lipofectamine RNAiMAX transfection reagent (LF), L-glutamine (200 mM), 0.25% trypsin–EDTA (1×) phenol red, McCoy's 5A (modified), Opti-MEM®, and 1,1′-dioctadecyl-3,3,3′,3′-tetramethylindodicarbocyanine perchlorate (DID) (λex = 644 nm, λem = 665 nm) were purchased from Invitrogen (Merelbeke, Belgium). Luciferase assay substrate was purchased from Promega (Madison, WI). Fetal bovine serum (FBS) was purchased from HyClone Thermo Scientific (Cramlington, UK). Passive lysis buffer and luciferase assay kits were purchased from Promega (Leiden, Netherlands). Negative-control siRNA (siNEG) and luciferase siRNA (siLuc) were purchased from Eurogentec (Searing, Belgium).

2.2 Preparation and characterization of the LPXs

Liposomes corresponding to 5 mM of DOTAP and 5 mM of DOPE lipids were prepared by mixing the appropriate amount of lipids in a round bottomed flask before evaporation. PEGylated liposomes were prepared by adding the desired amounts of C16 Cer-PEG dissolved in chloroform (corresponding to 5 mol %) to the lipids before evaporation. A lipid film was formed by rotary evaporation of the chloroform at 40 °C. Liposomes were prepared by rehydrating the lipid film with HEPES buffer (20 mM, pH 7.4), followed by sonication using a probe sonicator (Branson Ultrasonics Digital Sonifier, Danbury, USA). LPXs with a charge ratio of ±8 were prepared by adding the appropriate amounts of liposomes to siRNA. The mixture was incubated at room temperature to allow the formation of the LPXs. Lipofectamine RNAiMAX LPXs were prepared as described by the manufacturer. Briefly, the appropriate volume of lipofectamine RNAiMAX was added to a solution of siNEG, siLuc, or fluorescently labeled siRNA, respectively, and incubated at room temperature for 15 min before use. Throughout the manuscript, lipofectamine RNAiMAX LPXs will be termed LF-LPXs.

The average size and ζ-potential of all formulations were measured by a Zetasizer Nano-ZS (Malvern, Worcestershire, UK).

2.3 Cell Culture

The human ovarian cancer cell line SKOV-3, which stably expresses firefly luciferase, was used for *in vitro* experiments. Cells were cultured in McCoy's 5A medium supplemented with FBS and penicillin−streptomycin. Cells were cultured until 80% to 90% confluency and detached from tissue-culture dishes with 0.25% trypsin. Cells were maintained in an incubator at 37 °C in a humidified atmosphere with 5% CO2.

2.4 Transfection efficiency

SKOV-3 cells were cultured overnight on 24 well plates (35 000 cells per well) in 500 μL of medium containing 10% FBS. Cells were then washed and incubated with the LPXs and LF-LPXs in Opti-MEM® for 4 h. After 4 h of incubation, the transfection medium was replaced by culture medium, and cells were returned to the incubator for 24 h. The siLuc concentration in the wells equaled 25 nM. LF-LPXs, prepared as recommended by the manufacturer, were used as the positive control. Each LPX containing siLuc was compared with its own control (e.g., siNEG). After overnight incubation, cells were lysed with passive lysis buffer and analyzed for firefly luciferase expression using the luciferase assay kit (Promega). The bioluminescence (relative light units, RLU) was measured using a GloMax luminometer (Promega). The percentage of luciferase downregulation was determined by the following equation:

$$\% \text{ transfection} = 100 - (100 \times RLU_{Luc}/RLU_{NEG})$$

Where RLU_{NEG} and RLU_{Luc} are the mean bioluminescence as measured for siNEG and siLuc, respectively. The data shown in Figure 1 are based on three experiments performed on three different days. For transfections in the ascites fluid, 300 μL LPXs (of each formulation) were first added to 700 μL ascites fluid and incubated for 1 h. Then, 300 μL of this mixture was added to 700 μL of Opti-MEM® in each well of a 24 well-plate. Thereafter, the medium was replaced with growth medium and cells were returned to the incubator for 24 h as described above. So-named "upside-down transfections" were performed as follows: 300 μL of LF-LPXs was incubated for 1 and 3 h at 37°C in 700 μL of human ascites fluid. SKOV-3 cells were cultured (during 24 h) on 12 mm coverslips. Subsequently, the cells (on the coverslips) were mounted upside-down on plastic tubes (diameter of 1.3 cm and height of 0.9 cm) filled with 700 μL of Opti-MEM®. A total of 300 μL of LFLPXs was then added to these tubes as such or after incubation in the ascites fluid. After 4 h of exposure of the LF-LPXs to the cells, the coverslips were placed in the wells of a 24 well plate and kept in the incubator for 24 h after adding growth medium to the cells. Subsequently, the cells were lysed, and the percentage of luciferase inhibition was calculated as mentioned above. It should be noted that in this upside-down transfection mode, the precipitation of LF-LPXs on the cells due to gravity is avoided.

Statistical analysis (shown in Figure 1) was performed using GraphPad Prism 6. Statistically significant differences were calculated by using an analysis of variance (ANOVA) at a 0.05 significance level, followed by Sidak's post-test. For each formulation, transfection experiments carried out in Opti-MEM® were compared to those in ascites.

2.5 Fluorescence Correlation Spectroscopy on LPXs

Fluorescence correlation spectroscopy (FCS) is a microscopy-based technique that monitors the fluorescence intensity fluctuations of (fluorescent) molecules diffusing in and out of the focal volume of a confocal microscope.[7,10] Single-color FCS measurements were performed on LPXs containing 30% Cy5 siRNA and having a charge ratio of ±8. A total of 5 µL of such LPXs was diluted to a final volume of 45 µL HEPES buffer or 45 µL of ascites fluid (~90 vol % of biofluid); the samples were analyzed by FCS immediately, 1 and 24 h after incubation in the biofluids at 37 °C. During the incubation and FCS measurements, the well plate was covered with adhesive plates seals (Thermo Scientific, UK) to avoid evaporation of the sample and to minimize flow. FCS measurements were performed on the experimental setup described before [7].

2.6 Fluorescence Single-Particle Tracking

Fluorescence single particle tracking (fSPT) is a fluorescence microscopy technique that is very well-suited for the determination of diffusion and aggregation of NPs in undiluted biological fluids, as was previously shown [11]. fSPT measurements were performed on LPXs (cationic, 5% C16 Cer-PEG, and LF-LPXs), labeled with DID or containing Alexa-Fluor 488 (AF-488)-labeled siRNA. LPXs were dispersed in biofluids as follows. First, formulations were diluted 400 times in HEPES buffer. Then, 5 µL was added to 45 µL of human ascites fluid (~90 vol % of biofluid) and incubated for 1, 2, and 3 h, respectively, at 37°C in a 96 well plate (Greiner Bio-One, Frickenhausen, Germany). At the end of the incubation time, the samples were placed on a custom-built fSPT setup [11], and movies were recorded at about 5 µm above the bottom of the 96 well plate. Videos were analyzed as was previously explained using the following values of viscosity at room temperature: 1.39 cP for the ascites fluid and 0.94 cP for the HEPES buffer [7]. Human ascites fluid was obtained from a patient diagnosed with PC at the Medical Oncology Department of Ghent University Hospital (approved by the Ethics Committee of the Ghent University Hospital (no. 2013/589)).

2.7 Internalization of siRNA into SKOV-3 cells

SKOV-3 cells were plated on 24 well plates (35 000 cells in each well) and allowed to grow in an incubator for 24 h. For uptake experiments, cells were incubated in Opti-MEM® with fluorescent LPXs containing 10% of AF-488 siRNA for 4 h at 37 and 4°C. At the end of the incubation, cells were washed extensively with warm growth medium and PBS, then detached using trypsin and analyzed by FACS (FACSCalibur flow cytometer, BD Biosciences). Uptake experiments were performed with LPXs as such (directly after preparation) or after incubation of the LPXs with ~70% ascites fluid for 1 h before adding them to the cells, as described above under transfection efficiency.

3. Results

3.1 Characterization of the liposomes and LPXs in HEPES buffer

As depicted in Table 1, all the formulations resulted in nano-sized vesicles, as determined by dynamic light scattering (DLS). Despite the fact that the average size of the LF-based liposomes (LF-LP) and LF-LPXs were in the same range as the other formulations, the polydispersity of the LF-LP and LF-LPXs was higher (polydispersity index (PDI) >0.5). The size increased for all formulations upon complexation of the liposomes with siRNA (except for LF-LPXs). The cationic liposomes and LPXs showed the highest positive surface charge (as reflected from their ζ potential). As expected, PEGylation lowered the surface charge of the liposomes and the LPXs. LF-LP and LF-LPXs showed an intermediate surface charge.

Table 1. Z-Average diameter and ζ-Potential of the different formulations used in this study

Formulation	Z-average diameter ± SD (nm)	Polydispersity index (PDI)	ζ-potential (mV) (mean ±SD)	Abbreviation
Cationic liposomes	85 ± 1	0.2	56 ± 1	Cationic LP
Cationic LPX	107 ± 1	0.2	53 ± 1	Cationic LPXs
5% C16 Cer-PEG liposomes	115 ± 2	0.2	6 ± 1	5% C16 Cer-LP
5% C16 Cer-PEG LPX	151 ± 2	0.2	5 ± 1	5% C16 Cer-LPXs
Lipofectamine RNAiMAX liposomes	137 ± 12	0.6	26 ± 2	LF-LP
Lipofectamine RNAiMAX LPX	106 ± 3	0.6	22 ± 3	LF-LPXs

3.2 Transfection efficiency of the LPXs in reduced serum conditions and protein-rich conditions

To evaluate the ability of the LPXs to knock down the expression of a specific gene, we incubated SKOV-3 cells stably expressing luciferase with the LPXs containing siRNA against luciferase (siLuc). To verify the knockdown specificity, we used formulations loaded with a scrambled sequence (siNEG) as well. Figure 1 (dark gray bars) demonstrates the transfection efficiency of the LPXs following incubation in Opti-MEM®. All of the formulations efficiently downregulated luciferase expression. Considering the fact that NPs for *in vivo* IP gene therapy will come into contact with peritoneal fluids, we were interested to see whether incubation of the LPXs in the ascites fluid obtained from a human PC patient would influence their transfection efficiency. The white bars in Figure 1 show a dramatic significant decrease in the transfection efficiency for the cationic LPXs and 5% C16 Cer-LPXs while the LF-LPXs remain active. This raised the question as to why the LPXs and 5% C16 Cer-LPXs significantly lost their biological activity upon exposure to human ascites fluid.

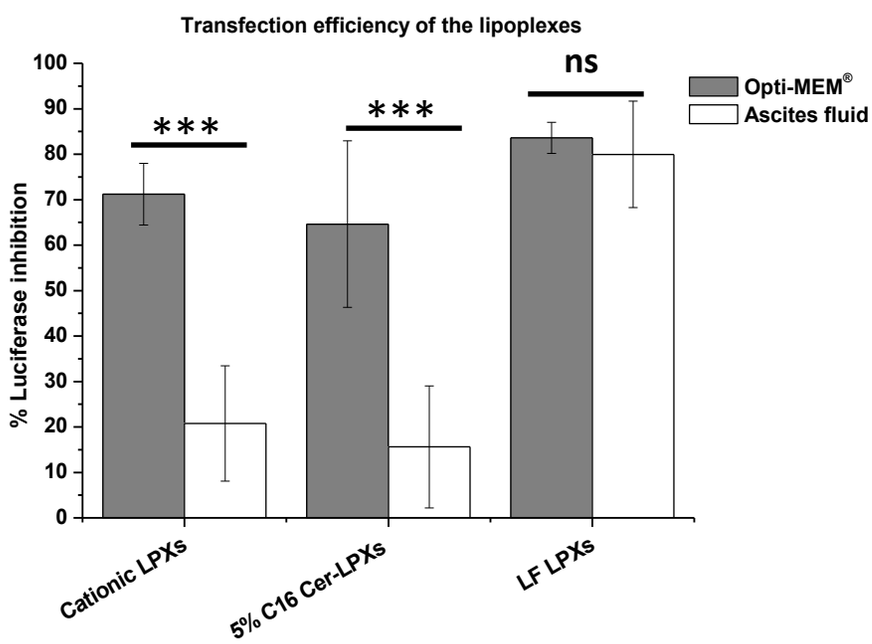

Figure 1. Inhibition of luciferase in SKOV-3 cells by the LPXs in Opti-MEM® (dark gray bars) following incubation of the LPXs for 1 h in ascites fluid (70 vol %) (white bars). The values in the graph represent the average from at least three experiments that were performed on different days.

3.3 Release of siRNA from LPXs in undiluted human ascites fluid

A possible reason why LPXs are less efficient in human ascites fluid could be a premature release of siRNA from the formulations. Indeed, the more siRNA is released from the carriers, the less siRNA remains available for uptake in cells. As demonstrated previously by us, FCS is a suitable method for determining the amount of siRNA that is present in nanocarriers [9,10]. Likewise, FCS can be used to follow the release of siRNA from NPs upon incubating them in buffer and biological fluids [7]. Figure 2 shows the percentage of siRNA that is associated with the different formulations in HEPES buffer immediately following preparation (e.g., complexation efficiency) and after incubation for 1 and 24 h in human ascites fluid (90% vol). In HEPES buffer (gray bars), cationic LPXs show the highest complexation efficiency, with more than 90% of the siRNA associated with the cationic liposomes. PEGylation of the cationic liposomes seems to reduce the complexation efficiency because only 75% of the siRNA is bound to the 5% C16-Cer LPXs. LF-LPXs have the lowest loading efficiency, with 65% of siRNA complexed. Following 1 h of incubation in human ascites fluid (white bars), all formulations release a substantial amount of the initially complexed siRNA, leaving only 50%, 40%, and 40% of siRNA complexed in cationic LPX, 5% C16-Cer LPXs, and LF-LPXs, respectively. Following 24 h of incubation in human ascites fluid, the release of siRNA continues, resulting in less than 20% of siRNA remaining complexed in all of the formulations (dark gray bars). Taken together, human ascites fluid induces a massive release of siRNA from all liposomal formulations, reducing the amount of complexed siRNA that remains available for biological activity to about 20%. The substantial loss of siRNA following incubation in ascites fluid could explain the lower transfection efficiency of the cationic LPXs and 5% C16 Cer-LPXs in Figure 1. Nevertheless, LF-LPXs retain only 20% of complexed siRNA while maintaining their biological activity. In a next step, we evaluated the aggregation of the complexes in the undiluted human ascites fluids and whether or not this aggregation influences the biological activity of the complexes.

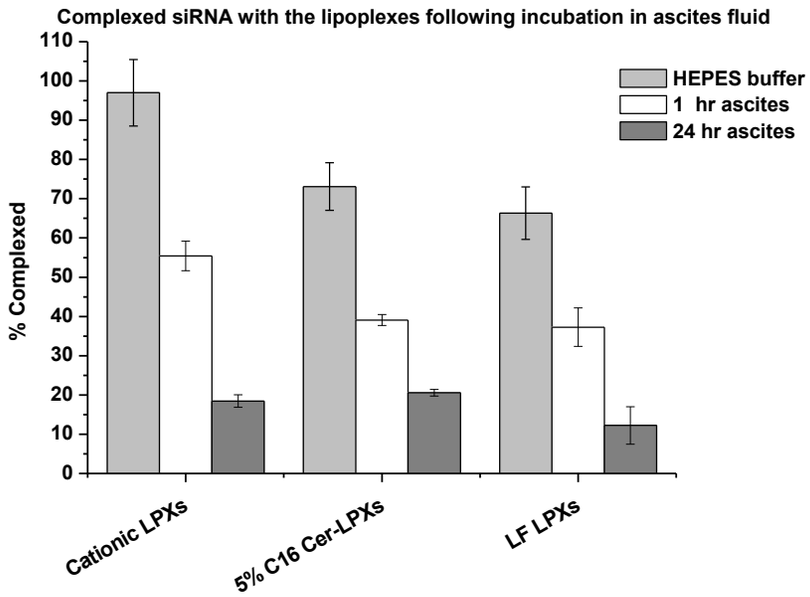

Figure 2. Complexation efficiency of liposomes immediately following preparation in HEPES buffer (gray bars) and percentage of siRNA still complexed after incubation of the lipoplexes in 90 vol% of human ascites fluid during 1 h (white bars) and 24 h (dark gray bars), respectively.

3.4 Aggregation of the LPXs in undiluted human ascites fluid

In our previous study [7], we have shown that dynamic light scattering (DLS) is not an ideal technique for quantifying the extent of aggregation of nanocarriers in (undiluted) ascites fluids, simply due to light scattering that results from the high amount of proteins in such samples. In our hands, fSPT has proven to be superior over DLS to study the aggregation of NPs in biological fluids [7,11-13]. Figure 3A shows the size distributions of the cationic LPXs incubated in undiluted human ascites fluid (~90 vol % of biofluid) during 1, 2, and 3 h. In HEPES buffer, the average diameter of the cationic LPXs is about 200 nm. In ascites fluid, aggregation in time clearly occurs with the formation of 1−2 μm sized aggregates. The 5% C16 Cer-LPXs have an average size of 150 nm in HEPES buffer (Figure 3B, black curve). Following 1 h of incubation in ascites fluid, the size distribution is (very) slightly shifted toward the right, showing the aggregation of a specific population of particles, particularly those that were initially smaller than 100 nm (Figure 3B, red curve). After 2 h of incubation, aggregation seems to become more prominent, with an average diameter of 200 nm (Figure 3B, blue curve). No further aggregation was observed following 3 h of incubation (Figure 3B, green curve). Figure 3B confirms our previous results, showing that PEGylation protects liposomes from aggregation in undiluted human ascites fluid [7]. LF-LPXs showed a high polydispersity in HEPES buffer, with particles ranging from tens of nanometers up to 1 μm in size (Figure 3C, black curve). Following incubation in ascites fluid, we observed a slight aggregation after 1 h of incubation (Figure 3C, red curve), followed by a pronounced aggregation after 2 and 3 h (Figure 3C, green and blue curve), with the presence of micron-sized particles. On the basis of the data in Figure 3C, it is clear that very severe aggregation occurs in ascites fluids

for LF-LPXs. Figure 1 demonstrates that LF-LPXs exposed to ascites fluids show the highest transfection efficiency, while the (more) colloidally stable cationic LPXs and 5% C16 Cer-LPXs lose their biological activity in ascites fluid (Figure 1, white bars). One possible reason for these observations could be that the larger LF-LPXs aggregates rapidly sediment onto the cells during transfection, leading to a forced increased uptake and transfection efficiency. To test this hypothesis, we evaluated the cell uptake of the LPXs before and after incubation of the formulations in ascites fluid.

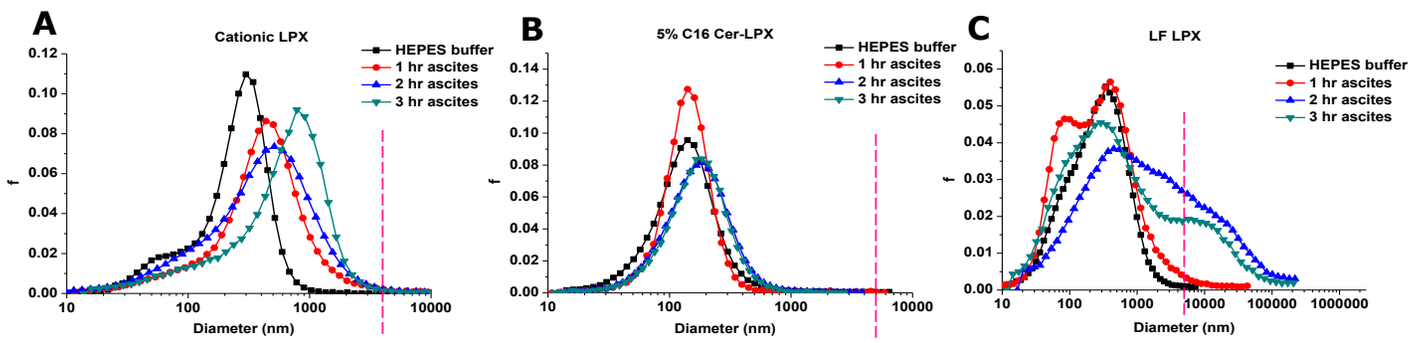

Figure 3. fSPT size distributions of the different lipoplexes following incubation in 90 vol % human ascites fluid at 37°C. (A) Cationic LPXs, **(B)** 5% C16 Cer-LPXs, and **(C)** LF-LPXs. The dotted pink line corresponds to aggregates of 5 µm in size. The Y-axis refers to the fraction (f) of NPs that appear with the corresponding size on the X-axis.

3.5 Influence of ascites fluid on the cellular uptake of the LPXs by SKOV-3 cells

To test the extent of LPX uptake in cells after incubation with ascites fluid, we exposed SKOV-3 cells to LPXs loaded with fluorescently labeled AF-488 siRNA and quantified their uptake by flow cytometry. Figure 4A indicates that in Opti-MEM® (and at 37°C), the various types of LPXs carried the fluorescent siRNA into SKOV-3 cells. At 4°C, intracellular AF-488 fluorescence was minimal (data not shown), indicating that at 37°C, the LPXs were indeed internalized and did not just attach at the surface of the cells. When the same experiment was performed with LPXs that were incubated in ascites fluid for 1 h, the cationic LPXs and the 5% C16 Cer-LPXs completely lost their ability to carry the fluorescent siRNA into the cells, as depicted in Figure 4B. Only LF-LPXs were still efficiently internalized into SKOV-3 cells.

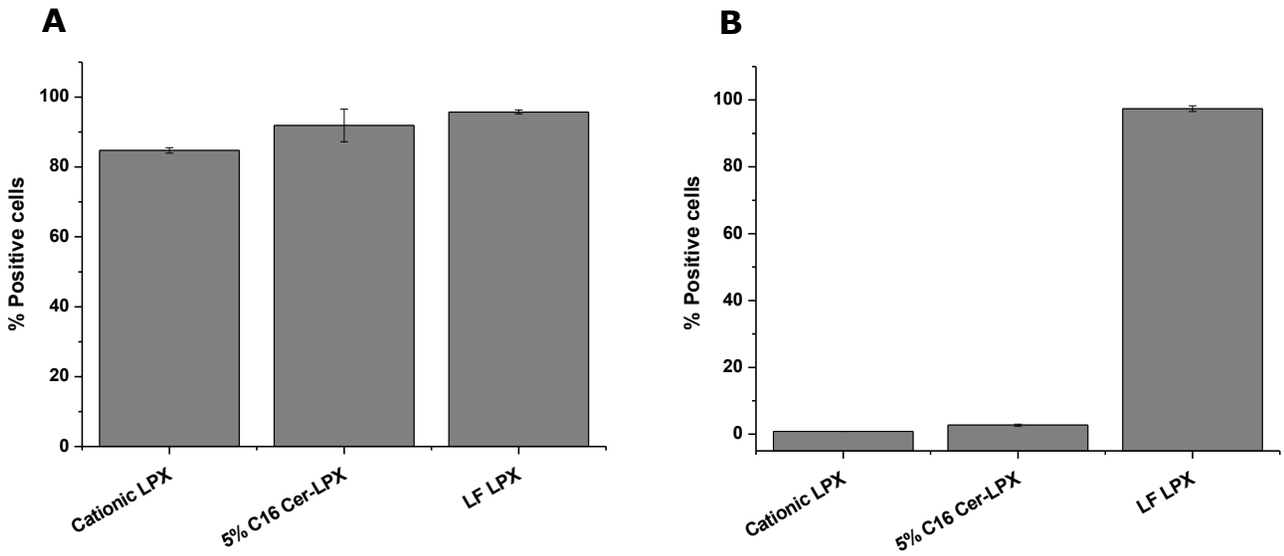

Figure 4. Uptake of AF-488 siRNA-labeled LPXs by SKOV-3 cells. LPXs were prepared in HEPES buffer and added to the cells in Opti-MEM® following preparation as such **(A)** or after incubation of the LPXs for 1 h in human ascites fluid before adding them on the cells **(B)**.

3.6 Aggregation: not the sole determinant of *in vitro* transfection efficiency

Because Figure 3C demonstrates that mainly LF-LPXs form large aggregates in ascites fluid, which may easily sediment on the cells, we wondered whether those severe aggregates explain why LF-LPXs keep transfecting the cells. Therefore, we tested the ability of LF-LPXs to transfect SKOV-3 cells in an "upside-down transfection mode" where cells are positioned at the top surface of the LPXs dispersions, thus avoiding the spontaneous sedimentation of aggregates on the cells. Upside-down transfections were performed with LF-LPXs in Opti-MEM® and with LF-LPXs that were incubated in ascites fluid during 1 or 3 h. As depicted in Figure 5, in Opti-MEM® luciferase down regulation remained 80%, which is similar to the "normal transfection mode" (see Figure 1). This demonstrates that in Opti-MEM®, LF-LPXs can transfect equally well cells that are below (Figure 1) or on top (Figure 5) of the LF-LPX solution, thereby ruling out the possibility that only aggregates contribute to the transfection efficiency. Following the incubation of LF-LPXs for 1 and 3 h in the ascites fluid, the transfection efficiency decreased to 40% in the upside-down transfection mode (Figure 5), while this decrease was not observed in the "normal transfection mode" (see Figure 1). Our data suggest that in the "upside-down transfection mode"', the non-aggregated fraction of the LF-LPXs can reach 40% of the cells, while in the "normal transfection mode" an additional 40% of cells are transfected by LF-LPXs aggregates that are formed in ascites fluid and sediment onto the cells. Therefore, aggregates can indeed contribute to the transfection efficiency, though they are not solely responsible for the observed biological activity.

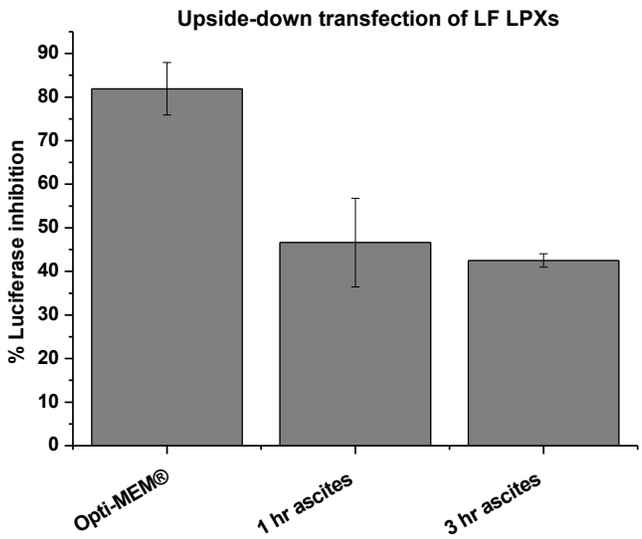

Figure 5. Luciferase inhibition, following upside-down transfections by LF-LPXs, respectively, in Opti-MEM® and following incubation of the complexes for 1 and 3 h in ascites fluid. The values in the graph represent the average from at least three experiments that were performed on different days.

4. Discussion

siRNA-mediated downregulation of disease-related proteins is a very promising therapeutic application. Although numerous efficient NPs have been identified for successful siRNA delivery *in vitro*, the actual number of formulations that withstand the harsh *in vivo* conditions is extremely disappointing. *In vivo*, NPs face additional barriers such as protein-rich biofluids that are not present in the widely used protein-low conditions when screening NPs *in vitro*. Hence, the influence of extracellular fluids on the nanoparticle performance after administration to the human body is often overlooked. In this study, we evaluated the potential of non PEGylated and PEGylated liposomal formulations to successfully deliver siRNA to a human ovarian cancer cell line. Considering the potential use of locoregional administration of lipid-based siRNA carriers to treat peritoneal metastasis, NPs in this study were tested in human ascites fluid obtained from a PC patient. Additionally, biological activity was determined in the widely used low protein content medium Opti-MEM®. Importantly, solely on the basis of the transfections in this low-protein medium, all formulations performed to expectations. Unfortunately, when incubating the formulations in a high-protein-content medium (i.e., ascites fluid in this study), only LF-LPXs were able to keep their original efficiency. To explain the drop in transfection efficiency, we evaluated three important properties of the NPs, namely premature siRNA release, nanoparticle aggregation, and cellular uptake in the presence of human ascites fluid. The complexation of siRNA to (cationic) carriers is necessary to enhance the cellular uptake of these negatively charged nucleic acids. Hence, the premature release of siRNA from the nanocarriers in the biofluids before cellular uptake has taken place will result in a lower amount of siRNA that is able to reach the cytoplasm of the

cells. Using FCS, we found that all tested formulations showed the release of siRNA in the presence of ascites fluid. This siRNA release most likely results from competition between siRNA and the abundantly present negatively charged proteins in the human ascites fluid for binding to the positively charged liposomes. Although testing the release of siRNA in protein-rich conditions can tell us something about the fraction of siRNA that is lost, it is important to note that the absolute values of complexed siRNA were not predictive for the expected biological activity. Indeed, all of the formulations end up with almost the same amount of remaining siRNA following 24 h of incubation (Figure 2), while clear differences in transfection efficiency exist (Figure 1). Because the uptake of NPs is both charge and size dependent, the aggregation of NPs can potentially influence the uptake profile and subsequent transfection efficiency [14]. Therefore, we evaluated whether the aggregation of the NPs was related to the obtained biological activity. Contrary to the release profile, the differences in aggregation between the formulations are much more pronounced. Aggregation is most pronounced in the case of the cationic LPXs, while in the case of C16 Cer-LPXs, the PEG chains protect the LPXs from aggregation. One could argue that the formation of large aggregates could be the reason why lipofectamine RNAiMAX is still efficiently transfecting cells after incubation in ascites fluid. Indeed, aggregates are expected to sediment onto cells and, in this way, a larger amount of NPs (and thus concentration of siRNA) comes into contact with cells during the 4 h incubation period. When we ruled out this sedimentation with an upside-down transfection setup, however, LF-LPXs still retained 50% of their transfection efficiency, demonstrating that aggregation alone cannot be the sole reason for the better transfection efficiency of LF-LPXs. Aggregation of particles remains, however, extremely important for the *in vivo* situation because large aggregates can cause severe toxicity, such as blocking the blood capillaries. Therefore, aggregation studies remain predictive of the suitability of NPs for the *in vivo* situation, and one should keep in mind that strongly aggregated NPs have no future for *in vivo* use, even when high *in vitro* transfection efficiencies were obtained. Cellular uptake is a first important step of the intracellular journey of NPs. Importantly, the drop in the transfection of the cationic and PEGylated LPXs does correspond with the observation that the complexes are no longer internalized into cells after incubation in ascites fluid (Figure 4B). Because we measured the uptake based on fluorescent siRNA, a premature release of siRNA in the ascites fluid would lower the amount of complexed siRNA that can enter the cells and be detected. The amount of released siRNA in ascites fluid is, however, comparable for the three formulations studied (Figure 2). Because all formulations contained at least 40% of complexed siRNA, the possible internalization of the complexes should be detectable. The fact that only LF-LPXs are still taken up in the cells after pre-incubation in ascites fluid could in theory also be ascribed to the sedimentation of a larger amount of particles onto the cells. As described above, however, LF-LPXs also transfect (and thus are taken up) in an upside-down transfection setup to which larger aggregates do not contribute. When NPs are dispersed in extracellular fluids, proteins in these biofluids may bind at the surface of the NPs, forming a so-called protein corona. It has been shown that the protein corona formed around transferrin functionalized NPs impairs their ability to bind transferrin

receptors on the cell surface following incubation in fetal bovine serum and human serum [15,16]. Also, the protein corona can alter the intracellular processing of particles, increasing the fraction that accumulates in the lysosomes [17]. Both the protein composition of the biofluid and the surface properties of the NPs will determine the composition of the protein corona that is eventually formed. We have previously shown that the protein concentration in human ascites fluid is half the concentration of proteins present in human serum, while the protein composition of human ascites fluid is very similar to that of human serum, with albumin as main fraction (62%) [7]. We hypothesize that the poor uptake observed following the incubation of cationic LPXs and PEGylated LPXs in the ascites fluid results from the surface coating of these formulations with negatively charged proteins [5]. It is worth mentioning that this is not the first study showing that NPs lose their ability to interact with biological membranes following incubation with a protein rich biological environment. Interestingly, very recently, Hadjidemetriou et al. also reported that bare and PEGylated liposomes significantly lost their ability to internalize into cells following incubation in undiluted plasma [18]. This points out that the detrimental effect of human ascites fluid on the internalization of NPs could be a common problem for many nanoparticle formulations exposed to various biological fluids. As for nucleic acid delivery, uptake is necessary for biological activity, and testing the uptake of gene delivery systems following incubation in undiluted biological fluids is extremely important and should become a routine test before performing *in vivo* studies. Taken together, the "protein corona field" is rapidly growing with new findings that are extremely important for translating the *in vitro* to the *in vivo* situation but is still not getting enough attention among scientists in the RNAi-delivery community.

5. Conclusion

Importantly, we found that good complexation and transfection properties in reduced serum conditions like Opti-MEM® are not predictive of the actual performance of NPs after being exposed to more complex biological fluids, such as human ascites fluid. On the basis of our results, we determined that the most important factor that eventually determines the biological activity is the biological fluid in which the particles are incubated with prior to adding them onto cells. The composition of the biological fluid may substantially influence the extent of release, aggregation, uptake, and biological activity of nano-sized siRNA formulations. Therefore, we strongly recommend performing *in vitro* optimization of nano-sized siRNA formulations in undiluted biological fluids, taking into account the route of administration regardless of the type of the formulation (lipid-based or polymer-based), before assessing the transfection efficiency of NPs *in vivo*. Because most biofluids, such as peritoneal fluid in the case of IP gene delivery and serum or blood in the case of intravenous (IV) delivery, are relatively easily accessible, testing NPs in these more complex biological environments is very feasible and far more representative for the *in vivo* situation.

On the basis of assays performed in protein free (Opti-MEM®) conditions only, we determined that one runs the risk of selecting NPs that are able to cross an empty street, hoping they will also survive the busy traffic conditions *in vivo*. Just like earning a driving license, however, NPs should be tested in realistic *in vitro* conditions so that *in vivo* animal testing can be restricted to only those particles that passed the relevant screening conditions.

Acknowledgements

This research was supported by the Research Foundation, Flanders (FWO) (grant no. G006714N) for K.R., J.D., S.D., and W.C. and the BOF Special Research Fund of Ghent University (grant no. 01B01108) for K.B. and S.D. We thank Senne Cornelis for his help with the experiments.

References

[1] S.M. Elbashir, J. Harborth, W. Lendeckel, A. Yalcin, K. Weber, T. Tuschl, Duplexes of 21-nucleotide RNAs mediate RNA interference in cultured mammalian cells, Nature, 411 (2001) 494-498.
[2] A. Fire, S.Q. Xu, M.K. Montgomery, S.A. Kostas, S.E. Driver, C.C. Mello, Potent and specific genetic interference by double-stranded RNA in Caenorhabditis elegans, Nature, 391 (1998) 806-811.
[3] M.R. Lares, J.J. Rossi, D.L. Ouellet, RNAi and small interfering RNAs in human disease therapeutic applications, Trends Biotechnol, 28 (2010) 570-579.
[4] D. Dell'Orco, M. Lundqvist, S. Linse, T. Cedervall, Mathematical modeling of the protein corona: implications for nanoparticulate delivery systems, Nanomedicine-Uk, 9 (2014) 851-858.
[5] C.C. Fleischer, C.K. Payne, Nanoparticle-Cell Interactions: Molecular Structure of the Protein Corona and Cellular Outcomes, Accounts Chem Res, 47 (2014) 2651-2659.
[6] C.D. Walkey, W.C.W. Chan, Understanding and controlling the interaction of nanomaterials with proteins in a physiological environment, Chem Soc Rev, 41 (2012) 2780-2799.
[7] G.R. Dakwar, E. Zagato, J. Delanghe, S. Hobel, A. Aigner, H. Denys, K. Braeckmans, W. Ceelen, F.C. De Smedt, K. Remaut, Colloidal stability of nano-sized particles in the peritoneal fluid: Towards optimizing drug delivery systems for intraperitoneal therapy, Acta Biomater, 10 (2014) 2965-2975.
[8] J. Conde, N. Artzi, Are RNAi and miRNA therapeutics truly dead?, Trends Biotechnol, 33 (2015) 141-144.
[9] K. Buyens, B. Lucas, K. Raemdonck, K. Braeckmans, J. Vercammen, J. Hendrix, Y. Engelborghs, S.C. De Smedt, N.N. Sanders, A fast and sensitive method for measuring the integrity of siRNA-carrier complexes in full human serum, J Control Release, 126 (2008) 67-76.
[10] K. Braeckmans, K. Buyens, W. Bouquet, C. Vervaet, P. Joye, F. De Vos, L. Plawinski, L. Doeuvre, E. Angles-Cano, N.N. Sanders, J. Demeester, S.C. De Smedt, Sizing Nanomatter in Biological Fluids by Fluorescence Single Particle Tracking, Nano Lett, 10 (2010) 4435-4442.
[11] K. Buyens, J. Demeester, S.C. De Smedt, N.N. Sanders, Elucidating the Encapsulation of Short Interfering RNA in PEGylated Cationic Liposomes, Langmuir, 25 (2009) 4886-4891.
[12] B. Naeye, H. Deschout, V. Caveliers, B. Descamps, K. Braeckmans, C. Vanhove, J. Demeester, T. Lahoutte, S.C. De Smedt, K. Raemdonck, In vivo disassembly of IV administered siRNA matrix nanoparticles at the renal filtration barrier, Biomaterials, 34 (2013) 2350-2358.
[13] B. Naeye, H. Deschout, M. Roding, M. Rudemo, J. Delanghe, K. Devreese, J. Demeester, K. Braeckmans, S.C. De Smedt, K. Raemdonck, Hemocompatibility of siRNA loaded dextran nanogels, Biomaterials, 32 (2011) 9120-9127.
[14] J. Rejman, V. Oberle, I.S. Zuhorn, D. Hoekstra, Size-dependent internalization of particles via the pathways of clathrin-and caveolae-mediated endocytosis, Biochemical Journal, 377 (2004) 159-169.
[15] G. Caracciolo, Liposome-protein corona in a physiological environment: Challenges and opportunities for targeted delivery of nanomedicines, Nanomed-Nanotechnol, 11 (2015) 543-557.
[16] A. Salvati, A.S. Pitek, M.P. Monopoli, K. Prapainop, F.B. Bombelli, D.R. Hristov, P.M. Kelly, C. Aberg, E. Mahon, K.A. Dawson, Transferrin-functionalized nanoparticles lose their targeting capabilities when a biomolecule corona adsorbs on the surface, Nat Nanotechnol, 8 (2013) 137-143.
[17] F.J. Wang, L. Yu, M.P. Monopoli, P. Sandin, E. Mahon, A. Salvati, K.A. Dawson, The biomolecular corona is retained during nanoparticle uptake and protects the cells from the damage induced by cationic nanoparticles until degraded in the lysosomes, Nanomed-Nanotechnol, 9 (2013) 1159-1168.
[18] M. Hadjidemetriou, Z. Al-Ahmady, M. Mazza, R.F. Collins, K. Dawson, K. Kostarelos, In Vivo Biomolecule Corona around Blood-Circulating, Clinically Used and Antibody-Targeted Lipid Bilayer Nanoscale Vesicles, ACS Nano, 9 (2015) 8142-8156.

5

EXPLORING THE HYDRATION METHOD FOR LOADING SIRNA ON LIPOSOMES: THE INTERPLAY BETWEEN STABILITY AND BIOLOGICAL ACTIVITY IN HUMAN UNDILUTED ASCITES FLUID

Parts of this chapter are published as:

George R. Dakwar[1], Kevin Braeckmans[2], Wim Ceelen[3], Stefaan C. De Smedt[1], Katrien Remaut[1], Exploring the HYDRAtion method for loading siRNA on liposomes: The interplay between stability and biological activity in human undiluted ascites fluid. *Drug Delivery and Translational Research* (2016).

[1] Ghent Research Group on Nanomedicines, Faculty of Pharmaceutical Sciences, Laboratory for General Biochemistry and Physical Pharmacy, Ghent University, Ghent, Belgium

[2] Center for Nano- and Biophotonics, Ghent University, Ghent, Belgium

[3] Department of Surgery, Laboratory of Experimental Surgery, Ghent University Hospital, Ghent, Belgium

Abstract

Delivery of small interfering RNA (siRNA) is recently gaining tremendous attention for the treatment of ovarian cancer. The present study investigated the potential of different liposomal formulations composed of (2,3-Dioleoyloxy-propyl)-trimethylammonium (DOTAP) and 1,2-Dioleoyl-sn-glycero-3-phosphoethanolamine (DOPE) encapsulating siRNA (hydration method) for their ability to knockdown luciferase (Luc) activity in human ovarian cancer SKOV-3 cells. Fluorescence Single Particle Tracking (fSPT) and fluorescence correlation spectroscopy (FCS) in human undiluted ascites fluid obtained from a PC patient revealed that cationic hydra-lipoplexes (HYDRA-LPXs) and HYDRA-LPXs decorated with stable DSPE-PEG (DSPE HYDRA-LPXs) showed high stability during at least 24 h. HYDRA-LPXs decorated with sheddable C8 and C16 PEG-Ceramides (Cer HYDRA-LPXs) resulted in rapid and premature release of siRNA already in the first hours. Despite their role in preventing aggregation, liposomes decorated with stable PEG residues resulted in a poor transfection compared to the ones decorated with sheddable PEG residues in reduced serum conditions. Yet, the transfection efficiency of both Cer HYDRA-LPXs significantly decreased following 1 hour of incubation in ascites fluid due to a drastic drop in the cellular uptake, while DSPE HYDRA-LPXs are still taken up by cells, but too stable to induce efficient gene silencing.

Keywords: siRNA delivery, siRNA encapsulation, peritoneal metastasis, sheddable PEG, ascites

1. Introduction

Small interfering RNA (siRNA) therapeutics hold great potential for the treatment of different diseases, such as neurodegenerative pathologies, genetic and metabolic disorders and cancer [1, 2]. To ensure their therapeutic activity, siRNA-based medicines should be delivered into the cytoplasm of the target cell where the natural RNAi machinery could be engaged. Towards this goal, complexation or encapsulation of siRNA within nano-sized particles is being utilized to protect the siRNA from blood nucleases and other extracellular components with the aim to increase the fraction that enters into cells following administration. Apart from protection of the siRNA against nucleases , these nano-carriers should also (i) be resistant to the formation of large aggregates while circulating in the extracellular biofluids, (ii) prevent premature release of the siRNA before reaching the target cell [3], and (iii) (sufficiently) interact extracellularly with the plasma membrane and intracelluarly with the endosomal membrane, an interaction which is essential for therapeutic activity of siRNA [3, 4].

Over the last decade, both polymeric and lipid nanoparticles (LNPs) were employed for siRNA delivery [2, 5]. Due to the negative charge of the siRNA, cationic lipid-based and polymeric NPs are widely used to obtain spontaneous electrostatic interactions and protect the siRNA from degradation [6-8]. The most important difference between the lipid-based and polymeric vehicles is that the majority of the cationic polymers do not contain a hydrophobic tail, and thus are completely soluble in water. Also, cationic polymers can be synthesized in different molecular weights and shapes (linear versus branched) and can be more easily tuned with functional groups, to influence, for example, the intracellular trafficking of the vehicles and their biological activity [8, 9]. Generally speaking, LNPs contain a lipid bilayer-disrupting lipids that are activated by low endosomal pH, whereas polymers are very easy to modify and control their structure in a way that they become positively charged in acidic endosomes in order to enhance endosomal escape of siRNA [10].

Lipid nanoparticles (LNPs) have been extensively investigated as candidates for siRNA delivery in cancer therapy [11]. Currently, LNPs represent the most promising platform for systemic delivery of siRNAs, with lipid-based formulations in clinical trials for the treatment of different diseases [2, 5]. Despite major advances with LNPs for siRNA delivery, the main challenge remains their colloidal stability within the fluids of the body. In this context, grafting LNPs with polyethylene glycol (PEG) is the most common strategy to prevent aggregation and prolong their half-life in the circulation [12]. PEGylation, however, has been associated with poor biological activity of siRNA [12]. It is speculated that PEG chains significantly decrease the uptake of LNPs by cells and disrupt their interaction with the endosomal membrane [4, 13]. For instance, increasing the PEGylation of siRNA-lipoplexes (siRNA-LPXs) from 2 to 5 mol% dramatically diminished the siRNA gene silencing *in vivo* [14]. Furthermore, it has been postulated that multiple administration of stabilized PEGylated lipid particles (SPLP), induced a strong immune response against PEG,

resulting in accelerated blood clearance [15-17]. Worth mentioning also is that PEG residues interfere with the electrostatic interactions between negatively charged siRNA and positively charged lipids resulting in a low complexation/encapsulation efficiency. Also, we observed that PEGylation leads to the rapid premature release of the siRNA from the surface of the liposomes in different biological fluids [18-20]. Therefore, when tailoring LNPs for *in vivo* siRNA delivery, a delicate balance between avoiding (i) aggregation, (ii) premature release, (iii) immune responses and realizing efficient intracellular release of siRNA in the cytoplasm of cells should be installed to overcome PEG-associated problems. In this respect, an interesting approach could be the use of 'exchangeable' PEG-derivatized lipids, also called "sheddable PEG", which diffuse out of LPXs upon contact with biological membranes, depending on the length of the acyl chain of the lipid anchor. Among the most used sheddable PEG-lipids are ceramides (Cer-PEG) and diacylglycerols (PEG-S-DAGs) [21, 22].

Ovarian cancer leads to more than 140,000 deaths annually in women around the world [23]. In the majority of the cases, ovarian cancer often migrates to the peritoneal cavity forming fatal PC. Interestingly, IP administration of different drugs has recently shown some advantages to treat peritoneal tumors when compared to intravenous administration, mainly due to high concentrations of drug at the tumor site following IP administration [24-26]. Also, the delivery of siRNA to ovarian cancer cells using different nano-sized carriers is recently gaining increasing attention in cancer therapy [27-30]. It has been reported that the co-delivery of chemotherapeutic agents with siRNA is an efficient strategy to enhance tumor killing effect and overcome resistance of cancer cells when compared to delivery systems carrying either siRNA or chemotherapeutics alone [31-33]. First of all, siRNAs can specifically silence cancer associated genes, causing less side effects in non-cancer cells. Moreover, siRNA is not limited to target receptors that are expressed on the surface of cancer cells, but can also silence genes associated with intracellular targets [34].

In this study, we investigate the suitability of different liposomes (cationic, PEGylated and grafted with diffusible Cer-PEG) composed of DOTAP and DOPE (as lipids) encapsulating siRNA within the aqueous core (prepared by the hydration method) [18, 35] to knockdown luciferase in the human ovarian cancer cell line SKOV-3. Initially we employ advanced fluorescence microscopy techniques, such as fluorescence correlation spectroscopy (FCS) and fluorescence single particle tracking (fSPT) [36, 37] to follow the release and aggregation of the LPXs in ascites fluid obtained from a PC patient. Additionally, we test the uptake, toxicity and silencing efficiency of all the formulations. We hypothesized that liposomes encapsulating siRNA and decorated with diffusible Cer-PEG may be an attractive strategy to target tumors confined within the peritoneal cavity following IP adminstration, as they represent a fine balance between PEGylation and de-PEGylation [38].

2. Materials and methods

2.1 Materials

(2,3-Dioleoyloxy-propyl)-trimethylammonium-chloride (DOTAP) and 1,2-Dioleoyl-sn-glycero-3-phosphoethanolamine (DOPE) were purchased from Corden Pharma LLC (Liestal, Switzerland).

1,2-distearoyl-*sn*-glycero-3-phosphoethanolamine-N-[methoxy(polyethyleneglycol)-2000] (DSPE-PEG), N-palmitoyl-sphingosine-1-{succinyl[methoxy(polyethylene-glycol)2000]} (C16 mPEG 2000 Ceramide)**,** N-octanoyl-sphingosine-1-{succinyl[methoxy(polyethylene glycol)2000]} (C8 mPEG 2000 Ceramide) were purchased from Avanti Polar Lipids (Alabaster, AL, USA). Chloroform, 4-(2-hydroxyethyl)-1-piperazineethanesulfonic acid (HEPES), 3-(4,5-Dimethyl-2-thiazolyl)-2,5-diphenyl-2H-tetrazolium bromide (MTT) and sodium chloride (NaCl) were purchased from Sigma Aldrich (Bornem, Belgium).

Penicillin-Streptomycin (5000 U/ml), L-Glutamine (200 mM), 0.25% Trypsin-EDTA (1X) Phenol Red, McCoy's 5A (Modified), Opti-MEM® and 1,1'-dioctadecyl-3,3,3',3'-tetramethylindodicarbocyanine perchlorate (DID) (λex= 644 nm, λem= 665 nm) were purchased from Invitrogen (Merelbeke, Belgium). Luciferase Assay Substrate was purchased Promega (Madison, WI, USA). Fetal Bovine Serum (FBS) was purchased from HyClone® Thermo Scientific (Cramlington, UK). Passive Lysis Buffer and Luciferase Assay Kit were purchased from (Promega, Leiden, Netherlands).

2.2 Preparation and characterization of the HYDRA LPXs

Liposomes corresponding to 5 mM of DOTAP and 5 mM of DOPE lipids were prepared by mixing the appropriate amount of each lipid in a round bottomed flask before evaporation. PEGylated liposomes were prepared by adding the desired amounts of DSPE-PEG, or C8 Cer-PEG or C16 Cer-PEG dissolved in chloroform (corresponding to 5 mol% the total lipids) to the lipids before evaporation. A lipid film was formed by rotary evaporation of the chloroform at 40°C.
To obtain the so named 'HYDRA LPXs', the dried lipid film was hydrated with a siRNA solution in HEPES buffer (20 mM, pH 7.4) resulting in LPXs with a charge ratio of ± 8. Finally, the obtained solution was sonicated using a probe sonicator (Branson Ultrasonics Digital Sonifier®,Danbury,USA).We showed previously that this method results in the encapsulation of 50% of the complexed siRNA inside the liposomes and 50% bound to the outer surface of the liposomes [35]. The average size and zeta potential of all formulations were measured using Zetasizer Nano-ZS (Malvern, Worcestershire, UK).

2.3 Fluorescence Single Particle Tracking (fSPT)

Fluorescence Single particle tracking (fSPT) is a fluorescence microscopy technique which is used to characterize the diffusion of nanoparticles. Briefly, fSPT makes use of a fast CCD camera and wide-field laser illumination to obtain movies of single, fluorescently labeled particles in biological media. The movies are then analyzed by using in-house image processing software [36], where the motion trajectories and subsequently the diffusion coefficient of each individual particle is calculated. Based on the trajectories of all the particles, it is possible to make a distribution of diffusion coefficients, which is then converted into size distribution using the Stokes-Einstein equation given the viscosity of the biofluid at which the experiment was performed is known. Finally, the distribution is refined by the maximal entropy method [36]. We have previously shown that fSPT is ideally suited to characterize the size (and thus the extent of aggregation) of nanoparticles in biological fluids like human serum, ascites fluid, human plasma, and blood [3, 20, 36]. The main advantage of fSPT over the widely used sizing techniques such as Dynamic Light Scattering (DLS), is the ability to perform sizing measurements in undiluted biological fluids, without the influence of the proteins present in these fluids [3].

fSPT measurements were performed on the HYDRA-LPXs (Cationic, 5% DSPE-PEG, 5% C8 Cer-PEG, 5% C16 Cer-PEG) labeled with the lipophilic dye DID, that labels the lipid bilayer of the liposomes). LPXs were dispersed in biofluids as follows. First, formulations were diluted 400 times in HEPES buffer. Then 5 µl was added to 45 µl of biofluid (~90 vol% of ascites fluid), and incubated for 1, 2 and 3 h at 37°C in a 96-well plate (Greiner bio-one, Frickenhausen, Germany). fSPT-videos of the different formulations in the biofluids were recorded with the NIS Elements software (Nikon) driving the EMCCD camera (Cascade II:512, Roper Scientific, AZ, USA) and a TE2000 inverted microscope equipped with a 100_ NA1.4 oil immersion lens (Nikon) as previously described [3, 20] using the following values of viscosity at room temperature: 1.39 cP for human ascites fluid and 0.94 for HEPES buffer [3]. Human ascites fluid was obtained from a patient diagnosed with PC at the Medical Oncology Department of Ghent University Hospital (approved by the Ethics Committee of the Ghent University Hospital (no. 2013/589).

2.4 Fluorescence Correlation Spectroscopy (FCS) on HYDRA LPXs

FCS is a microscopy-based technique that monitors the fluorescence intensity fluctuations of molecules diffusing in and out of the focal volume of a confocal microscope [3]. When free fluorescently labeled siRNA molecules pass through the focal volume, a fluorescence baseline with an intensity that corresponds to the concentration of the free labeled siRNA molecules is obtained. When the siRNA is complexed/encapsulated within a carrier, the concentration of free siRNA drops and subsequently, a drop in the baseline intensity of the fluorescence signal occurs, accompanied with fluorescence fluctuations (i.e. peaks) each time a complex passes the focal volume. Release of siRNA, on its turn, results in an increase in the fluorescence baseline. An important advantage

of FCS is the low volume of samples needed to perform the experiments (~50 µl). Our group showed before that FCS is ideally suited to measure the amount of siRNA that is released/associated from/with nano-sized carriers in various types of biofluids [3,4,15].

FCS measurements were carried-out on HYDRA-LPXs containing 30% Cy-5 siRNA and 70% non-labeled siRNA, with a charge ratio of ± 8. 5 µl of LPXs were diluted to a final volume of 50 µl in respectively HEPES buffer or ascites fluid (~ 90 vol%) and FCS measurements were done (i) immediately after diluting the LPXs (in HEPES or ascites fluid), (ii) 1 h and (iii) 24 h after incubation with the biofluids at 37°C. FCS measurements were performed on a C1si laser scanning confocal microscope (Nikon, Japan), equipped with a time-correlated single photon counting (TCSPC) data acquisition module (Picoquant, Berlin, Germany). The laser beam was held stationary and focused through a water immersion objective lens (Plan Apo 60, NA 1.2, collar rim correction, Nikon, Japan) at ~ 50 µm above the bottom of the glass-bottom 96-well plate (Grainer Bioone, Frickenhausen, Germany), which contained the fluorescent LPXs. The 633 nm laser beam was used to record fluorescence intensity fluctuations using SymPhoTime (Picoquant, Berlin, Germany).

2.5 Cell culture

The human ovarian cancer cell line SKOV-3 which stably expresses firefly luciferase was used for *in vitro* experiments. Cells were cultured in McCoy's 5A medium supplemented with FBS, Penicillin-Streptomycin and L-Glutamine. Cells were cultured until 80% to 90% confluency and detached from tissue culture dishes with 0.25% trypsin. Cells were maintained in an incubator at 37°C in a humidified atmosphere with 5% CO_2.

2.6 Cell viability assay

The MTT assay was used as a measure of cell viability following incubation of the studied formulations with a final negative control siRNA concentration of 10, 15 and 20 nM. SKOV-3 cells were cultured on 24-well tissue culture plates (35,000 cells per well). On the next day, cells were incubated for 4 h with 500 µl Opti-MEM® containing the LPXs of interest or 30% of ethanol as positive control. Then, cells were washed and incubated with McCoy's 5A medium for an additional 24 h. Thereafter, 100 µl of MTT stock solution (5 mg/ml MTT in PBS) in McCoy's 5A was added to each well and incubated for 3 h. After aspirating the medium, 500 µl of DMSO was added to each well in order to dissolve the formazan crystals. The plates were covered with aluminum foil, placed on an orbital shaker for 10 min and the absorbance of the formed formazan crystals was determined at 590 nm with reference at 690 nm using a Wallac Envision™ multilabel reader (PerkinElmer, Zaventem, Belgium). Percentages of cell viability for each sample were calculated as follows: (absorbance of the sample / absorbance of the negative control) x 100%.

2.7 Internalization of siRNA into SKOV-3 cells

SKOV-3 cells were plated on 24-well plates (35,000 cells in each well) and allowed to grow in an incubator for 24 h. Cells were incubated with the formulations containing 10% Alexa Fluor-488 siRNA at a final siRNA concentration of 15 nM for 4 h at 37°C. At the end of the incubation, cells were washed extensively with warm growth medium and PBS, then detached using trypsin and analyzed by FACS (FACSCalibur Flow Cytometer, BD Biosciences, USA). Uptake experiments were done with LPXs administered in Opti-MEM® or with LPXs which were first incubated for 1 h in human ascites fluid, as previously described [20]. Uptake experiments in the ascites fluid were performed by incubating 300 µl of each of the studied formulations with 700 µl of ascites fluid for 1 h at 37°C. Then, 300 µl of the mixture were added in triplicates to 700 µl of Opti-MEM® in each well of a 24 well-plate. After 4 h of incubation at 37°C, cells were washed, detached and analyzed as described above.

2.8 Transfection efficiency

SKOV-3 cells were cultured on 24-well plates (35,000 cells/well) in 500 µl of medium containing 10% FBS 24 h prior to the transfection. Cells were incubated with HYDRA-LPXs at a final siRNA concentration of 15 nM respectively in Opti-MEM® or following 1 h of pre-incubation in ascites fluid as previously explained [20]. After 4 h incubation, the transfection medium was replaced by culture medium and cells were returned to the incubator for 24 h. Then, cells were lysed with Passive Lysis Buffer and analyzed for firefly luciferase expression using the luciferase assay kit (Promega). The bioluminescence (Relative Light Units, RLU) was measured using a GloMax Luminometer (Promega). The percentage of luciferase downregulation was determined by the following equation:

% transfection = 100 – (100 x RLU_{luc}/RLU_{ctrl}), where RLU_{ctrl} is the mean for control siRNA and RLU_{luc} is the mean for luciferase siRNA. Transfection experiments were performed in triplicates on three different days. For transfections in the ascites fluid, 300 µl of each HYDRA-LPX (of each formulation) were incubated with 700 µl ascites fluid and incubated for 1 h at 37°C. Thereafter, 300 µl of the mixture was added to 700 µl of Opti-MEM® in each well of a 24 well-plate. Then, the medium was replaced with growth medium and cells were returned to the incubator for 24 h, as described above.

2.9 Statistical analysis

Statistical analysis on the transfection data (Figure 5) was performed using GraphPad Prism 6. Data are presented as means ± SD. Statistically significant differences were calculated by using an analysis of variance (ANOVA) at a 0.05 significance level, followed by Sidak's post-test. For each formulation, transfection experiments carried out in Opti-MEM® were compared to these in ascites fluid.

3. Results

3.1 Characterization of the studied LPXs

Table 1 shows the size and zeta potential of the different used formulations. In the hydration method, formulations were prepared by hydrating the lipid film with siRNA directly. This results in liposomes in which the siRNA is also encapsulated inside the aqueous core of the resulting LPXs, as well as being complexed to the outer surface of the liposomal formulations. As depicted in Table 1, all the studied formulations resulted in nano-sized vesicles, as determined by dynamic light scattering (DLS). When compared to empty liposomes, the size increased for all formulations when LPXs were formed, except for the 5% C16 Cer HYDRA-LPXs.

As expected, both PEGylation and the addition of siRNA influenced the charge of the liposomes. Introducing PEG chains on the surface of the liposomes results in shielding of the positive charge from about 56 mV for the cationic liposomes to about 17-20 mV for the PEGylated ones. Encapsulation of siRNA resulted in a further decrease of the charge, except for the 5% C16 Cer HYDRA-LPXs.

Table 1. Hydrodynamic diameter and ζ-Potential of the liposomes only or loaded with siRNA at pH 7.4.

Formulation	Z-average diameter ± SD (nm)	Polydispersity index (PDI)	ζ-potential (mV) (mean ±SD)	Abbreviation
Cationic liposomes	86 ± 1	0.2	56 ± 1	Cationic LP
HYDRA-LPX	135 ± 3	0.25	46 ± 1	HYDRA- LPXs
5% DSPE-PEG LP	93 ± 1	0.2	17 ± 1	DSPE-LP
5% DSPE-PEG LPX	129 ± 3	0.25	14 ± 1	DSPE HYDRA-LPX
5% C8 Cer-PEG	93 ± 1	0.33	18 ± 1	5% C8 Cer-LP
5% C8 Cer-PEG LPX	106 ± 1	0.24	13 ± 1	5% C8 Cer HYDRA-LPX
5% C16 Cer-PEG LP	115 ± 2	0.24	6 ± 1	5% C16 Cer-LP
5% C16 Cer-PEG LPX	115 ± 1	0.25	6 ± 1	5% C16 Cer HYDRA-LPX

3.2 Aggregation of the formulations in undiluted ascites fluid

In our previous study we have shown that DLS is not an ideal technique for characterizing aggregation of nanoparticles in biological fluids, simply due to scattering that results from e.g. the proteins in the biofluids [3]. fSPT has proven to be superior over DLS for this purpose [3, 36]. Figure 1A shows the size distributions of the HYDRA-LPXs as measured by fSPT. In agreement with the DLS outcomes in Table 1, HYDRA-LPXs have an average size around 100 nm when measured in HEPES buffer (Figure 1A, black curve). Following 1 h of incubation in ascites fluid, the size distribution is shifted to the right (red curve), with a peak diameter around 200 nm. Upon longer times in ascites fluids, aggregation of the HYDRA-LPXs seemed somehow to continue, resulting in HYDRA-LPXs with a peak diameter of 300 nm (Figure 1A, blue curve). After 3 h of incubation, the size distributions did not further change, indicating the aggregation reached an equilibrium already after 2 h (Figure 1A, green curve).

Next, we were interested if PEGylation would further inhibit the aggregation of HYDRA-LPXs. Two types of PEGylation were tested, namely the incorporation of respectively stable, non-exchangeable DSPE-PEG chains, and exchangeable PEG-Ceramides. In the case of the DSPE-PEG HYDRA-LPXs (Figure 1B), initially a minor aggregation was observed following incubation in ascites fluid when compared to the distribution in HEPES buffer (~ 150 nm). Then, the PEGylated complexes remained stable, resulting in particles of about 250 nm in diameter. For the 5% C8 Cer HYDRA-LPXs, the size in HEPES buffer was around 100 nm (Figure 1C) and increased to 200 nm after 1 h of incubation in ascites fluid. Surprisingly, further incubation in ascites fluid for 2 and 3 h resulted again in smaller 5% C8 Cer HYDRA-LPXs of 150 nm and less. The SPT data in Figure 1D for the C16 Cer HYDRA-LPXs exhibit a similar behavior to the C8 Cer HYDRA-LPXs, with an equilibrium reached after 1 h of incubation in ascites fluid, and a peak diameter of about ~250 nm. Taken together, all the formulations seemed sufficiently stable in the ascites fluid: no micrometer-sized aggregates were observed and the size of all LPXs remained sufficiently small to allow endocytosis by cells.

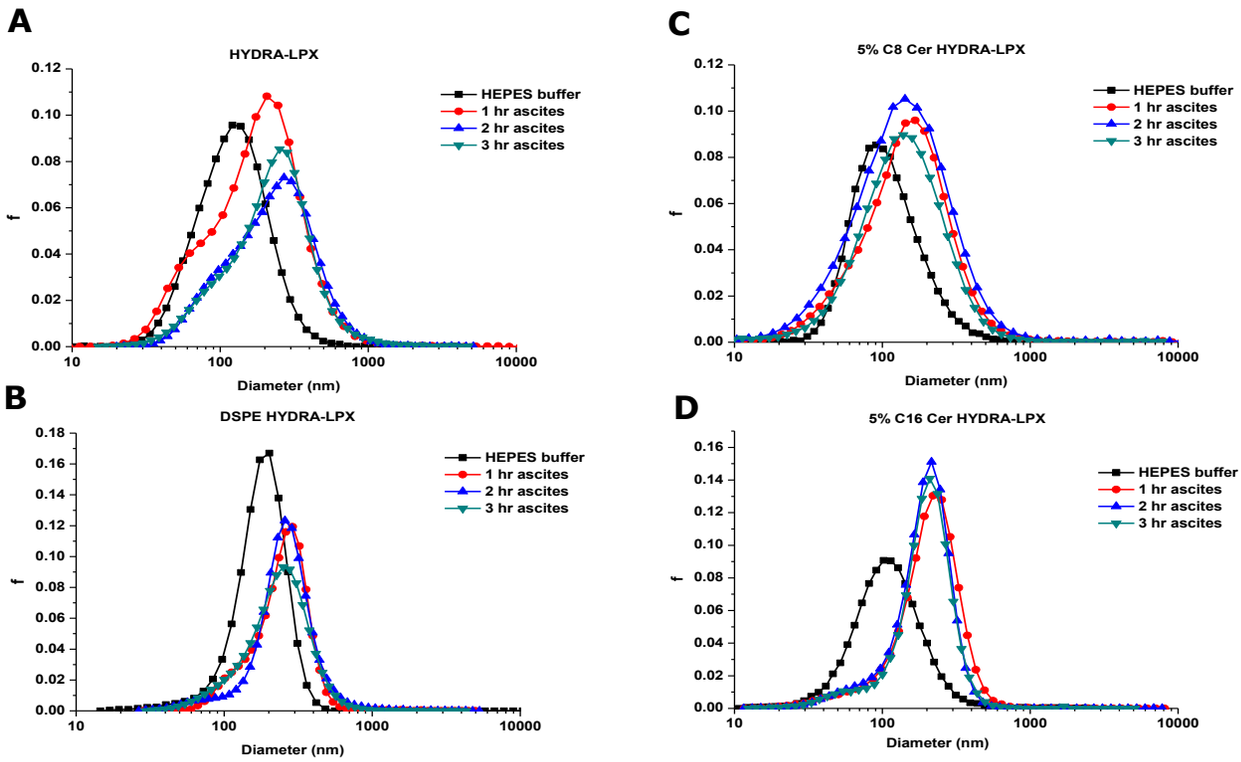

Figure 1. fSPT size distributions of the different formulations following incubation in 90 vol % human ascites fluid at 37 °C. (A) HYDRA-LPX, **(B)** DSPE HYDRA-LPX, **(C)** 5% C8 Cer HYDRA-LPX and **(D)** 5% C16 Cer HYDRA-LPX.

3.3 Release of siRNA from the formulations in undiluted ascites fluid

As demonstrated previously, FCS is a suitable method to follow the release of siRNA from different types of formulations in undiluted biological fluids [3, 19, 20]. Figure 2 displays the complexation efficiency of the studied formulations. HYDRA-LPXs show a high complexation efficiency with about 80% of the siRNA complexed with the liposomes immediately after preparation in HEPES buffer (Figure 2, white bars) and during 24 h (grey and green bars). Following 1 h of incubation (Figure 2, blue bars), a burst release was observed leading to about 40% complexed siRNA (60% of free siRNA). This release is highly likely ascribed to the siRNA which is bound on the surface of the liposomes and not actually encapsulated inside. No substantial further release was noted after 24 h of incubation in ascites fluid, demonstrating that eventually about 35% of the siRNA was encapsulated within the aqueous core of the liposomes (magenta bars). PEGylation clearly influenced the complexation efficiency and release profile of the studied formulations. For DSPE HYDRA-LPXs, only 50% of the siRNA is complexed immediately after preparation, suggesting that PEGylation lowers the siRNA complexation efficiency (white bars). This 50% of siRNA, however, can be retained in the DSPE HYDRA-LPXs for the complete 24 h incubation period and is therefore most likely encapsulated inside the liposomes (Figure 2, magenta bars). For the Cer HYDRA-LPXs, the effect of PEGylation was even more pronounced, with 70% and 75% of free siRNA (e.g. uncomplexed) as such in HEPES buffer for the 5% C8 Cer and 5% C16 Cer HYDRA-LPXs respectively. Following 24 h of incubation in ascites fluid, both Cer HYDRA-LPXs resulted in around 90% of free siRNA (Figure 2, magenta bars).

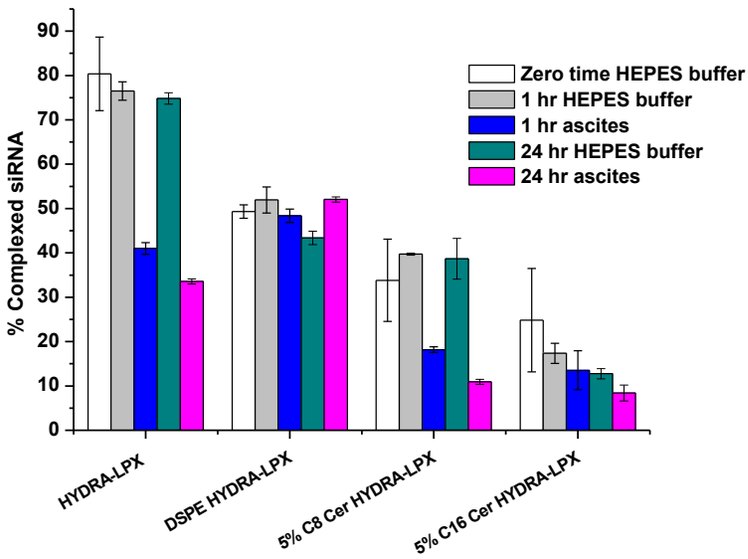

Figure 2. Complexation efficiency of the studied formulations immediately following preparation (white bars), 1 h (grey bars) and 24 h (green bars) following incubation in HEPES buffer, and percentage of complexed siRNA after incubation of the formulations in 90 vol % of human ascites fluid during 1 h (blue bars) and 24 h (magenta bars).

3.4 Cytotoxicity of the studied formulations

The toxicity of the formulations was assessed on SKOV-3 human ovarian cancer cells using a MTT assay. As can be seen in Figure 3, the formulations did not exhibit any severe decrease in the metabolic activity of the cells, with maximum 20% mortality for the highest siRNA concentrations of 20 nM. A decrease in the cell viability was observed with increasing siRNA concentrations. To stay within the non-toxic range of concentrations, we decided to perform uptake and transfection experiments with a final concentration of 15 nM.

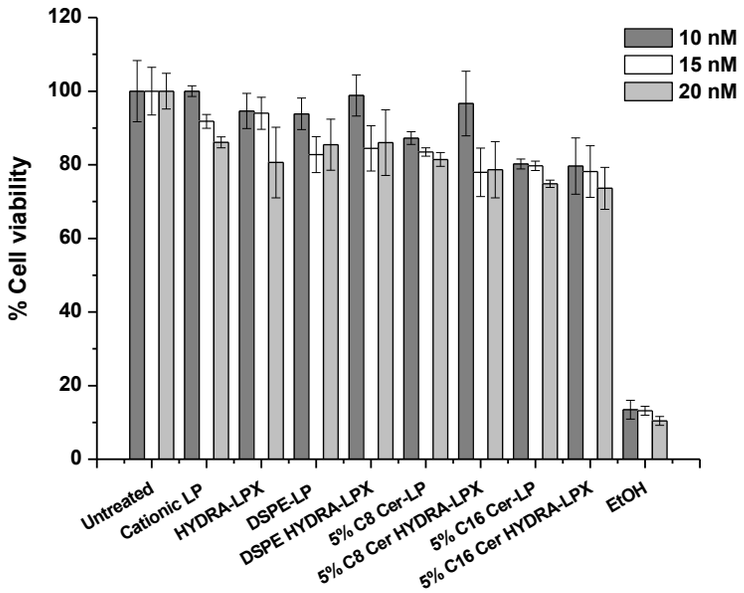

Figure 3. Outcomes of the cell viability assay (MTT). For each formulation the toxicity of the liposomes and LPXs was evaluated using 3 different concentrations, 10 nM (dark grey bars), 15 nM (white bars) and 20 nM (grey bars), respectively. Results are expressed as mean ± SE.

3.5 Cellular uptake and transfection efficiency of the formulations by SKOV-3 cells

To evaluate the ability of the different formulations to knockdown the expression of a specific gene, SKOV-3 cells stably expressing luciferase were incubated with the formulations containing siRNA against luciferase (luc siRNA). To verify the knockdown specificity, luc siRNA formulations were compared to the same formulations loaded with a scrambled negative control siRNA.

We have recently proven the importance of performing uptake experiments of formulations carrying siRNA in the relevant biofluid [20]. Uptake is a key feature in siRNA delivery, since naked siRNA cannot internalize into cells due to its negative charge and hydrophilicity. To test whether the formulations are capable of delivering siRNA into cells, we incubated SKOV-3 cells with fluorescently labeled LPXs and followed their uptake with flow cytometry. The outcomes of the uptake experiments shown in Figure 4 indicate that all the formulations are internalized into SKOV-3 cells at 37°C when incubated in serum reduced media (i.e. Opti-MEM®), represented by high percentage of positive cells (Figure 4, white bars). Following 1 h of incubation in ascites fluid (Figure 4, grey bars), however, all the formulations significantly lose their ability to be taken up by cells, except for the DSPE-HYDRA LPXs where cellular uptake still occurs.

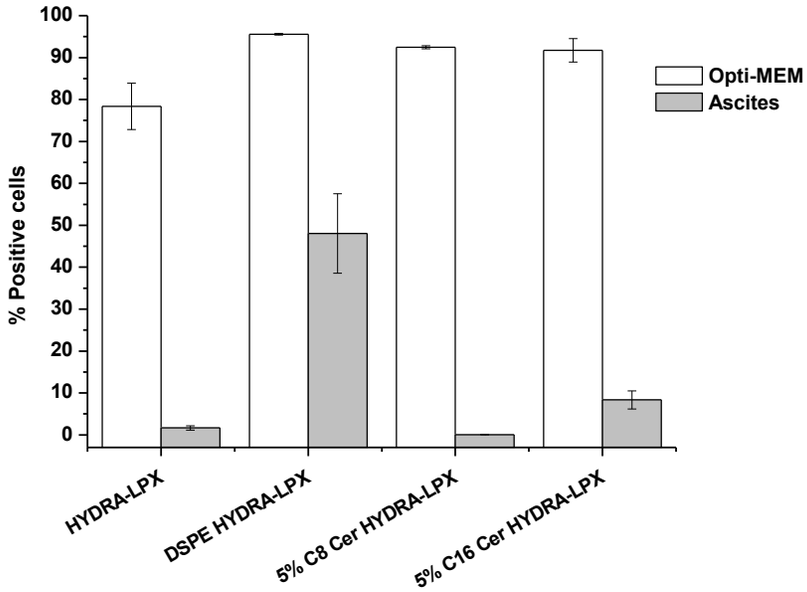

Figure 4. Uptake of AF-488 siRNA-labeled formulations by SKOV-3 cells. The studied formulations were prepared in HEPES buffer and added to the cells in Opti-MEM® following preparation as such (white bars) or after incubation for 1 h in human ascites fluid before adding them on the cells (grey bars).

Figure 5 depicts the transfection efficiency of the studied formulations in Opti-MEM® (white bars) and following 1 h of incubation in ascites fluid (grey bars). In Opti-MEM®, it can be seen that only DSPE HYDRA-LPXs resulted in a very poor transfection efficiency (37%). All other formulations demonstrated high and significant downregulation of 70% for the HYDRA-LPXs, 73% for the 5% C8 Cer HYDRA-LPXs and 80% for the 5% C16 Cer HYDRA-LPXs. Following incubation in ascites fluid, however, all the formulations lost their ability to silence luciferase, when compared with the situation in Opti-MEM®.

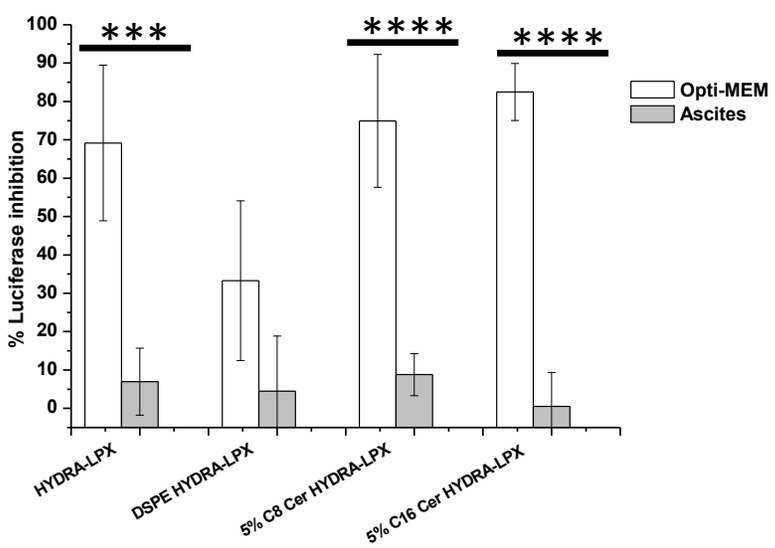

Figure 5. Inhibition of luciferase in SKOV-3 cells by the formulations in Opti-MEM® (white bars) and following incubation of the LPXs for 1 h in ascites fluid (70 vol %) (grey bars). The values in the graph represent the average from at least three experiments that were performed on different days.

4. Discussion

4.1 Choice of the study

The final goal of this study is to assess the suitability of liposomal-based formulations loaded with siRNA via the hydration method and possessing different surface modifications in undiluted ascites fluid obtained from a PC patient for siRNA delivery. As a follow-up of our previous study [3] and towards enhancing the stability of LPXs and maximizing their biological activity, we focused on two main aspects: 1) the siRNA loading method and 2) the PEGylation strategy. On the level of loading, we used the hydration method [18, 35], while on the level of PEGylation we decided to evaluate the stable DSPE-PEG, diffusible C8 and C16 Cer-PEG. The different PEG-chains were chosen to understand whether Cer-PEGylation can still play a role in preventing aggregation in the extracellular IP fluid, while the diffusion of the PEG-chains out of the liposomal formulations upon interaction with biological membranes would enhance the cellular uptake and endosomal escape on the intracellular level. In this context, Cer-PEG with shorter C8 acyl chain lipids (C8) seems to be best candidates for local IP delivery, due to the rapid exchange rate of the Cer-PEG from the surface of the liposomes, compared to the longer acyl chains (C20) [39]. Additionally, C8 Cer-PEG were successfully exploited to deliver plasmid DNA for regional gene therapy [40].

4.2 Influence of PEGylation on encapsulation efficiency

It is of interest to point out the differences between the hydration technique used in this study and the widely used complexation technique. With the conventional complexation technique, liposomes are prepared by hydrating the lipid film with a buffer solution. Then, LPXs are prepared by the simple mixing of siRNA and the preformed liposomes, taking advantage of the electrostatic interactions between the negatively charged siRNA and the cationic liposomes. In this case the siRNA binds on the surface of the liposomes, and is not encapsulated into the aqueous core. We have previously demonstrated, however, that the surface bound siRNA in this classic complexation protocol is easily displaced when the liposomes are dispersed in biofluids such as human serum or ascites fluid, especially when PEGylated liposomes are used [3].

We hypothesized that when using the hydration protocol [35], which ensures an even distribution of the negatively charged siRNA over the inner and outer core of a cationic lipid, the premature release of siRNA in the ascites fluid could be overcome [35]. Indeed, only the surface bound siRNA is expected to be released from the LPXs in the biofluids, while the siRNA encapsulated in the aqueous core is protected from premature release. Figure 2 demonstrated that this hypothesis was valid to some extent. We have previously shown that 5% DSPE-PEG LPXs prepared with the classic complexation method, release the majority of the complexed siRNA immediately after incubation with ascites fluid [3]. For DSPE HYDRA-LPXs, however, 50% of the siRNA is still encapsulated within the liposomes following 24 h of incubation in ascites fluid (Figure 2). This agrees with our assumption that with the hydration method, the siRNA within the aqueous

core of the liposomes is protected from the external environment, and thus the negatively charged proteins (mainly albumin) which compete for binding to the liposomes. Also the non-PEGylated HYDRA-LPXs retain about 35-40% of the complexed siRNA within the aqueous core after 24 h of incubation in ascites fluid, following the initial burst release of the siRNA which is complexed on the surface of the liposomes and exposed to the proteins in the ascites fluid. Unfortunately, the high stability of the HYDRA-LPXs and DSPE HYDRA-LPXs was not observed for the formulations containing C8 and C16 Cer-PEG chains. Both formulations resulted in the formation of complexes with a low complexation efficiency of siRNA. Also, the majority of siRNA that was complexed, is released almost immediately following incubation in ascites fluid. This rapid and premature release most likely stems from a re-organization on the level of the lipid bilayer upon introducing the C8 and C16 Cer-PEG chains within the lipid bilayer, resulting in a smaller aqueous core and consequently lower complexation efficiency where most of the siRNA is free or attached to the surface of the complexes.

4.3 Influence of stability on biological activity

While extracellular stability is one of the major concerns when designing siRNA delivery systems, the internalization and intracellular interactions with the different organelles are key factors to ensure maximal biological activity. The size and the charge of the studied formulations (Table 1) suggest that these complexes can cross biological membranes and deliver the siRNA into cells (Figure 4). Also, all PEGylated formulations used in this study succeeded in preventing the aggregation of the liposomal formulations for at least 3 hours when incubated in ascites fluid (Figure 1). Therefore, each PEGylation strategy seems suitable to stabilize the formulations and to assure the presence of nano-sized formulations for a sufficiently long time to warrant cellular uptake. Following internalization, endosomal escape is essential to ensure delivery of siRNA in the cytoplasm and to induce efficient silencing of the target gene [4]. For the HYDRA-LPXs and Cer HYDRA-LPXs, substantial luciferase inhibition was observed when the incubation took place in Opti-MEM® (Figure 5, white bars), except for the DSPE HYDRA-LPXs formulation. In the case of the HYDRA-LPXs, the cationic charge facilitates the interaction and destabilization of the endosomes, leading to fusion and eventually release of the siRNA into the cytosol. The fusion is further enhanced when a fusogenic "helper lipid" is incorporated within the liposomal formulation, such as DOPE in this case. It has been shown that upon acidification of the endosomal compartment DOPE triggers a conformational change from the stable lamellar phase into the highly unstable inverted hexagonal phase, which is thought to destabilize the endosomal membrane and release the cargo into the cytosol [41] . This conformational transition is not possible in the DSPE HYDRA-LPXs [42]. This explains the relatively low transfection efficiency of this formulation when compared with other formulations (Figure 5).

When PEGylation is performed with sheddable Cer-PEG instead of stable DSPE-PEG chains, it can be seen that both Cer-PEG HYDRA-LPXs result in high transfection efficiency. The transfection efficiency of the Cer-PEG formulations is highly likely ascribed to the "de-PEGylation" that occurs

upon interaction of the Cer-PEG formulations with the cell membrane [42], and consequently, similar interaction with the endosomes as the one described above for the HYDRA-LPXs is expected.

Since the final goal of this study is to determine the biological activity of the studied formulations in a relevant undiluted biofluid, we tested the transfection efficiency of all the formulations following incubation in ascites fluid obtained from a PC patient (Figure 5, grey bars). We are convinced that undiluted ascites fluids better resembles the *in vivo* peritoneal situation, not only in terms of stability, but also biological activity [20]. The drop in the transfection efficiency observed upon incubation in ascites fluid can be discussed on two levels: 1) cellular uptake of the studied formulations and 2) intracellular trafficking of the DSPE HYDRA-LPXs specifically following internalization. In particular, the HYDRA-LPXs and Cer HYDRA-LPXs are not internalized into SKOV-3 cells following 1 h of incubation in ascites fluid (Figure 4). Consequently, the cargo (i.e. siRNA) is not delivered into the cytoplasm of the cell where it should be further processed by the RNAi machinery, leading eventually to the absence of biological activity depicted in Figure 5.

Based on the stability data in Figure 1 and Figure 2, DSPE HYDRA-LPXs are protected from aggregation in the presence of ascites fluid and are able to keep the siRNA encapsulated for a sufficient long time to allow internalization into the cells. Therefore, the poor transfection efficiency observed for the DSPE HYDRA-LPXs is mainly due to the poor interaction with the endosomes, as also observed for the transfections in Opti-MEM®. The poor transfection efficiency of the DSPE-PEG formulation stands in line with recently published data, where DOTAP/cholesterol pDNA LPXs with 2% DSPE-PEG diminished the transfection compared to the non-PEGylated LPXs *in vitro* [43]. Additionally, DOTAP DOPE LPXs loaded with survivin siRNA and grafted with 1% DSPE-PEG successfully downregulated the activity of survivin in cultured cells, but lost its activity in peritoneal tumors *in vivo* [33].

Taken together, the findings of this study provide an evidence of the sensitive interplay that exists between extracellular stability, cellular uptake and biological activity when developing nano-sized siRNA formulations in protein-rich biological fluids. An optimal formulation designated for *in vivo* applications should fulfill all the requirements of colloidal stability, interaction with biological barriers, and intracellular trafficking in the relevant biofluid. One should keep in mind that formulations that show good stability and transfection characteristics in protein-free conditions such as Opti-MEM®, do not necessarily translate in potent formulations when transfections are being performed in the relevant biological fluids. For the formulations tested in this study, cellular uptake was the bottleneck for obtaining efficient gene knockdown, whereas poor intracellular processing was most probably the reason for the low gene knockdown observed with the only formulation taken up by the cells following incubation in undiluted ascites fluid (i.e. DSPE HYDRA-LPX).The cellular uptake in this case was not a problem, since this formulation exhibited low transfection efficiency (Figure 5) even in protein-free conditions (i.e. Opti-MEM®), where efficient internalization occurred.

5. Conclusions

In this study we tested the stability of different liposomal formulations for IP siRNA delivery based on the hydration technique and different types of PEGylation in human undiluted ascites fluid, as well as, the transfection efficiency in the SKOV-3 ovarian cancer cell line. We hypothesized that liposomes encapsulating siRNA and grafted with Cer-PEG chains would be an ideal platform for IP siRNA delivery. Nonetheless, our findings revealed that these carriers are not taken up by SKOV-3 cells in protein-rich conditions (i.e. ascites fluid). On the contrary, liposomes encapsulating siRNA and coated with stable DSPE-PEG are endocytosed by SKOV-3 cells in protein-rich conditions, but are associated with poor biological activity highly likely due to insufficient intracellular processing.

Acknowledgments

GD is a doctoral fellow of the Flemish Government (Vlaamse overheid). WC is a senior clinical investigator of the Fund for Scientific Research – Flanders (FWO). The research was supported by the Research Foundation-Flanders (research project G006714N). We thank Senne Corneils for his help with the experiments.

References

[1] M.R. Lares, J.J. Rossi, D.L. Ouellet, RNAi and small interfering RNAs in human disease therapeutic applications, Trends Biotechnol, 28 (2010) 570-579.
[2] A. Wittrup, J. Lieberman, Knocking down disease: a progress report on siRNA therapeutics, Nat Rev Genet, 16 (2015) 543-552.
[3] G.R. Dakwar, E. Zagato, J. Delanghe, S. Hobel, A. Aigner, H. Denys, K. Braeckmans, W. Ceelen, S.C. De Smedt, K. Remaut, Colloidal stability of nano-sized particles in the peritoneal fluid: towards optimizing drug delivery systems for intraperitoneal therapy, Acta Biomater, 10 (2014) 2965-2975.
[4] T.F. Martens, K. Remaut, J. Demeester, S.C. De Smedt, K. Braeckmans, Intracellular delivery of nanomaterials: How to catch endosomal escape in the act, Nano Today, 9 (2014) 344-364.
[5] R. Kanasty, J.R. Dorkin, A. Vegas, D. Anderson, Delivery materials for siRNA therapeutics, Nature Materials, 12 (2013) 967-977.
[6] C.K. Chen, C.H. Jones, P. Mistriotis, Y. Yu, X.N. Ma, A. Ravikrishnan, M. Jiang, S.T. Andreadis, B.A. Pfeifer, C. Cheng, Poly(ethylene glycol)-block-cationic polylactide nanocomplexes of differing charge density for gene delivery, Biomaterials, 34 (2013) 9688-9699.
[7] D.C. Forbes, N.A. Peppas, Polycationic Nanoparticles for siRNA Delivery: Comparing ARGET ATRP and UV-Initiated Formulations, Acs Nano, 8 (2014) 2908-2917.
[8] C.H. Jones, C.K. Chen, A. Ravikrishnan, S. Rane, B.A. Pfeifer, Overcoming Nonviral Gene Delivery Barriers: Perspective and Future, Mol Pharmaceut, 10 (2013) 4082-4098.
[9] A. Elouahabi, J.M. Ruysschaert, Formation and intracellular trafficking of lipoplexes and polyplexes, Mol Ther, 11 (2005) 336-347.
[10] S.K. Samal, M. Dash, S. Van Vlierberghe, D.L. Kaplan, E. Chiellini, C. van Blitterswijk, L. Moroni, P. Dubruel, Cationic polymers and their therapeutic potential, Chem Soc Rev, 41 (2012) 7147-7194.
[11] C. Wan, T.M. Allen, P.R. Cullis, Lipid nanoparticle delivery systems for siRNA-based therapeutics, Drug Delivery and Translational Research, 4 (2014) 74-83.
[12] L.C. Gomes-da-Silva, N.A. Fonseca, V. Moura, M.C.P. de Lima, S. Simoes, J.N. Moreira, Lipid-Based Nanoparticles for siRNA Delivery in Cancer Therapy: Paradigms and Challenges, Accounts of Chemical Research, 45 (2012) 1163-1171.
[13] S. Mishra, P. Webster, M.E. Davis, PEGylation significantly affects cellular uptake and intracellular trafficking of non-viral gene delivery particles, European Journal of Cell Biology, 83 (2004) 97-111.
[14] A. Santel, M. Aleku, O. Keil, J. Endruschat, V. Esche, G. Fisch, S. Dames, K. Loffler, M. Fechtner, W. Arnold, K. Giese, A. Klippel, J. Kaufmann, A novel siRNA-lipoplex technology for RNA interference in the mouse vascular endothelium, Gene Therapy, 13 (2006) 1222-1234.
[15] A. Judge, K. McClintock, J.R. Phelps, I. MacLachlan, Hypersensitivity and loss of disease site targeting caused by antibody responses to PEGylated liposomes, Mol Ther, 13 (2006) 328-337.
[16] T. Tagami, K. Nakamura, T. Shimizu, T. Ishida, H. Kiwada, Effect of siRNA in PEG-coated siRNA-lipoplex on anti-PEG IgM production, Journal of Controlled Release, 137 (2009) 234-240.
[17] T. Tagami, K. Nakamura, T. Shimizu, T. Ishida, H. Kiwada, Effect of siRNA in PEG-Coated siRNA-Lipoplex on the Anti-PEG IgM Production as Induced by the PEG-Coated siRNA-Lipoplex, Mol Ther, 17 (2009) S253-S253.
[18] K. Buyens, S.C. De Smedt, K. Braeckmans, J. Demeester, L. Peeters, L.A. van Grunsven, X.D. du Jeu, R. Sawant, V. Torchilin, K. Farkasova, M. Ogris, N.N. Sanders, Liposome based systems for systemic siRNA delivery: Stability in blood sets the requirements for optimal carrier design, Journal of Controlled Release, 158 (2012) 362-370.
[19] K. Buyens, B. Lucas, K. Raemdonck, K. Braeckmans, J. Vercammen, J. Hendrix, Y. Engelborghs, S.C. De Smedt, N.N. Sanders, A fast and sensitive method for measuring the integrity of siRNA-carrier complexes in full human serum, Journal of Controlled Release, 126 (2008) 67-76.
[20] G.R. Dakwar, K. Braeckmans, J. Demeester, W. Ceelen, S.C. De Smedt, K. Remaut, Disregarded Effect of Biological Fluids in siRNA Delivery: Human Ascites Fluid Severely Restricts Cellular Uptake of Nanoparticles, ACS Applied Materials & Interfaces, 7 (2015) 24322-24329.
[21] E. Ambegia, S. Ansell, P. Cullis, J. Heyes, L. Palmer, I. MacLachlan, Stabilized plasmid-lipid particles containing PEG-diacylglycerols exhibit extended circulation lifetimes and tumor selective gene expression, Biochimica Et Biophysica Acta-Biomembranes, 1669 (2005) 155-163.
[22] M.S. Webb, D. Saxon, F.M.P. Wong, H.J. Lim, Z. Wang, M.B. Bally, L.S.L. Choi, P.R. Cullis, L.D. Mayer, Comparison of different hydrophobic anchors conjugated to poly(ethylene glycol): Effects on the pharmacokinetics of liposomal vincristine, Biochimica Et Biophysica Acta-Biomembranes, 1372 (1998) 272-282.
[23] J. Hunn, G.C. Rodriguez, Ovarian Cancer: Etiology, Risk Factors, and Epidemiology, Clinical Obstetrics and Gynecology, 55 (2012) 3-23.
[24] W.P. Ceelen, M.F. Flessner, Intraperitoneal therapy for peritoneal tumors: biophysics and clinical evidence, Nature Reviews Clinical Oncology, 7 (2010) 108-115.

[25] P. Zahedi, J. Stewart, R. De Souza, M. Piquette-Miller, C. Allen, An injectable depot system for sustained intraperitoneal chemotherapy of ovarian cancer results in favorable drug distribution at the whole body, peritoneal and intratumoral levels, Journal of Controlled Release, 158 (2012) 379-385.
[26] G.R. Dakwar, M. Shariati, W. Willaert, W. Ceelen, S.C. De Smedt, K. Remaut, Nanomedicine-based intraperitoneal therapy for the treatment of peritoneal carcinomatosis - Mission possible?, Adv Drug Deliv Rev, (2016).
[27] R.D. George, S.C.D.S. Stefaan, R. Katrien, Intraperitoneal nonviral nucleic acid delivery in the treatment of peritoneal cancer, Intraperitoneal Cancer Therapy, CRC Press2015, pp. 359-371.
[28] M.S. Goldberg, siRNA Delivery for the treatment of ovarian cancer, Methods, 63 (2013) 95-100.
[29] H.J. Kim, A. Kim, K. Miyata, K. Kataoka, Recent progress in development of siRNA delivery vehicles for cancer therapy, Adv Drug Deliv Rev, 104 (2016) 61-77.
[30] S.J. Lee, M.J. Kim, I.C. Kwon, T.M. Roberts, Delivery strategies and potential targets for siRNA in major cancer types, Adv Drug Deliv Rev, 104 (2016) 2-15.
[31] M. Creixell, N.A. Peppas, Co-delivery of siRNA and therapeutic agents using nanocarriers to overcome cancer resistance, Nano Today, 7 (2012) 367-379.
[32] M. Saraswathy, S.Q. Gong, Recent developments in the co-delivery of siRNA and small molecule anticancer drugs for cancer treatment, Mater Today, 17 (2014) 298-306.
[33] J. Wang, Z. Lu, B.Z. Yeung, M.G. Wientjes, D.J. Cole, J.L.S. Au, Tumor priming enhances siRNA delivery and transfection in intraperitoneal tumors, Journal of Controlled Release, 178 (2014) 79-85.
[34] D. Bumcrot, M. Manoharan, V. Koteliansky, D.W.Y. Sah, RNAi therapeutics: a potential new class of pharmaceutical drugs, Nature Chemical Biology, 2 (2006) 711-719.
[35] K. Buyens, J. Demeester, S.C. De Smedt, N.N. Sanders, Elucidating the Encapsulation of Short Interfering RNA in PEGylated Cationic Liposomes, Langmuir, 25 (2009) 4886-4891.
[36] K. Braeckmans, K. Buyens, W. Bouquet, C. Vervaet, P. Joye, F. De Vos, L. Plawinski, L. Doeuvre, E. Angles-Cano, N.N. Sanders, J. Demeester, S.C. De Smedt, Sizing Nanomatter in Biological Fluids by Fluorescence Single Particle Tracking, Nano Letters, 10 (2010) 4435-4442.
[37] K. Braeckmans, K. Buyens, B. Naeye, D. Vercauteren, H. Deschout, K. Raemdonck, K. Remaut, N.N. Sanders, J. Demeester, S.C. De Smedt, Advanced fluorescence microscopy methods illuminate the transfection pathway of nucleic acid nanoparticles, Journal of Controlled Release, 148 (2010) 69-74.
[38] S.D. Li, L. Huang, Stealth nanoparticles: High density but sheddable PEG is a key for tumor targeting, Journal of Controlled Release, 145 (2010) 178-181.
[39] J.J. Wheeler, L. Palmer, M. Ossanlou, I. MacLachlan, R.W. Graham, Y.P. Zhang, M.J. Hope, P. Scherrer, P.R. Cullis, Stabilized plasmid-lipid particles: construction and characterization, Gene Therapy, 6 (1999) 271-281.
[40] Y.P. Zhang, L. Sekirov, E.G. Saravolac, J.J. Wheeler, P. Tardi, K. Clow, E. Leng, R. Sun, P.R. Cullis, P. Scherrer, Stabilized plasmid-lipid particles for regional gene therapy: formulation and transfection properties, Gene Therapy, 6 (1999) 1438-1447.
[41] I.S. Zuhorn, U. Bakowsky, E. Polushkin, W.H. Visser, M.C.A. Stuart, J.B.F.N. Engberts, D. Hoekstra, Nonbilayer phase of lipoplex-membrane mixture determines endosomal escape of genetic cargo and transfection efficiency, Mol Ther, 11 (2005) 801-810.
[42] F.X. Shi, L. Wasungu, A. Nomden, M.C.A. Stuart, E. Polushkin, J.B.F.N. Engberts, D. Hoekstra, Interference of poly(ethylene glycol)-lipid analogues with cationic-lipid-mediated delivery of oligonucleotides; role of lipid exchangeability and non-lamellar transitions, Biochemical Journal, 366 (2002) 333-341.
[43] J.L. Betker, J. Gomez, T.J. Anchordoquy, The effects of lipoplex formulation variables on the protein corona and comparisons with in vitro transfection efficiency, Journal of Controlled Release, 171 (2013) 261-268.

6

NANOPARTCLES' INCUBATION IN FETAL BOVINE SERUM IS NOT REPRESENTATIVE FOR PROTEIN CORONA FORMATION IN UNDILUTED BIOLOGICAL FLUIDS

This Chapter is in preparation:

George R. Dakwar[1], Artur Ghazaryan[2], Kevin Braeckmans[1,3], Wim Ceelen[4], Volker Mailänder[2], Stefaan C. De Smedt[1], Katrien Remaut[1], Nanoparticles' incubation in fetal bovine serum is not representative for protein corona formation in undiluted biological fluids.

[1] Ghent Research Group on Nanomedicines, Faculty of Pharmaceutical Sciences, Laboratory for General Biochemistry and Physical Pharmacy, Ghent University, Ghent, Belgium

[2] Max Planck Institute for Polymer Research, Mainz, Germany

[3] Center for Nano- and Biophotonics, Ghent University, Ghent, Belgium

[4] Department of Surgery, Laboratory of Experimental Surgery, Ghent University Hospital, Ghent, Belgium

Abstract

Upon exposure of nanomedicines to protein-rich biofluids, a layer of proteins termed as « protein corona » is formed around the particles. It has become increasingly clear that the protein corona might affect the cellular uptake, intracellular trafficking and eventually the biological activity of nanomedicines. In an attempt to predict the influence of the protein corona on their stability and performance, nanomedicines are often incubated with fetal bovine serum (FBS). Here, we investigate if incubation in FBS is representative for the protein corona formed in undiluted biofluids such as human serum and ascites fluid obtained from a carcinomatosis patient. As nanomedicines, small interfering RNA (siRNA) containing lipoplexes (LPXs) were prepared from different molar ratios of the cationic lipid DOTAP and cholesterol (CHOL). All LPXs were taken up and were biologically active in Opti-MEM®. In FBS, nanoparticles' uptake was not altered, but the biological activity severely decreased. In human serum and ascites fluid, nanomedicines lost their activity mainly due to impaired cellular uptake. As demonstrated by qualitative SDS-PAGE and quantitative LC-MS analysis, increasing amounts of cholesterol in the LPXs diminished the amount of proteins bound, whereas the type of biofluid determined the composition of proteins present. We conclude that incubation in FBS is not representative for the protein corona formed in undiluted biofluids. Therefore, we suggest to always incubate nanoparticles in the representative biofluid and not FBS to predict the formation of a protein corona around nanomedicines, especially when mechanistic studies on the transfection pathway are being considered.

Keywords: Protein Corona, siRNA delivery, Undiluted biofluids, Cellular uptake, Gene downregulation, FBS

1. Introduction

The fate of nano-sized nucleic acid delivery systems, both *in vitro* and *in vivo*, depends on their behavior in biological milieu. To date, *in vitro* optimization of nucleic acid delivery systems is routinely performed in reduced serum conditions (Opti-MEM®) or in fetal bovine serum (FBS), before performing *in vivo* experiments. Unfortunately, such optimization does not take into account the composition and high concentration of proteins that exist in undiluted biological fluids, which in fact better resemble the *in vivo* situation. The protein corona might influence the uptake, intracellular trafficking, targeting ability and eventually the biological activity of nanomedicines [1-6]. Therefore, evaluating nanomedicines upon exposure to different biofluids is key to enhance the *in vitro in vivo* correlations.

When small interfering RNA (siRNA) is used as cargo, siRNA should be delivered to the cytoplasm of the cells. Different steps in the transfection pathway include interaction of the delivery vehicle with the plasma membrane of cells, cellular uptake and intracellular release of the siRNA. Nano-sized delivery systems should protect the siRNA from the proteins present in the biological environment and avoid the extracellular release of siRNA. Also, aggregation of nanomedicines in the extracellular fluid should be prevented to avoid clogging of capillaries and maintain sufficient cellular uptake [7, 8].

We have previously shown that lipid-based delivery vehicles are good candidates for siRNA delivery. A wide variety of lipids is available for the formation of liposomes. Often, the cationic lipid DOTAP is used to bind the negatively charged siRNA and enhance interaction with the negatively charged cell membrane. Also, PEGylated lipids are often included as Poly-Ethylene-Glycol (PEG) prevents aggregation of the liposomal formulations [8, 9]. A number of research groups have demonstrated the ability of cholesterol (CHOL) to resist serum aggregation, thereby functioning as an alternative for the widely used PEG. Also, DNA lipoplexes (LPXs) containing high mol% of CHOL resulted in a high transfection efficiency following exposure to FBS or fetal calf serum (FCS) [10-13]. In our previous study, we showed the importance of performing *in vitro* optimization of siRNA delivery systems in undiluted biological fluids [7]. Furthermore, we provided an experimental evidence that cellular uptake is a key parameter that eventually dictates the biological activity of siRNA LPXs in undiluted ascites fluid obtained from a PC patient [7].

To gain a mechanistic insight on the effect of different protein coronas formed around siRNA LPXs upon exposure to different biofluids, we prepared siRNA LPXs composed of the positively charged lipid DOTAP, supplemented with different molar ratios of cholesterol (CHOL). The cellular uptake and downregulation efficiency in SKOV-3 human ovarian cancer cells following incubation of the LPXs in Opti-MEM® and culture medium containing 10% and 50% FBS was compared to the

efficiency of LPXs incubated with undiluted ascites fluid from a PC patient and human serum. Additionally, we investigate the colloidal stability (i.e. aggregation and siRNA release) of the LPXs by fluorescence single particle tracking (fSPT) and fluorescence correlation spectroscopy (FCS) in the ascites fluid. Finally, the composition of the protein corona surrounding the different LPXs was analyzed qualitatively and quantitatively by SDS-PAGE and liquid-chromatography mass spectroscopy (LC-MS) respectively. With this set of experiments, we aimed to investigate whether the protein corona is mainly determined by the nature of the nanoparticles or by the respective biofluids in which these nanoparticles where dispersed. We observed that increasing amounts of cholesterol in the LPXs diminished the amount of proteins bound, whereas the type of biofluid determined the composition of proteins present. Importantly, the protein corona formed around the LPXs following incubation in FBS was not representative of the protein corona formed in the undiluted biofluids from human origin.

2. Materials and methods

2.1 Materials

(2,3-Dioleoyloxy-propyl)-trimethylammonium-chloride (DOTAP), cholesterol (CHOL), were purchased from Avanti Polar Lipids (Alabaster, AL). Chloroform, 4-(2-hydroxyethyl)-1-piperazineethanesulfonic acid (HEPES), Sodium Dodecyl Sulfate (SDS), 3-(4,5-dimethyl-2-thiazolyl)-2,5-diphenyl-2H-tetrazolium bromide (MTT), and sodium chloride(NaCl) were purchased from Sigma-Aldrich (Bornem, Belgium). Penicillin−streptomycin (5000 U/ml), L-glutamine (200 mM), 0.25% trypsin−EDTA (1×) phenol red, McCoy's 5A (modified), Opti-MEM®, and 1,1-dioctadecyl-3,3,3,3-tetramethylindodicarbocyanine perchlorate (DID) (λex = 644 nm, λem = 665 nm) were purchased from Invitrogen (Merelbeke, Belgium). Luciferase assay substrate was purchased from Promega (Madison, WI). Fetal bovine serum (FBS) was purchased from HyClone Thermo Scientific (Cramlington, UK). Passive lysis buffer and luciferase assay kits were purchased from Promega (Leiden,Netherlands). Negative-control siRNA (siNEG), luciferase siRNA (siLuc) and 5' Cy® siRNA (Cy5 siRNA) were purchased from Eurogentec (Searing, Belgium).

2.2 Preparation and characterization of the lipoplexes (LPXs)

Liposomes composed of DOTAP and CHOL were prepared by mixing the appropriate amount of lipids in a round bottomed flask before evaporation to obtain a 50:50 or 20:80 molar ratio of DOTAP:CHOL. A lipid film was formed by rotary evaporation of the chloroform. Liposomes were prepared by rehydrating the lipid film with HEPES buffer (20 mM, pH 7.4), followed by sonication using a probe sonicator (Branson Ultrasonics Digital Sonifier®,Danbury,USA). LPXs were prepared with a charge ratio of ±8 by adding the appropriate amounts of liposomes to siRNA. The mixture was incubated at room temperature to allow the formation of the LPXs. The average size and zeta potential of all formulations, was measured in HEPES buffer by a Zetasizer Nano-ZS (Malvern, Worcestershire, UK). Throughout the manuscript, siRNA-liposome complexes composed of DOTAP CHOL 50:50 and DOTAP CHOL 20:80 will be termed DOTAP CHOL 50:50 LPXs and DOTAP CHOL 20:80 LPXs respectively.

2.3 Cell culture

The human ovarian cancer cell line SKOV-3, which stably expresses firefly luciferase was used for *in vitro* toxicity, uptake and transfection experiments. Cells were grown and cultured in McCoy's 5A medium supplemented with 10% FBS, and Penicillin-Streptomycin. Cells were cultured until 80% to 90% confluency and detached from tissue-culture dishes using 0.25% trypsin. Cells were maintained in an incubator at 37°C and humidified atmosphere of 5% CO_2 as previously described.

2.4 Internalization of siRNA into SKOV-3 cells

SKOV-3 cells were seeded on 24-well plates (35,000 cells in each well) and allowed to grow in an incubator for 24 h. For uptake experiments, cells were incubated in different biological media with fluorescent LPXs containing 10% of Alexa-Fluor-488 siRNA for 4 h. At the end of the incubation, cells were washed with Phosphate Buffered Saline (PBS) and growth medium and, then detached using trypsin and analyzed by FACS (FACSCalibur Flow Cytometer, BD Biosciences, USA). Uptake experiments were performed with LPXs at 4°C, Opti-MEM®, medium containing 10% or 50% FBS, and finally after incubation of the LPXs in ~70% ascites fluid or human serum for 1 h before adding them to the cells, as described previously [7]. LPXs were incubated with SKOV-3 cells at a final siRNA concentration of 15 nM, which shows limited toxicity as determined by an MTT assay (Supplementary Figure 1.).

Human ascites fluid was obtained from a patient diagnosed with PC at the medical oncology department of Ghent University hospital (approved by the ethical committee of the Ghent University hospital (# 2013/589)).

2.5 Transfection Efficiency

SKOV-3 cells were cultured overnight on 24 well plates (35, 000 cells per well) in 500 µL of growth medium containing 10% FBS. Cells were then incubated with the LPXs in Opti-MEM®, medium containing 10% FBS and medium containing 50% FBS for 4 h. After 4 h of incubation, the transfection medium was replaced by culture medium, and cells were returned to the incubator for 24 h. Each LPX containing siRNA against luciferase (siLuc) was compared with the same formulation containing control siRNA (siNEG). After overnight incubation, cells were lysed with passive lysis buffer and analyzed for firefly luciferase expression using the luciferase assay kit (Promega). The bioluminescence (relative light units, RLU) was measured using a GloMax luminometer (Promega). The percentage of luciferase downregulation was determined by the following equation:

% transfection = $100 - (100 \times RLU_{Luc}/RLU_{NEG})$ where RLU_{NEG} and RLU_{Luc} are the mean bioluminescence as measured for siNEG and siLuc, respectively. The data shown in Figure 1B is based on three experiments performed on three different days. For transfections in the ascites fluid and human serum, 300 µL LPXs (of each formulation) were first added to 700 µL ascites fluid or human serum and incubated for 1 h. Then, 300 µL of this mixture was added to 700 µL of Opti-MEM® in each well of a 24 well-plate and incubated for 4 h. Thereafter, the medium was replaced with growth medium and cells were returned to the incubator for at least 18 h.

Statistical analysis (shown in Figure 1B) was performed using GraphPad Prism 6. Statistically significant differences were calculated by using an analysis of variance (ANOVA) at a 0.05 significance level, followed by Sidak's post test. For each formulation, transfection experiments carried out in Opti-MEM® were compared to the other biological fluids.

2.6 Fluorescence Correlation Spectroscopy on LPXs

Fluorescence Correlation Spectroscopy (FCS) is a microscopy-based technique that enables to follow the fluorescence intensity fluctuations of (fluorescent) molecules diffusing in and out of the focal volume of a confocal microscope. Eventually, FCS allows to quantify the fraction of complexed/released siRNA from the LPXs at different time points following incubation in undiluted biological fluids [14]. Single color FCS measurements were performed on LPXs containing 30% Cy5 siRNA. 5 µl of each LPXs was diluted to a final volume of respectively 50 µl HEPES buffer or 50 µl ascites fluid (~ 90 vol% of biofluid). The samples were analyzed by FCS respectively immediately, 1 h and 24 h after incubation in the biofluids at 37°C. During the incubation and FCS measurements, the well plate was covered with Adhesive Plates Seals (Thermo Scientific, UK) to avoid evaporation of the sample. FCS measurements were performed on the experimental set-up described before [7, 8].

2.7 Fluorescence single particle tracking

Fluorescence single particle tracking (fSPT) is a fluorescence microscopy technique which is used for the determination of diffusion and size of nanoparticles in undiluted biological media, as was previously shown [9].

fSPT measurements were performed on LPXs labeled with DID. LPXs were first diluted 400 times in HEPES buffer. Then, 1 µl of this dilution was added to 49 µl of human ascites fluid (~ 98 vol% of biofluid), and incubated for respectively 1, 2 and 3 h at 37°C. Movies were recorded using the same set-up as was previously described [7, 8]. Videos were analyzed as was previously explained using the following values of viscosity at room temperature: 1.39 cP for the ascites fluid and 0.94 cP for HEPES buffer [8].

2.8 Protein corona preparation

DOTAP CHOL 50:50 LPXs and DOTAP CHOL 20:80 LPXs were prepared in fresh HEPES buffer as described above. Subsequently, 200 µl of LPXs were incubated with 200 µl of FBS, human ascites fluid or human serum in triplicates for 1 h at 37°C. The incubation time of 1 h is sufficient to obtain a stable protein corona as has been demonstrated by Walcyzk et al. [15]. Also, this is the same time frame as was used when LPXs were preincubated with undiluted biological fluids for the uptake and transfection experiments. The ratio between the LPXs (100 µl) and each of the biological fluids (100 µl) was kept constant for all the samples.

The LPXs were separated from the biological fluid (i.e. supernatant) by centrifugation at 15000g for 15 minutes. The obtained pellet was resuspended in HEPES buffer and washed by two more centrifugation steps at 15000g for 15 minutes. Thereafter, the supernatant was discarded and the

obtained pellet was resuspended in 100 µl of freshly prepared SDS-Tris buffer (2% (w/v) SDS, 62.5 mM Tris-HCl solution) and incubated at 95°C for 5 minutes followed by centrifugation at 15000 g and 4°C for 15 minutes.

Quantification of the total protein concentration in each sample was performed using the Pierce 660 nm protein assay (Thermo Fisher Scientific) according to the manufacturer's instructions. Bovine Serum Albumin (BSA) was used as a standard.

2.9 SDS polyacrylamide gel electrophoresis

16.25 µL protein sample, equivalent to 1 µg, was mixed with 6.25 µL NuPAGE LDS Sample Buffer and 2.5 µL NuPAGE Sample Reducing Agent, heated at 70°C for 10 min and loaded onto a NuPAGE 10% Bis-Tris Protein Gel (Novex, Thermo Fisher Scientific). The electrophoretic run was carried out in NuPAGE MES SDS Running Buffer at 150V for 2 h using SeeBlue Plus2 Pre-Stained Standard as a molecular marker (Invitrogen). The gel was then silver-stained using SilverQuest Silver Staining Kit (Thermo Fischer Scientific).

2.10 Protein in-solution digestion and Liquid-chromatography mass-spectrometry (LC-MS) analysis

The digestion of corona proteins and subsequent LC-MS analysis was carried out following the protocol described in Schöttler et al. [6] with subtle modifications. 25 µg of each protein was precipitated and digested by Trypsin with an enzyme-to-protein ratio of 1:50. For LC-MS analysis, the digested samples were diluted 4-fold with aqueous 0.1% formic acid and spiked with Hi3 *E.coli* Standard (final concentration of 20 fmol/µL) (Waters Corporation) for absolute quantification. 2 µL sample was injected into the LC-MS.

Quantitative analysis of protein samples was performed using a nanoACQUITY UPLC system coupled with a Synapt G2-S*i* mass spectrometer (Waters Corporation). Tryptic-digested peptides were separated on the nanoACQUITY system equipped with a C18 nanoACQUITY Trap Column (5 µm, 180 µm x 20 mm, Waters Corporation) and a C18 analytical reversed-phase column (1.7 µm, 75 µm x 150 mm, Waters Corporation). Samples were processed with mobile phase A consisting of 0.1% (v/v) formic acid in water and mobile phase B consisting of acetonitrile with 0.1% (v/v) formic acid. The separation was performed at a sample flow rate of 0.3 µL/min using a gradient of 2-40% mobile phase B for 65 minutes. As a lock-mass reference compound 150 fmol/µL Glu-Fibrinopeptide was infused at a flow rate of 0.8 µL/min. Data-independent acquisition (MS^E) experiments were performed on the Synapt G2-S*i* operated in resolution mode. Electrospray Ionization was performed in positive ion mode using a NanoLockSpray source. Data was acquired over a range of m/z 50-2000 Da with a scan time of 0.5s and a total acquisition time of 80 min. All samples were analysed in two technical replicates and averaged. Data acquisition and processing was carried out using MassLynx v4.1, and Progenesis QI for Proteomics v2.0 software was used to

process data and identification of proteins. The generated peptide masses were searched against a reviewed human or bovine protein sequence databases downloaded from UniProt.

3. Results

3.1 Characterization of the LPXs

Table 1 depicts the average size and surface charge of the liposomes and LPXs used in this study. All the formulations show an increase in their average diameter following complexation with siRNA, with the largest hydrodynamic diameter for the DOTAP CHOL 20:80, most likely due to the formation of cholesterol domains when the molar ratio of CHOL in the formulation exceeds 66 mol% [12]. The zeta-potential of the LPXs was positive due to the presence of the positively charge lipid DOTAP in the formulation. Taken together, both the surface charge and the size of the LPXs should enable interaction with biological membranes and subsequently, cellular uptake.

Table 1. Characterization of the studied LPXs

Formulation		Z-Average diameter ± SD (nm)	Polydispersity index (PDI)	ζ-potential (mV) (mean ± SD)
DOTAP CHOL 50:50	Liposomes	76.6 ± 0.6	0.22	46.8 ± 2.2
	LPXs	137.9± 2.9	0.24	51.7 ± 0.4
DOTAP CHOL 20:80	Liposomes	103.2 ± 1.1	0.36	49.9.7 ± 1.6
	LPXs	202.2 ± 1.2	0.23	51.8 ± 2.2

3.2 Internalization and biological activity of the LPXs in SKOV-3 cells

To test whether the LPXs are capable to deliver the siRNA into SKOV-3 cells, we carried-out uptake experiments in different biofluids. The rationale behind such an experiment is to understand whether there are alterations in the interaction between the LPXs and the cellular membranes (and subsequent internalization) following the formation of a protein corona around the surface of the LPXs [16].

Figure 1A shows the uptake of the complexes in different conditions. As control, LPXs carrying fluorescently labeled AF-488 siRNA were incubated with the cells for 4 h at 4°C, to block the temperature dependent internalization of the LPXs. The amount of complexes binding to the outside of the cells without being internalized is negligible (Figure 1A, black bars). In Opti-MEM®,

both LPXs are taken up by SKOV-3 cells, although the uptake of the DOTAP CHOL 20:80 LPXs was lower when compared with DOTAP CHOL 50:50 LPXs (Figure 1A, white bars). In the presence of 10% FBS (Figure 1A, red bars) however, the cellular uptake of DOTAP CHOL 20:80 LPXs increased and became comparable to the level of uptake for the DOTAP CHOL 50:50 LPXs. This indicates that LPXs containing a high molar ratio of CHOL (above 66 mol%) have a better interaction with the cell membrane in the presence of FBS, as was observed before [11,12]. Further increasing the FBS content of the cell medium to 50% slightly decreased the percentage of positive cells of both LPXs (Figure 1A, blue bars). After pre-incubation of the complexes with human serum, however, only the DOTAP CHOL 50:50 LPXs were still taken up in more than 70% of the SKOV-3 cells (Figure 1A, magenta bars), while no uptake was observed for DOTAP CHOL 20:80 LPXs. Following exposure to the ascites fluid (Figure 1A, cyan bars) both LPXs lost their ability to carry the fluorescently labeled siRNA into SKOV-3 cells.

Also on the level of the biological activity of the DOTAP CHOL LPXs, the influence of the different tested biofluids became clear (Figure 1B). The LPXs were only able to downregulate luciferase expression in the SKOV-3 cells when incubated in the low protein containing Opti-MEM®, resulting in 65% and 50% of luciferase downregulation for DOTAP CHOL 50:50 LPXs and DOTAP CHOL 20:80 LPXs, respectively. Unfortunately, a significant decrease in luciferase inhibition occurred for both LPXs in all the tested biological fluids (Figure 1B). It should be noted the lack of transfection efficiency is expected for the formulations that are not taken up, as the siRNA needs to be delivered intracellularly. Some LPXs, however, clearly had a good intracellular uptake profile in the SKOV-3 cells, yet did not result in a productive siRNA delivery at the intracellular level.

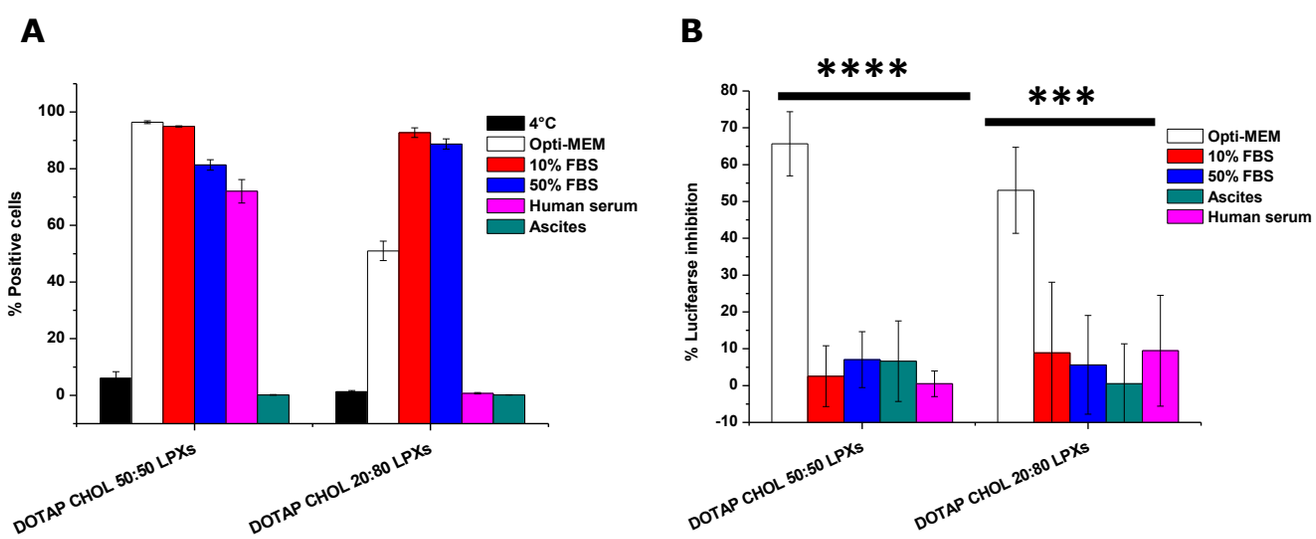

Figure 1. Uptake and transfection efficiency of the DOTAP CHOL LPXs. LPXs were prepared in HEPES buffer and added on the cells in Opti-MEM®, 10% FBS and 50% FBS or after incubation for 1 h in human ascites fluid or human serum before adding them on the cells. **(A)** Uptake of Af-488 siRNA labeled LPXs by SKOV-3 cells and **(B)** inhibition of luciferase in SKOV-3 cells by the LPXs. The values represent the average from at least three experiments that were performed on 3 different days.

3.3 Colloidal stability of the LPXs in undiluted ascites fluid

As the ascites fluid had such a drastic effect on the cellular uptake of the LPXs, we tested the stability of the LPXs in the undiluted ascites fluid. Figure 2A shows the fraction of siRNA complexed with the LPXs immediately following preparation in HEPES buffer (black bars). DOTAP CHOL 50:50 LPXs complex around 60% of siRNA, whereas about 80% of the siRNA is complexed in the case of DOTAP CHOL 20:80 LPXs. Following 1 h of incubation in the ascites fluid (Figure 2A, red bars), a fraction of the siRNA is released from the LPXs, resulting in about 45% of siRNA that remains complexed for both formulations. After 24h incubation in ascites fluid, almost all complexed siRNA has been released from the formulations, showing the poor long term stability of these complexes in a protein rich environment. As the uptake experiments above were performed following 1 h incubation in ascites fluid, however, the pre-mature release of siRNA at the 1 h time point cannot be responsible for the drastic decrease in cellular uptake following exposure to the ascites fluid.

Next, we tested if aggregation of the LPXs could be responsible for the lack of cellular internalization. Therefore, we carried-out fSPT to obtain size distributions of the LPXs following incubation in full ascites fluid. Both formulations showed good stability in the ascites fluid, with the higher molar fraction of CHOL in the formulations preventing aggregation in undiluted ascites fluid the most. The size distributions of DOTAP CHOL 50:50 following 1, 2, and 3 h of incubation in ascites fluid (Figure 2B) are slightly shifted towards higher sizes, when compared to HEPES buffer (black curve). For the DOTAP CHOL 20:80 LPXs (Figure 2C), however, the peak diameter of the size distribution in HEPES buffer (black curve) overlaps with the size distributions following 1, 2, and 3 h of incubation in ascites fluid. Taken together, both the release and aggregation data point out to the fact that the LPXs are sufficiently colloidally stable following 1 h of incubation in ascites fluid, both in terms of the amount of siRNA that they carry as for the size range of the complexes that should enable crossing biological membranes.

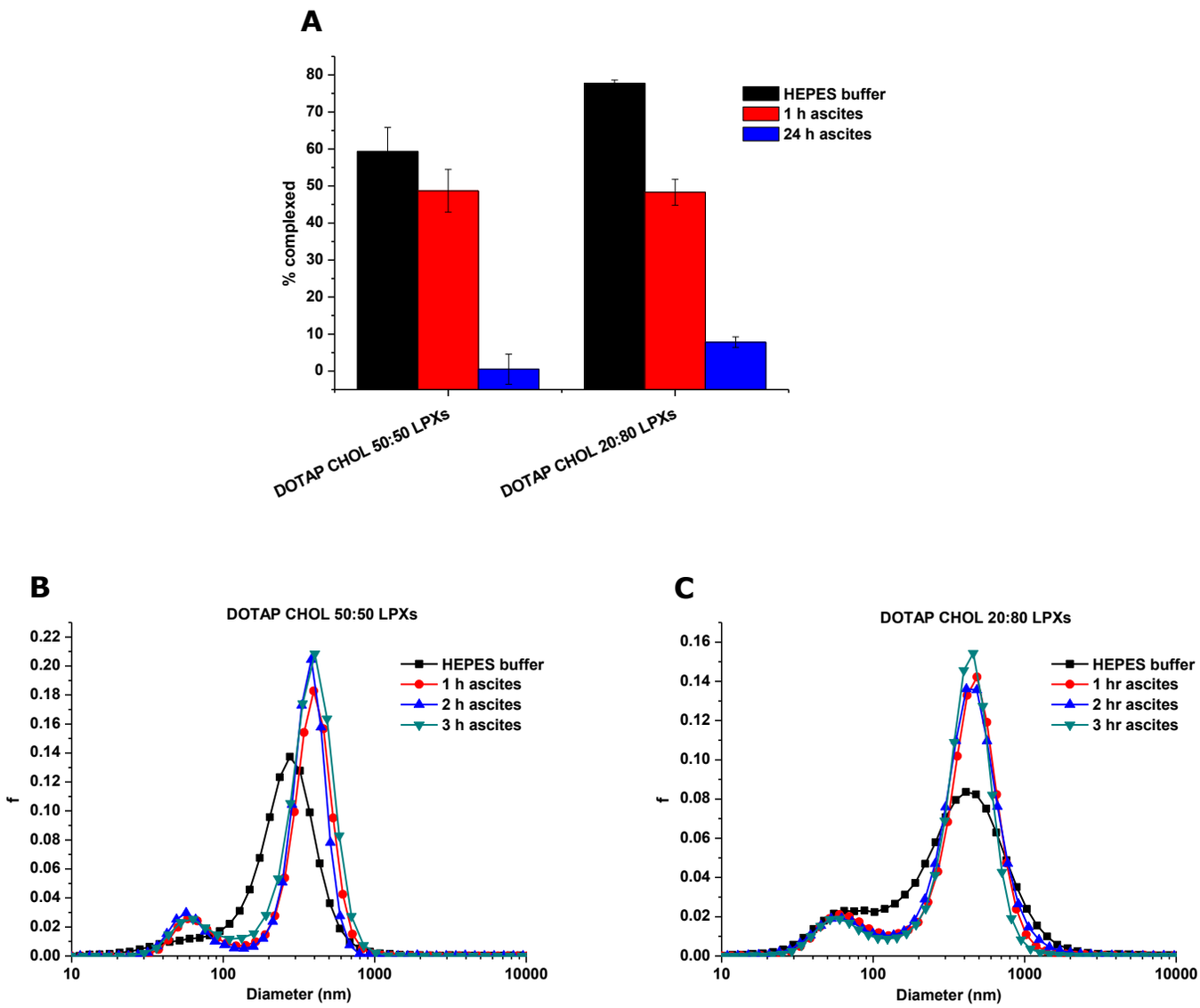

Figure 2. Colloidal stability of the LPXs in human ascites fluid. (A) Complexation efficiency of the LPXs immediately following preparation in HEPES buffer (black bars), and after incubation in 90 vol % of ascites fluid during 1 h (red bars) and 24 h (blue bars), respectively. **(B)** fSPT size distributions of the DOTAP CHOL 50:50 LPXs and **(C)** DOTAP CHOL 20:80 LPXs in 98 vol % of ascites fluid.

3.4 Protein corona of the LPXs

In a next set of experiments, we aimed to evaluate whether the differences in cellular uptake and biological activity could stem from different protein coronas that are formed upon incubation of the LPXs in the different biofluids. It should be noted that the centrifugation and washing steps for the separation of the LPXs from the biofluids results in the removal of proteins that are loosely bound to the surface of the LPXs – known as the 'soft' protein corona. Therefore, the obtained data represent the 'hard' protein corona which is more strongly bound to the LPXs [17]. First, we quantified the amount of adsorbed proteins on the surface of the LPXs following 1 h of incubation with each of the biological fluids. Figure 3A shows that the amount of CHOL in the formulations clearly influences the amount of proteins that bind to the LPXs. Specifically, the DOTAP CHOL 50:50 LPXs exhibit protein binding which is 22, 47 and 6 fold higher than the one measured for the

DOTAP CHOL 20:80 LPXs in respectively FBS, ascites fluid and human serum. For the DOTAP CHOL 20:80 LPXs, the highest protein adsorption was measured in human serum. For DOTAP CHOL 50:50 LPXs, both ascites fluid and human serum resulted in a higher amount of absorbed proteins when compared to FBS.

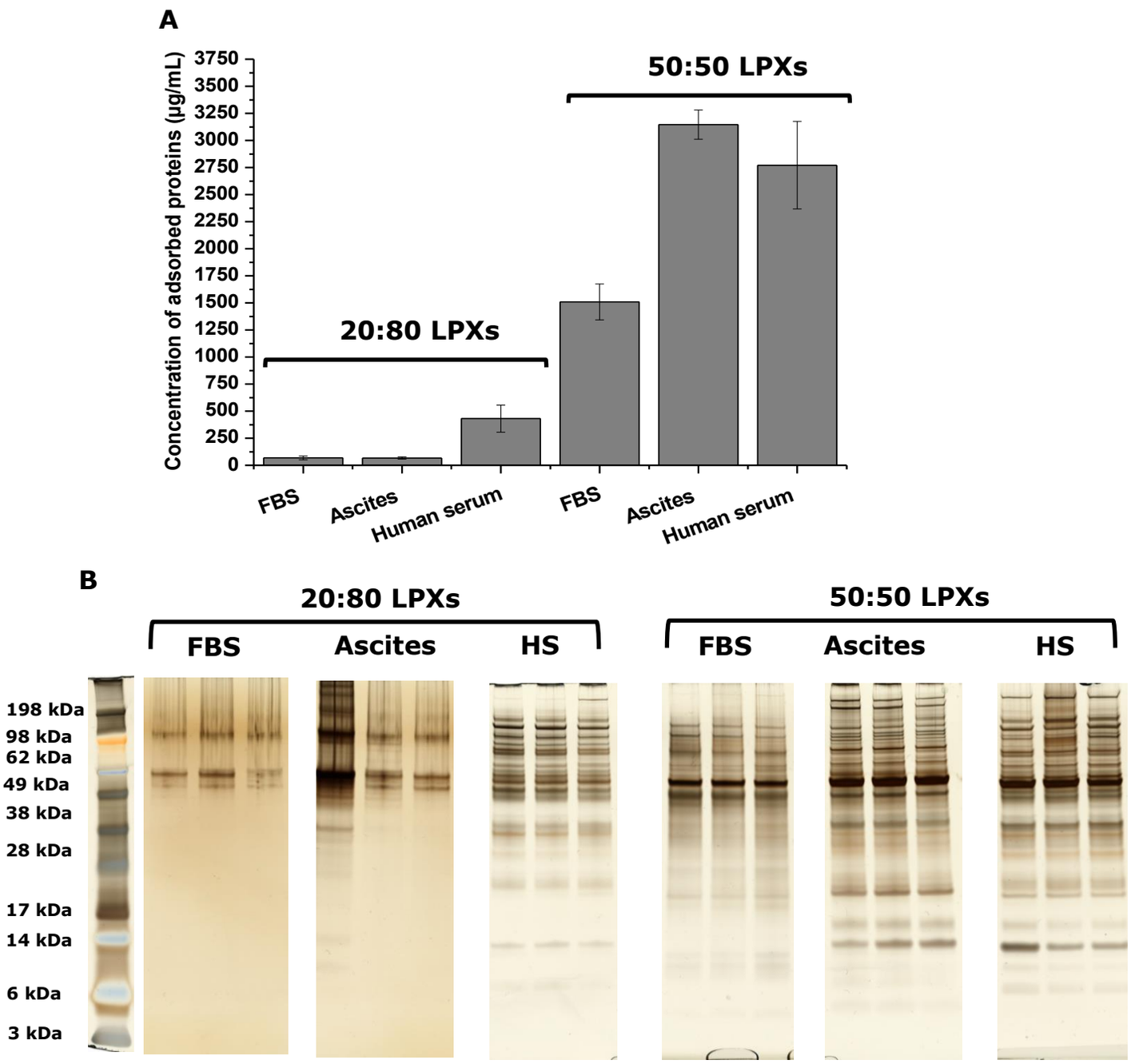

Figure 3. Protein adsorption to the surface of DOTAP CHOL 20:80 and DOTAP CHOL 50:50 LPXs following incubation in the different biological fluids. The formulations were incubated with FBS, ascites fluid obtained from a peritoneal carcinomatosis patient and human serum (HS). (A) Quantification of the concentration of adsorbed proteins with Pierce 660 nm assay. Values are expressed mean ± SD of three biological replicates. **(B)** SDS-PAGE was performed to qualitatively determine the composition of the protein corona formed around the LPXs following incubation in the different biological environments.

Apart from the amount of proteins, a clear difference was also observed in the protein pattern as seen with SDS-PAGE (Figure 3B). For all formulations, a band is detected around 62 kDa, representing albumin. The DOTAP CHOL 20:80 LPXs incubated with human serum show additional bands around 14 and 38 kDa, which are not observed for FBS and ascites fluid. Also for the DOTAP CHOL 50:50 LPXs, additional bands are observed around 14 kDa, 17 kDa, 38 kDa and 200 kDa for ascites fluid and human serum, but not for the LPXs incubated with FBS.

The SDS-PAGE provides a qualitative insight on the composition of the protein corona. To identify the specific proteins involved in each of the coronas formed around the LPXs and to quantify their abundance, quantitative LC-MS analysis was carried out. Unfortunately, the low amount of proteins bound to the DOTAP CHOL 20:80 LPXs in FBS and ascites fluid didn't enable us to perform LC-MS analysis on these samples. Therefore, only the 4 formulations that exhibited the highest amount of proteins bound were used, namely DOTAP CHOL 20:80 LPXs in human serum and all DOTAP CHOL 50:50 LPXs. Table 2 highlights the most abundant proteins in the composition of each of the coronas formed following incubation of the LPXs with different biofluids. For the DOTAP CHOL 50:50 LPXs in FBS, ascites fluid, and human serum. Serum albumin was the most abundant protein forming 19.23%, 31.91% and 22.67% of the protein coronas respectively. Also, for the biofluids from human origin (i.e. ascites and human serum) complement C3 was the second abundant protein composing the coronas with 5.64% and 7.18% respectively. In line with the SDS-PAGE data, the composition of the corona for the DOTAP CHOL 20:80 LPXs in human serum differs from the one of the DOTAP CHOL 50:50 LPXs in human serum. Interestingly, vitronectin but not serum albumin was the most abundant protein, with 9.38% of the DOTAP CHOL 20:80 LPXs corona. Other key proteins that were identified are complement C3 and clusterin, compromising 7.1% and 3.7% of the corona respectively (Table 2). Of relevance for the optimization of nucleic acid delivery systems, major differences in the composition of the protein corona of the DOTAP CHOL 50:50 LPXs in FBS is observed compared to the one obtained for DOTAP CHOL 50:50 LPXs in human serum (Table 2). Several proteins such as clusterin, fibronectin, and vitronectin are present in the corona of the 50:50 LPXs in human serum but not in the corona of the DOTAP CHOL 50:50 LPXs in FBS. This data highlight the fact that biological fluids (and the resulting protein corona) originating from humans significantly differ from those from bovine origin, both in terms of concentration and composition of the proteins that are bound.

Table 2. Representative proteins composing the corona formed around each LPX following incubation in FBS, ascites, and HS as determined by LC-MS. The values correspond to the molar percentage of each protein in each sample. The list represents the most abundant proteins. The size of the grey circles was calculated based on the molar percentage of each protein, and is correlated with the abundancy of each protein. The dashed lines represent proteins that are not present in the corona.

	50:50 FBS	50:50 ascites	50:50 HS	20:80 HS
ALB protein	10.09	------	------	------
Alpha-1-antitrypsin	------	3.2	1.8	------
Alpha-1-acid glycoprotein 1	------	1.0	0.7	------
Alpha-2-HS-glycoprotein	16.0	------	------	------
Alpha-1B-glycoprotein	1.4	------	------	------
Apolipoprotein A-I	1.4	1.8	0.7	------
Apolipoprotein A-IV	------	0.7	0.9	------
Apolipoprotein E	0.7	0.6	------	------
Complement C1q subcomponent subunit B	------	------	0.7	0.5
Complement C3	1.8	5.6	7.2	7.1
Complement C4-A	------	1.0	2.1	1.6
Complement C4-B	------	0.7	1.6	1.2
Complement factor H	------	------	0.5	0.6
Clusterin	------	1.1	3.2	3.7
Cytoplasmic dynein 1 light intermediate chain 1	------	1.9	1.0	------
Fibronectin	------	0.6	1.6	1.1
Fibrinogen gamma chain	------	2.8	------	------
Haptoglobin	------	1.8	2.0	------
Ig gamma-1 chain C region	------	1.7	1.8	4.4
Ig kappa chain C region	------	1.7	3.6	6.8
Ig kappa chain V-III region VG (Fragment)	------	-----	------	1.2
Ig mu chain C region	------	0.7	1.2	4.9
Inter-alpha-trypsin inhibitor heavy chain H1	------	1.1	3.2	7.9
Inter-alpha-trypsin inhibitor heavy chain H2	------	1.4	3.1	7.4
Inter-alpha-trypsin inhibitor heavy chain H3	0.8	------	------	1.7
Protein AMBP	3.0	0.8	1.4	3.8
Prothrombin	0.8	1.3	1.5	1.7
Serum albumin	19.2	31.9	22.7	2.2
Transthyretin	------	2.0	1.5	1.0
Vitronectin	------	1.5	3.0	9.4

4. Discussion

Over the past several years, it has become evident that upon incubation of nanoparticles with protein-rich biofluids, a protein layer is formed on the surface of nanoparticles. This layer changes the identity of the nanoparticles, and consequently their ability to interact with biological barriers [18, 19]. Worth mentioning in this context, that the vast majority of the protein corona research is focused on nanoparticles that are not biologically active, and its impact on the biological activity of nanomedicines in general and nucleic acid delivery systems in particular, remains to be elucidated.

In our previous work, we demonstrated that cationic and PEGylated siRNA LPXs composed of DOTAP DOPE lose their ability to be taken up by cells. Consequently, they exhibited a significant decrease in their transfection efficiency after incubation in ascites fluid obtained from a PC patient [7]. Nevertheless, we didn't provide any experimental evidence that the loss of uptake is related to the protein corona of the LPXs. Here, we investigated whether the same phenomenon still occurs with LPXs composed of DOTAP CHOL and in different biofluids from human (i.e. human serum and ascites) and bovine origin (i.e FBS). Generally speaking, it is possible to think about the chosen undiluted biofluids (human serum and ascites) in a way that each resembles a relevant model for *in vivo* administration, namely the human serum for intravenous (IV) administration and the ascites fluid for intraperitoneal (IP) administration [8]. FBS, however, is widely used to carry-out *in vitro* experiments, and is considered the « golden standard » for the uptake and transfection of LPXs, especially when used at high percentages (e.g. 50%). Finally, Opti-MEM® is a standard, reduced serum fluid used for transfection experiments, which unlike the other biofluids does not influence the biological activity of siRNA LPXs as we have previously shown [7].

4.1 Interaction of the corona-coated LPXs with biological membranes

Based on the results obtained in this study, it is possible to classify the different studied conditions as schematically illustrated in Figure 4. In reduced serum conditions (i.e. Opti-MEM®) - uptake of the LPXs leads to gene downregulation. This indicates that the LPXs were able to internalize in the cells and efficiently deliver their siRNA to the cytoplasm of the cells, were downregulation of the target protein occurred (Figure 4, situation 1). In some cases, however, uptake of the LPXs by the cells was followed by the loss of biological activity (e.g. LPXs in 10% and 50% FBS and DOTAP CHOL 50:50 LPXs in human serum). In this case, it seems that the proteins involved in the protein corona around the LPXs still allow efficient uptake of the LPXs, but interfere on the level of efficient intracellular delivery of the siRNA (Figure 4, situation 2). The lack of biological activity under these conditions may be attributed to a disrupted interaction between the corona covered LPXs and the endosomal membrane following uptake. It has already been demonstrated by Wang et al. [20] that the protein corona is retained on the surface of nanoparticles following internalization, and consequently, unlike the Opti-MEM® conditions, the LPXs with the surrounding corona in this case interact with the endosomal membrane. Although the mechanism by which DOTAP CHOL siRNA

LPXs escape the endosomes was never investigated, Pozzi et al. [11] showed that DOTAP CHOL DNA LPXs enter the cells by fusion with the plasma membrane, a process which also facilitates the subsequent endosomal escape. According to the authors, the fusion is possible due to the presence of CHOL in the formulations. Importantly, the experiments show in Pozzi et al. were performed in cell culture medium supplemented with 10% FBS. Assuming that the enodsomal escape under Opti-MEM® conditions in the case of DOTAP CHOL-siRNA LPXs occurs via fusion, it is logical to claim that the fusion with the endosomal membrane which in most of the cases requires a specific surface characteristics of the LPXs, is hampered by the corona proteins in the case of FBS and human serum. Thus the LPXs are entrapped in the endosomes, leading eventually to their degradation in the lysosomal compartment. It should be noted, however, that we do not have experimental evidence for this hypothesis up to date.

Finally, in some cases complete inhibition of the cellular uptake which results in a complete loss in the ability of the LPXs to downregulate a specific gene was observed (e.g. DOTAP CHOL 20:80 in human serum and all LPXs in ascites fluid) (Figure 4, situation 3). Since these LPXs are colloidally stable in the ascites fluid (Figure 2), premature release of siRNA and/or aggregation of the LPXs cannot be the sole reason for the loss in cellular uptake. Therefore, the complete inhibition of cell internalization and the logical subsequent loss in downregulation ability (compared with the Opti-MEM® condition) is most likely ascribed to the protein corona formed around the LPXs. More specifically, the combination of proteins bound on the surface of these LPXs does apparently not allow interaction with the cell membrane. In spite of the clear differences in the composition of the corona in each biofluid, it is difficult to define what combination of proteins facilitate or inhibit the cellular uptake, or which proteins are on the surface and specifically involved in the interaction with the plasma membrane. It has already been suggested that by forming a single protein corona around nanoparticles, the uptake could be enhanced or inhibited [4]. Nevertheless, this approach never resembles the real corona which is formed around the LPXs. Here, we do not aim to pinpoint specific proteins responsible for inhibiting/facilitating cellular uptake, but rather to focus to emphasize the importance of the protein corona and its influence on the biological performance of siRNA delivery systems *in vitro*. Nonetheless, we can conclude that corona proteins, specifically the ones participating in the interaction with the plasma membrane and also with the endosomes play an important role and even regulate the transfection efficiency of siRNA LPXs. The type and concentration of those proteins change as a function of the biofluid. Importantly, FBS cannot be used to predict the effect of the protein corona formed around LPXs in more complex biological fluids. Therefore, optimization of LPXs is best performed in the actual biofluid the particles will encounter upon *in vivo* administration.

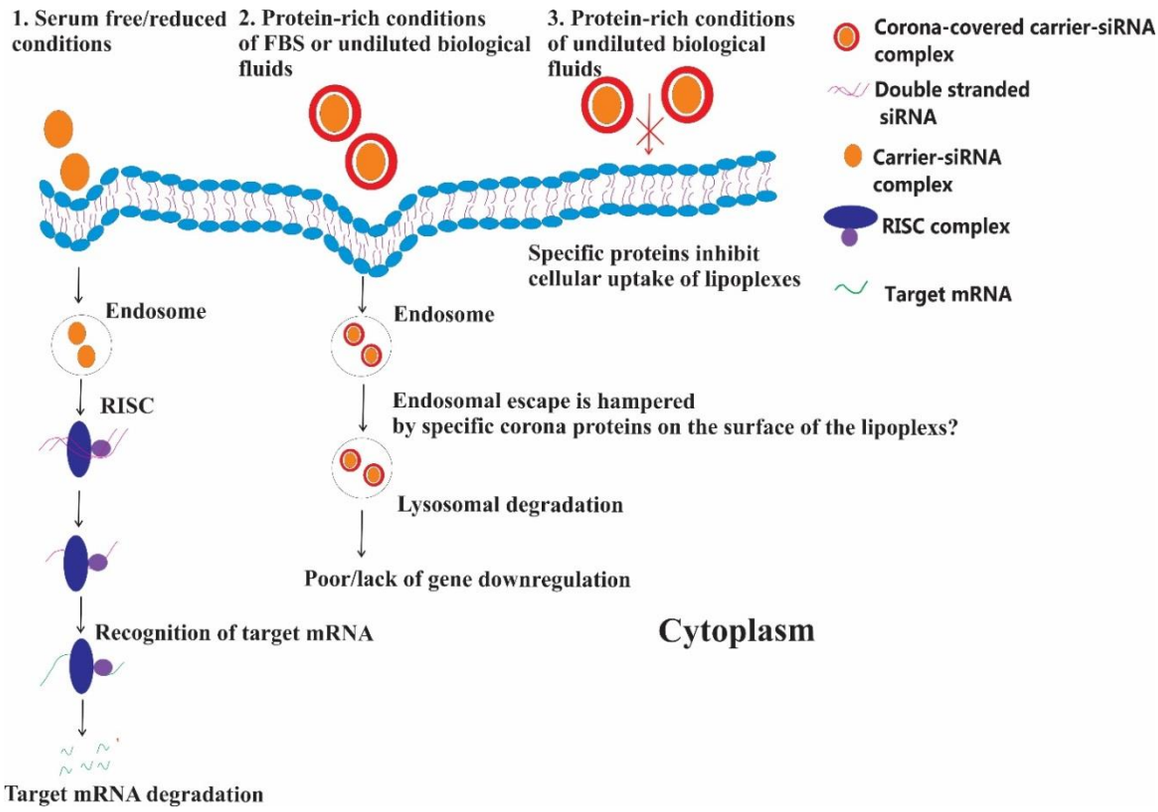

Figure 4. Schematic illustration summarizing the influence of the absence/presence of a protein corona formed around the DOTAP CHOL-siRNA LPXs in the different biofluids on the cellular uptake and gene downregulation.

5. Conclusions

In this study we investigate the ability of DOTAP CHOL-siRNA LPXs to downregulate genes in serum reduced media and also in protein-rich conditions. We showed that the loss of biological activity is associated with the presence of a protein corona. Broadly speaking, the results demonstrate significant differences in cellular uptake in high percentage of fetal bovine serum (50%) compared with undiluted biological fluids from human origin. We recommend to perform *in vitro* optimization of siRNA delivery systems in the relevant biofluid before performing *in vivo* experiment, as well as, not to correlate uptake and transfection efficiency data obtained in FBS to the *in vivo* situation in mice or in humans. Towards a better fundamental understanding that resembles the *in vivo* situation, the outcomes of this study encourage in-depth investigation of the effects of different biological environments (and the resulting corona) on the interaction with biological membranes on the extracellular and intracellular level.

Acknowledgements

George Dakwar is a doctoral fellow at the Ghent Research Group on Nanomedicines. W.C. is a senior clinical investigator of the Fund for Scientific Research Flanders, (FWO). This work was supported by the FWO (grant No. G006714N) for G.D., K.R., S.D., and W.C.

Supplementary information

Supplementary Figure 1.

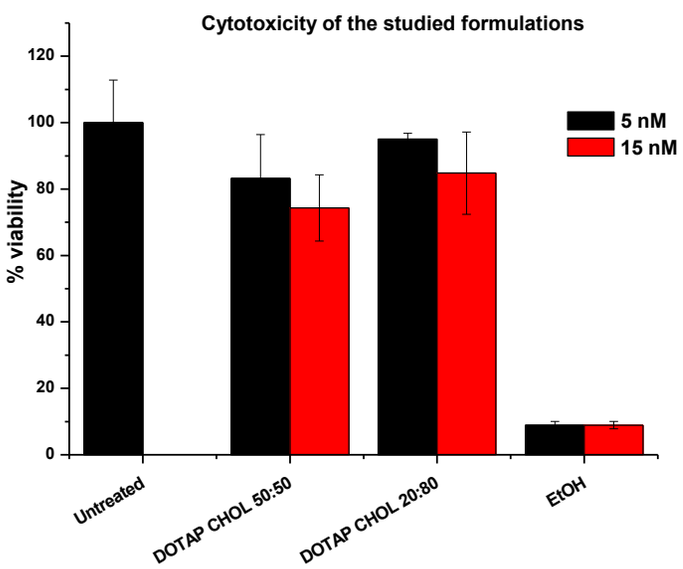

Outcomes of the cell viability assay (MTT). For each formulation the toxicity of the LPXs was evaluated using 2 different concentrations, 5 nM (black bars), 15 nM (red bars), respectively. Results are expressed as mean ± SE.

References

[1] Q. Dai, Y. Yan, J.L. Guo, M. Bjornmalm, J.W. Cui, H.L. Sun, F. Caruso, Targeting Ability of Affibody-Functionalized Particles Is Enhanced by Albumin but Inhibited by Serum Coronas, Acs Macro Lett, 4 (2015) 1259-1263.
[2] M. Hadjidemetriou, Z. Al-Ahmady, M. Mazza, R.F. Collins, K. Dawson, K. Kostarelos, In Vivo Biomolecule Corona around Blood-Circulating, Clinically Used and Antibody-Targeted Lipid Bilayer Nanoscale Vesicles, Acs Nano, 9 (2015) 8142-8156.
[3] Q. Peng, H.L. Mu, The potential of protein-nanomaterial interaction for advanced drug delivery, J Control Release, 225 (2016) 121-132.
[4] S. Ritz, S. Schottler, N. Kotman, G. Baier, A. Musyanovych, J. Kuharev, K. Landfester, H. Schild, O. Jahn, S. Tenzer, V. Mailander, Protein Corona of Nanoparticles: Distinct Proteins Regulate the Cellular Uptake, Biomacromolecules, 16 (2015) 1311-1321.
[5] A. Salvati, A.S. Pitek, M.P. Monopoli, K. Prapainop, F.B. Bombelli, D.R. Hristov, P.M. Kelly, C. Aberg, E. Mahon, K.A. Dawson, Transferrin-functionalized nanoparticles lose their targeting capabilities when a biomolecule corona adsorbs on the surface, Nat Nanotechnol, 8 (2013) 137-143.
[6] S. Schottler, K. Klein, K. Landfester, V. Mailander, Protein source and choice of anticoagulant decisively affect nanoparticle protein corona and cellular uptake, Nanoscale, 8 (2016) 5526-5536.
[7] G.R. Dakwar, K. Braeckmans, J. Demeester, W. Ceelen, S.C. De Smedt, K. Remaut, Disregarded Effect of Biological Fluids in siRNA Delivery: Human Ascites Fluid Severely Restricts Cellular Uptake of Nanoparticles, Acs Appl Mater Inter, 7 (2015) 24322-24329.
[8] G.R. Dakwar, E. Zagato, J. Delanghe, S. Hobel, A. Aigner, H. Denys, K. Braeckmans, W. Ceelen, F.C. De Smedt, K. Remaut, Colloidal stability of nano-sized particles in the peritoneal fluid: Towards optimizing drug delivery systems for intraperitoneal therapy, Acta Biomater, 10 (2014) 2965-2975.
[9] K. Braeckmans, K. Buyens, W. Bouquet, C. Vervaet, P. Joye, F. De Vos, L. Plawinski, L. Doeuvre, E. Angles-Cano, N.N. Sanders, J. Demeester, S.C. De Smedt, Sizing Nanomatter in Biological Fluids by Fluorescence Single Particle Tracking, Nano Lett, 10 (2010) 4435-4442.
[10] J.L. Betker, J. Gomez, T.J. Anchordoquy, The effects of lipoplex formulation variables on the protein corona and comparisons with in vitro transfection efficiency, J Control Release, 171 (2013) 261-268.
[11] D. Pozzi, C. Marchini, F. Cardarelli, H. Amenitsch, C. Garulli, A. Bifone, G. Caracciolo, Transfection efficiency boost of cholesterol-containing lipoplexes, Bba-Biomembranes, 1818 (2012) 2335-2343.
[12] L. Xu, T.J. Anchordoquy, Cholesterol domains in cationic lipid/DNA complexes improve transfection, Bba-Biomembranes, 1778 (2008) 2177-2181.
[13] S.Y. Yang, Y. Zheng, J.Y. Chen, Q.Y. Zhang, D. Zhao, D.E. Han, X.J. Chen, Comprehensive study of cationic liposomes composed of DC-Chol and cholesterol with different mole ratios for gene transfection, Colloid Surface B, 101 (2013) 6-13.
[14] K. Buyens, B. Lucas, K. Raemdonck, K. Braeckmans, J. Vercammen, J. Hendrix, Y. Engelborghs, S.C. De Smedt, N.N. Sanders, A fast and sensitive method for measuring the integrity of siRNA-carrier complexes in full human serum, J Control Release, 126 (2008) 67-76.
[15] D. Walczyk, F.B. Bombelli, M.P. Monopoli, I. Lynch, K.A. Dawson, What the Cell "Sees" in Bionanoscience, J Am Chem Soc, 132 (2010) 5761-5768.
[16] D. Docter, D. Westmeier, M. Markiewicz, S. Stolte, S.K. Knauer, R.H. Stauber, The nanoparticle biomolecule corona: lessons learned - challenge accepted?, Chem Soc Rev, 44 (2015) 6094-6121.
[17] S. Winzen, S. Schoettler, G. Baier, C. Rosenauer, V. Mailaender, K. Landfester, K. Mohr, Complementary analysis of the hard and soft protein corona: sample preparation critically effects corona composition, Nanoscale, 7 (2015) 2992-3001.
[18] D. Maiolo, P. Del Pino, P. Metrangolo, W.J. Parak, F.B. Bombelli, Nanomedicine delivery: does protein corona route to the target or off road?, Nanomedicine-Uk, 10 (2015) 3231-3247.
[19] S. Motta, V. Rondelli, L. Cantu, E. Del Favero, M. Aureli, D. Pozzi, G. Caracciolo, P. Brocca, What the cell surface does not see: The gene vector under the protein corona, Colloid Surface B, 141 (2016) 170-178.
[20] F.J. Wang, L. Yu, M.P. Monopoli, P. Sandin, E. Mahon, A. Salvati, K.A. Dawson, The biomolecular corona is retained during nanoparticle uptake and protects the cells from the damage induced by cationic nanoparticles until degraded in the lysosomes, Nanomed-Nanotechnol, 9 (2013) 1159-1168.

7

THE EFFECT OF THE CARRIER SOLUTION ON THE *IN VIVO* RESIDENCE TIME OF NANOPARTICLES IN THE PERITONEAL CAVITY IN MICE

George R. Dakwar[1], Felix Gremonprez[2], Charlotte Carlier[2], Elodie Melsens[2], Natacha Rosseel[2], Ranhua Xiong[1,3], Kevin Braeckmans[1,3], Benedicte Descamps[4], Christian Vanhove[4], Wim Ceelen[2], Stefaan C. De Smedt[1], Katrien Remaut[1], The effect of the carrier solution on the *in vivo* residence time of nanoparticles in the peritoneal cavity in mice.

[1] Ghent Research Group on Nanomedicines, Faculty of Pharmaceutical Sciences, Laboratory for General Biochemistry and Physical Pharmacy, Ghent University, Ghent, Belgium

[2] Department of Surgery, Laboratory of Experimental Surgery, Ghent University Hospital, Ghent, Belgium

[3] Center for Nano- and Biophotonics, Ghent University, Ghent, Belgium

[4] Small animal imaging laboratory (Infinity), Ghent University Hospital, Ghent, Belgium

Abstract

Developing nanomedicine-based intraperitoneal (IP) therapy for the treatment of peritoneal carcinomatosis (PC) requires prolonged exposure of the drug loaded nanoparticles (NPs) to the tumor. A major problem of IP injected NPs is their rapid clearance from the peritoneal cavity to the liver and spleen. Here, we investigate the residence time and clearance of nanomaterials following IP administration in healthy mice for different carrier solutions. First, isotonic phosphate buffered saline (PBS) was used to inject the NPs in the peritoneal cavity. The NPs were cleared together with the carrier solution in the first 2 h following injection. When 7.5% icodextrin was used as a carrier solution, the colloid osmotic effect allowed the carrier solution to remain in the peritoneal cavity for at least 2 h. Also, the concentration of NPs in the carrier solution did not decrease. Both the amount of carrier solution present in the peritoneal cavity and the concentration of NPs in the remaining carrier solution, however, strongly decreased 4 h following injection. Biodistribution studies showed that NPs accumulated mainly in liver and spleen 24 h following injection, with only limited amount of NPs found in the peritoneal cavity. Finally, fluorescence recovery after photobleaching (FRAP) was performed on mixtures of FITC dextrans (FDs) with different molecular weights (corresponding to sizes between 3 and 30 nm), in order to identify if a particular size of FD shows more potential to be retained in the peritoneal cavity. The clearance from the peritoneal cavity, was however independent of the Mw of the FD molecules. In summary, the carrier solution for injection of NPs in the peritoneal cavity has an important role in the residence time of nanomedicines in the peritoneal cavity. More optimized carrier solutions could aid to maintain high concentrations of the injected material in the peritoneal cavity for several hours or even days following administration.

Keywords: Residence time, carrier solution, Icodextrin, colloid osmosis, clearance

1. Introduction

IP therapy for the treatment of PC following surgical debulking might possess several advantages over the IV route mainly because of a higher exposure time and concentration of the drug to the tumor and lower systemic toxicity [1]. Ideally, to maximize the efficacy of anti-cancer drugs, prolonged exposure of tumors to the drugs in the abdomen is essential. In this context, different strategies aiming at increasing the residence time of anti-cancer drugs in the peritoneal cavity are being investigated, as IP administration of 'simple' solutions of chemotherapeutics results in their rapid clearance to the systemic circulation [2]. For example, one strategy to prolong the residence time of the chemotherapeutics is the use of depot systems which slowly release the drugs in the abdomen [3].

Generally speaking, transport of fluids across the peritoneal cavity is governed by two major forces: (1) hydrostatic pressure gradient between the peritoneal cavity and underlying tissue layers results in the absorption of water from the peritoneal cavity and (2) osmotic pressure gradient which is induced by an osmotic agent and leads to the removal of water from the tissue and blood to the peritoneal cavity. The flow of water by osmotic pressure is called ultrafiltration. Solutes are transported from and to the peritoneal cavity by diffusion and/or convection. It has been shown that diffusion is the main transport mechanism for solutes with Mw lower than 600 Da (e.g. urea, creatinine, and glucose), whereas convection is the dominant mechanism for large molecules, with Mw higher 40,000 Da (e.g. proteins)[4].

Nanomedicines (i.e. nanoparticles loaded with drugs) have emerged as an attractive strategy for the treatment of PC, due to their potential to not only deliver chemotherapeutics to the peritoneal cavity, but also nucleic acids [5, 6]. In spite of the progress made in nanomedicine-based IP therapy, nanomedicines still suffer from a short residence time in the peritoneal cavity following IP administration, as they are rapidly cleared from the abdomen to the systemic circulation, mainly via the lymphatic system [7]. To date, several studies have evaluated the therapeutic efficacy of nanoparticles loaded with chemotherapeutics or nucleic acids [6, 8] against peritoneal tumors following IP injection. Apart from the type of NPs, also the carrier solution used to inject the NPs in the peritoneal cavity, can be varied. Up to date, however, there is no recommendation as on which carrier solution is most optimal for the IP injection of nanoparticles.

Clearly, a good carrier solution should retain the NPs in the peritoneal cavity as long as possible without destabilizing the injected NPs. A good possible candidate could be Extraneal®, a commercial icodextrin-based solution (average Mw of 16.2 kDa), widely used in peritoneal dialysis. A proposed pathway of the peritoneal transport of fluids during peritoneal dialysis as suggested by Krediet et al. [9] is shown in Figure 1. In crystalloid osmosis, water is transported down an osmotic gradient, from regions with low concentration of molecules to regions with high concentration of molecules (Figure 1A). A net water flow to the peritoneal cavity thus requires the

administration of a hypertonic solution. In colloid osmosis, however, macromolecules can induce the transport of water in the direction of an excess of large macromolecules, even when the solution is isotonic. Icodextrin is such a macromolecule that induces colloid osmosis. It is a starch-derived polymer composed of glucose units linked by α-1-4 glucosidic bonds and branched at the α-1-6 glucosidic bonds (less than 10%). It results in an effective ultrafiltration through colloid osmosis, in which waste products are absorbed from the blood capillaries to the peritoneal cavity and regularly removed together with the icodextrin solution. Icodextrin is not metabolized inside the peritoneum, but slowly absorbed into the bloodstream through the lymph vessels. After absorption, it is slowly degraded to disaccharides (maltose) and then to the monosaccharide glucose [10, 11]. As the osmotic activity of icodextrin results in the attraction of water to the peritoneal cavity (Figure 1B), the icodextrin solution is kept in the peritoneal cavity for a longer time when compared to the isotonic solution of PBS. We hypothesized that when used as a carrier for NPs, icodextrin could extend the residence time of NPs up to several hours in the abdomen and potentially attenuate their clearance in the reticuloendothelial system (RES) organs, such as the liver and spleen. Therefore, the clearance of NPs from the peritoneal cavity was determined by concentration measurements on the carrier solutions collected from the peritoneal cavity at different time points following injection, by using Single Particle Tracking (SPT). Furthermore, we made use of a recently developed Fluorescence Recovery After Photobleaching (FRAP) method from our laboratory, able to simultaneously measure the concentration of each molecular weight fraction of FITC-Dextrans (FDs) present in a mixture. This allows us to estimate if a certain MW range of FDs (between 10 and 500 kDa) is better suited to be retained in the peritoneal cavity. If so, solutions prepared with this Mw of FDs could be a good alternative for the icodextrin solution to contribute to colloid osmotic effects in order to increase the residence time of NPs administered in this solution.

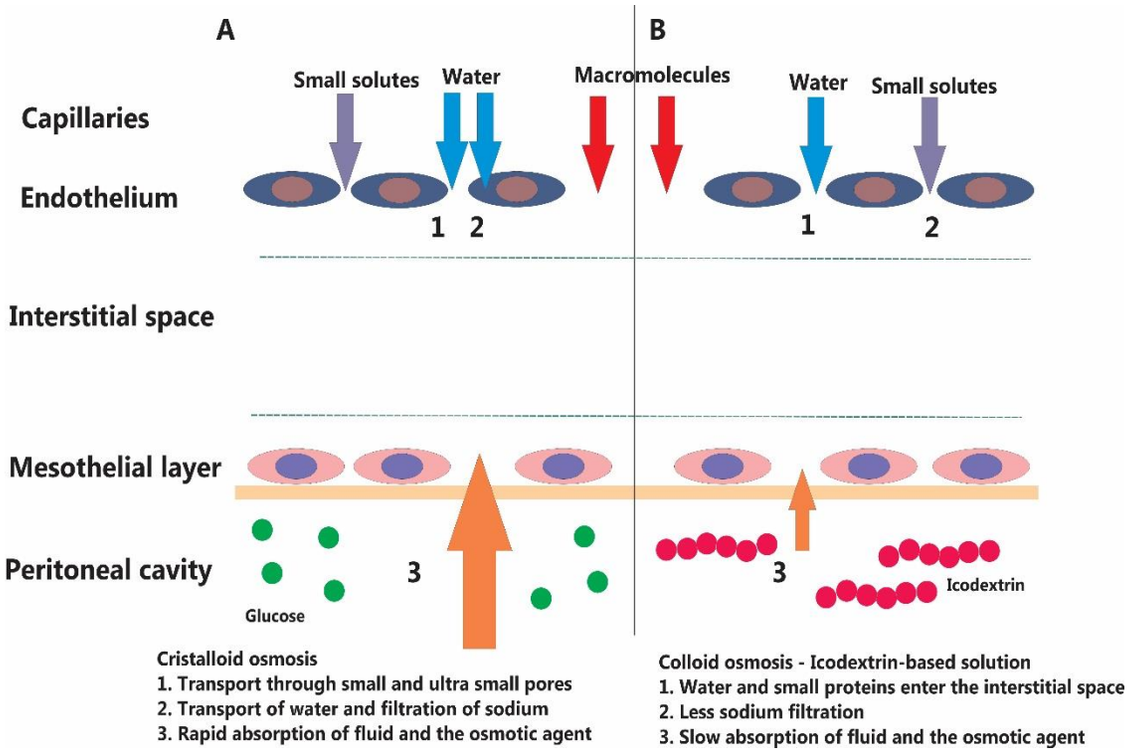

Figure 1. Proposed pathways for the peritoneal transport of fluids and solutes as suggested by Krediet et al.

2. Materials and methods

2.1 Materials

FluoSpheres® carboxylate-modified 0.2 µm dark red (λ_{ex}= 660, λ_{em}= 680) was purchased from molecular probes®, Thermo Fisher Scientific. Dulbecco's Phosphate Buffered Saline (DPBS) was purchased from gibco®, life technologies™ (Merelbeke, Belgium). Fluorescein isothiocyanate-dextran (FD) of average molecular weight 10, 40, 150 and 500 kDa were purchased from Sigma-Aldrich® (Bornem, Belgium). Extraneal®; 7.5% icodextrin solution was purchased from Baxter Healthcare (IL, USA). Functionalization of 200 nm anionic NPs to PEGylated ones was performed according to previously published procedures [12]. The size and surface charge of the NPs was measured using the Zetasizer Nano-ZS (Malvern, Worcestershire, UK), as shown in Table 1.

2.2 Animals

Healthy female nude Foxn1^nu 5 weeks old mice (15-20 g) were purchased from Harlan laboratories (Indianapolis, IN, USA). All animal procedures were approved by the Ghent University Hospital (UZ Gent) ethical committee on animal experiments (ECD No. 14/78). The animals were maintained by the animal core facility at the Ghent University Hospital and kept at 22°C in a humidified atmosphere with food and water ad libitum.

2.3 Colloidal stability and residence time of the anionic and PEGylated PS NPs following IP administration in mice

1 µl of the stock solution of the anionic PS NPs was diluted up to 1 ml in PBS, and IP administered in mouse. Samples from the abdominal cavity of mouse were obtained 1 h and 3 h following administration. Both the size and concentration of the PS NPs were determined using fSPT as explained below.

1 µl of the stock solution of the PEGylated PS NPs was diluted up to 1 ml 7.5% icodextrin solution. Subsequently, this 1 ml of PEGylated PS NPs was IP administered in healthy mice (n=3). Samples from the peritoneal cavity of mice were obtained 2 h and 4 h following injection, as explained under section 2.4 The obtained samples were analyzed on a wide-field fSPT set-up as described under section 2.9 in Chapter 3 [13]. To obtain size distributions of the NPs following injection, the value of the viscosity was set to 1 cP. Note that an accurate determination of the viscosity using a viscometer was impossible due to the low volume of fluids that remain in the abdomen 2 h and 4 h following injection. To determine the concentration of the PS NPs in the IP fluids by fSPT experiments, we made use of the method reported by Roding et al., which is based on the correlation which exists between the number of trajectories (recorded in the fSPT experiments) and the concentration of particles in the sample. Given the detection volume, track length and

diffusion coefficient of each NP, the concentration of the NPs can be calculated using the maximum likelihood estimation [14, 15].

2.4 Biodistribution of the PEGylated PS NPs following IP administration in mice

To study the biodistribution of the PS NPs following IP injection, 1 ml of the PS NPs solution in icodextrin was injected in 3 mice. Whole body fluorescence imaging was performed by the IVIS Lumina II 1,2,3,4 and 24 h following injection under anesthesia as described under section 2.6. Thereafter, the intestines, liver and spleen were collected and imaged separately to determine the fluorescence intensity. All fluorescence images were obtained using the 640 nm excitation filter, Cy5.5 emission filter and exposure time of 10 sec.

2.5 Residence time of 150 kDa FDs in the abdomen following IP administration in mice in PBS or icodextrin

1 ml of a 150 kDa FD solution, with the FD dissolved in respectively PBS or 7.5% icodextrin, was IP injected (using a 30G needle) in healthy mice (n=3). Samples from the peritoneal cavity of the mice were obtained 2 h and 4 h following injection. Therefore mice were anesthetized using isoflurane (5% induction, 2% maintenance), and the abdomen was opened to obtain the fluids with a 1 ml 20G syringe. 7 µl of the obtained samples was used for FRAP analysis as described under 2.7. It should be noted that the volume that could be collected from the abdomen decreased as a function of time. For example, it was possible to recover about 100 µl of fluid 2 h following injection, while only 20-30 µl could be collected from the abdomen 4 h following administration.

2.6 Residence time of a mixture of FDs with varying molecular weight following IP administration in mice in icodextrin

A mixture of FDs was prepared containing 2.5 mg/ml of the 10 kDa FD, 1.5 mg/ml of the 40 kDa FD and 1 mg/ml of respectively the 150 kDa and 500 kDa FD. The concentrations and molecular weights of the FDs in the mixure were chosen to allow the analysis of the FD-mixture by fluorescence recovery after photobleaching (FRAP), following a recently published FRAP-method as outlined below [16]. The unique property of using these FD mixtures, is that the clearance of different molecular weight fractions can be evaluated in a single FRAP experiment. Based on the FRAP measurements performed by Xiong et al. the average size is 3 nm for the 10 kDa FD, 10 nm for the 40 kDa FD, 16 nm for the 150 kDa FD and 31 nm for the 500 kDa FD [16]. FRAP basically allows to measure the distribution of the diffusion coefficients of the FD-mixture, which can be used to calculate size distributions through the stokes-Einstein equation. Based on these size distributions, it can be estimated if one molecular weight fraction of FDs is cleared from the peritoneal cavity more rapidly. 1 ml of the FD mixture in 7.5% icodextrin, was IP injected (using a 30G needle) in healthy mice (n=3). Samples from the peritoneal cavity of the mice were obtained 2 h and 4 h following injection and analysed as described above.

2.7 Fluorescence Recovery after photobleaching (FRAP)

In a FRAP experiment, a sample containing fluorescently labeled molecules or NPs is photobleached in a micron size area by an excitation pulse, followed by a recovery at a rate that is proportional to the diffusional rate of the fluorescent components. Using continuous FRAP (cFRAP) that was recently developed in our laboratory, a rectangle is photobleached, and the recovery curve is fitted to a theoretical recovery model that enables to extract a continuous distribution of diffusion coefficients.

In brief, FRAP experiments were performed on a C1-si confocal microscope (Nikon, Japan) equipped with a 488 nm Ar-ion laser of 40 mW and acoustic optical tunable filter (AOTF) to modulate the laser intensity for bleaching and imaging (fastest imaging rate ~0.5 frame s^{-1}). Rectangular areas were photobleached and the fluorescence recovery was imaged using the Nikon NIS Elements AR software package. A 10× NA 0.45 plan apochromat objective lens was used for bleaching and imaging. The laser power was adjusted to obtain 25-50% bleaching, in accordance with the theoretical requirement of limited bleaching. The recovery time depends on the diffusion coefficient as well as the size of the bleach area. To capture the diffusion from the smallest (10 kDa) and largest (500 kDa) FD components we used a bleach area of 50 µm with a sampling time that starts at 0.5 s per frame and increases to 16 s per frame towards the end of the time lapse recording. FRAP measurements were performed at room temperature, and the obtained diffusion distributions were converted to size distributions using the stokes-Einstein equation. In order to calculate the size distributions, the following viscosity values were used: 0.94 cP before injection and 1 cP after injection.

3. Results

3.1 Residence time of IP injected 200 nm anionic PS NPs in the peritoneal cavity with PBS as carrier solution

Our initial aim was to determine at what time following IP administration NPs are cleared from the abdomen. Therefore, NPs dispersed in PBS were injected in the peritoneal cavity of mice and fluid samples were collected from the peritoneal cavity at different time points. On these fluids, SPT was performed to determine the size and concentration of the NPs that remained. The size and surface charge of anionic PS NPs are given in Table 1 below. The data in Figure 2A demonstrate the size distributions of the 200 nm anionic PS NPs in PBS before injection (black curve), and 1 h (red curve) and 3 h (blue curve) following IP injection in mouse. When compared to the size distribution before injection, both the red and blue distributions are shifted towards higher sizes, indicating that aggregation of the 200 nm anionic PS NPs has occurred in the abdomen of the mouse. The data is in line with our previously published outcomes, where we showed that 100 nm anionic PS NPs aggregate in diluted peritoneal fluid obtained from mice and in undiluted human

ascites fluids obtained from a PC patient [13]. The increase in size 1 h and 3 h following administration was accompanied with a linear decrease in the concentration of the anionic PS NPs measured in the collected fluid from the abdomen, as observed in Figure 2B. It should be noted that very low amount of fluid (10 µl) could be retrieved from the peritoneal cavity 3 h following administration. Together, these results suggest that the injected solution is rapidly absorbed from the abdomen and that almost no freely diffusing NPs are present in the peritoneal cavity at the 3 h time point. To make more firm conclusions, however, the experiments should be repeated in more mice, as the data in Figure 2A and Figure 2B was obtained from one mouse only.

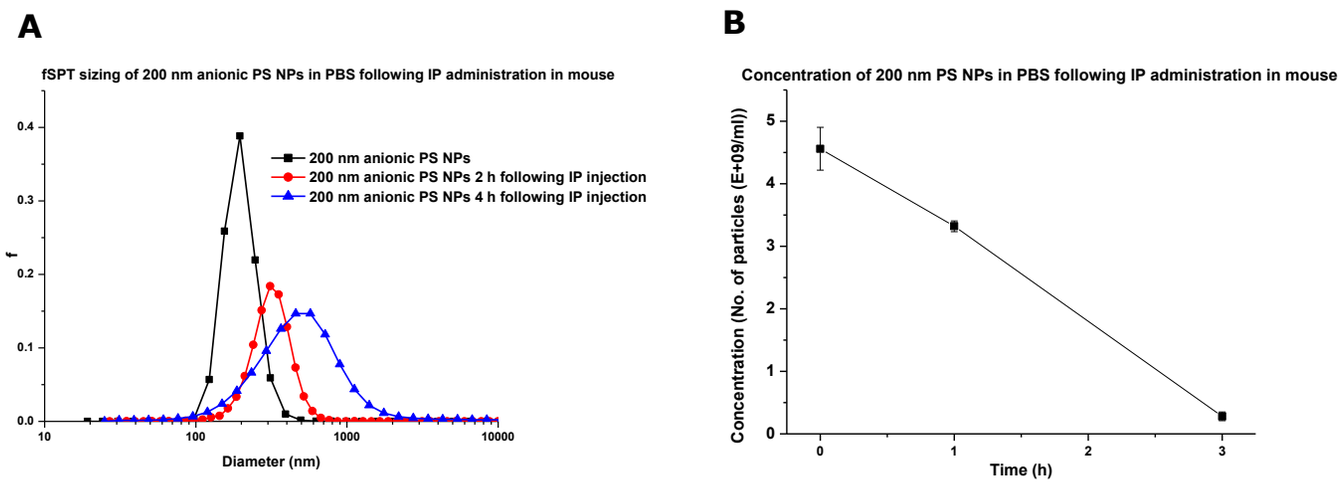

Figure 2. Size distributions and concentration of 200 nm anionic PS NPs following IP administration. (A) fSPT sizing of 200 nm anionic PS NPs before injection (black curve), 1 h (red curve) and 3 h (blue curve) following IP administration in mouse. **(B)** Concentration of the PS NPs before injection, 1 h and 3 h after injection as measured in the collected fluids. Samples collected from 1 mouse at three different time points.

3.2 Influence of the carrier solution on the residence time of IP injected 150 kDa FD in the peritoneal cavity

Based on the outcomes presented in Figure 2, we decided to test whether rapid clearance could be prevented by changing the carrier solution for injection. As the anionic beads aggregated in the peritoneal cavity, we first tested the effect of changing the carrier solution on FD molecules of 150 kDa. As outlined in the introduction, we hypothesize that, due to the colloid osmosis, dispersing NPs in an icodextrin solution instead of in PBS might prolong the residence of IP injected NPs in the abdomen. Icodextrin has indeed been reported to remain in the peritoneal cavity of humans for several hours and even days, due to the attraction of water into the abdomen [17].

Mice were IP injected with 1 ml 150 kDa FD either in PBS or in icodextrin as carrier solutions. When possible, 50 µl of the injected solution was retrieved from the peritoneal cavity and the size distributions of the FD was measured with FRAP as mentioned in the materials and methods section. When 150 kDa FD was dissolved in PBS, IP fluids could be collected from the animals up to approximately 2 h after IP injection. Fluid was no longer found in the peritoneal cavity 2.5 and 3

h following injection. The data in Figure 3A demonstrate the size distribution (obtained by FRAP) of the 150 kDa FD in respectively PBS (i.e. in the injected solutions; black curve) and in the IP fluid collected 2 h after IP injection (red curve). A small shift in the size distribution can be observed, originating from a slightly slower diffusion of the FD molecules. This could stem from slight differences in the viscosity of the fluids before and after injection. Alternatively (but less likely), some smaller fraction of the FD solution might preferentially have left the peritoneal cavity, resulting in a shift to the larger size range of FD molecules.

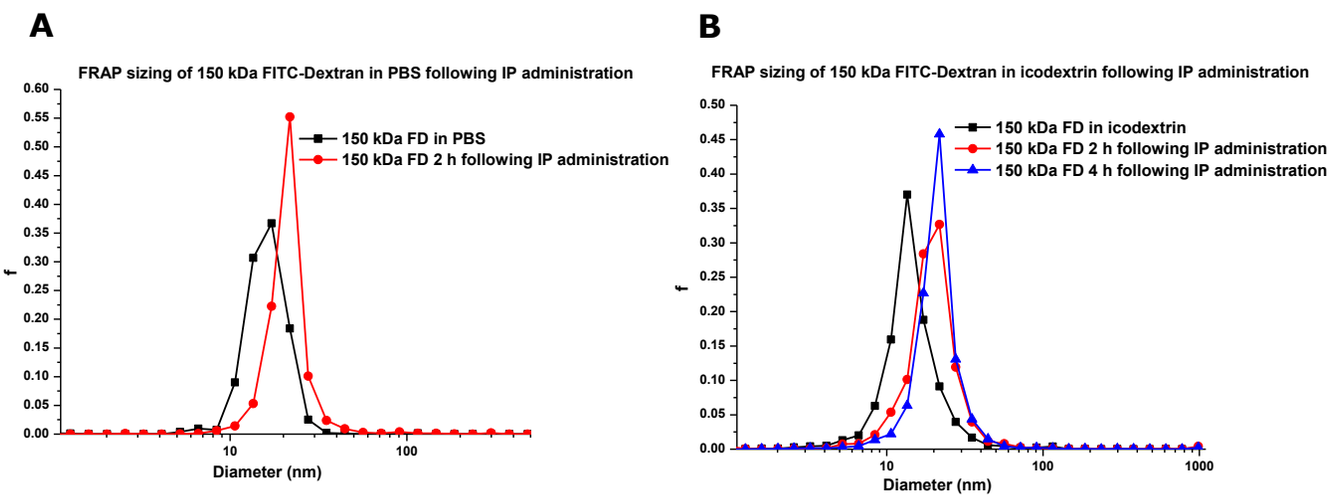

Figure 3. **Size distributions of (A)** 150 kDa FD in PBS (black curve) and in IP fluids collected 2 h following IP injection in mice (red curve). **(B)** Size distribution of 150 kDa FD in icodextrin solution (black curve), in IP fluids collected respectively 2 h (red curve) and 4 h (blue curve) after IP injection. Each of the distributions is an average calculated from fluids that were collected from 3 mice at different time points.

When 150 kDa FD was resuspended in icodextrin, it was possible to collect 50 µl fluid samples from the abdomen 2 h and 4 h following the IP injection. The size distribution of the 150 kDa FD component as shown in Figure 3B, again shows a small increase in size when compared to the initial size distributions obtained in the icodextrin (black curves). This stems most likely from small differences in viscosity of the obtained samples. No further increase in the size of the 150 kDa FD occurred, however, between 2 to 4 hours following injection. The data in Figure 3 suggest that the use of icodextrin, instead of PBS, prolongs the residence of IP injected 150 kDa FD in the abdomen. Therefore, Figure 3 supports our hypothesis that an increase in the abdominal retention of the injected soltuion occurs when icodextrin is used as carrier solution for the 150 kDa FD. The time frame in which 50 µl samples could be taken from the peritoneal cavity, however, remained rather short (e.g. maximally 4 h). Worth mentioning in this context that the FRAP and fSPT experiments are based on the diffusion of nanomaterials in a solution, and hence when the residence time of the fluid is extended, the residence time of the nanomaterials diffusing is also extended. Upon clearance of the solution, however, it is possible that not all the particles are cleared simultaneously with the solution, leading to their sedimentation in the peritoneal cavity.

3.3 Optimization of the icodextrin solution for prolonged residence time in the abdomen

The abdominal residence time of 4 h could stem from the intrinsic ability of the icodextrin solution to induce the colloid osmosis effect as discussed in the introduction. Nevertheless, a residence time of 4 h is still insufficient when thinking of prolonged exposure of the tumor to drugs in the abdomen. In order to optimize the icodextrin solution to reside for a longer time in the abdomen, we IP injected the icodextrin solution in combination with FDs of different molecular weights, namely 10, 40, 150, and 500 kDa. Such an experiment will allow us to understand whether in addition to the colloid osmosis effect of the icodextrin, the Mw of the FDs in the injected solution could play an important role in extending the residence time of icodextrin in the abdomen. The final goal of this experiment was to select the FD component that exhibits the slowest clearance from the abdomen, and make use of this Mw to prepare a carrier solution for IP injection of NPs.

Figure 4 depicts the size distributions of the FDs mixture in respectively the icodextrin solution (i.e. before injection; black curve), IP fluids collected 2 h (red curve) and 4 h (blue curve) following IP injection. The size distributions in Figure 4 suggest that the clearance of FDs from the abdomen is independent of the Mw, as the size distributions remain around the initial values, indicating that all the FD components are cleared simultaneously. In addition, no fluid was present in the abdomen 4.5 and 5 h following injection, indicating that in spite of the high Mw of the FDs components, no additional extension in the abdominal retention was observed. Therefore, none of the FD components seems to be preferred to prepare a carrier solution that would show extended residence time in the peritoneal cavity when compared to the icodextrin solution.

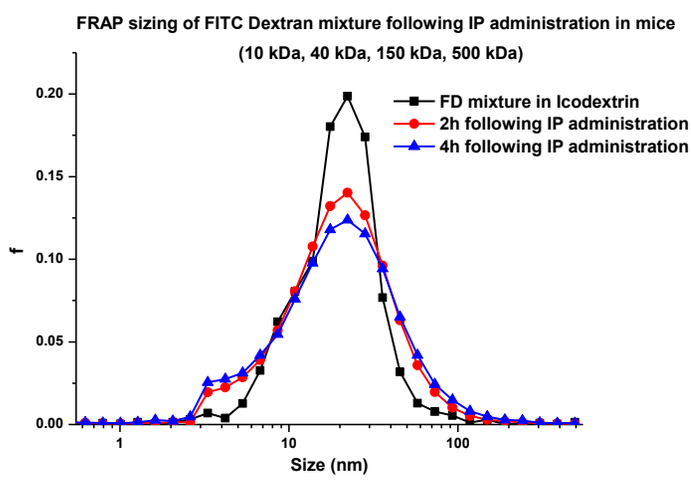

Figure 4. Size distributions of the FD mixture composed of different Mws in icodextrin following IP injection in mice obtained by FRAP. The black curve represents the mixture of FDs in icodextrin before IP injection in mice. Samples were obtained from the peritoneal cavity of mice 2 h (red curve) and 4 h (blue curve) following injection. Each of the red and blue curves was obtained following administration in three different mice (3 mice for each time point).

3.4 Residence time and biodistribution of IP injected 200 nm PEGylated PS NPs in the peritoneal cavity of mice with icodextrin as carrier solution

The experiments above show that adding high molecular weight FDs to the icodextrin solution does not increase the residence time of the fluid into the peritoneal cavity. We did observe, however, that icodextrin is preferred over PBS to follow the fate of 150 kDa FDs in the peritoneal cavity. In order to investigate whether the icodextrin solution would also prolong the residence time of nanoparticles following IP administration, 200 nm PEGylated PS NPs were injected in icodextrin into the peritoneal cavity. PEGylated PS NPs were used to prevent the aggregation of anionic PS NPs following IP injection as was observed in Figure 2. The size and surface charge of the anionic PS NPs (i.e. before functionalization with PEG) and PEGylated PS NPs are given in Table 1. As expected, grafting the surface with PEG increases the diameter and decreases the surface charge of the NPs.

Table 1. Average diameter and zeta-potential of the anionic and PEGylated PS NPs

NPs	Average diameter (nm) ± SD	Polydispersity index (PDI)	ζ-potential (mv) mean ± SD
Anionic PS	210 ± 1	0.036	-65.1 ± 4.7
PEGylated PS	254 ± 1	0.119	-8.5 ± 0.1

Initially, we IP injected 1 ml of 200 nm PEGylated PS NPs dispersed in icodextrin in mice and collected 50 µl of the fluids from the abdomen, respectively 2 h and 4 h after administration. Worth mentioning the fact that using FRAP to measure the size of the PS NPs is not possible since the PS NPs are fluorescently labeled with a photostable dye which is hard to bleach even by using high laser intensities. Therefore, we made use of fSPT to determine simultaneously the size and concentration of PS NPs before and after injection. Figure 5A highlights the size distributions of the 200 nm PEGylated PS NPs before injection in mice (black curve), and following IP injection in mice (red and blue curves). When compared to the size distribution before injection in mice, the size distribution of the PEGylated PS NPs in fluids collected 2 h and 4 h after IP injection was slightly shifted towards the right. This could be due to (i) either small differences in the viscosity or (ii) minor aggregation of the NPs in the abdomen. Figure 5B depicts the concentration of the PS NPs as a function time. The zero time point corresponds to the concentration of the PS NPs in icodextrin before injection. Unlike the linear decrease in concentration observed for the anionic PS NPs following administration in PBS (Figure 2B), Figure 5B demonstrates a non-linear decrease in the concentration of the PEGylated PS NPs when administered in icodextrin. A slight drop in the concentration is observed 2 h following administration, while a more steep decrease was

documented 4 h following injection. The data in Figure 5B suggest that only a minor fraction of the PEGylated PS NPs are cleared from the abdomen within the first two hours, whereas the majority of the PS NPs leave the abdomen between 2 to 4 h following administration. Of note, the calculated NPs concentration in Figure 5B does not include NPs that possibly sedimented or stayed somehow in the abdomen, but only those that are freely diffusing in the solutions that were collected from the peritoneal cavity.

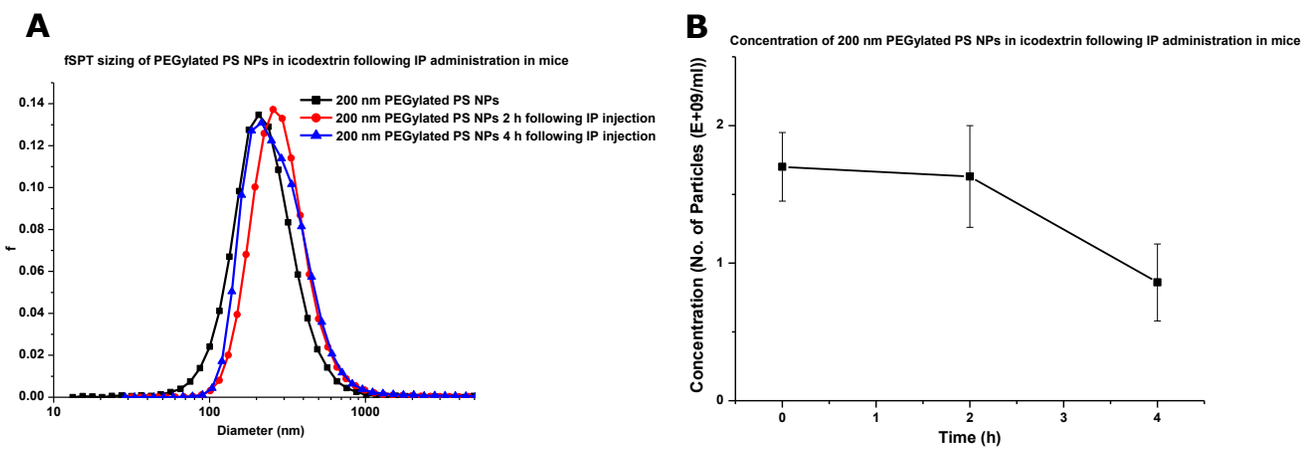

Figure 5. fSPT sizing and clearance of the 200 nm PEGylated PS NPs in icodextrin solution following IP administration in mice. (A) The black curve represents size of the PS NPs before injection. Fluids were collected from the peritoneal cavity of mice 2 h (red curve) and 4 h (blue curve) following IP injection and analyzed by fSPT. Each of the red and blue curves was obtained following administration in three different mice (3 mice for each time point). **(B)** Concentration of the PS NPs before injection and in the fluids collected from the abdomen 2 h and 4 h following injection.

To study the biodistribution of the PS NPs following IP injection in the icodextrin, we injected the fluorescently labeled PS NPs in 3 different mice, and determined the fluorescence intensity of the excised intestines, liver and spleen of each mouse 24 h following IP administration (Figure 6). The highest fluorescence intensity (in yellow) was detected in the liver, followed by the spleen. Some fluorescence signal is detected in the intestines, as pointed out by the white arrows in Figure 6, although the vast majority of NPs clearly have left the peritoneal cavity. The total flux (expressed in photons per second) collected from the liver and spleen is given in Table 2. The data confirms that in spite of the extended residence time (4 h) achieved by icodextrin in the abdomen, the carrier solution does not succeed in keeping a high amount of NPs in the peritoneal cavity 24 h following injection. Whether or not the injection of PS NPs in the peritoneal cavity in Icodextrin significantly alters the biodistribution of NPs (e.g. the amount of NPs that are retained in the peritoneal cavity) at the 4 hours time scale, remains to be seen.

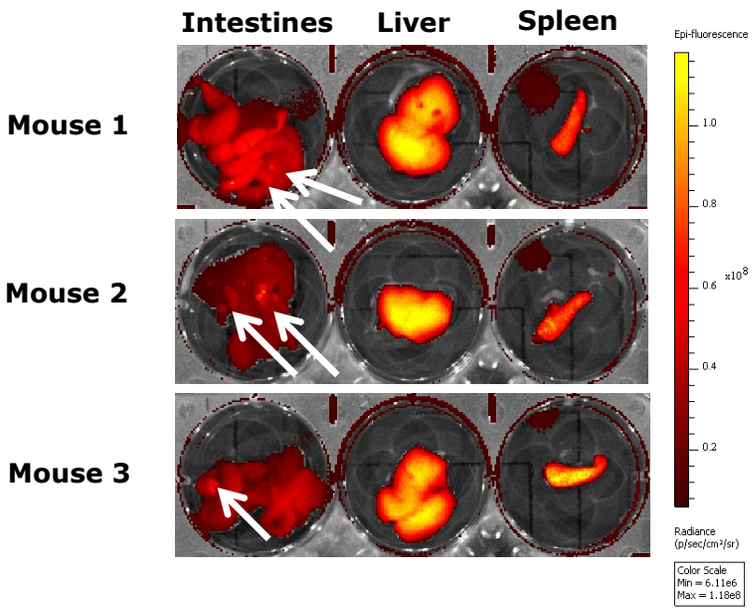

Figure 6. biodistribution of fluorescently labeled PS NPs in icodextrin following IP administration in mice. The intestines, liver and spleen from each mouse were collected 24 h following injection and the fluorescence signal was determined by the IVIS Lumina II. The red signal represents the fluorescence background and the yellow signal corresponds to the fluorescence of the 200 nm PEGylated PS NPs. The white arrows represent the fluorescence signal of the PS NPs that accumulated in the intestines.

Table 2. Values of the total flux [p/s] of the organs collected from each mouse

Mouse	Liver	Spleen
1	3.4E+09	4.9E+08
2	2.8E+09	2.4E+08
3	3.3E+09	8.2E+08

4. Discussion

The above-described set of experiments aims to optimize a carrier solution for prolonged residence time of NPs in the peritoneal cavity following IP injection. We first assessed the residence time of NPs dispersed in PBS and then compared it with icodextrin which is used in the clinic for peritoneal dialysis. We expected that due to the colloid osmosis effect and the formation of a pressure gradient across the peritoneal membrane, the 7.5% icodextrin solution will increase the peritoneal retention time of the fluid (and thus also of the NPs dispersed in this fluid) to several hours. We observed, however, that icodextrin was only available to prolong the residence time of NPs to 4 h, compared to 2 h when the NPs were dispersed in PBS. The reason beyond the relatively short increase in the peritoneal residence time following IP administration of nanomaterials dispersed in icodextrin compared to PBS, is due to two main forces that exist in the abdomen. On the one hand, icodextrin is iso-osmolar (not hypertonic) in relation to the plasma, ensuring that no transport occurs through the ultra-small pores from the capillaries to the interstitium, leading to a

pressure gradient across the peritoneal membrane which is maintained for several hours [18]. This pressure gradient does not exist when the isotonic PBS is used as carrier solution. On the other hand, the presence of lymphatic vessels accelerates the drainage of nanomaterials from the peritoneal cavity via an one way system to the circulation [19]. It is therefore logical to assume that the retention time of icodextrin in the abdomen (Figure 3 and Figure 4) is in fact a balance between the pressure gradient across the peritoneal membrane and the clearance. It is very important to mention in this context, that in addition to the increase in the residence time achieved by using icodextrin as carrier solution, a high concentration of the PS NPs was maintained in the abdomen during the first two hours (Figure 5B) compared to the situation in PBS (Figure 2B) where a decrease in the PS NPs concentration was noticeable even 1 h following injection. This effect is most likely attributed to the colloid osmosis effect, keeping the solution together with the NPs in the abdomen, which is essential when developing IP therapy for the treatment of PC as explained in Chapter 1 of this thesis. The biodistribution of the PS NPs (Figure 6) 24 h following IP administration demonstrates, however, that also NPs injected with the icodextrin solution were cleared to the liver and spleen 24 hours after injection. It is highly likely that the NPs accumulated first in the spleen, since the spleen but not the liver is a primary lymphoid organ [18], and then to the systemic circulation ending up eventually in the liver. To confirm this, further experiments that include collecting tissues at shorter time points following administration (e.g. 4, 6 h) should be performed. Worth mentioning also that the biodistribution data are in line with the outcomes of the studies reviewed in Chapter 1 of this thesis, where NPs dispersed in PBS solution accumulated mainly in the liver and spleen following IP administration.

As for the findings with the FDs mixture (Figure 4), we hypothesized that the Mw of the FDs would influence the residence time and clearance from the abdomen. Subsequently, we aimed to prepare a carrier solution based on the optimal Mw of FDs that remained the longest time in the peritoneal cavity. Nevertheless, the data in Figure 4 demonstrate that there is no influence of the Mw of the FDs neither on the residence time of the injection fluid nor on the clearance of the FDs from the abdomen. Therefore, in our hands, the icodextrin solution remained the most suited to exhibit colloid osmosis and a prolonged residence time of the fluid in the peritoneal cavity.

To evaluate the impact of the carrier solution on the pharmacokinetics of IP chemotherapy, Sugarbaker and co-workers [21] studied the dwelling of the anti-cancer drugs 5-fluorouracil or gemcitabine in the abdomen of rats. The drugs were IP administered in rats using different carrier solutions that varied in tonicity (0.3%, 0.9%, or 3% sodium chloride) or were isotonic and varied in Mw (0.9% sodium chloride, 4% icodextrin, and 6% hetastarch). The authors demonstrated that the use of high molecular weight carrier solutions or a hypertonic sodium chloride (i.e. 3%) result in a prolonged dwell of chemotherapy and consequently maintained high volumes of fluid in the abdomen, for 6 h following administration. Worth mentioning in this context that the findings of this study can’t be directly compared with our outcomes, since we used different carriers solutions and administered NPs in mice, while Pestieau et al. administered chemotherapeutics in rats.

Importantly, the 7.5% icodextrin solution used in this study was previously used as carrier solution in the treatment of PC. Kerr et al. [17] used 7.5% icodextrin solution as carrier for 5-fluorouracil in a phase I study to determine the maximal tolerated dose and toxicity. The study demonstrated IP steady state concentrations of 5-fluorouracil that were 1000-fold higher than the systemic level, due to the long abdominal retention achieved by icodextrin [22]. The fact that the 7.5% icodextrin solution significantly increased the residence time of drugs in the abdomen of humans, but not in rats or mice is most probably ascribed to the presence of high concentrations of amylase in the tissues of mice and rats, which more rapidly metabolizes starch than in humans [23]. Therefore, the use of icodextrin solution as drug carrier to extend the residence time of drugs/nanomedicines in the abdomen of mice or rats does not resemble the situation in humans, which makes it harder to extrapolate the results into the human situation. In this case, experiments in humans are required in order to determine whether 7.5% icodextrin solution enhances the residence of nanomedicines in the abdomen.

Broadly speaking, since the icodextrin solution is approved for use in the clinic for peritoneal dialysis, it is possible to use it also when applying solutions containing anti-cancer drugs or nanomedicines in the peritoneal cavity. Nevertheless, based on the findings of this study, a residence time of 4 h in the abdomen of mice and even 24 h in humans if achieved, is most probably not sufficient to achieve sustained release of anti-cancer drugs from nanomedicines for the local treatment of PC. Such approach, if used, would require multiple administrations in patients in order to achieve maximal exposure of peritoneal tumors to the drug.

5. Conclusions

In this study we investigate the influence of the carrier solution on the residence time and clearance of nanomaterials following IP injection in mice. Namely, we evaluated the residence and clearance of FD solutions or PS NPs when IP injected in two carrier solution – PBS and icodextrin. Compared with the PBS solution, an extended residence time of 4 h in the abdomen was achieved when the FDs and PS NPs were dispersed in 7.5% icodextrin and IP administered. In our hands, the clearance from the abdomen was independent of the Mw of the injected material. Importantly we observed that when injected in icodextrin, higher concentration of PS NPs is retained in the abdomen when compared to PBS where the concentration decreases rapidly while the solution is being cleared. We also demonstrated that PEGylated NPs are stable in the abdomen, as no increase in size was observed 4 h following IP administration. Finally, we demonstrate that NPs following IP administration in icodextrin, accumulate mainly in the liver 24 h following administration. Based on the outcomes, we think that the use of icodextrin is a good strategy to increase the residence time of nanomaterials in the abdomen on the short scale. Yet the prolonged residence time when compared to PBS (from 2 hours to 4 hours) might not be sufficient to achieve maximal therapeutic efficacy when exploiting nanomedicines for the treatment of PC.

Acknowledgements

We thank the Infinity laboratory at the Ghent University Hospital for the assistance with the *in vivo* experiments and access to imaging equipment. We thanks the laboratory of experimental surgery at the Ghent University Hospital for their help with designing and performing *in vivo* experiments.

References

[1] G. Bajaj, Y. Yeo, Drug Delivery Systems for Intraperitoneal Therapy, Pharm Res, 27 (2010) 735-738.
[2] C. Hasovits, S. Clarke, Pharmacokinetics and Pharmacodynamics of Intraperitoneal Cancer Chemotherapeutics, Clin Pharmacokinet, 51 (2012) 203-224.
[3] F. Ramazani, C.F. van Nostrum, G. Storm, F. Kiessling, T. Lammers, W.E. Hennink, R.J. Kok, Locoregional cancer therapy using polymer-based drug depots, Drug Discov Today, 21 (2016) 640-647.
[4] S.-P. Joanna, W. Jacek, Mathematical models of intraperitoneal drug delivery, Intraperitoneal Cancer Therapy, CRC Press2015, pp. 153-169.
[5] G.R. Dakwar, M. Shariati, W. Willaert, W. Ceelen, S.C. De Smedt, K. Remaut, Nanomedicine-based intraperitoneal therapy for the treatment of peritoneal carcinomatosis - Mission possible?, Adv Drug Deliv Rev, (2016).
[6] R.D. George, S.C.D.S. Stefaan, R. Katrien, Intraperitoneal nonviral nucleic acid delivery in the treatment of peritoneal cancer, Intraperitoneal Cancer Therapy, CRC Press 2015, pp. 359-371.
[7] M. Tsai, Z. Lu, J. Wang, T.K. Yeh, M.G. Wientjes, J.L.S. Au, Effects of carrier on disposition and antitumor activity of intraperitoneal paclitaxel, Pharm Res, 24 (2007) 1691-1701.
[8] T.R. van Oudheusden, H. Grull, P.Y.W. Dankers, I.H.J.T. de Hingh, Targeting the Peritoneum with Novel Drug Delivery Systems in Peritoneal Carcinomatosis: A Review of the Literature, Anticancer Res, 35 (2015) 627-634.
[9] R.T. Krediet, The peritoneal membrane in chronic peritoneal dialysis, Kidney Int, 55 (1999) 341-356.
[10] C.D. Mistry, R. Gokal, Can Ultrafiltration Occur with a Hypoosmolar Solution in Peritoneal-Dialysis - the Role for Colloid Osmosis, Clin Sci, 85 (1993) 495-500.
[11] R. Pecoits, S. Mujais, B. Lindholm, Future of icodextrin as an osmotic agent in peritoneal dialysis, Kidney Int, 62 (2002) S80-S87.
[12] J. Suh, K.L. Choy, S.K. Lai, J.S. Suk, B.C. Tang, S. Prabhu, J. Hanes, PEGylation of nanoparticles improves their cytoplasmic transport, Int J Nanomed, 2 (2007) 735-741.
[13] G.R. Dakwar, E. Zagato, J. Delanghe, S. Hobel, A. Aigner, H. Denys, K. Braeckmans, W. Ceelen, F.C. De Smedt, K. Remaut, Colloidal stability of nano-sized particles in the peritoneal fluid: Towards optimizing drug delivery systems for intraperitoneal therapy, Acta Biomater, 10 (2014) 2965-2975.
[14] M. Roding, H. Deschout, K. Braeckmans, M. Rudemo, Measuring absolute number concentrations of nanoparticles using single-particle tracking, Phys Rev E, 84 (2011).
[15] M. Roding, H. Deschout, K. Braeckmans, M. Rudemo, Measuring absolute nanoparticle number concentrations from particle count time series, J Microsc-Oxford, 251 (2013) 19-26.
[16] R. Xiong, R.E. Vandenbroucke, K. Broos, T. Brans, E. Van Wonterghem, C. Libert, J. Demeester, S.C. De Smedt, K. Braeckmans, Sizing nanomaterials in bio-fluids by cFRAP enables protein aggregation measurements and diagnosis of bio-barrier permeability, Nat Commun, 7 (2016) 12982.
[17] D.J. Kerr, A.M. Young, J.P. Neoptolemos, M. Sherman, P. VanGeene, A. Stanley, D. Ferry, J.W. Dobbie, B. Vincke, J. Gilbert, D. ElEini, N. Dombros, G. Fountzilas, Prolonged intraperitoneal infusion of 5-fluorouracil using a novel carrier solution, Brit J Cancer, 74 (1996) 2032-2035.
[18] R.T. Krediet, M.M. HodacPannekeet, A.L.T. Imholz, D.G. Struijk, Icodextrin's effects on peritoneal transport, Periton Dialysis Int, 17 (1997) 35-41.
[19] I. Choi, S. Lee, Y.K. Hong, The New Era of the Lymphatic System: No Longer Secondary to the Blood Vascular System, Csh Perspect Med, 2 (2012).
[20] D.R. Getts, A.J. Martin, D.P. McCarthy, R.L. Terry, Z.N. Hunter, W.T. Yap, M.T. Getts, M. Pleiss, X.R. Luo, N.J.C. King, L.D. Shea, S.D. Miller, Microparticles bearing encephalitogenic peptides induce T-cell tolerance and ameliorate experimental autoimmune encephalomyelitis (vol 30, pg 1217, 2012), Nat Biotechnol, 31 (2013) 565-565.
[21] S.R. Pestieau, K.J. Schnake, O.A. Stuart, D. Yoo, P.H. Sugarbaker, The impact of carrier solutions on pharmacokinetics of intraperitoneal chemotherapy in a rat model, 3rd International Gastric Cancer Congress, (1999) 767-772.
[22] C.S. Mcardle, D.J. Kerr, P. Ogorman, H.A. Wotherspoon, H. Warren, D. Watson, B.J. Vinke, J.W. Dobbie, D.I.D. Eleini, Pharmacokinetic Study of 5-Fluorouracil in a Novel Dialysate Solution - a Long-Term Intraperitoneal Treatment Approach for Advanced Colorectal-Carcinoma, Brit J Cancer, 70 (1994) 762-766.
[23] R.L. Mcgeachin, J.R. Gleason, M.R. Adams, Amylase Distribution in Extrapancreatic, Extrasalivary Tissues, Arch Biochem Biophys, 75 (1958) 403-411.

8

BROADER INTERNATIONAL CONTEXT, RELEVANCE AND FUTURE PERSPECTIVES

1. *In vitro* evaluation of nano-sized siRNA formulations in biofluids

A general overview on the *in vitro* findings shown in **Chapters 3, 4, 5, and 6** of this work reveals that a bottom-up approach of formulation development for a specific route of administration requires performing experiments under conditions that resemble as much as possible the *in vivo* situation. The advanced microscopy techniques employed in this work allow to predict the behavior of formulations and their optimization before carrying-out *in vivo* experiments. The importance of such experiments lies in the fact that to date, it is not possible to monitor and quantify cargo release and aggregation of nanomedicines upon their administration *in vivo* while circulating in the fluids of the body, which could be the reason for the lack or low biological activity in a lot of cases. In the case of the formulations evaluated in this project, the colloidal stability (i.e. release and aggregation) was not the bottleneck for efficient gene knockdown in protein-rich conditions, but the cellular uptake and subsequent intracellular processing. Of significance in this respect, each formulation is a special case and it is hard to predict the behavior of different formulations before performing the experiments. The fact that the colloidal stability was not the limiting factor for gene knockdown in biofluids, does not necessary imply that the colloidal stability can't be a problem when using other nano-sized siRNA formulations. Finally, the data in **Chapter 6** involve the use of different biofluids, confirming and emphasizing the significance of assessing nano-sized siRNA formulations in biofluids. The biofluids used in **Chapter 6** resemble not only IP administration of nanomedicines but also intravenous (IV) administration. Overall, the use of biofluids is still an overlooked aspect in siRNA delivery and deserves more attention from the drug delivery community.

2. Ascites as a model for studying the colloidal stability and biological activity of nanomedicines: advantages and limitations

Ascites fluid [1] obtained from a peritoneal carcinomatosis (PC) patient was used in this project to study the colloidal stability and biological activity of siRNA LPXs *in vitro*. The rationale behind using the ascites fluid was to resemble as much as possible the human situation of the peritoneal cavity. Nevertheless, it is important to mention that for the vast majority of the PC cases in the clinic, ascites is not the ideal model. Ascites is considered a sign of advanced disease and poor prognosis [2], and thus patients with ascites are not subject to CRS and subsequent therapy, but receive palliative care which consists mainly of treatment of bowel obstruction and/or ascites. Therefore, ascites does not resemble the fluid that exists in the abdomen of PC patients following cytoreductive surgery (CRS).

In spite of the above-mentioned, when thinking of peritoneal fluids that resemble the real situation for *in vitro* experiments, only two were accessible as shown in **Chapter 3**. The first one is a diluted fluid obtained from healthy mice following flushing of the abdominal cavity with a physiological solution or water and the second is ascites from a PC patient, which is similar in its composition to the human serum as demonstrated in **Chapter 3**. In other words, ascites is the most "aggressive" fluid that can exist in the peritoneal cavity of humans diagnosed with PC. Therefore, the use of ascites for *in vitro* evaluation of nanomedicines and/or depot systems intended to reside for several days or weeks in the abdomen, increases the chances that these systems will be biologically active *in vivo* even if deterioration occurs and ascites is present in the peritoneal cavity. The data presented in **Chapters 3, 4, 5, and 6** demonstrate that the presence of only a low volume of fluid which is similar in its composition to the ascites fluid in the peritoneal cavity may influence the stability and/or biological activity. Under these conditions the ascites fluid seems a relevant model.

Of note, all experiments performed in this project were performed using ascites fluid from a single patient, which means that the inter- or intra-patient variability on the composition of the ascites, and its possible effects on the outcomes of the study was not taken into account. Obtaining ascites fluid from multiple patients is not an easy task. First, ascites formation is limited to tumors that originate from specific organs within the peritoneal cavity and not all peritoneal tumors. Second, despite of the fact that the ascites punctured from patients in the clinic is not further used, the use of ascites for research requires informed consent from the patient, and also approval of the ethical committee after explanation on the planned experiments to be done with ascites. The ascites fluid used in this project represents the typical ascites in the clinic in terms of protein composition and concentration as shown in **Chapter 3**.

In conclusion, the use of human ascites for *in vitro* optimization of nanomedicines possesses advantages and limitations. Yet, the fact that several formulations investigated in this project exhibited very low or no biological activity following incubation in ascites does not imply that those will behave similarly following IP administration *in vivo* in the absence of ascites. In this context, extrapolation of the data obtained in ascites *in vitro* to the *in vivo* situation requires a thorough evaluation of the formulations *in vivo* in the presence and absence of ascites, and establishing *in vitro in vivo* correlations. In the absence of ascites, formulations can be injected in solutions that are typically used in the clinic, such as 5% dextrose.

3. Residence time of the fluid vs. residence time of nanomedicines in the abdomen

As reviewed in **Chapter 1**, the residence time of nanomedicines in the abdomen is a very important factor in IP therapy of PC. Nevertheless, different methods and techniques were utilized to estimate the residence time of nanomedicines in the abdomen without clearly distinguishing between the residence time of the fluid and that of nanomedicines. As mentioned in **Chapter 7**, the absence of fluid in the peritoneal cavity several hours after IP administration, does not necessarily mean that the nanomedicines are not present. Consequently, the question whether nanomedicines that sediment on the abdominal wall and are immobile could exert biological activity has not been addressed yet. It is logical to assume that non-diffusing immobile nanomedicines would hardly come in contact with tumors, and induce tumor killing. For instance, Tsai et al. [3] investigated the residence time and anti-tumor activity of gelatin nanoparticles (NPs) loaded with radiolabeled PTX in mice. By obtaining peritoneal lavage samples at different time points following IP administration, the recovered dose of PTX in the peritoneal cavity was quantified and a PK model was established. Nevertheless, the residence time of the fluid was not estimated, and it is not clear whether the low anti-tumor activity (compared to gelatin MPs loaded with PTX) obtained stems only from PTX encapsulated within the gelatin NPs that were mobile and diffusing following IP injection or also from PTX that remained immobile in the peritoneal cavity. Overall, the residence time of the drug but not the fluid in the abdomen was determined.

Based on the above-mentioned, future research should focus on determining the residence time of both the nanomedicines and fluids, as well as to assess the time frame following administration during which nanomedicines come in contact with peritoneal tumors. The time frame in this case, will depend on the carrier solution of the nanomedicines as discussed in **Chapter 7**.

4. Nanomedicines for IP therapy of PC: The way forward

With approximately 250,000 new cancer cases annually in the USA [4], there is no doubt that developing efficacious post-surgical strategies for the treatment of PC will have a global clinical and economic impact. Based on the findings obtained and reviewed in this project, it is possible to exclude some strategies of being successfully translated into the clinic, and propose others that should be further investigated. In this section, different strategies and concepts that could be exploited for future IP therapy of PC will be discussed. Before proceeding in the discussion, worth mentioning the fact that to date, pharmaceutical companies did not show any interest in joining the effort that is being put together both in the academia and in clinical practice towards developing new IP therapies or formulations loaded with anti-cancer agents for the treatment of PC. This is may be related to difficulties encountered when registering new patents as anti-cancer formulations/drugs, or simply due to the general perception that investing in such therapies is not economically viable.

As mentioned earlier in this thesis, particularly in **Chapter 1**, an ideal post-surgical therapy for PC would be the one that resides in the abdomen for weeks or even months, and releases the anti-cancer agent in a sustained manner. To this end, we have shown in this work that NPs dispersions are rapidly cleared to the systemic circulation, following IP administration, precluding the requirement of long residence time in the abdomen. The same applies for free chemotherapeutics in solution following IP administration [5]. The use of depot systems [6, 7], capable of releasing anti-cancer agents for a prolonged period of time in the abdomen, therefore holds promise as a comparable strategy. This latter approach has been successfully translated into the clinic for the treatment of malignant glioma in the brain. Similar to PC where surgical debulking takes place, after the removal of malignant tumors in the brain, wafers based on a matrix of a biodegradable polymer poly[1,3-bis(carboxyphenoxy)propane-*co*-sebacic-acid (PCPP-SA 20:80) loaded with the chemotherapeutic drug carmustine are placed in the area where the tumor was located. Upon degradation, these wafers release the drug into surrounding cells and prevent disease recurrence. These wafers are known in clinical oncology as Giladel® [8]. Such formulations for IP therapy of PC should exhibit some desirable characteristics to ensure successful translation into the clinic. Examples are: (1) prevention of adhesions in the abdomen [9, 10], (2) the ability of the developed depot system to cover and distribute over the large surface area of the peritoneum [11] and (3) slow degradation of the depot system in a way that it attenuates as much as possible the clearance of the encapsulated drug/nanomedicine to the systemic circulation [3, 5]. While the first one is being extensively investigated [12], less attention has been paid to the design of biomaterials that take into consideration the last two characteristics. Indeed, suppression of peritoneal tumors was observed when hydrogels were used as depot systems for the release of free chemotherapeutics or NPs loaded with chemotherapeutics in the abdomen of mice, but not in humans [13-15]. Towards the translation of depot systems to the clinic, an important question remains unanswered; that is whether the *in vivo* degradation kinetics in the abdomen of mice (8

days – 2 weeks) is optimal to increase the survival of PC patients compared to the current post-surgical techniques mentioned in **Chapter 1**. It is possible that insufficient residence time of the depot system in the abdomen of humans requires multiple injections, once every two or three weeks. Of relevance in this context, that the release of chemotherapeutics from depot systems in the abdomen does not require the use of NPs, since chemotherapeutics due to their hydrophobic nature, enter cells by themselves. For IP gene-based therapy of PC, however, NPs are essential to deliver the desired cargo (e.g., DNA, siRNA) into tumors.

In the context of overcoming the rapid clearance of NPs from the peritoneal cavity, a novel strategy which involves the adhesion of NPs to the mesothelial cells in the peritoneal cavity has been recently described by Deng et al. [16]. The bioadhesive NPs loaded with a chemotherapeutic agent extend the residence in the abdomen and result in a significant tumor inhibition when compared to the NPs not owing bioadhesive properties or free drug. Such strategies require more detailed investigation, using different chemotherapeutics and also tumor models.

Another recent technique for the treatment of PC, introduced in **Chapter 1**, involves nebulization of chemotherapeutics under pressure in the peritoneal cavity – PIPAC. Pressurized Intraperitoneal Aerosol Chemotherapy (PIPAC) is not considered as post-operative technique as it is only performed in patients who have irresectable PC because of the advanced stage of the disease. Unlike the above-described depot systems, PIPAC is currently being used in several clinical centers for the treatment of PC patients and has shown initial promising results [17-19]. Moreover, prospective studies (NCT02604784, NCT02320448, NCT01854255) are ongoing to further assess the efficacy of PIPAC. As for now, chemotherapeutics are nebulized under constant abdominal pressure of 20 bar (12 mmHg), in order to enhance tissue (and tumor) penetration. Whether the same anti-tumor efficacy can be achieved by applying lower pressure is a topic for future investigation. Nebulization of nanomedicines under high pressure might lead to the destabilization of nanomedicines and limit their biological activity. The ability to obtain the same effect with pressure values less than 12 mmHg is likely to increase the probability of successful application of nanomedicines with PIPAC. This in turn will facilitate co-delivery of siRNA and conventional chemotherapeutics to overcome multi-drug resistance of peritoneal tumors [20, 21].

The strategies proposed above rely on targeting tumors using chemotherapeutics and/or nucleic acids, a process which requires direct interaction and penetration of the IP administered drug/nanomedicine into the tumor to exert anti-tumor activity. Other strategies, however, make use of NPs, but do not require direct exposure of the tumor to the NPs, such as cancer immunotherapy.

The last decade has witnessed significant progress in cancer immunotherapy [22]. Simply defined, **cancer immunotherapy,** is a treatment that uses parts of the body's immune system against cancer cells. This can be achieved in several ways; one is *via* the use of monoclonal antibodies as checkpoint inhibitors [23, 24]. Another approach is *in vivo* vaccination, targeting dendritic cells (DCs) [25, 26]. Adoptive T cell therapy [27] is another approach, which has proven useful in treatment of blood cancer. With respect to PC, immunotherapy, more specifically the *in vivo* vaccination, might possess some advantages over the conventional chemotherapeutics currently used in the clinic. First, immunotherapy exhibits reduced off-target side effects and prompts anti-tumor memory, preventing disease recurrence [28]. Furthermore, immune responses can be directed not only against neoplastic cells, but also metastases. The results in this thesis provide an evidence that NPs drain into lymphatic organs (such as the spleen) following IP administration. This builds a rationale for considering *in vivo* vaccination *via* the IP route as future nanomedicine-based treatment of PC, especially that such approach does not require prolonged residence time of the nanomedicines in the peritoneal cavity like in the case of nucleic-acids or chemotherapy-based IP therapy. On the contrary, the rapid clearance of nanomedicines from the peritoneal cavity would facilitate the below-described immunotherapeutic strategy.

A very common way to induce anti-tumor immunity is by the activation of (DCs) [29]. DCs function as mediators between the innate and adaptive immune system. The main role of DCs is to capture antigens and present them to T cells on molecules known as the major histocompatibility complexes (MHCs). The presented antigen is then recognized by $CD8^+$ or $CD4^+$ T cells, which in turn induce their proliferation and differentiation into cytotoxic T lymphocytes (CTLs) and helper T cells (Th), respectively. Both CTLs and Th cells play an important role in the immune response against different viruses and cancer cells. Of importance for cancer immunotherapy, tumors specifically express tumor-associated antigens (TAAs) that induce CTL responses [30]. DC-based vaccination is based on the modification of DCs to present TAAs to T cells leading to specific TAA CTL activation. A successful activation requires first loading of the TAAs on the DCs, and second turning the DCs from immature to mature. Worth mentioning in this respect, that mature and immature DCs exist in the lymph nodes, and tissues [31, 32] as well as in the blood, but can only be activated after their migration into the lymph nodes. NPs are being extensively investigated as carriers of antigenic materials towards DCs in the lymphatics or other tissues [33, 34]. Several research groups have recently demonstrated a strong antigen-specific T-cell responses against tumors following systemic administration of (m)RNA (as antigen) complexed with lipid NPs in mice [35, 36]. The NPs protect the (m)RNA from degradation by extracellular ribonucleases, facilitate the cellular uptake and subsequent expression of the encoded antigen by DCs. Consequently, the (m)RNA-NPs complexes induce the release of interferon-α by plasmacytoid DCs, in addition to DCs maturation, leading eventually to antigen-specific T cell responses [37, 38].

A comparable strategy which involves IP delivery of vaccine antigens using NPs into DCs may be an attractive post-operative (i.e. following surgical debulking) treatment for PC, in particular due to the clearance and biodistribution of NPs following IP administration as stated and reviewed in **Chapter 1**. Specifically, since it has been shown that NPs are mainly cleared from the peritoneal cavity via the lymphatics in the spleen and liver [3, 39], IP injection of NPs-antigen complexes is expected to result in a more potent antigen-specific T cell responses compared to the IV one as the lymphatics lead to the lymph nodes and spleen where a lot of DCs reside, which is a crucial factor for the potency of the immune response. There is no doubt that DC vaccine research for cancer immunotherapy is receiving a great deal of attention over the past few years, however, it has not been employed against tumors confined within organs in the peritoneal cavity. In this case also, a proof of concept of antigen-specific T cell responses followed by tumor growth inhibition is required as first step in mice before moving to trials in humans, due to the complexity of the immune system and the possibility of inducing immunosuppression [40].

In summary, the outcomes of this project did not provide a clear-cut answer whether the use of nanomedicines *via* the IP route of administration would improve the current post-surgical techniques used in clinical management of PC. Nevertheless, the findings of this project clearly demonstrate that IP administration of nanomedicine dispersions are rapidly cleared from the peritoneal cavity and are not suitable for prolonged and sustained release of anti-cancer agents in the abdomen.

Therefore, different tactics using nanomedicines such as the nebulization of NPs loaded with chemotherapeutics and/or nucleic acids and their release from depot systems in the abdomen, as well as, NPs for the delivery of antigens to DCs to tackle peritoneal tumors and metastases, are the next steps towards a firm assessment with regard to the use of nanomedicines for IP therapy of PC. In the near future, however, IP post-operative therapy of PC with (H)IPEC and catheter-based chemotherapy, as well as the application of PIPAC to nebulize chemotherapeutics in the IP cavity are expected to remain the most widely applied treatment strategies.

References:

[1] E. Kipps, D.S.P. Tan, S.B. Kaye, Meeting the challenge of ascites in ovarian cancer: new avenues for therapy and research, Nat Rev Cancer, 13 (2013) 273-282.
[2] A.A. Ayantunde, S.L. Parsons, Pattern and prognostic factors in patients with malignant ascites: a retrospective study, Ann Oncol, 18 (2007) 945-949.
[3] M. Tsai, Z. Lu, J. Wang, T.K. Yeh, M.G. Wientjes, J.L.S. Au, Effects of carrier on disposition and antitumor activity of intraperitoneal paclitaxel, Pharm Res, 24 (2007) 1691-1701.
[4] A.C. Society, Cancer Facts & Figures 2015, American Cancer Society, (2015).
[5] C. Hasovits, S. Clarke, Pharmacokinetics and Pharmacodynamics of Intraperitoneal Cancer Chemotherapeutics, Clin Pharmacokinet, 51 (2012) 203-224.
[6] F. Ramazani, C.F. van Nostrum, G. Storm, F. Kiessling, T. Lammers, W.E. Hennink, R.J. Kok, Locoregional cancer therapy using polymer-based drug depots, Drug Discov Today, 21 (2016) 640-647.
[7] J.B. Wolinsky, Y.L. Colson, M.W. Grinstaff, Local drug delivery strategies for cancer treatment: Gels, nanoparticles, polymeric films, rods, and wafers, J Control Release, 159 (2012) 14-26.
[8] F.J. Attenello, D. Mukherjee, G. Datoo, M.J. McGirt, E. Bohan, J.D. Weingart, A. Olivi, A. Quinones-Hinojosa, H. Brem, Use of Gliadel (BCNU) wafer in the surgical treatment of malignant glioma: A 10-year institutional experience, Ann Surg Oncol, 15 (2008) 2887-2893.
[9] K. De Clercq, C. Schelfhout, M. Bracke, O. De Wever, M. Van Bockstal, W. Ceelen, J.P. Remon, C. Vervaet, Genipin-crosslinked gelatin microspheres as a strategy to prevent postsurgical peritoneal adhesions: In vitro and in vivo characterization, Biomaterials, 96 (2016) 33-46.
[10] T. Liakakos, N. Thomakos, P.M. Fine, C. Dervenis, R.L. Young, Peritoneal adhesions: Etiology, pathophysiology, and clinical significance - Recent advances in prevention and management, Digest Surg, 18 (2001) 260-273.
[11] R.L. Dedrick, M.F. Flessner, Pharmacokinetic problems in peritoneal drug administration: Tissue penetration and surface exposure, J Natl Cancer I, 89 (1997) 480-487.
[12] B. Schnuriger, G. Barmparas, B.C. Branco, T. Lustenberger, K. Inaba, D. Demetriades, Prevention of postoperative peritoneal adhesions: a review of the literature, Am J Surg, 201 (2011) 111-121.
[13] E.J. Cho, B. Sun, K.O. Doh, E.M. Wilson, S. Torregrosa-Allen, B.D. Elzey, Y. Yeo, Intraperitoneal delivery of platinum with in-situ crosslinkable hyaluronic acid gel for local therapy of ovarian cancer, Biomaterials, 37 (2015) 312-319.
[14] B. Sun, M.S. Taha, B. Ramsey, S. Torregrosa-Allen, B.D. Elzey, Y. Yeo, Intraperitoneal chemotherapy of ovarian cancer by hydrogel depot of paclitaxel nanocrystals, J Control Release, 235 (2016) 91-98.
[15] S.X. Xu, H.X. Fan, L. Yin, J.H. Zhang, A.J. Dong, L.D. Deng, H. Tang, Thermosensitive hydrogel system assembled by PTX-loaded copolymer nanoparticles for sustained intraperitoneal chemotherapy of peritoneal carcinomatosis, Eur J Pharm Biopharm, 104 (2016) 251-259.
[16] Y. Deng, F. Yang, E. Cocco, E. Song, J.W. Zhang, J.J. Cui, M. Mohideen, S. Bellone, A.D. Santin, W.M. Saltzman, Improved i.p. drug delivery with bioadhesive nanoparticles, P Natl Acad Sci USA, 113 (2016) 11453-11458.
[17] C. Demtroder, W. Solass, J. Zieren, D. Strumberg, U. Giger-Pabst, M.A. Reymond, Pressurized intraperitoneal aerosol chemotherapy with oxaliplatin in colorectal peritoneal metastasis, Colorectal Dis, 18 (2016) 364-371.
[18] G. Nadiradze, U. Giger-Pabst, J. Zieren, D. Strumberg, W. Solass, M.A. Reymond, Pressurized Intraperitoneal Aerosol Chemotherapy (PIPAC) with Low-Dose Cisplatin and Doxorubicin in Gastric Peritoneal Metastasis, Journal of Gastrointestinal Surgery, 20 (2016) 367-373.
[19] W. Solass, R. Kerb, T. Murdter, U. Giger-Pabst, D. Strumberg, C. Tempfer, J. Zieren, M. Schwab, M.A. Reymond, Intraperitoneal Chemotherapy of Peritoneal Carcinomatosis Using Pressurized Aerosol as an Alternative to Liquid Solution: First Evidence for Efficacy, Ann Surg Oncol, 21 (2014) 553-559.
[20] M. Creixell, N.A. Peppas, Co-delivery of siRNA and therapeutic agents using nanocarriers to overcome cancer resistance, Nano Today, 7 (2012) 367-379.
[21] M. Saraswathy, S.Q. Gong, Recent developments in the co-delivery of siRNA and small molecule anticancer drugs for cancer treatment, Mater Today, 17 (2014) 298-306.
[22] C.G. Drake, E.J. Lipson, J.R. Brahmer, Breathing new life into immunotherapy: review of melanoma, lung and kidney cancer, Nat Rev Clin Oncol, 11 (2014) 24-37.
[23] C. Kyi, M.A. Postow, Checkpoint blocking antibodies in cancer immunotherapy, Febs Lett, 588 (2014) 368-376.
[24] D.M. Pardoll, The blockade of immune checkpoints in cancer immunotherapy, Nat Rev Cancer, 12 (2012) 252-264.
[25] K. Palucka, J. Banchereau, Cancer immunotherapy via dendritic cells, Nat Rev Cancer, 12 (2012) 265-277.
[26] E.J. Small, P.F. Schellhammer, C.S. Higano, C.H. Redfern, J.J. Nemunaitis, F.H. Valone, S.S. Verjee, L.A. Jones, R.M. Hershberg, Placebo-controlled phase III trial of immunologic therapy with sipuleucel-T (APC8015) in patients with metastatic, asymptomatic hormone refractory prostate cancer, J Clin Oncol, 24 (2006) 3089-3094.

[27] N.P. Restifo, M.E. Dudley, S.A. Rosenberg, Adoptive immunotherapy for cancer: harnessing the T cell response, Nat Rev Immunol, 12 (2012) 269-281.
[28] H.J. Braam, T.R. Van Oudheusden, I.H.J.T. De Hingh, S.W. Nienhuijs, D. Boerma, M.J. Wiezer, B. Van Ramshorst, Patterns of recurrence following complete cytoreductive surgery and hyperthermic intraperitoneal chemotherapy in patients with peritoneal carcinomatosis of colorectal cancer, J Surg Oncol, 109 (2014) 841-847.
[29] M. Merad, P. Sathe, J. Helft, J. Miller, A. Mortha, The Dendritic Cell Lineage: Ontogeny and Function of Dendritic Cells and Their Subsets in the Steady State and the Inflamed Setting, Annual Review of Immunology, Vol 31, 31 (2013) 563-604.
[30] P.G. Coulie, B.J. Van den Eynde, P. van der Bruggen, T. Boon, Tumour antigens recognized by T lymphocytes: at the core of cancer immunotherapy, Nat Rev Cancer, 14 (2014) 135-146.
[31] B. Malissen, S. Tamoutounour, S. Henri, The origins and functions of dendritic cells and macrophages in the skin, Nat Rev Immunol, 14 (2014) 417-428.
[32] M.M. Velasquez-Lopera, L.A. Correa, L.F. Garcia, Human spleen contains different subsets of dendritic cells and regulatory T lymphocytes, Clin Exp Immunol, 154 (2008) 107-114.
[33] B. Choi, H. Moon, S.J. Hong, C. Shin, Y. Do, S. Ryu, S. Kang, Effective Delivery of Antigen-Encapsulin Nanoparticle Fusions to Dendritic Cells Leads to Antigen-Specific Cytotoxic T Cell Activation and Tumor Rejection, ACS Nano, (2016).
[34] H. Dewitte, R. Verbeke, K. Breckpot, S.C. De Smedt, I. Lentacker, Nanoparticle design to induce tumor immunity and challenge the suppressive tumor microenvironment, Nano Today, 9 (2014) 743-758.
[35] K. Broos, K. Van der Jeught, J. Puttemans, C. Goyvaerts, C. Heirman, H. Dewitte, R. Verbeke, I. Lentacker, K. Thielemans, K. Breckpot, Particle-mediated Intravenous Delivery of Antigen mRNA Results in Strong Antigen-specific T-cell Responses Despite the Induction of Type I Interferon, Mol Ther Nucleic Acids, 5 (2016) e326.
[36] L.M. Kranz, M. Diken, H. Haas, S. Kreiter, C. Loquai, K.C. Reuter, M. Meng, D. Fritz, F. Vascotto, H. Hefesha, C. Grunwitz, M. Vormehr, Y. Husemann, A. Selmi, A.N. Kuhn, J. Buck, E. Derhovanessian, R. Rae, S. Attig, J. Diekmann, R.A. Jabulowsky, S. Heesch, J. Hassel, P. Langguth, S. Grabbe, C. Huber, O. Tureci, U. Sahin, Systemic RNA delivery to dendritic cells exploits antiviral defence for cancer immunotherapy, Nature, 534 (2016) 396.
[37] D.A. Mitchell, S.K. Nair, RNA-transfected dendritic cells in cancer immunotherapy, J Clin Invest, 106 (2000) 1065-1069.
[38] P. Ponsaerts, V.F.I. Van Tendeloo, Z.N. Berneman, Cancer immunotherapy using RNA-loaded dendritic cells, Clin Exp Immunol, 134 (2003) 378-384.
[39] K. Yang, H. Gong, X.Z. Shi, J.M. Wan, Y.J. Zhang, Z. Liu, In vivo biodistribution and toxicology of functionalized nano-graphene oxide in mice after oral and intraperitoneal administration, Biomaterials, 34 (2013) 2787-2795.
[40] G.A. Rabinovich, D. Gabrilovich, E.M. Sotomayor, Immunosuppressive strategies that are mediated by tumor cells, Annu Rev Immunol, 25 (2007) 267-296.

SUMMARY AND CONCLUSIONS

Primary cancer within organs in the peritoneal cavity metastasizes often leads peritoneal carcinomatosis (PC). Current clinical management of PC which is based on cytoreduction followed by IV administration of chemotherapeutics results in low survival rates of the treated patients. Several Local (IP) therapy strategies following CRS have already been under investigation for more than two decades. In spite of the progress made in IP therapy of PC, efficient IP post-operative techniques are utterly needed. In this context, the use of nanomedicines for IP therapy in general, and for siRNA-based treatment in particular, is still poorly understood. A better insight on the physico-chemical properties and cellular processes of nanomedicines loaded with siRNA following IP administration offer to open new avenues for gene therapy of PC and accelerate its translation to the clinic.

In **Chapter 1**, we provided a general introduction on the anatomy and role of the peritoneal membrane under normal conditions and upon formation of ascites fluid. Furthermore, we briefly explained the rationale behind developing local therapy for the treatment of PC. Importantly, the advantages and drawbacks of current IP techniques in the clinical management of PC, such as flushing the peritoneal cavity with a chemotherapeutic solution (i.e. (H)IPEC), as well as, nebulization of chemotherapeutics under high pressure in the abdomen known as PIPAC, are discussed. A major disadvantage of applying chemotherapeutics intraperitoneally is the rapid clearance from the peritoneal cavity to the systemic circulation, as well as, the lack of specificity and the resulting adverse effects. In the second part of Chapter 1, we focused on the biodistribution of nanomedicines following IP injection *in vivo*, emphasizing that IP injected nanomedicines dispersed in solution suffer from short residence time in the peritoneal cavity as they are rapidly cleared in the liver and spleen. We then proposed several strategies that may increase the residence time of nanomedicines in the peritoneal cavity, including: (1) the release of nanomedicines from depot systems such as hydrogles, (2) nebulization of nanomedicines in the abdomen under high peritoneal pressure (i.e. PIPAC of nanomedicines), (3) flushing the peritoneal cavity with nanomedicines (i.e. (H)IPEC of nanomedicines), and (4) continuous IP administration of nanomedicines at low doses known as metronomic chemotherapy. Finally, we shed the light on 2 ongoing clinical trials of nanomedicines that were administered via the IP route. Although both trials (phase I) showed an advantage of IP instilled nanomedicines over the IV administered nanomedicines, it is not clear whether a phase II clinical trial is planned. We concluded that in-depth investigation of the discussed strategies is needed in order to answer the question whether nanomedicines are suitable for the treatment of PC.

While in Chapter 1 the focus was on nanomedicines in general and those loaded with chemotherapeutics, in **Chapter 2,** we summarized the recent progress in non-viral nucleic acid delivery systems, especially of pDNA and siRNA, for the treatment of PC. We first defined the structure and role of pDNA and siRNA, their working mechanisms, and the need to carry them into the cells due to their negative charge and incapability to cross biological membranes. Subsequently, we described both the extracellular and intracellular barriers that nano-sized vehicles should overcome upon administration in the peritoneal cavity in order to downregulate (in the case of siRNA) or overexpress (in the case of pDNA) the desired gene. Then, we reviewed intraperitoneally administered nano-sized vehicles loaded with pDNA or siRNA for the treatment of PC *in vivo* in animal models. We concluded that nucleic acids when used as monotherapy is a promising strategy for the treatment of PC, however, optimal anti-tumor activity will be achieved when delivered with chemotherapeutics.

In **Chapter 3**, we evaluated the colloidal stability in terms of aggregation and cargo (i.e. siRNA) release of cationic, negatively charged and PEGylated (coated with PEG) NPs (namely PS NPs and liposomes) in diluted peritoneal fluid obtained from a healthy mice and undiluted ascites fluid obtained from a PC patient. We performed the same experiments in undiluted human serum which is used as an *in vitro* model for IV administration of NPs. To do so, we employed advanced microscopy techniques such as fluorescence correlation spectroscopy (FCS) and fluorescence single particle tracking (fSPT). Strong aggregation was observed for the cationic and anionic NPs, whereas PEGylation protected the NPs from aggregation in the peritoneal fluids. We concluded that PEGylation is necessary to protect the NPs from aggregation in the peritoneal fluids. When LPXs were prepared by electrostatic interactions between the negatively charged siRNA and the positively charged liposomes, PEGylation leads to a premature release of the siRNA. The release of siRNA is ascribed to the competition between the negatively charged siRNA and the negatively charged proteins in the ascites fluid on the binding to the positively charged liposomes. Therefore, we suggested that future studied should focus on different loading methods where the siRNA is protected within the aqueous core of the liposomes, and not exposed to the proteins in the biofluids.

While in Chapter 3 the colloidal stability of NPs in peritoneal fluids was evaluated, in **Chapter 4** both the gene knockdown efficiency and colloidal stability of cationic, decorated with C16 ceramide-PEG DOTAP DOPE liposomes, and the commercial reagent lipofectamine RNAiMAX (LF) siRNA LPXs in or following incubation in ascites fluid were investigated. In protein-free conditions, all the formulations efficiently decreased the expression of luciferase which is stably expressed on SKOV-3 cells, on the contrary to the situation where the LPXs were incubated for 1 h in ascites fluid and then added onto cells. In this case both the cationic and C16 Cer-PEG LPXs lost their ability to decrease the expression of luciferase, but not the LF-LPXs. We hypothesized that the decrease in knockdown efficiency following incubation in the ascites fluid compared with the protein-free conditions stems from poor colloidal stability of the cationic and C16 Cer-PEG LPXs in

ascites fluid. Surprisingly, fSPT experiments showed severe aggregation for the LF-LPXs following incubation in ascites fluid, whereas the C16 ceramide-PEG LPXs were more stable. Similarly, LF-LPXs exhibited the lowest complexation with siRNA in protein-free conditions as demonstrated by FCS experiments. Importantly, all the LPXs still retain a fraction of complexed siRNA following 1 h incubation in ascites fluid, confirming that the colloidal stability (i.e. aggregation and siRNA release) is not the reason for the significant drop in the transfection efficiency following incubation in ascites fluid.

Finally, all the LPXs exhibited high cellular uptake in protein-free conditions, but a significant decrease following incubation in the ascites fluid except for the LF-LPXs, where the cellular uptake was comparable to that in protein-free conditions. We concluded that aggregation is not the only determinant of the transfection efficiency *in vitro*. Broadly speaking, *in vitro* optimization of siRNA delivery systems should be performed in biological fluids that resemble the *in vivo* situation based on the desired route of administration. In the case of IV administration for example, *in vitro* assessment of siRNA delivery systems should be carried-out in human plasma or human serum. Such approach enables a safer transition from the *in vitro* to the *in vivo* situation and provides a better insight on parameters that are not possible to monitor in a lot of cases following *in vivo* administration, like cellular uptake, cargo release, and aggregation.

Next, as a follow-up to the data presented in Chapter 3 and Chapter 4 where siRNA LPXs were prepared by the formation of electrostatic interactions between the negatively charged siRNA and the positively charged liposomes, in **Chapter 5** we used the HYDRAtion method for loading siRNA on liposomes. In theory, hydration of the lipid film with a siRNA solution is supposed to result in an equal distribution of the siRNA over the liposomes – in the aqueous core and also on the surface. Additionally, on the level of PEGylation (i.e. coating the LPXs with PEG) we studied LPXs grafted with stable PEG residues (DSPE-PEG), and "sheddable" PEG chains (C8 and C16 Cer-PEG) that diffuse out the surface upon contact with the plasma membrane and hence, facilitate endosomal escape which is essential to obtain gene knockdown. On the one hand, the DSPE-PEG formulation was highly stable in terms of cargo release and aggregation, with 50% of the siRNA encapsulated in the aqueous core following 24 h of incubation in ascites fluid. In spite of its high stability and efficient cellular uptake in the ascites fluid, the DSPE-PEG formulation exhibited low gene knockdown, most likely due to poor intracellular processing. On the other hand, the cationic and Cer-PEG LPXs prepared with the HYDRAtion method successfully downregulated a specific gene in protein-free conditions, but lost their ability to be taken up by the human ovarian cancer SKOV-3 cells following incubation in human undiluted ascites fluid.

In **Chapter 6**, we intended to understand whether the inhibition of cellular uptake observed in Chapter 4 and Chapter 5 also occurs in other biofluids than the ascites fluid and for other lipid composition of the LPXs. To do so, we prepared siRNA LPXs composed from different molar ratios of the positively charged lipid DOTAP and the neutral helper lipid cholesterol (CHOL), namely

DOTAP CHOL 50:50 and DOTAP CHOL 20:80 LPXs. Subsequently, we studied the cellular uptake and gene knockdown efficiency of the DOTAP CHOL LPXs in Opti-MEM®, 10% and 50% fetal bovine serum (FBS), ascites fluid obtained from a PC patient, and human serum. In Opti-MEM® both LPXs were taken up by SKOV-3 cells and successfully downregulated the expression of luciferase. In FBS, however, the LPXs lost their ability to knockdown luciferase despite the efficient uptake. Consistently, no gene knockdown was observed following incubation of the LPXs in ascites fluid or human serum, due to the inhibition of cellular uptake in all cases except for DOTAP CHOL 50:50 LPXs following incubation in human serum.

To elucidate the reason behind the loss of cellular uptake, we carried-out siRNA release (by FCS) and aggregation (by fSPT) experiments of the DOTAP CHOL LPXs following incubation in ascites fluid, where both DOTAP CHOL 50:50 and DOTAP CHOL 20:80 LPXs are not taken up by SKOV-3 cells. The outcomes of the stability experiments demonstrated that the LPXs are colloidally stable in ascites fluid, and didn't provide any explanation for the loss of cellular uptake. Qualitative (by SDS-PAGE) and quantitative (by LC-MS) analysis revealed major differences in the type and amount of proteins bound to the LPXs (i.e. the protein corona) following incubation in FBS, ascites fluid and human serum, which in turn alters the interaction of the LPXs with the plasma membrane and also intracellularly, most likely with the endosomal compartment. Consequently, we deduced that using undiluted biological fluids and not FBS which is used by the majority of the scientists for *in vitro* optimization of siRNA delivery systems is crucial. Furthermore, the protein corona which is formed around LPXs following incubation in biofluids strongly influences the interaction of the LPXs extracellularly, as well as intracellularly and eventually their biological performance.

In **Chapter 7**, we tested the effect of the NPs' carrier solution on their residence time in the peritoneal cavity and also on their biodistribution following IP administration in mice. As mentioned in Chapter 1, NPs tend to be cleared mainly in the liver and spleen after IP injection. While the vast majority of the studies reviewed in Chapter 1 didn't pay attention to the NPs' carrier solution and administered the NPs in physiological isotonic solutions such as phosphate buffered saline (PBS), we investigated whether 200 nm PEGylated PS NPs dispersed in 7.5% icodextrin solution reside for a longer period in the abdomen when compared to other solutions and influence the clearance of the NPs from the peritoneal cavity to the systemic circulation. The 7.5% icodextrin solution is used in the clinic with patients undergoing peritoneal dialysis (PD) owing to its high abdominal retention. Indeed, the 7.5% icodextrin solution increased the residence time of the PS NPs and FITC-dextrans (FDs) in the peritoneal cavity to 4 h when compared to PBS where the injected solution was completely cleared 2 h following injection. On the level of biodistribution, however, no differences between the PBS and 7.5% icodextrin solution were observed, as the NPs accumulated in the liver and spleen 24 h following injection. Also, no aggregation of the FDs and PS NPs was documented 2 h and 4 h following IP injection. Moreover, clearance of FDs from the peritoneal cavity was independent of the Mw, as FDs that vary in Mw were simultaneously cleared

from the abdomen. In summary, NPs dispersed in icodextrin solution seem not to be a suitable strategy for prolonged delivery in the peritoneal cavity of mice.

In **Chapter 8**, we reflected on the outcomes of this project and highlighted several therapeutic strategies where nanomedicines could be exploited in IP therapy for PC. Yet, in-depth investigation of these approaches is required to ensure their successful translation into the clinic.

Conclusions

To conclude, we have established an *in vitro* model based on ascites fluid obtained from a PC patient to study the stability and biological activity of NPs in general and liposomal nano-sized siRNA formulations in particular. We demonstrated the significance of performing *in vitro* assessment of siRNA delivery systems in protein-rich biological fluids due to the influence of these proteins on the siRNA release, aggregation and importantly the cellular uptake and subsequent intracellular processing. We have also shown that the carrier solution of the NPs influences their residence time in the peritoneal cavity of mice following IP administration. Based on our findings, nanomedicines dispersed in solution is not a good strategy to achieve prolonged delivery of drugs in the peritoneal cavity for the treatment of PC following surgical debulking. Other strategies like sustained release of nanomedicines from depot systems, repeated nebulization of nanomedicines in the abdomen, as well as the use of nanomedicines for immunotherapy of peritoneal tumors should be further investigated in order to understand whether nanomedicines are the magic bullet for the treatment of PC.

Samenvatting en Conclusies

Primaire kanker in organen in de buikholte leiden na uitzaaiing vaak tot peritoneale metastasen (PC). De huidige klinische behandeling van PC is gebaseerd op cytoreductie, gevolgd door intraveneuze (IV) chemotherapie toediening. Dit resulteert echter in lage overleving van de behandelde patiënten. Diverse lokale intraperitoneale (IP) therapieën zijn in ontwikkeling die post-operatief kunnen worden toegepast. Een mogelijkheid is het gebruik van nanomedicijnen voor de lokale toediening van chemotherapeutica of small interfering RNA (siRNA). Om deze therapieën ooit via IP administratie te kunnen aanbieden, is het noodzakelijk een beter inzicht te verkrijgen in de fysicochemische eigenschappen en cellulaire processen van nanomedicijnen die leiden tot een efficiënte afgifte van siRNA. Momenteel is er echter weinig gekend welke barrières nanomedicijnen die geïnjecteerd worden in de buikholte moeten overwinnen om klinisch toepasbaar te zijn.

Hoofdstuk 1, beschrijft kort de algemene anatomie en functie van het peritoneale membraan onder normale omstandigheden en na vorming van ascitesvloeistof in patiënten met PC. Verder worden de beweegredenen achter de ontwikkeling van een lokale therapie voor de behandeling van PC toegelicht. De voor- en nadelen van de huidige IP technieken in de klinische behandeling van PC worden besproken, zoals het spoelen van de peritoneale holte met een chemotherapeutisch oplossing ((H)IPEC), evenals de verneveling van chemotherapeutica onder hoge druk in de buikholte (PIPAC). Een belangrijk nadeel van de lokale toediening van chemotherapeutica is de snelle klaring uit de buikholte naar de systemische circulatie, het gebrek aan doelgericht afdoden van de kankercellen en de resulterende neveneffecten. Het tweede deel van hoofdstuk 1 geeft een overzicht van de biodistributie van nanomedicijnen na IP-injectie in vivo, met nadruk op de korte verblijftijd in de buikholte en de snelle klaring door de lever en de milt. Vervolgens stellen we een aantal strategieën voor om de verblijftijd van nanomedicijnen in de buikholte te kunnen verhogen, waaronder: (1) het vrijkomen van nanomedicijnen uit depot systemen zoals hydrogels, (2) verneveling van nanomedicijnen in de buik onder hoge peritoneale druk (dwz PIPAC van nanomedicijnen), (3) het spoelen van de buikholte met nanomedicijnen (dwz (H)IPEC van nanomedicijnen), en (4) constante IP toediening van een lage dosis van nanomedicijnen (metronomische chemotherapie). Tot slot bespreken we 2 lopende klinische proeven van nanomedicijnen die via de IP-route werden toegediend. Hoewel beide proeven (fase I) een voordeel aantonen van IP geïnjecteerde nanomedicijnen ten opzicht van IV toegediende nanomedicijnen, is het niet duidelijk of een fase II klinische studie wordt gepland. We concludeerden dat verder onderzoek momenteel noodzakelijk is om te evalueren of nanomedicijnen geschikt zijn om PC te behandelen na lokale IP toediening.

Terwijl in hoofdstuk 1 de focus lag op nanogeneesmiddelen in het algemeen en deze geladen met chemotherapeutica, vatten we in **hoofdstuk 2** de recente vooruitgang samen voor niet-virale nucleïnezuur afgiftesystemen, voor de toediening van plasmide DNA (pDNA) en siRNA voor de behandeling van PC. De structuur en de rol van pDNA en siRNA, hun werkingsmechanisme, en de noodzaak om door biologische celmembranen te migreren om het intracellulair milieu te bereiken, werden besproken. Vervolgens werden de extracellulaire en intracellulaire barrières opgelijst, die niet-virale nucleïnezuur afgiftesystemen moeten overwinnen om na toediening in de buikholte te leiden tot downregulatie van proteïne expressie (bij siRNA) of overexpressie van proteïnen (in het geval van pDNA). Tenslotte werden de niet-virale nucleïnezuur afgiftesystemen met pDNA of siRNA opgelijst, die reeds getest worden voor de behandeling van PC in vivo in diermodellen. We concludeerden dat de lokale toediening van nucleïnezuren een veelbelovende strategie is voor de behandeling van PC, en dat optimale anti-tumor activiteit kan worden bereikt indien deze nucleïnezuren samen worden toegediend met chemotherapeutica.

In **hoofdstuk 3** evalueerden we de colloïdale stabiliteit van nanopartikels (NPs) waarbij we de aggregatie van de NPs en de vrijgave van siRNA uit kationische, negatief geladen en gePEGyleerde (gecoat met polyethyleenglycol (PEG)) NPs opvolgden in verdund peritoneale vloeistof verkregen uit gezonde muizen en in onverdund ascitesvloeistof verkregen van een PC patiënt. Onverdund humaan serum werd gebruikt als een in vitro model voor de IV toediening van NPs. We maakten gebruik van geavanceerde microscopische technieken zoals fluorescentie correlatie spectroscopie (FCS) en fluorescentie single particle tracking (fSPT). Sterke aggregatie werd waargenomen voor de kationische en anionische NPs, terwijl PEGylatie de NPs beschermde tegen aggregatie in de peritoneale vloeistoffen. PEGylatie lijkt dus noodzakelijk om stabiele partikels te bekomen. Wanneer echter lipide nanopartikels (LPXs) werden bereid door middel van elektrostatische interactie met negatief geladen siRNA, leidde PEGylatie tot de voortijdige afgifte van het siRNA. Vermoedelijk treedt er concurrentie op tussen het negatief geladen siRNA en de negatief geladen eiwitten aanwezig in de ascites vloeistof, voor binding aan het positief geladen liposomen. We concludeerden dat methoden die ervoor zorgen dat het siRNA geëncapsuleerd zit in de binnenzijde van de liposomen en niet electrostatisch gebonden blijft aan het oppervlak van de liposomen, deze blootstelling aan de eiwitten in de biologische vloeistoffen zou kunnen vermijden.

Terwijl in hoofdstuk 3 de colloïdale stabiliteit van NPs in peritoneale vloeistoffen werd geëvalueerd, werd in **hoofdstuk 4** zowel de downregulatie efficiëntie en de colloïdale stabiliteit nagegaan van liposomen aangemaakt met kationische DOTAP DOPE lipiden, gedecoreerd met C16 ceramide-PEG of het commerciële reagens lipofectamine RNAiMAX (LF). In eiwitvrije omstandigheden waren alle formulaties doeltreffend om de expressie van luciferase te onderdrukken in SKOV-3 cellen. Wanneer de LPXs gedurende 1 uur in ascitesvloeistof werden geïncubeerd en vervolgens werden toegevoegd aan cellen, verloren zowel kationische als C16 gePEGyleerde LPXs hun vermogen om de expressie van luciferase te verminderen. Enkel LF-LPXs bleven biologisch actief. We vermoedden dat de afname van knock-down efficiëntie na incubatie in de ascitesvloeistof het

gevolg was van een slechte colloïdale stabiliteit van de kationische en C16 PEG-Cer LPXs in ascitesvloeistof. FSPT experimenten toonden echter aan dat voornamelijk de LF-LPXs ernstige aggregatie vertoonden in ascites vloeistof, terwijl de C16 ceramide-PEG LPXs stabieler waren. Ook de complexatie met siRNA bleek lager voor LF-LPXs, zoals aangetoond door FCS experimenten, al behouden alle onderzochte LPXs nog steeds een fractie van het gecomplexeerde siRNA na 1 uur incubatie in ascitesvloeistof. We stelden dus vast, dat de colloïdale stabiliteit (d.w.z. aggregatie en siRNA afgifte) niet de voornaamste oorzaak was van een scherpe daling van de transfectie-efficiëntie na incubatie in ascitesvloeistof. De cellulaire opname van de LPXs bleek echter wel een belangrijke factor te zijn om goede downregulatie te verkrijgen. Alle LPXs vertoonden een hoge cellulaire opname in eiwitvrije omstandigheden, maar een significante daling na incubatie in de ascitesvloeistof met als uitzondering de LF-LPXs, waarbij de cellulaire opname vergelijkbaar was met die in eiwitvrije omstandigheden.

We concludeerden dat de in vitro optimalisatie van siRNA afgiftesystemen best wordt uitgevoerd in biologische vloeistoffen die de in vivo situatie van de gewenste toedieningsroute reflecteren. Bij intraveneuze toediening, bijvoorbeeld, moeten siRNA afleveringssystemen in vitro in humane plasma- of serum condities worden getest. Zo'n aanpak heeft een grotere kans van slagen om de overgang te maken van de in vitro naar de in vivo situatie en geeft ons een beter inzicht in de parameters die bij in vivo toediening mogelijks worden aangetast, zoals de cellulaire opname, de vrijgave van siRNA en aggregatie.

In hoofdstuk 3 en hoofdstuk 4 werden siRNA LPXs bereid door de vorming van elektrostatische interacties tussen de negatief geladen siRNA en de positief geladen liposomen. In **hoofdstuk 5** gebruikten we de hydratatie methode voor het opladen van siRNA in de liposomen. In theorie leidt de hydratatie van de lipide film met een siRNA oplossing tot een gelijke verdeling van de siRNA moleculen in de waterige kern en op het oppervlak van de liposomen. We bestudeerden bovendien verschillende PEGylatie methoden, gebruik makende van stabiele PEG lipiden (DSPE-PEG) en "transiënte" PEGylatie (C8 en C16 Cer-PEG), waarbij de PEG-ketens uit het oppervlak van de liposomen kunnen diffunderen, wat de endosomale vrijgave van het siRNA zou bevordenen als essentiële stap om gen knockdown te verkrijgen. De DSPE-PEG formulering was zeer stabiel qua siRNA encapsulatie en aggregatie, met 50% van het siRNA nog steeds ingekapseld in de waterige kern na 24 uur incubatie in ascitesvloeistof. Ondanks zijn hoge stabiliteit en efficiënte cellulaire opname in de ascitesvloeistof, vertoonde de DSPE-PEG formulatie echter een lage gen knockdown, waarschijnlijk als gevolg van slecht intracellulair transport en gebrek aan endosomale vrijgave. De kationische en Cer-PEG LPXs bereid met de hydratatie werkwijze waren succesvol om het reporter luciferase gen in SKOV-3 cellen te onderdrukken in eiwitvrije omstandigheden, maar verloren hun onderdrukkend vermogen na incubatie in humaan onverdund ascitesvloeistof. De beoogde verbetering in transfectie efficiëntie met de alternatieve siRNA encapsulatie en de transiënte PEGylatie werd dus niet bekomen.

In **hoofdstuk 6** werd dieper ingegaan op mogelijke redenen waarom eiwitrijke omstandigheden de transfectie efficiëntie of cellulaire opname van LPXs kunnen afremmen. Bovendien werd een nieuwe lipide samenstelling geëvalueerd, omwille van de positieve effecten die worden toegeschreven aan cholesterol om NPs te stabiliseren. siRNA LPXs werden bereid uit verschillende molaire verhoudingen van het positief geladen lipide DOTAP en het neutrale helperlipide cholesterol (CHOL), namelijk DOTAP CHOL 50:50 en 20:80. Vervolgens hebben we de cellulaire opname en gen knockdown efficiëntie vergeleken van de DOTAP CHOL LPXs in Opti-MEM®, 10% en 50% foetaal runder serum (FBS), ascitesvloeistof verkregen van een PC patiënt en humaan serum. In Opti-MEM® werden beide LPXs door SKOV-3 cellen opgenomen en werd de expressie van luciferase succesvol gedownreguleerd. In FBS echter, verloren de LPXs hun vermogen om luciferase te onderdrukken ondanks de efficiënte opname. Tenslotte werd er ook geen gen knockdown waargenomen na incubatie van de LPXs in ascitesvloeistof of menselijk serum, wegens de inhibitie van de cellulaire opname van alle LPXs, behalve DOTAP CHOL 50:50 LPXs na incubatie in menselijk serum.

Om de reden achter het verlies van cellulaire opname op te helderen, voerden we siRNA afgifte (FCS) en aggregatie (door FSPT) experimenten uit met de DOTAP CHOL LPXs na incubatie in ascitesvloeistof. De LPXs bleken echter colloïdaal stabiel in ascitesvloeistof, en gaven dus geen verklaring voor het verlies van cellulaire opname. Kwalitatieve (met SDS-PAGE) en kwantitatieve (met LC-MS) analyse toonde echter wel grote verschillen aan in het type en de hoeveelheid eiwitten gebonden aan de LPXs (~de eiwit corona) na incubatie in FBS, ascitesvloeistof en humaan serum. De eiwit corona die aan het oppervlak van de LPXs bindt, wijzigt vermoedelijk de interactie van de LPXs met de plasmamembraan en/of de interactie van de LPXs op intracellulair niveau, zoals bijvoorbeeld ter hoogte van de endosomale membraan. We concludeerden bijgevolg dat het gebruik van onverdunde biologische vloeistoffen en niet FBS, cruciaal is indien we siRNA afleveringssystemen in vitro wensen te optimaliseren. Bovendien heeft de eiwit-corona die wordt gevormd rond de LPXs na incubatie in biologische vloeistoffen een grote invloed op de interactie van de LPXs met extracellulaire en intracellulaire membranen en bijgevolg de uiteindelijke biologische efficiëntie.

In **hoofdstuk 7**, tenslotte werd het effect van de injectievloeistof voor de IP injectie van NPs getest op hun verblijftijd in de peritoneale holte en op hun biodistributie na intraperitoneale toediening bij muizen. Zoals vermeld in hoofdstuk 1, hebben NPs de neiging om snel te worden geklaard door de lever en de milt na IP-injectie. Terwijl de overgrote meerderheid van de studies besproken in hoofdstuk 1 geen aandacht besteedt aan de injectieoplossing waarin de NPS zich bevinden, onderzochten we of 200 nm gePEGyleerde polystyreen (PS) NPs geïnjecteerd in 7.5 % icodextrine oplossing een langere verblijftijd hadden in de IP holte in vergelijking met de vaak gebruikte fysiologische oplossingen zoals phosphate buffered saline (PBS). De 7,5% icodextrine oplossing wordt immers klinische toegepast bij patiënten die peritoneale dialyse (PD) ondergaag, vanwege zijn hoge retentie tijd in de buikholte. We stelden vast dat de 7,5% icodextrine oplossing

de verblijftijd van de PS NPs en FITC-dextranen (FDs) in de peritoneale holte verhoogde tot 4 uur na injectie, in vergelijking met 2 uur indien PBS als injectie oplossing werd gebruikt. De biodistributie bleek echter weinig te verschillen tussen injecties uitgevoerd met PBS en 7,5% icodextrine, aangezien NPs steeds voornamelijk in de lever en de milt accumuleerden 24 uur na injectie. Tenslotte konden we waarnemen dat er geen aggregatie optrad van FDs en PS NPs 2 uur en 4 uur na IP-injectie en dat klaring van FDs uit de buikholte onafhankelijk was van het moleculair gewicht van de FDs. Samengevat kunnen we stellen dat NPs gedispergeerd in icodextrine oplossing een iets langere verblijftijd vertonen in de buikholte, maar nog niet in die mate dat een langdurige verblijftijd van NPs in de peritoneale holte van muizen werd geobserveerd.

In **hoofdstuk 8** belichten we verschillende therapeutische strategieën waarbij nanomedicijnen zouden kunnen worden benut in IP-therapie voor PC. We geven een persoonlijke visie op welke aanpak (na diepgaand onderzoek) mogelijks potentiëel heeft om succesvol vertaald te worden in de kliniek.

Conclusies

Concluderend kunnen we stellen dat we een in vitro model hebben ontwikkeld om op basis van ascitesvloeistof (van een PC patiënt) de stabiliteit en biologische activiteit van NPs te bestuderen in het algemeen en van liposomale siRNA formulaties in het bijzonder. We toonden het belang aan van het uitvoeren van in vitro evaluaties van siRNA afgiftesystemen in eiwitrijke biologische vloeistoffen, aangezien de aanwezige eiwitten een belangrijke invloed kunnen hebben op de siRNA afgifte, NP aggregatie en vooral de cellulaire opname en het intracellulair gedrag van de NPs. We hebben ook aangetoond dat de injectie oplossing de verblijftijd van NPs in de peritoneale holte kan beïnvloeden na intraperitoneale toediening in muizen. Op basis van onze bevindingen lijkt het momenteel niet mogelijk om de langdurige verblijftijd van nanomedicijnen te verkrijgen na injectie van deze NPs in oplossing in de peritoneale holte voor de behandeling van PC na chirurgische debulking. Andere strategieën zoals de gecontroleerde vrijgave van nanomedicijnen vanuit depot systemen, de herhaalde verneveling van nanomedicijnen in de buikholte, en het gebruik van nanomedicijnen voor immunotherapie van peritoneale tumoren moeten verder worden onderzocht om te begrijpen of nanomedicijnen een belangrijke rol kunnen spelen bij de behandeling van PC in de nabije toekomst.

CURRICULUM VITAE

Personalia

Last name	Dakwar
First name	George
Nationality	Israeli
Date of birth	March 17th 1987
Place of birth	Nazareth
Private address	Muilaardstraat 72, 9000 Ghent, Belgium
Private telephone	+32 468 15 38 72
Professional address	Laboratory for General Biochemistry and Physical Pharmacy, Faculty of Pharmaceutical Sciences, Ghent University, Ottergemsesteenweg 460, 9000 Ghent, Belgium
Professional telephone	+32 9 264 80 74
E-mail	George.Dakwar@ugent.be/george.dakwar@gmail.com
Websites	https://www.researchgate.net/profile/George_Dakwar http://www.biofys.ugent.be

Education

10/2012 – 10/2016: PhD candidate Ghent Research Group on Nanomedicines, Faculty of Pharmaceutical Sciences, Ghent University, Ghent, Belgium.

10/2010 – 09/2012: Master of Medical Sciences Clinical Pharmacology Department, Ben-Gurion University of the Negev, Beer-Sheva, Israel.

10/2006 – 01/2010: Bachelor of Science in Chemistry and Life Sciences Hebrew University Jerusalem, Jerusalem, Israel.

International peer-reviewed publications

Research articles:

[1] **G.R. Dakwar**, Kevin Braeckmans, Wim Ceelen, Stefaan C. De Smedt, Katrien Remaut Exploring the HYDRAtion method for loading siRNA on liposomes: The interplay between stability and biological activity in human undiluted ascites fluid Drug Delivery and Translational Research (2016).

[2] B. Colzani, G. Speranza, R. Dorati, B. Conti, T. Modena, G. Bruni, E. Zagato, L. Vermeulen, **G.R. Dakwar**, K. Braeckmans, I. Genta, Design of smart GE11-PLGA/PEG-PLGA blend nanoparticulate platforms for parenteral administration of hydrophilic macromolecular drugs: synthesis, preparation and in vitro/ex vivo characterization, Int J Pharm, (2016).

[3] **G.R. Dakwar**, M. Shariati, W. Willaert, W. Ceelen, S.C. De Smedt, K. Remaut, Nanomedicine-based intraperitoneal therapy for the treatment of peritoneal carcinomatosis - Mission possible?, Adv Drug Deliv Rev, (2016).

[4] T. Furst, **G.R. Dakwar**, E. Zagato, A. Lechanteur, K. Remaut, B. Evrard, K. Braeckmans, G. Piel, Freeze-dried mucoadhesive polymeric system containing pegylated lipoplexes: Towards a vaginal sustained released system for siRNA, J Control Release, 236 (2016) 68-78.

[5] R.S. Santos, **G.R. Dakwar**, R.H. Xiong, K. Forier, K. Remaut, S. Stremersch, N. Guimaraes, S. Fontenete, J. Wengel, M. Leite, C. Figueiredo, S.C. De Smedt, K. Braeckmans, N.F. Azevedo, Effect of Native Gastric Mucus on in vivo Hybridization Therapies Directed at Helicobacter pylori, Mol Ther-Nucl Acids, 4 (2015).

[6] **G.R. Dakwar**, K. Braeckmans, J. Demeester, W. Ceelen, S.C. De Smedt, K. Remaut, Disregarded Effect of Biological Fluids in siRNA Delivery: Human Ascites Fluid Severely Restricts Cellular Uptake of Nanoparticles, Acs Appl Mater Inter, 7 (2015) 24322-24329.

[7] L. Novo, K.M. Takeda, T. Petteta, **G.R. Dakwar**, J.B. van den Dikkenberg, K. Remaut, K. Braeckmans, C.F. van Nostrum, E. Mastrobattista, W.E. Hennink, Targeted Decationized Polyplexes for siRNA Delivery, Mol Pharmaceut, 12 (2015) 150-161.

[8] L. Novo, L.Y. Rizzo, S.K. Golombek, **G.R. Dakwar**, B. Lou, K. Remaut, E. Mastrobattista, C.F. van Nostrum, W. Jahnen-Dechent, F. Kiessling, K. Braeckmans, T. Lammers, W.E. Hennink, Decationized polyplexes as stable and safe carrier systems for improved biodistribution in systemic gene therapy, J Control Release, 195 (2014) 162-175.

[9] **G.R. Dakwar**, E. Zagato, J. Delanghe, S. Hobel, A. Aigner, H. Denys, K. Braeckmans, W. Ceelen, F.C. De Smedt, K. Remaut, Colloidal stability of nano-sized particles in the peritoneal fluid: Towards optimizing drug delivery systems for intraperitoneal therapy, Acta Biomater, 10 (2014) 2965-2975.

[10] Y. Aizner, O. Sharabi, J. Shirian, **G.R. Dakwar**, M. Risman, O. Avraham, J. Shifman, Mapping of the Binding Landscape for a Picomolar Protein-Protein Complex through Computation and Experiment, Structure, 22 (2014) 636-645.

[11] L. Philosof-Mazor*****, **G.R. Dakwar***, M. Popov, S. Kolusheva, A. Shames, C. Linder, S. Greenberg, E. Heldman, D. Stepensky, R. Jelinek, Bolaamphiphilic vesicles encapsulating iron oxide nanoparticles: New vehicles for magnetically targeted drug delivery, Int J Pharmaceut, 450 (2013) 241-249. *** Both authors equally contributed to the manuscript.**

[12] **G.R. Dakwar**, V. Kaplun, L. Kojukarov, P. Gorenbein, I. Schumacher, D. Kontorovich, C. Forster, E. Beit-Yannai, D. Stepensky, Toxicity assessment of extracts from infusion sets in cEND brain endothelial cells, Int J Pharmaceut, 434 (2012) 20-27.

[13] **G.R. Dakwar**, I. Abu Hammad, M. Popov, C. Linder, S. Grinberg, E. Heldman, D. Stepensky, Delivery of proteins to the brain by bolaamphiphilic nano-sized vesicles, J Control Release, 160 (2012) 315-321.

Book chapter:

G.R. Dakwar, S.C. De Smedt, K. Remaut, Intraperitoneal nonviral nucleic acid delivery in the treatment of peritoneal cancer, Intraperitoneal Cancer Therapy, CRC Press 2015, pp. 359-371.

National and international conferences with oral presentation

Dakwar GR., The Disregarded Effect of Biological Fluids in siRNA Delivery: Human Ascites Fluid Severely Restricts Uptake of Nanoparticles. The Belgian-Dutch Biopharmacy Day, University of Leuven, Leuven, Belgium, Nov. 23rd, 2015.

Dakwar GR., Remaut K., Demeester J., De Smedt S., Braeckmans K. Advanced microscopy techniques to study the stability of nanoparticles in undiluted biological fluids. 1st COMPACT face to face meeting, GlaxoSmithKline (GSK), Stevenage, United Kingdom, Feb. 11-12, 2014.

Dakwar GR., Zagato E., Linder C., Delanghe J., Hobel S., Aigner A., Denys H., Braeckmans K., Ceelen W., De Smedt S., Remaut K. Stability of Colloidal Nano-Sized Systems In The Peritoneal Fluid: Towards Optimizing Drug Delivery Systems For Intraperitoneal Therapy. The 17th Forum organized by the Belgian Society of Pharmaceutical Sciences. SPA, Belgium, Oct. 17-18, 2013.

Dakwar GR. Brain delivery of proteins using bolaamphiphilic nano-sized vesicles: mechanisms and efficiency. The 8th Annual Meeting of the Israeli Chapter of the Controlled Release Society, Maalot-Tarshiha, Israel, Sep. 5, 2012.

Dakwar GR. Delivery of proteins to the brain using bolaamphiphilic nano-sized vesicles. Seminar at MERCK research laboratories – RNA therapeutics, delivery biology, Sumneytown Pike, West Point, PA,USA, Oct. 20, 2011.

National and international conferences with poster presentation

Dakwar GR., Ghazaryan A., Verbeke R., Braeckmans K., Ceelen W., Mailänder V., De Smedt S., Remaut K. Protein Corona of fetal bovine serum and undiluted biological fluids alters the interaction of siRNA lipoplexes with biological membranes extracellularly and intracellularly. The 14th European Symposium on Controlled Drug Delivery. Apr. 13-15, 2016.

Dakwar GR., Zagato E., Linder C., Delanghe J., Hobel S., Aigner A., Denys H., Braeckmans K., Ceelen W., De Smedt S., Remaut K. Stability of Colloidal Nano-Sized Systems In The Peritoneal Fluid: Towards Optimizing Drug Delivery Systems For Intraperitoneal Therapy. The 2nd NanoFar Autumn School . University of Santiago De Compostella, Santiago De Compostella, Spain, Oct. 21-25, 2013.

Dakwar GR., Braeckmans K., Ceelen W., De Smedt S., Remaut K. siRNA Delivery for the Treatment of Ovarian Cancer: In vitro Optimization of liposomes in SKOV-3 Ovarian Cancer Cell line. The 9th International Conference on Peritoneal Surface Malignancies. NH Grand Hotel Krasnapolsky, Amsterdam, Netherlands, Oct. 9-11, 2014.

Dakwar GR., Braeckmans K., Ceelen W., De Smedt S., Remaut K. Intraperitoneal Lipid-Based siRNA Delivery: The PEG Dilemma. The 13th European Symposium on Controlled Drug Delivery. Apr. 16-18, 2014.

Teaching activities

Teaching assistant in Organic Chemistry for Medical students, Ben-Gurion University of the Negev, Faculty of Health Sciences from 10/2011 till 06/2012.

Scholarships and awards

08/2012 Scholarship for the academic year 2012-2013 granted by the Flemish Community of Belgium.

07/2013 Scholarship for the academic year 2013-2014 granted by the Flemish Community of Belgium.

05/2012 Excellence in biomedical research award granted by the Faculty of Health Sciences, Ben-Gurion University of the Negev. Amount: $2625

Specialist courses

FeLaSa class C degree in laboratory animal science from the Faculty of Veterinary Medicine, March 2014, Ghent University, Belgium.

ACKNOWLEDGEMENTS

First and foremost I would like to express my special appreciation to my advisor **Katrien Remaut,** thanks for the supervision, input, and patience at the moments when I was too excited and impatient about doing something. In my opinion, this work was successful thanks to the communication we had throughout the last 4 years. You gave me the flexibility to develop ideas, plan and execute experiments towards reaching our goals, but in the same time you always made very good suggestions that were very useful to sharpen the ideas and conclusions drawn from the performed experiments, as well as to position them in a broader context within the frame of our research question. Moreover, I appreciate the trust you gave me in establishing new collaborations and make steps forward in the project. I think that we were a very good team.

Katrien, in 2012 when I started my PhD you served as post-doctoral researcher, now you are a professor, teaching, supervising PhD students and also a mom of two cute boys. I am convinced that this combination is not easy at all, keeping you up late at nights. I am genuinely happy that you are moving up in your field and wish you a lot of success in the future.

Stefaan, many thanks for giving me the opportunity to be part of this excellent research group. I still remember the first time we met in February 2012 during the interview as if it was yesterday when you told me: "We are looking for serious people" and then I had doubts for several months if I am serious enough to start a PhD or not. I would like to express my gratitude for the scientific supervision, suggestions and deep discussions we had on my project. I always enjoyed discussing scientific matters with you. The most important thing I learned from our discussions is that a lot concepts and ideas start from imagination, and that good science is not necessarily limited to what is possible to do at a certain situation. I have no doubts that you will keep leading the group towards excellence in research.

Wim, without your help major parts of this work would not have been possible. I am thankful for discussions, critical questions, support with the ethical committee and the access you provided to your laboratory in order to perform animal experiments. Overall, your contribution to my PhD project made it more coherent, updated with the latest clinical developments, and relevant to a large audience of scientists and also clinicians. So again many thanks!

Kevin, we collaborated successfully on many levels. After every meeting we had you used to say: "well, this was an efficient meeting". I really enjoyed working with you within the frame of the European project but also on all other occasions. You are a smart and ambitious researcher and I think that some more "ERC-like" grants are on their way! Thanks for the corrections of my research articles, suggestions, and for guiding me through the first steps in fSPT.

Jo, your effort to make sure that "everything is fine" with me during my first weeks in Belgium is much appreciated. You always made sure to speak in Dutch with me so that I practice and this was very important for me.

I would like to thank all the PhD students, Post-doctoral fellows and staff members I worked with since October 2012 at the Ghent Research Group on Nanomedicines.

In every laboratory there is a person who knows everything and without him it is impossible. **Bart,** I would like to thank you for sparing no effort to ensure that we got all the materials, equipment and conditions to perform our research. The fact that you are a very social and kind person gave always the impression that you are much more than a colleague at work, but a very good friend. **Hilde,** thanks for being so kind open and social. Together with Bart you make a great team that facilitate the work in our laboratory and make it more organized ☺

Koen Raemdonck, congratulations with the new academic position, I am sure that you will keep doing high-quality research! **Ine Lentacker,** the door of your office was always open to ask questions and you are always willing to help ☺

Toon the "IT-GOD", you joined the group one and a half years ago, but to me it feels like you have been there from the beginning of my PhD. You got very rapidly integrated in the group because you are so friendly, social and open to others. Thanks for making our day-to-day research life easier. I will never forget your help to arrange the projector at the faculty room 20 minutes before the beginning of my internal PhD defense…

Hendrik Deschout, thanks for the help with fSPT, I used the tips you gave me until the end of my PhD. I enjoyed discussing politics with you. **Ine De Cock,** we were office buddies for more than 3 years, we shared good moments and frustrations, I hope that you are enjoying your time in Seattle and I am sure that you are having a successful post-doctoral experience. **Ranhua,** my office buddy since I started my PhD and until now – you helped me a lot with everything I asked for, starting from science to IT problems and other things. You are a very intelligent, wise and hard working person – I am convinced that a very successful academic career is waiting for you. Keep going and up to the next Nature publication ☺. **Oliwia,** you used to wait for the moments when I was very serious and then to tell a joke or something funny – I liked that ☺

Rein, you are a very nice office buddy and frankly I like to hear you speaking in Dutch on the phone simply because I can't get 90% of the words, so for me in one way or another it is a challenge! I am glad that I got to know you better during our stay in Mainz! I greatly appreciate your kind and encouraging words during the last months while I was writing my PhD ☺

I thought that I am a very social and friendly person until I met you **Karen.** You are a great person and friend. I like the fact that you are always willing to accept other people, and your

curiosity to explore and respect other cultures. I appreciate your will to volunteer and contribute for building a better society. I wish you all the best from the bottom of my heart!

Freya, the more we talked, the more I realized what a good and open person you are. I wish you all the best with writing and defending your PhD thesis, as well as in your future career! **Elisa,** what I really like about you is that you express what is on your mind loudly and you sing it! **Thomas,** thanks for being there whenever I needed help and by the way I missed a lot the " spreekwoord van de dag" translated into English ☺. **Katrien Forier,** I hope that my explanation of the problems in the middle east was not complicated and I miss "Friday haha". **Koen Rombouts,** you always did things till the end, and when you used to party you did it till the very end – cheers ☺. **Stephan,** very ambitious, devoted and hardworking friend! Over the past 4 years we met a lot on weekends at work, at the beginning we were surprised but then we both understood that we are going in the same way and we did it! I am sure that you will have a very successful post-doctoral experience and career! Oh wait, I owe you an apology – I didn't mean to scare you while driving in Scotland! **Eline,** I guess that our first meeting was very long and stressful for you but you got your IWT because you are a very smart person and you deserve it. I assume that I am forgiven ☺. I have to say that you are working with a lot of passion, long days and nights – just make sure you keep some energy for the next two years ☺. Thanks a million for the help with cover of this book ☺ **Lotte,** we went on 3 conferences together (enjoyed COMPACT meetings together ☺) and during this time I got to know you much better. Specially, I enjoyed our discussions in Dresden. **Joke,** I seriously think that you are talented in many ways. Your PhD project is progressing very well and I am looking forward to your PhD defense!

Heleen, Lynn, when I started my PhD both of you were already with a lot of experience. I always felt very welcome to come in your office to ask questions or to report on a problem, I always got an answer and I am very grateful for that ☺. Thanks for making sure that a lot of things are in order and proper before and nowadays! **Laura,** first I wish you all the best with your new career ! Thanks for being there to listen especially during your last year in the group. What I really like about you is that you can't stand injustice and would immediately talk about it without any fear and frankly! **PieterJan,** already from the first weeks in the office I realized that you are a very serious, wise and dedicated person. I am impressed by your knowledge on different topics we discussed! I am sure that you are going to make the best out of your PhD! Many thanks for correcting texts that I wrote in Dutch ☺. **Silke,** I am curious to know what will happen with the aggregates (sorry I mean the spheroids) at the end ☺. **Heyang,** I really enjoyed working with you specially for the *in vivo* experiments ☺. You are working very hard, just try to keep one day on weekends to rest. **Molood,** it is always hard at the beginning to have experiments up and running, keep yourself motivated and everything will be alright ☺. **Jing,** you are a polite, warm, and smart person. Keep up the good work!

Roberta, Laurens, Jelter, Aranit, Thijs: " A journey of a thousand miles begins with a single step". I wish all of you the best of luck with your doctoral studies. Judging by what I saw until now the first step for all of you was full of motivation…keep it this way till the end! **Juan,** I wish you all the best with the new beginnings in life!

Ilse and Katharine, thanks for being so nice to work with, considerate, helpful, wonderful, efficient, and fun. A lot of times you helped me so much me that I felt really spoiled ! I can't thank you enough for all what you have done for me!

Last but not least, **Rita.** I would write pages in this case but I will try to make a long story short. On your first day, I was lucky to be given the mission to introduce you to the group and guide you through the different research techniques. I remember We went to the rectoraat together by bus…and then when we had to walk you said that I walk very fast and you added: "life is meant to be enjoyed". Within a few weeks, it evolved into a strong friendship. We went out to eat, drink, shared secrets, told jokes, and discussed a lot of topics. I always felt so comfortable to share with you a lot things that I didn't share with anyone else, this is because of the awesome friend you are! Thanks for the support, listening, and giving advices during hard times. You will be leaving soon to Portugal and for me it is a great loss – I will be missing you, but in the same time I am very pleased that you are going back to your family and loved ones. I wish you much success in your professional and personal life! Finally, I would like to mention that I have never been to Portugal and now I got a very very very good excuse to do so ☺…to be continued ☺

Now I wish to thank all the colleagues and collaborators from the Ghent University Hospital. A very special thank you to **Natacha, Felix, Charlotte, and Elodie** from the experimental surgery laboratory for their help with the animal experiments. I always felt welcome, I learned a lot from you, and you made me feel as one of the laboratory members – much appreciated ! **Wouter,** thanks for the discussions, ideas and contribution to my review article. Many thanks for the support I received from **Dr. Benedicte Descamps** and **Prof. Christian VanHove** at the Infinity laboratory before and during the animal experiments. I greatly appreciate the help of **Prof. Hannelore Denys** from the medical oncology department to obtain ascites fluid from patients. The help of **Prof. Joris Delanghe** from the department of clinical chemistry with the protein analysis of the biofluids is greatly acknowledged.

I acknowledge the help of **Prof. Achim Aigner** and **Dr. Sabrina Hobel** for their help to obtain peritoneal fluid from the abdomen of mice. The support provided by **Prof. Volker Mailänder** and **Dr. Artur Ghazaryan** with the protein corona experiments is gratefully acknowledged.

I would like to acknowledge the funding received towards my PhD from the Flemish Ministry of Education, European consortium – COMPACT, and the Research Foundation – Flanders (FWO).

I want to thank **Bernice De Regge**, **Hubert Goeminne**, **Renaat De Paepe** and **Ronny Verhoeven** for the help with a lot of matters especially upon my arrival in Belgium. Thanks for opening your homes to me and make me feel part of your families.

I would like to thank my PhD examination committee: **Prof. Chris Vervaet**, **Prof. Veronique Preat**, **Prof. Enrico Mastrobattista, Dr. Pieter Colin** and **Dr. Wouter Willaert** for the valuable comments on my PhD work.

My best friends in Belgium, **Pieter** and **Sharaz**, although we met one and a half years ago, for me it feels we know each other for several years! I am so lucky to have met you, you guys are super friendly, always willing to help, go out and have fun! As my PhD is done now, I promise to work less and be more social ☺

I wish to thank **Dr. Muhammad Safadi** for his guidance (back in 2010) that resulted in choosing drug delivery as a research topic for my M.Sc studies, which was later on my PhD research field.

This journey would not have been possible without the support of my relatives and all my family members. To my uncles and cousins, thanks for encouraging me forward to follow my ambitions and dreams. I am especially grateful to my grandmother **Nuha** and my grandfather **Sameer**, for their love and continuous support from my childhood until this moment. To my grandfather, **Sameer**, you taught me what "working hard" is about and I am very thankful for that. Without the spirit of working hard, this PhD project would not have been in the same quality as it is now.

Special and profound thanks to my brother **Azar**, for the invaluable support, tips, advices and humor over the years.

I am indebted and especially thankful and especially grateful to my parents: my mom **Suhair** and my father **Read** for the love, care, unlimited moral, emotional and financial support from the moment I was born until now. I was always sure that you believed in me and wanted the best for me. Without the opportunities and chances you have given me over the years I would never have made it here. Thank you for everything!

Katrina, thanks for the support, encouragement and great moments we spent together over the last 7 months. You were the light in this difficult and stressful period of my life ☺.

George